A Dissertation

entitled

Prediction of Glucose for Enhancement of Treatment and Outcome:

A Neural Network Model Approach

by

Scott M. Pappada

Submitted to the Graduate Faculty as partial fulfillment of the requirements for the

Doctor of Philosophy Degree in Engineering

_____
Brent Cameron PhD, Committee Chair

_____
Ronald Fournier PhD, Committee Member

_____
Thomas Papadimos MD, Committee Member

_____
Marilyn Borst MD, Committee Member

_____
William Olorunto MD, Committee Member

_____
Dr. Patricia Komuniecki, Dean
College of Graduate Studies

The University of Toledo

May 2010

An Abstract of

Prediction of Glucose for Enhancement of Therapy and Outcome: A Neural Network Model Approach

Submitted to the Graduate Faculty as partial fulfillment of the requirements for the Doctor of Philosophy Degree in Engineering

The University of Toledo

May 2010

Critical care (e.g. trauma and cardiothoracic surgical) and diabetic patients are prone to variability in glucose concentration on a daily basis. Hypoglycemic and hyperglycemic glucose values in these patient populations have been associated with decreased patient outcomes. In diabetic patients, persistently elevated glucose values are associated with development of long term complications such as, but not limited to retinopathy, neuropathy, and nephropathy. In the critical care patient population, elevated glucose has been correlated to increases in mortality, length of stay in the intensive care unit (ICU), and morbidities. The maintenance of tight glycemic control in these patients without severe hypoglycemia or glycemic variability appears to improve outcomes in these patients.

Various factors are associated with future glycemic excursions such as, but not limited to: lifestyle/activities (e.g. sleep-wake cycles), emotional factors (e.g. stress), nutritional intake, medication dosages, and ICU medical records (in critical care patients). In the field of diabetes research, models for prediction of glucose and/or models used to maintain tight glycemic control have been the focus of research. In the critical care

patient population, very little research into development of such models has been completed to date.

Multiple factors affect or are indicators of future glucose concentration. A suitable modeling technique needs to incorporate the effect of such factors for accurate prediction of glucose. A modeling technique well suited for this task is a neural network model.A neural network is an adapative modeling technique, which learns and updates model parameters based on determining patterns/trends existent in input data.This adapative capability, makes neural network modeling well suited for prediction of glucose where multiple factors impact future glycemic excursions.

This dissertation summarizes the development and optimization of various neural network model architectures for the real-time prediction of glucose in diabetic and critical care patients. Neural network models were configured to predict glucose using prediction horizons >60 minutes, which have not been attained in many predictive models to date. The performance of the neural network model is assessed via determination of overall model error, percentage of glycemic extremes predicted, and clinical acceptability of model predictions as determined via Clarke Error Grid Analysis.

ACKNOWLEDGEMENTS

This dissertation is a result of five years of work, which was possible only with the support and encouragement of many people. I would like to express sincere thanks to Dr. Brent Cameron my advisor for his advisement and guidance throughout my graduate career. Without the insight and support provided by Dr. Cameron throughout my career this work would not have been possible. I would also like to thank and acknowledge the help and support given by Drs. Fournier, Papadimos, Borst, Olorunto, Molitor and Relue for serving on my graduate advisory committees.

I would like to thank the University of Toledo for project funding, as well as the Departments of Surgery and Anesthesiology in the University of Toledo, College of Medicine, Tamara Phares the Bioengineering Lab Coordinator, and my colleagues in the Biooptics Laboratory Anthony Webb and Rui Zheng for their input, insight, help and support provided throughout my graduate career.

I would also like to thank and acknowledge the various physicians, nursing staff, and medical/graduate students at the University of Toledo Medical Center, for their numerous contributions in the clinical investigations: Dr. Paul M. Rosman (diabetes investigation), and Drs. Papadimos, Borst, Olorunto, Bourey, and Chiricolo (critical care investigation), Jennifer Low, Desmond Shipp, Steven Stanek, Jason Lather, Tyler Sbrocchi, Abhilash Felix, Christine Collins, and Brittiany Sheard.

TABLE OF CONTENTS

LIST OF FIGURES

LIST OF TABLES

LIST OF ABBREVIATIONS

AR……..autoregressive

CGM……..Continuous Glucose Monitoring

eCIDL…….electronic clinical intensive data-logger

FF……feed forward

GUI……..graphical user interface

Hypo……..……hypoglycemia

Hyper…….……hyperglycemia

ICU…….intensive care unit

MAD%.....mean absolute difference percent

MFNN……multifunctional neural network

MICU…….medical intensive care unit

MLR……multiple linear regression

MSE……..mean squared error

PID……..proportional integral derivative

PLS…….partial least squared

POC……..point of care

RMSECV……..root mean squared error of cross validation

SICU……..surgical intensive care unit

TLFF……..time-lagged feed forward

UTMC……..University of Toledo Medical Center

CHAPTER 1

INTRODUCTION

Lack of glycemic control in patients with diabetes is a well known phenomenon. This is especially difficult in patients with type I or insulin dependent diabetes as the body no longer produces insulin and insulin injections or continuous subcutaneous insulin infusion via an insulin pump must be optimized. Optimum control of glucose concentration in patients with diabetes is the main goal of diabetes therapy. Optimized control of glucose in patients with diabetes is obtained via frequent sampling of blood glucose and adjustment of insulin based on these sampled values. Research has been completed which substantiates that such intensive treatment is necessary for reduction of long term complications associated with persistently elevated glucose. [1-4]

What is less known however, is the lack of glycemic control in critical care patients (e.g. trauma and cardio thoracic surgical patients). Research has also substantiated that an intensive insulin infusion protocol in critical care patients in the intensive care unit can help reduce mortality. [5]

The optimization of glycemic control can be enhanced with advanced knowledge of unwanted glycemic excursions. Given the prediction of hyperglycemic and hypoglycemic excursions, patients and clinicians can adjust insulin and therapeutic delivery to mitigate occurrences of these unwanted glucose values. The enhancement of glycemic control can be correlated with enhancement of outcome in both diabetic and critical care patient populations.

Recent advances in technology for monitoring of glucose include the development and utilization of real-time continuous glucose monitoring (CGM) devices. These devices measure glucose concentration in the interstitial fluid every one to five minutes depending on CGM technology. Currently patients with diabetes monitor blood glucose anywhere from 2-6 times daily. These values are discrete time measurements and do not provide insight to glycemic excursions when such metered values are not obtained. In the critical care patient population, current convention of care is to monitor a patient's blood glucose concentration every 1-4 hours. Based on the metered glucose readings obtained, the patient is given insulin according to a specific institutions insulin delivery protocol. Even in the event that a patient is monitored every hour, there is an hour time span where glycemic excursions and response to the insulin infusion protocol are unknown. There is thus a need to predict and forecast future glucose concentration when discrete metered glucose readings are not obtained. The utilization of real-time CGM technologies will provide considerable data on which to develop models for prediction of glucose which can be therefore used for therapeutic direction/guidance and eventually automation.

This dissertation summarizes the results of two clinical investigations. In these investigations, the development and performance analysis of neural network models for prediction of glucose in diabetic and critical care patients was accomplished. These models were developed using data derived from utilization of CGM technologies. The clinical acceptability and applicability of the developed predictive models is summarized.

CHAPTER 2

LITERATURE REVIEW

2.1 Glycemic Excursions and Diabetes Mellitus: A Multivariate System

Type I diabetes is an autoimmune disease in which the beta-cells of the body are destroyed thus resulting in a lack of insulin production. This leads to an inability to control blood glucose concentration as insulin facilitates the cellular uptake of glucose. If glucose levels remain high for extended periods of time, long-term complications such as but not limited to neuropathy, nephropathy, and retinopathy can arise. Due to the lack of insulin production, type I diabetics are required to take insulin subcutaneously as their primary method of therapy.

The major difficulty involving the successful treatment of diabetes is the appropriate dosing of insulin such that a therapeutic range of glucose concentration (80-120 mg/dl) can be achieved. There are a multitude of factors which influence subsequent glucose concentrations in diabetics including but not limited to: insulin dosage, carbohydrate and nutritional intake, lifestyle (i.e. sleep-wake cycles and sleep quality, exercise, etc.), and emotional states (i.e. stress, depression, contentment, etc.). [6-16] The effect of these various factors on subsequent glucose concentration is not fully understood, and may be similar across all diabetic patients or patient specific. In order to optimize control in diabetic patients, there needs to be some method for quantifying or

predicting future occurrences of dysglycemia (i.e. high and low blood glucose concentration also referred to as hyperglycemia and hypoglycemia, respectively).

Fluctuations in glucose concentration experienced on an everyday basis appear to be chaotic, however, prior research does identify possible patterns which may exist. [15,17-22] Circadian rhythms in sleep and subsequent glucose regulation have been identified in previous research. [15] Other patterns in glucose tolerance, insulin activity, insulin sensitivity, insulin clearance, and hormone levels (e.g. cortisol, epinephrine, norepinephrine) and their subsequent effect on glucose concentration have also been identified in previous research. [11,15,17-31] The existence of rhythms in insulin activity, and subsequent quantifiable patterns in glucose fluctuations, provide a foundation and hypothetical construct for the development of modeling techniques for prediction and ultimately control of glucose.

2.2 Historical Attempts at Prediction and Control of Glucose in Patients with Diabetes

The major goal in treatment of patients with diabetes is the optimization of insulin therapy such that a normal glucose concentration may be obtained. Previous and ongoing research has been focused on the development of mathematical models for optimal glycemic control using various analytical and mathematical approaches. The goal of many of these previous and ongoing studies is the development of a closed loop artificial pancreas to maintain euglycemia (normal glucose) in patients with diabetes.

One of the most well known methods for development of an artificial pancreas for optimal glycemic control is a classic PID algorithm developed by researchers at Medtronic Minimed/Diabetes. [32-34] The basis of this model is that the PID controller

mimics the biphasic nature and function of the beta cell in the body. The PID control algorithm has three components the proportional, integral, and derivative components. The function of these components, are based on tracking of glucose in the body. The proportional component is proportional to glucose concentration, the integral component slowly increments up or down based on response to glucose, and the derivative component reacts to the rate of change of glucose.

Another investigation was completed by Schaller and colleagues involved generation of a model predictive control algorithm for optimization of glycemic control in fasting type I diabetic patients. [35] In this investigation, venous glucose concentration sampled at 15 minute intervals, carbohydrate intake, and insulin dosages were inputs to the model predictive control algorithm. Furthermore, the model predictive control algorithm developed in this investigation, had eight adaptable parameters.

Further investigations such as the investigation by Sparancino et al., demonstrated the prediction of glucose using continuous glucose monitoring (CGM) and description of past glucose data by either a first-order polynomial or a first-order autoregressive (AR) model, both with time-varying parameters determined by weighted least squares. [36] This research demonstrated that prediction of glucose was possible implementing a prediction horizon of 30 minutes. The investigation substantiated that utilizing this prediction horizon gives the patient adequate time to compensate and avoid predicted hypoglycemic extremes.

Further investigation completed by Reifman et al. demonstrated the usage of autoregressive modeling for prediction of glucose using CGM in patients with diabetes. [37] In this investigation, 15 patients were confined to a study site and limited in physical

activity while undergoing CGM. Meals and snacks were kept consistent. The investigation demonstrated that prediction of glucose utilizing prediction horizons of 30 and 60 minutes resulted in considerably accurate predictions with 95.9-100% of the predictions being determined as clinically acceptable and not leading to adverse therapeutic direction. Analysis of predictions generated using a prediction horizon of 120 minutes was also completed. It was determined that implementation of this prediction horizon resulted in considerably less predictive accuracy in comparison to the 30-60 minute predictions.

2.3 Necessity of Glycemic Control in Critical Care Patients

It is known that patients with type 1 diabetes mellitus routinely experience lack of glucose control due to inability to produce insulin. In these patients, there is need for intensive monitoring of glucose followed by modification of insulin dosages to maintain a normal glycemic state. It is less known however, that critical care patients (i.e. trauma, cardiothoracic surgical patients, and other intensive care unit patients) also experience glycemic variability and lack of optimal glucose control. It has been reported that critical care patients experience insulin resistance and corresponding hyperglycemia. [38] Similarly to the patients with diabetes, lack of optimal glucose control is correlated with decreased outcomes in this critical care patient population.

Glycemic variability following trauma is a common phenomena. Following severe trauma, research indicates that approximately 25% of individuals may experience hyperglycemia. [39] If hyperglycemia is sustained, mortality and requirements for care

are potentially increased. [40-43] Published data indicate that lowering glucose levels after trauma may decrease mortality, the length of stay on ventilators, incidence of infection, and length of stay in the intensive care unit (ICU) and in the hospital. Aggressive therapy to maintain glucose levels below 150 mg/dl was shown to improve outcomes although the ability to sustain this goal in post-traumatic circumstances may be difficult as the patient recovers. [41] If glucose levels exceed 200 mg/dl in severely injured patients on admission to trauma centers, their expected survival has been reported to be reduced by more than 50%. [40] Persistence of this hyperglycemia during the first two days after trauma has been shown to further reduce survival [43] and increasing glucose levels during this early post-trauma period has been shown to potentially predict adverse outcomes in these patients. [40] Glucose levels greater than 150 mg/dl during the first two post- trauma days is also associated with an increased risk of mortality and/or other complications and subsequent euglycemic maintenance does not appear to improve these outcomes. [39]

In addition to trauma patients, cardiothoracic surgical patients also experience a considerable degree of glycemic variability and associated elevated glucose. Patients who undergo some form of cardiovascular surgical intervention are prone to glycemic fluctuations. Control of glucose concentration in such patients is a desired goal for improving patient outcomes. Tight glycemic control in cardiac surgical patients has been correlated to reduced morbidity and mortality rates. [44-48] Thus, it is integral to patient outcome that tight glycemic control be obtained in cardiac surgical patients both interoperatively/perioperatively as well as postoperatively.

A considerable percentage of patients who undergo some form of cardiothoracic

surgical intervention are diagnosed with some type of diabetes. Over the years, various treatment protocols have been designed for optimization of glycemic control in such a patient base. These protocols, however, are often tedious and difficult to maintain. The development of such treatment protocols for tight glycemic control began in 1987, with the Portland Protocol. [49] The Portland Protocol is a well-defined intravenous insulin infusion protocol for hospitalized patients for use in both intensive care units and general inpatient wards. The Portland Protocol has been in use since 1992 and has been modified by various institutions worldwide to provide tight glycemic control. Further investigation to date substantiates that intensive insulin delivery in these patients has been correlated with decreased occurrences of morbidity (e.g. deep sternal wound infections), decreased length of stay in the hospital, and mortality. [49-54]

Utilization of intensive insulin therapeutic protocols across the critical care patient populations with lack of optimal glycemic control has been a major research focus by Van Den Berghe and colleagues. [55] Furthermore, Van Den Berghe stressed that such intensive insulin therapy in critically ill patients directly benefits patient outcomes. [56]

2.4 Patterns in Glycemia in Critical Care Patients: A Justification for Predictability

The reported patterns in glucose, insulin clearance, insulin sensitivity, hormone levels, etc. by previous research in both diabetic and non-diabetic individuals are also present in patients in the critical care setting. [11,15,17-31] Furthermore, research has been completed which demonstrates the existence of patterns in glucose in critical care patients receiving intensive insulin therapy and insulin infusions. [57-59]

Patterns in glucose can be correlated with hormone levels of cortisol in the critical

care patient population. Research has demonstrated that cortisol plays a significant role in the human counter-regulatory response to hypoglycemia. [60] Furthermore, patients with critical illness have elevated cortisol levels which can be correlated to the elevated glucose observed in this patient population. It is important to note however, that both insufficient and excessive hypothalamic-pituitary-adrenal axis is associated with increased mortality in critical care patients. [61] The measurement of serum free cortisol in this patient population has therefore been subject of previous research endeavors. [62]

While cortisol has been demonstrated to have a significant impact on glycemic excursions in the critical care patient population, other factors also are indicators or significantly impact future glucose concentration. Various factors are documented in patient medical records throughout the course of a patient's stay in the intensive care unit. These factors include but are not limited to: vital signs, lab results, ventilation data, pain indices, organ systems analysis, nutritional intake, medications, etc. A major difficulty facing caregivers in the intensive care unit is to determine the effect of these factors on future glucose such that corresponding changes in insulin therapy can be adapted to optimize glycemic control. The utilization of these records, in combination with glucose values collected throughout the patient's length of stay in intensive care will provide a hypothetical construct for development of predictive and/or models for optimizing glycemic control in these patients. The optimization of glycemic control in these patients has been correlated with enhancement of patient outcome and further research is needed for the development of strategies to facilitate optimal glycemic control. [56,63-66]

2.5 Models for Prediction and Control of Glucose in Critical Care Patients

Due to the large quantity of research substantiating that increased glycemic control is correlated with enhancement of critical care patient outcome, research has shifted towards the development of predictive and/or control models/algorithms for enhancement of glycemic control. Currently, monitoring and control of glucose in critical care patients is completed via discrete point of care monitoring with handheld glucose monitors by caregivers. Insulin requirements for maintaining normal glucose concentration are determined from the point of care glucose values. [67] The development of predictive and assistive models to enhance this conventional therapeutic approach is subject of ongoing research.

A method utilizing a model predictive control algorithm for control of glucose was compared against conventional critical care glucose management protocols by Plank et al. [68] Results of this investigation demonstrated that utilization of the model predictive control algorithm resulted in a higher percentage of the time the patients glucose values were maintained within target normal glucose ranges.

The implementation of the PID control algorithm for optimized glycemic control in patients with diabetes [32-34] has been investigated in pediatric intensive care unit patients as well. [69] This investigation was preliminary and completed on six pediatric patients. Results demonstrated that hyperglycemia could be significantly reduced via implementation of the PID control algorithm. In addition to this PID control algorithm, a similar approach has been investigated and applied to the general critical care population. [70]

The development of a computer program (GRIP) for enhancement of glycemic

control has been investigated for its applicability in the critical care setting. In this computer program an insulin pump rate for maintaining glucose within a target range is approximated via Equation 1. In this equation, ΔI is the estimated insulin pump rate, $\bar{I}_{-4h}$ is the mean insulin pump rate over the previous four hours, G_0 is the most recent glucose value, G_{target} is the target glucose value, and $\Delta_{-4h}G$ is the change between the last glucose value and the glucose value measured four hours earlier. [71] In addition to this estimation, the GRIP program also estimates the time between which nursing and clinical staff should measure point of care glucose values. Results of this investigation demonstrated that usage of GRIP enhanced glycemic control with respect to a previously implemented paper-based sliding scale protocol.

$$\Delta I = \left(1 + 0.25 \cdot \bar{I}_{-4h}\right) \cdot (0.2) \cdot \left(G_0 - G_{target}\right) + 0.3 \cdot \Delta_{-4h}G \quad \text{[Equation 1]}$$

2.6 Advances in Monitoring Technology: Continuous Glucose Monitoring (CGM)

Historically, both diabetic and critical care patients are monitored via handheld blood glucose monitors. Patients with diabetes use these handheld glucose monitoring devices to measure glucose concentration 2-6 times daily. Critical care patients are monitored more frequently with point of care glucose being monitored every 1-6 hours depending on an institution's insulin infusion protocol. Recent advances in glucose monitoring include the development of continuous glucose monitoring devices which measure glucose in interstitial fluid every 1-5 minutes depending upon technology. [72-74] Further advances have led to the development of real-time implementations of these continuous glucose monitoring devices. The utilization of this technology would thus

provide patients and caregivers, insight into glycemic control and effectiveness of therapy when discrete glucose monitoring is not provided. [75] Additionally, the glucose data acquired via these devices can be utilized for development, implementation, and subsequent optimization of predictive and/or optimal control models for glucose implemented in the diabetic and critical care populations as previously discussed.

Utilization of continuous glucose monitoring in patients with diabetes has been demonstrated to provide significant insight into glycemic excursions when discrete meter-based glucose concentrations are not routinely obtained. The usage of this technology in this patient base has thus been demonstrated to enhance glycemic control via providing addition insight into glycemic excursions otherwise unseen via conventional discrete glucose monitoring. [74-83] The major goal of diabetes therapy is the maintenance of a normal glucose concentration. An indicator used to gauge glycemic control in this patient population is the glycated hemoglobin A1C value (HbA1C). Utilization of CGM in patients with diabetes has been demonstrated to lower HbA1C values and correlate with increased ability to control blood glucose values. [76] The utilization of CGM in patients with diabetes is an emerging and continuously growing field.

While CGM in patients with diabetes has been considerably investigated over the past 5-10 years, the utilization of CGM in critical care patients is a relatively new field. [84-90] Given that a critical care patient is intensively monitored during their length of stay in intensive care, the utilization of CGM will provide insight to the quality of care the patient receives. The utilization of CGM may also provide insight as to which documented variables in the patient's medical record affect or are indicators of subsequent glycemic excursions. The quantification of these various factors would thus

provide significant insight into optimizing the control of blood glucose concentration in this patient population.

Real-time CGM technologies have been developed and integrated with real-time alarms based on real-time sensor glucose values as well as trends in the CGM data. [91-95] The Medtronic Diabetes© Guardian RT® real-time CGM device alerts patients when their glucose crosses programmable thresholds for hypoglycemia and hyperglycemia thus providing some form of real-time feedback.[95] In contrast, the Abbott Diabetes© Freestyle Navigator® real-time CGM device alerts users of pending hypoglycemia and hyperglycemia based on trends in real-time CGM data and predicts the occurrence of unwanted glucose values based on these trends. [94] Patients with diabetes often experience hypoglycemic unawareness where they are unaware when their glucose reaches dangerously low glucose values and there is a degree of cognitive dysfunction.[96-98] The utilization of real-time CGM and these alarms and alerts for pending dysglycemia are extremely important. The utilization of real-time CGM technologies provides a unique foundation for improving glycemic control. The development of further predictive models utilizing these real-time CGM devices as a platform for prediction and or automated closed loop insulin delivery is therefore warranted of future research endeavors.

There has been some controversy in utilizing real-time CGM technology and its applicability in a clinical setting. A time-lag existent between interstitial glucose (subcutaneous glucose) and blood glucose concentrations has been determined. [99-102] Mathematical analysis of the time-lag existent between interstitial and blood glucose revealed that this time–lag was on the order of 12.5 minutes. [101] The utilization of

closed loop controllers such as the PID controller may have some limited adverse effects given this time lag, however, predictive models with large enough prediction horizons ($\geq$60 minutes) will minimize the effect of this time-lag.

Given that there are a variety of factors which impact and are indicators of future glycemic excursions in both diabetic and critical care patients as previously discussed, a successful modeling technique should be capable of quantifying the effects of these variables. Previously reported modeling techniques do not take into account a majority of these factors which at times may inhibit model success. For example, overly aggressive insulin therapy with PID controllers is possible if glucose changes rapidly due to other variables and factors which will lead to unwanted hypoglycemia. [32-34] Research demonstrates patients with an extended history of diabetes often have impaired counter-regulation in response to hypoglycemia due to autonomic insufficiency/failure. [103-105] A PID controller configured for automated insulin delivery given changes in glucose may give an inappropriate increase in insulin infusion given delayed counter-regulatory response in this patient base which would lead to further hypoglycemia and a dangerous cycle. Most of the initial studies completed using the PID control algorithm for automated closed loop glucose control were implemented in a controlled inpatient setting and variations/factors in everyday life were negated. [32-34]

2.7 Introduction to Neural Network Modeling and Attempts to Control and Predict Glucose

An artificial neural network model or neural network is a mathematical or computational modeling technique. Neural network models contain a connected series of processing elements called neurons. These neurons exhibit complex global behavior

which is determined by the connections existent between various processing elements and related parameters within the neural network architecture. Neural network modeling and the concept thereof is derived from knowledge of the central nervous system and specifically neurons (consisting of axons, dendrites, and synapses) which are the most basic information processing elements in neuroscience. Neural network models are desirable as they are adaptive technologies, which learn based on determining patterns/trends existent in input data. Based on this learning process, weights within the neural network architecture are modified to minimize error in neural network model output and complete a specific task. Historically, neural network modeling has been used in a variety of applications. These applications include but are not limited to: time series prediction, function approximation, regression analysis, classification, and data processing (e.g. filtering, and clustering).

Historically, neural network modeling has been investigated to predict glucose and/or optimum insulin therapy for maintaining normal glucose levels in patients with diabetes. One such investigation was completed by Tresp et al., in which his research group investigated the utilization of recurrent neural network models and time series convolution neural networks to model glucose metabolism in diabetic patients. [106] In this investigation, a dataset of 63 days with a total of 463 blood glucose measurements were used to model glucose metabolism in a male diabetic patient. This correlates to approximately seven discrete glucose measurements per day acquired for the investigation.

Investigation by Prank et al. was also completed to develop neural network models for learning the time course of blood glucose levels from the complex interaction

of counter-regulatory hormones. [107] In this investigation, neural network modeling was utilized to model blood glucose given activity of counterregulatory (glucose raising) hormones and their subsequent effect on future glycemic excursions.

Davide and his research group investigated the utilization of fuzzy logic combined with neural network techniques to modify intravenous insulin administration in diabetic patients subjected to glucose and potassium infusion. [108] Insulin infusion rates were adjusted every 4 hours between -1.5 and 1.5 units per hour, based on results of the fuzzy logic and neural network control algorithm. Glycemic control obtained using this method was compared against utilization of a conventional insulin estimation algorithm. The system was found to be effective in improving glycemic control without increasing the risk of hypoglycemia.

Research efforts by El-Jabali were completed to develop a neural network system for prediction and control of glucose in diabetic patients. The system was configured to predict the long term and short term insulin requirements for maintaining normal glucose levels. The neural network model inputs were discrete blood glucose measurements, insulin dosages, meals, and exercise. [109] Results demonstrated that reliable estimation of the next glucose level and insulin needed to maintain a normal glucose concentration can be obtained.

In these attempts at prediction and/or control of glucose using the neural network modeling techniques outlined above, discrete glucose monitoring was utilized as inputs to the neural network models. The utilization of CGM as inputs to these neural network models would likely provide better quality training data on which patterns in glucose can be learned and processed by the neural network models. Various modeling techniques

take into account other factors known to impact glucose such as meals, insulin dosages, exercise, sleep, and counterregulatory hormone levels. [107,109] The utilization of CGM in these cases would better help quantify the effect of these factors on future glucose concentration as well.

2.8 Summary of Literature Review

The optimization of glycemic control in patients with diabetes is a well known problem. Similarly, critical care patients such as but not limited to, trauma, and cardiothoracic surgical patients experience glycemic variability and elevated glucose during their course of stay in the intensive care unit which has been linked to increases in morbidity and mortality rates. Research has demonstrated that a multitude of factors affect and are indicators of subsequent glycemic excursions in both of these patient bases. Successful models for prediction and ultimately optimization of glycemic control in these patient bases would likely need to incorporate the occurrence and effect of such factors. To date, this issue has not been fully addressed in both patient populations. In diabetic patients, lifestyle and emotional factors (unincorporated by previous modeling techniques) have been demonstrated in previous research to impact glucose. [6-8,12,14-16,24] In critical care patients, modeling has been completed for predicting optimized insulin delivery for maintaining a normal glycemic state, however, considerable research regarding development of predictive models for glucose has not been the subject of research. Furthermore, there are a variety of factors documented in patient medical records throughout the course of their stay in intensive care. Many of these factors impact or are indicators of future glycemia in this patient base. To date, a modeling technique incorporating these factors which impact or are indicative of future glucose has not been

developed.

Recent advances in glucose monitoring technology, includes the development of real-time CGM technologies. The utilization of these technologies has and will be, implemented in closed loop insulin delivery applications in both the diabetic and critical care patient populations. The proportional integral derivative (PID) controller has been investigated for its potential in closed loop insulin delivery and automated glycemic control. This classical control algorithm closely mimics the beta cell, which is the primary insulin delivery mechanism in the human body. There are limitations accompanied with the utilization of this control algorithm as well. Studies on patients using such PID controllers were done in a controlled setting (i.e. hospital bed) where nutritional intake, activity, and other factors were controlled and did not parallel everyday variability in lifestyle and other factors a patient would expect in the course of their everyday lives. In critical care patients, utilization of these control algorithms would likely need to include the effect of various factors such as but not limited to medications, vitals, nutritional intake, ventilation data, and other factors routinely documented in medical records throughout a patient's stay in intensive care. If the PID control algorithm is implemented, changes in glucose, may be correlated to other factors and the PID control algorithm could not differentiate this and lead to overly aggressive insulin infusion. This may potentially lead to unwanted hypoglycemia which has also been correlated to adverse outcomes.[110]

Neural network modeling is a technique which has considerable potential to the prediction and control of glucose in these patient bases. What makes neural network modeling an attractive technique is its adaptive capabilities. Neural network models learn

based on patterns in input data and can quantify the effect of various input factors on a desired/predicted output. Given that a variety of factors impact or are indicators of future glucose in the patient bases discussed, neural network modeling is well suited for quantification of these factors and subsequent prediction of glucose. Neural network modeling techniques for prediction and control of glucose in patients with diabetes have historically utilized only discrete metered glucose values and did not include factors which may have an effect or impact on future glycemic excursions. In regards to the critical care population, CGM has only recently been investigated for clinical utility. The development of predictive models for glucose in this patient population has not been a major focus of research endeavors to date.

While control algorithms such as the PID controller have been successful in automated glycemic control, this investigation outlines a unique and different approach towards optimization of glycemic control. This dissertation includes the development of various renditions of neural network modeling techniques for prediction of glucose in diabetic and critical care patient populations. These neural network models were developed using CGM data, and the documentation of other factors known to affect or be indicators of future glucose concentration. In the diabetic patient population neural network models were configured to utilize inputs including: time, insulin dosages, nutritional intake, metered glucose readings, CGM data, lifestyle, emotional factors, and presence of hypoglycemic and hyperglycemic symptoms. For the critical care population, a genetic algorithm was utilized to determine which inputs documented in patient medical records were relevant to include in neural network model architecture. Using the medical records known to impact or be indicative of glycemic excursions, neural network models

were developed using this –optimized" training set. The neural network models developed were integrated into a computer application for real-time prediction of glucose in both patient bases, and the predictions generated in real-time were analyzed for clinical acceptability.

The application of the neural network models outlined in this dissertation will provide patients and caregivers insight into future glucose concentration and provide a means for therapeutic intervention to mitigate occurrences of unwanted hyperglycemic and hypoglycemic excursions. Furthermore, the utilization of these neural network models may provide a means to gauge the effect of the various input factors on subsequent glycemic excursions. This information can be utilized both as an instructive tool as well as provide a means for optimizing predictive model accuracy. Although neural network models were developed for both diabetic and critical care patient populations, the major focus of this dissertation will be the development/optimization of the neural network models for the critical care patient population. The development of such predictive models, especially those utilizing CGM, has not received much research attention. The development and utilization of such models will fill a gap in research and lead to advances in care, safety, and outcome of diabetic and critical care patients.

The neural network models presented in this dissertation can be utilized for intelligent therapeutic direction and assistance for patients and caregivers. Given increased model accuracy, the development of models for estimation of insulin needed for optimized glycemic control can be constructed. From this, the creation of semi-closed loop (i.e. closed loop implementation with user entering of input factors to predict and control glucose), and fully automated closed loop systems can be developed.

CHAPTER 3

MATERIALS AND METHODS

3.1 Introduction

Neural network modeling provides a well suited construct for predictive models for glucose given the effect/impact of a variety of factors on glucose concentration. Neural network models have the ability to distinguish the effect of individual as well as multiple factors on a desired/predicted output.

This chapter will outline the procedures used for data collection, development, and testing/validation of the various neural network models developed in two clinical investigations. This chapter will be divided into two sections. One section will focus on clinical study and model development for patients with diabetes. A second section will include the clinical study and model development for critical care patients.

3.2 Neural Network Model Development for Patients with Insulin Dependent Diabetes

3.2.1 Generation of Pocket PC based Electronic Diary for Initial Data Collection

The initial step in development of the neural network models was data acquisition. A Pocket PC based electronic diary facilitating documentation of a patient's meter blood glucose readings, insulin dosages, carbohydrate intake, hyperglycemic and hypoglycemic symptoms, lifestyle (activities and events), and emotional states was created using Visual C# .NET. The graphical user interface

(GUI) of the developed software application is included in Figure 3-1. Emotional factors and lifestyle factors were selected from drop-down menus with pre-defined selectable inputs. Based on the input selected from the interface the input is binary encoded via Equation 2. In Equation 2, $V_{encoded}$ is the encoded value, i is the selected index of the drop-down menu and i_{max} is the number of selectable indices in the drop-down menu.

$$V_{encoded} = \frac{2^{i}}{2^{i_{\max}}} \quad \text{[Equation 2]}$$

The Pocket PC based electronic diary was configured to output a file containing all data-logged from the intensive electronic diary, which is used for subsequent integration with CGM data and neural network model training and development. CGM data and electronic diary data were integrated via merging the data into a single tab-delimited text file. The electronic diary automatically updated the date and time of each entry to facilitate real-time data acquisition and mitigate instances of erroneous input.

Figure 3-1. GUI of Electronic Diary for Initial Data Acquisition

3.2.2 Patient Training and Data Collection

The patient population utilized for neural network algorithm/model development was obtained from a private endocrine practice in Warren, OH. The only inclusion criterion for the study was that patients must have insulin dependent diabetes mellitus. Using the developed electronic diary, 27 patients were subjected to usage of the diary in combination with a Medtronic CGMS (Continuous Glucose Monitoring System) Gold® device. Patient utilization of CGM varied from patient to patient between 3-9 day monitoring periods. The electrochemical sensor for the device was changed every three days in accordance with manufacturer and FDA recommendations for sensor life and stability period. Patients were instructed on calibration of the CGM unit, as well as, trained in usage of the electronic diary before their involvement in the study.

It is important to note that the data logged via the usage of the electronic diary may have been entered incorrectly. Data was evaluated after each patient monitoring period, and erroneous inputs were removed. It was impossible to monitor the patients involved in the study over the course of their everyday lives. To mitigate such errors, patients were instructed and trained to record data using the electronic diary prior to their involvement in the study.

3.2.3 Neural Network Model Design and Development

Neural network models were generated using NeuroSolutions® software (Neurodimension, Gainesville, FL). These neural networks were configured to forecast future glycemic levels within a certain pre-defined time frame or prediction horizon. Models were developed with prediction horizons ranging from 50-180 minutes. These prediction horizons were chosen for two reasons: to cover a wide range of time, and to gain a predictive view of 120-180 minutes which is very important for a diabetic patient specifically after meals and insulin dosages. Each glucose value obtained from the Medtronic CGM device was collected every five minutes, therefore, for a 100 minute prediction horizon, the neural network was configured to predict 20 CGM values.

The neural networks developed in this investigation were time-lagged feed forward neural networks. These neural networks are multi-layer perceptrons which have memory components to store previous values of data within the network. The existence of such memory components provides the network the ability to learn relationships/patterns existent in the data over time. These neural networks consist of multiple layers of processing elements which are connected together in a feed forward

manner. Various connections (synapses) were constructed to facilitate connections between the processing elements of the neural network (axons).

The neural networks generated were trained using a method known as the backpropagation of errors. Elements in the neural network known as backpropagation axons (BackAxons) facilitated the training process. BackAxons derive a relative error at their input which is to be back propagated to any processing elements which precede them in the neural network design. Backpropagation of errors is completed as an error is presented at the output of each BackAxon in the neural network, and the BackAxon is charged with calculating the gradient information associated with calculating weights for minimization of total error in the neural network. Optimal weights for minimization of error in the predictive model are obtained via a gradient descent with momentum algorithm performed within the BackAxon elements. This gradient descent algorithm calculates the optimal weight for minimization of total error in the neural network model. The optimization value of step size in such an algorithm is integral in the amount of time it takes to train the neural network. A small step size could lead to large training time, and conversely a large step size could lead to over estimation of the desired local minimum. Neural networks were configured with a forward trajectory of 50 samples and the back propagation of 40 samples (i.e. single exemplar). The neural network model was configured to update weights after 200 exemplars were encountered. The neural networks were configured to terminate training if the mean squared error exceeded the threshold of 0.01 or after 1000 epochs (i.e. cycles through the dataset).

Optimization via usage of a genetic algorithm, which are useful computer aided design techniques, was completed during neural network model training. [111-113]

Optimization via a genetic algorithm was used to minimize the number of processing elements (neurons) and inputs into the neural network. The genetic algorithm also effectively determines which inputs have an impact on predictions and minimizes the various interconnections between neurons (i.e. processing elements in the neural network). The genetic algorithm also determines the best value for step-size and momentum for calculating the optimum weights for minimization of total error the neural network as well.

Figure 3-2 includes the neural network design/architecture of one of the processing and output layers of the neural network models designed using the NeuroSolutions® software. The various components in the neural network design are labeled 1-5. Component 1 is a hyperbolic tangent axon (Tanh axon). The Tanh axon has the processing elements for the hidden layer of the neural network. This processing element effectively processes inputs within the neural network between a range of -1 and 1. This range makes patterns in the data more easily interpreted due to the smaller range of potential values. For example, CGM values would have values between 40 and 400 mg/dl, utilizing the hyperbolic tangent processing element would limit this large range of values to a more quantifiable one. Each processing element sums the weighted connections from the inputs into the axon. Component 2 is a Laguarre Axon which functions to store delayed versions of the processing elements output and pass it onto the next layer of the neural network. The Laguarre axon, therefore, serves to provide the neural network with memory thus enabling the processing of information in time. Component 3 is the momentum/gradient descent component of the network. This component serves to adjust the weights with information about the error within the

network. Optimal step sizes and momentum values in these elements for minimization of error are determined via implementation of a genetic algorithm, as discussed previously. Component 4 is an example of the synapses of the neural network which serve to connect the various axons/processing elements of the neural network. Component 5 is the output layer of the neural network which consists of a Bias axon (leftmost element in component 5) and an Output Axon (rightmost element in component 5). The Bias axon component has the processing elements for the output layer, each of which sums the weighted connections from the second hidden layer. The Bias axon adds an offset to the weighted values obtained from the previous layer. The output axon yields the predicted values in the original format (i.e. desired response) as originally presented to the neural network.

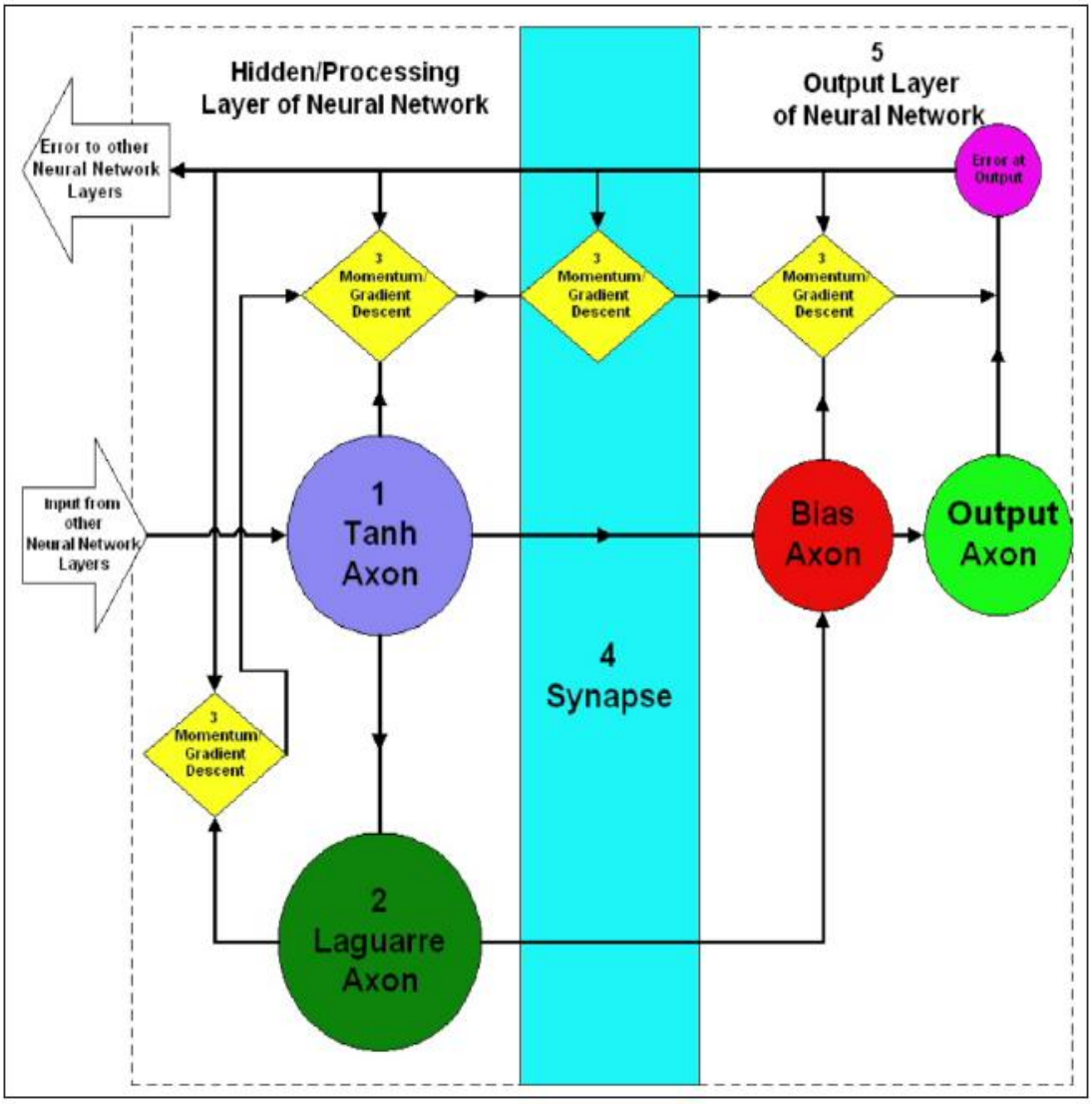

Figure 3-2. Hidden Layer and Output Layer Design of Time-Lagged Feed Forward (TLFF) Neural Network Model Architecture Implemented for Prediction of Glucose in Diabetic Patients

3.2.4 Testing/Validation of Developed Neural Network Models

Three methods were implemented to analyze the accuracy of the developed neural network's predictive abilities. The first method involved the validation of neural network models generated with variable length training sets. In this analysis, training sets using

11-17 patients were used to generate neural network models with a constant prediction horizon of 100 minutes. The performance of each neural network model was evaluated using the CGM and electronic diary data from a patient which was not included in the training data of any of the neural network models. MATLAB® was used for performance analysis of the neural network model. The mean absolute difference percent (MAD%) of the model's predictive abilities on the entire test data set (overall MAD%), hypoglycemic extremes (<=70 mg/dl) and hyperglycemic extremes (>=180 mg/dl), were calculated using Equations 3 and 4. Equation 3 is utilized for calculating the absolute difference percent (AD%) between each neural network predicted value and the corresponding actual CGM value. Equation 4 is used to calculate the mean absolute difference percent (MAD%), which is defined as the mean of all obtained absolute difference percent values in the dataset. The percentage of hyperglycemia and hypoglycemia predicted by the system was also calculated.

Note: *AD%(t)* is the calculated AD% at time t, $NNet_{predict}(t)$ is the predicted neural network glucose value at time *t*, and $CGM_{actual}(t)$ is the actual CGM data point at time *t*. N is the number of data points in the dataset, used for calculating the MAD%.

$$AD\%(t) = \frac{\left|NNet_{predict}(t) - CGM_{actual}(t)\right|}{CGM_{actual}(t)} * 100\% \qquad \text{[Equation 3]}$$

$$MAD\% = \frac{\sum_{i=1}^{N} AD\%(t)}{N} \qquad \text{[Equation 4]}$$

A second method of performance analysis involved the validation of the multiple neural network models generated using 12-17 patient datasets. The final patient included in each dataset, (i.e. the last 3-3.5 days of each dataset) was omitted from the training data and utilized to validate the accuracy/predictive abilities of the neural network on

unseen patient data. This analysis mimics real-time functionality of such models on multiple unseen patients as the data used to test model performance is a different patient each time. MATLAB® was utilized for performance analysis and used to calculate the previously described performance measures.

The final method of performance analysis was the validation of the various neural network models with variable prediction horizons ranging from 50-180 minutes, tested on data from a patient which was not included in the initial training data. The respective predictive abilities were analyzed using MATLAB®.

3.2.5 Development of a Real-Time Software Implementation of Neural Network Based Predictive Model for Patients with Diabetes

The neural network models developed in 3.2.3 above consisted of a complex architecture, which consisted of an input layer, and two hidden layers which contained memory structures for giving the network memory of the input signals past. These memory structures provide the neural network a medium through which trends and patterns in input data can be identified. The utilization of a neural network model with this architecture may not be ideally suited for utilization in a real-time setting with a CGM device which samples interstitial glucose concentration every five minutes. These neural network models, depending on configuration, can have increased processing time (i.e. time needed to train and generate predictions). For this reason, a neural network model was developed with a reduced complexity feed forward architecture, which differed from the neural network models developed in section 3.2.3. The neural network models were converted to C++ source code, and a dynamic linked library (DLL) was

developed to implement the neural network model in a real-time setting in a graphical user interface (GUI) based C++ application. The next sections outline the neural network architecture implemented in the real-time application as well as the procedure taken to test the performance of the developed neural network model in a simulated real-time setting. In addition to this reduced complexity neural network model, a model implementing the time-lagged feed forward architecture outlined in section 3.2.3 is also developed, and integrated into the real-time predictive system and outlined in the following sections.

3.2.6 Feed Forward Neural Network Architecture Implemented in Real-time Predictive System

The neural network model generated for the real-time application was configured to implement a feed forward neural network model architecture. The neural network architecture included a three layer design which included a single input layer, a hidden layer for processing (implementing a hyperbolic tangent transfer function), and an output layer. Figure 3-3 is an illustration of the neural network model architecture and three layer design. Figure 3-3 also demonstrates the flow of the data through the neural network model. The complexity of this neural network architecture was implemented as it would be well suited for a real-time predictive application. The utilization of such a model architecture will decrease computation time (which would benefit in a real-time application), and allow time for pre and post-processing algorithms and other supporting algorithms for enhancement of model accuracy.

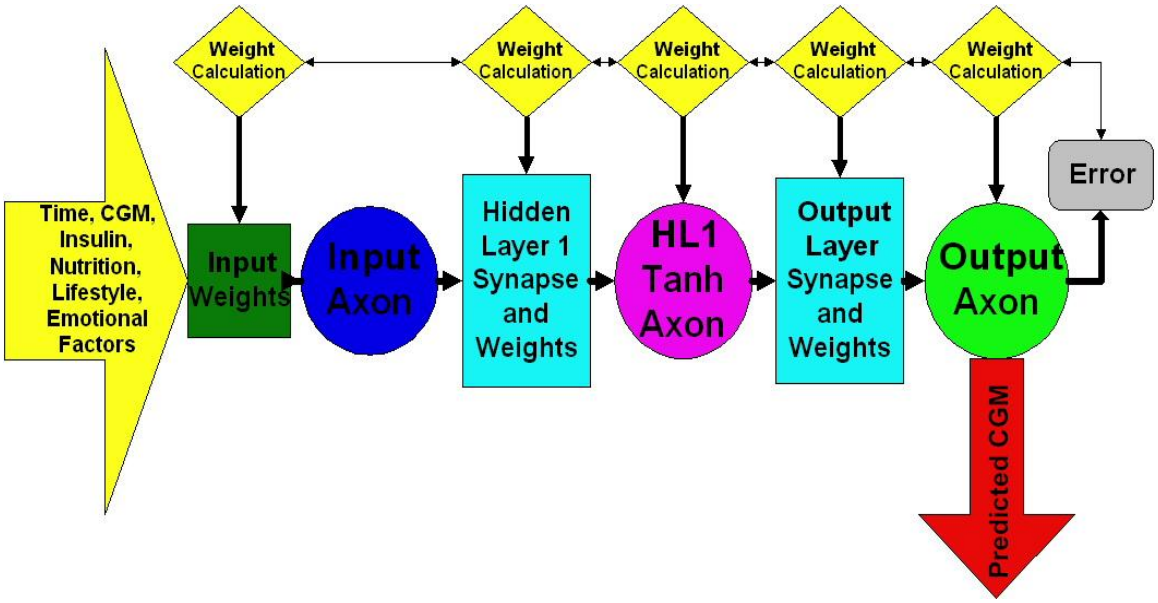

Figure 3-3. Real-time Predictive System Neural Network Architecture and Data Flow

The neural network model was developed using NeuroSolutions® software (Neurodimension, Gainesville, FL). The neural network model was configured to predict glucose using a prediction horizon of 75 minutes (i.e. 15 CGM values). The neural network model was trained via backpropagation of errors. As demonstrated in Figure 3-3, the error of the neural network predictions (i.e. mean squared error between actual and predicted CGM data) is backpropagated to previous layers of the neural network and optimum weights for minimization of error are calculated via a gradient descent with momentum algorithm. The neural network model was configured with a forward and backpropagation trajectory of a single input (i.e. exemplar). Additionally, the neural network model was configured to update weights after 200 exemplars and to terminate training after 1000 epochs (i.e. cycles through entire dataset), or if a mean squared error threshold of 0.01 is exceeded.

3.2.7 Integration of Neural Network Functionality into Real-time C++ Application

NeuroSolutions® software was utilized to generate a C++ source code representation of the developed neural network model. This C++ source code was limited in functionality and only worked for the initial training set used to generate the neural network model. For this reason, the source code was modified significantly and a DLL was generated which implemented functions to generate neural network model predictions in a real-time setting. The DLL was integrated into a graphical user interface (GUI) based program for real-time prediction of glucose, and the computer program was configured to formulate predictions within a five minute timeframe. This step was necessary for integration of this technology into a real-time system as most CGM technologies report glucose concentration every five minutes. The patient data used for testing the accuracy of the neural network model's predictions in a real-time setting included data from 10 patients not used in initial model development and training. These patients were derived from the private endocrine practice in Warren, OH and via the data collection procedures defined in section 3.2.2.

The neural network model accuracy was evaluated via two different methodologies. The first of these methods involved loading the model weights derived from model training using the initial 17 patient training set before each real-time prediction. A second method involved the utilization of the real-time application to update and adapt weights as new data is presented to the real-time system.

The application was designed to read from an input file which initially contained 800 inputs to the neural network. Of these 800 inputs, 799 contained historical CGM data. The final 800^{th} input represented the current real-time CGM value. Separately, a file

contained the desired predicted output of the neural network. This file consisted of 800 CGM values time shifted ahead to implement a prediction horizon of 75 minutes and was presented to the neural network for training and weight adaptation. The final 800^{th} value in the desired predicted output file was set to zero (i.e. unknown). The final 15 predicted values of the neural network output represent the neural networks prediction of glucose implementing the prediction horizon of 75 minutes. The application was configured to generate its predictions within 5 minutes (the sampling rate of the CGM device) such that upon reception of a new CGM value, another prediction may be generated. After each prediction, a new CGM value is appended to the end of the input data file, and the previous CGM value is added to the desired output file at the index before the current real-time data to maintain the prediction horizon and appropriate training/adaptation of the neural network. After a total of 100 predictions and file length of 900 is achieved, the application was configured to delete the first 100 inputs and predictions resume as outlined above.

The GUI of the computer program generated for this investigation is included in Figure 3-4. This GUI allows the user to select the prediction horizon, and displays the predictive results to the user.

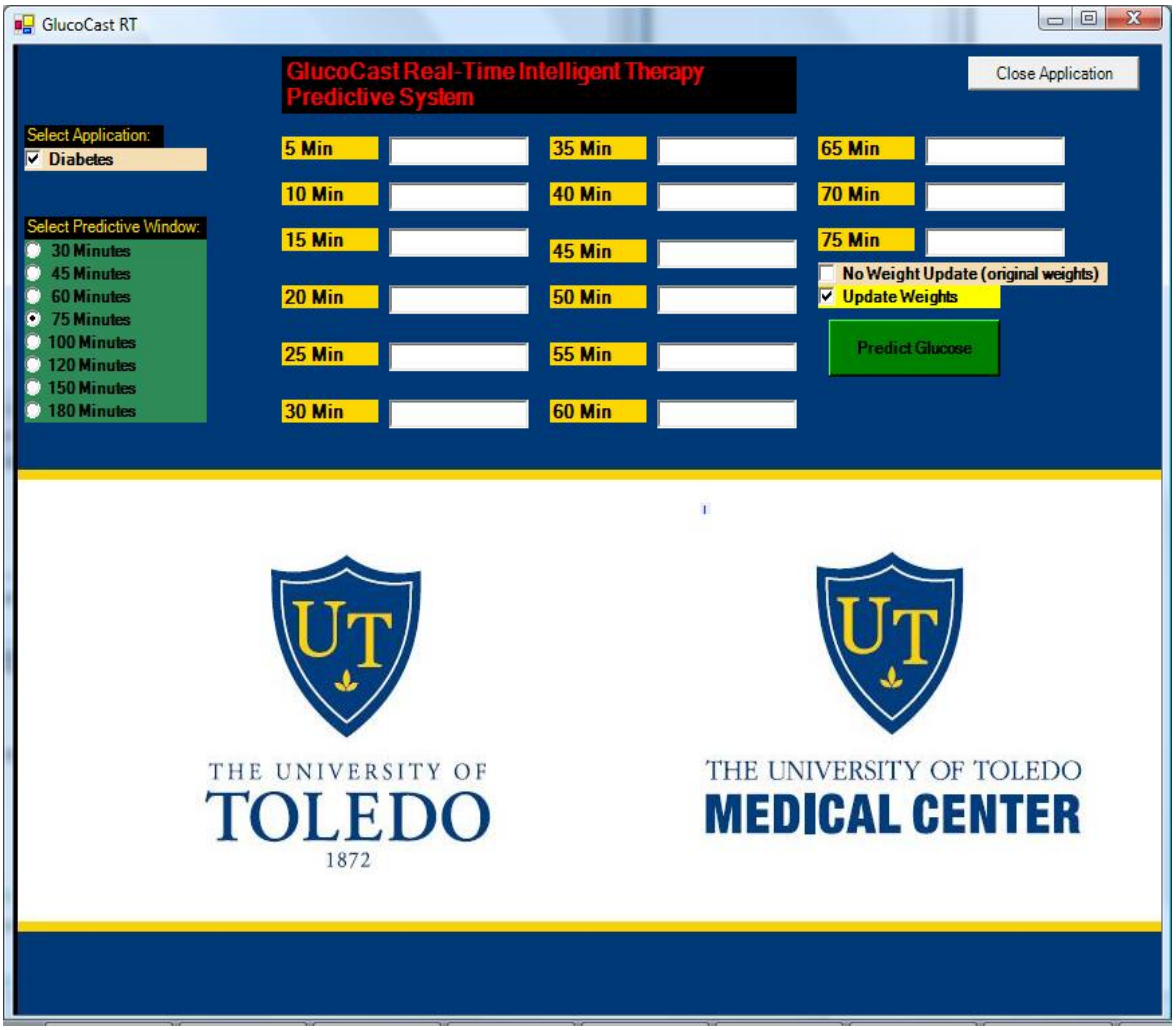

Figure 3-4. GUI of Real-Time System (GlucoCast RT) for Real-time Glycemic Forecasting

3.2.8 Enhanced Multifunctional Neural Network Model Architecture in Real-Time Application

A neural network model was designed implementing a model architecture similar to the initial neural network models developed in 3.2.3 and integrated into the real-time predictive application outlined in section 3.2.7. This neural network was designed to be a multifunctional neural network (MFNN) model which predicts glucose concentration

(CGM data) and glycemic states (i.e. glucose ranges based on numerical classification from 1-7). Glycemic states were defined as 1 (hypoglycemia [CGM≤70 mg/dl]), 2 (lower normal [CGM>70&CGM≤100 mg/dl]), 3(middle normal [CGM>100&CGM≤140 mg/dl]), 4(upper normal [CGM>140&CGM≤179 mg/dl]), 5(lower hyperglycemic [CGM>179&CGM≤220 mg/dl]), 6(middle hyperglycemic [CGM>220&CGM≤300 mg/dl]), 7 (upper hyperglycemic [CGM>300 mg/dl]).

The neural network models were designed with an input layer, 2 hidden processing layers, and an output layer. The input layer was designed with a memory component with 3 taps, and a tap delay line of 1 sample (i.e. delay of 2 samples between successive taps). The memory component thus provides memory of the current input as well as 2 historical inputs. The first hidden processing layer was designed with a hyperbolic tangent axon and a memory component with 8 taps and a tap delay line of 1 sample. This memory component provides memory of the current input, as well as 7 historical inputs. The second hidden processing layer was designed with a hyperbolic tangent axon and a memory component with 4 taps and a tap delay line of 1 sample. This memory component provides the memory of a current input and 3 historical inputs. The output layer of the neural network included a bias axon which adds an offset to the neural network data from the second hidden layer to generate the neural network model predicted output.

The real-time predictive application was generated via similar methodologies as outlined in section 3.2.7 In this implementation, the input file presented to the neural network model needs to be maintained at a constant file length. For this real-time implementation, the input file was maintained at a constant length of 800 values (799

historical and 1 real-time input data vector). Additional design modifications included the forward and back propagation trajectory of N samples (i.e. single exemplar). The forward trajectory is the number of input and desired values of which the neural network model looks ahead and calculates gradient information for modification of model weights. The back propagation trajectory is the calculated error between neural network output and desired response which is back-propagated to other neural network layers for weight adaptation. An additional design modification is the number of exemplars per weight update in the neural network model design.

3.2.9 Performance Analysis of Neural Network Models in Real-Time

The neural network models developed for prediction of glucose in the insulin dependent diabetic population were tested in a real-time setting. To test the performance of these real-time predictive models, Clarke Error Grid Analysis (CEGA) was implemented to determine the percentage of model predictions which can be deemed clinically acceptable. CEGA was utilized in this investigation to assess accuracy of predicted CGM values with respect to actual CGM values. CEGA was established in 1987 and was originally utilized to assess meter-based patient estimates of blood glucose compared to those obtained using a "gold-standard" reference glucose meter. [114] The accuracy of current CGM technologies is also assessed via utilization of CEGA to compare CGM performance to that of blood glucose meters. [81] Region A contains predicted values within 20% of the reference concentration and region B contains predictions outside 20%, however, would not lead to inappropriate treatment. Regions A and B therefore contain predicted values which can be classified as "clinically acceptable". Region C contains points which lead to unnecessary treatments, and region

D contains points indicating a potentially dangerous failure to detect hypoglycemia. Region E contains predicted values which would confuse treatment of hypoglycemia for hyperglycemia and vice-versa. A successful predictive model and system would thus need a majority of predicted CGM to fall within regions A and B in the Clarke Error Grid. Furthermore, a higher percentage of values falling within region A of the Clarke Error Grid is most desireable.

Additional performance analysis was completed via calculating the overall error of the neural network model predictions with respect to actual CGM values. Overall error was determined via calculation of mean absolute difference percent (MAD%) via equations 3 and 4 in 3.2.4. Error of CGM devices with respect to gold standard handheld blood glucose meters has been reported to be 14.0-21.0%. [115] A successful predictive model would therefore need predictive errors (MAD%) within this range. In addition to overall error, the percentage of hypoglycemic, hyperglycemic, and normal glucose extremes predicted was also calculated. For multifunctional neural network models, the percentage of general glycemic states (low (state 1), normal (states 2-4), and high (states 5-7)) was calculated. Additionally, the percentage of each specific glycemic state (1-7) predicted was calculated.

3.3 Neural Network Model Development for Critical Care Patient Population

The section will outline the procedures and methodologies implemented in the clinical study for prediction of glucose in critical care patients completed at the University of Toledo Medical Center (UTMC) in the surgical intensive care unit (SICU) and medical intensive care unit (MICU). This investigation was approved by the University of Toledo Biomedical Institutional Review Board (IRB) with approval

#106204. The approved IRB documents utilized for the patient consent process are included in the appendix of this dissertation (Appendix A.1).

3.3.1 Development of Electronic Clinical Intensive Data-Logger (eCIDL)

Currently, the medical records in the surgical and medical intensive care units (SICU and MICU) at the University of Toledo Medical Center (UTMC) are transcribed in paper format. The utilization of these medical records in a computer based mathematical model is therefore not possible in the current state. For this reason, a computer application was developed to facilitate documentation of the paper-based medical records into an electronic format. This electronic clinical intensive data-logger (eCIDL) was created as a GUI based C++ software application using Microsoft Visual Studio 2008 development environment.

The preliminary step in the development of the eCIDL was discussion with clinical investigators involved in the project to determine which medical records information needed to be logged using the developed eCIDL. A copy of the intensive care unit paper-based records were obtained, and these records were transcribed into the computer application. Discussion with clinical staff and the University of Toledo Department of Pharmacy generated a list of commonly utilized medications and labs in the critical care patient population. Following the derivation of specifications for eCIDL development from clinical staff, the eCIDL was developed and tested/validated for data entry. The main menu GUI of the developed eCIDL is presented in Figure 3-5.

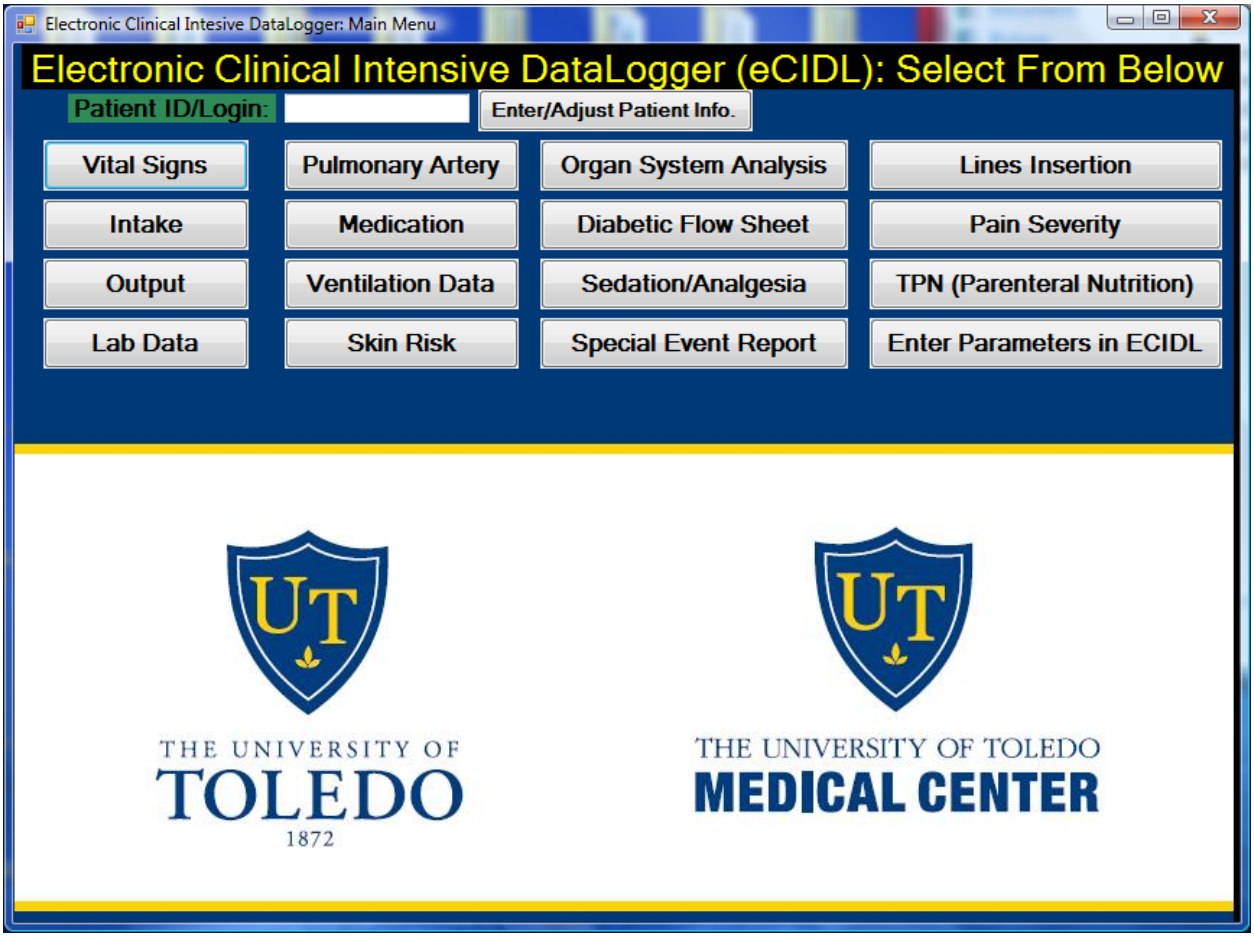

Figure 3-5. GUI of Developed Electronic Clinical Intensive Data-Logger (eCIDL)

The design of the eCIDL included a variety of text fields for documentation of numerical medical records. Non-numerical medical records were included in drop-down menus, and the inputs were logged based on the index of the selection from the drop-down menu. If the parameter was not logged (i.e. text field or drop down menu was blank), data was defined as 0 in the electronic medical record. The eCIDL was configured to log both a text based and numerical based (encoded for neural network model integration) rendition of the medical records. Each record logged using the eCIDL was time-stamped with the time and date of each entry so that data could be combined with CGM data acquired during a patient's intensive care unit stay. The numerical (i.e. neural

network) time was converted to a decimal value between 0 and 24 to document data on a 24 hour scale.

In the event that multiple medical records (e.g. medication, labs, and clinical events) were logged at the same time, the eCIDL was configured to encode the data based on the category, type, and number of the specific events (i.e. medication, lab results, or clinical events) logged at a single time stamp.

For example, if multiple medications were entered into the system at a single instance in time, Equations 5 and 6 are utilized to numerically encode the multiple medications. Equation 5 is a weighted ratio Wt_{med} , to scale individual medication dosages based on the binary encoding of medication category and medication type (i.e. specific medication) used. Binary encoding of medication category ($Med_{category}$) and medication type (Med_{type}) is completed via calculating 2 raised to the drop-down menu index+1 of each medication category and type as demonstrated in Equation 5. Equation 6 is the encoded dosage (Med_{dose}) of the medication such that for multiple medications, the neural network model input is unique. Multiple medication categories and types were encoded at a single time stamp via summing the values of the binary encoded categories types, and dosages logged using the eCIDL. If the medication logged is infused via a specific dose/hr, the infusion rate (dose/hr) is weighted via the same methodology as the medication dosage. NOTE: The same method of encoding was utilized for laboratory results logged using the eCIDL. Instead of dose, the lab result was weighted based on the lab category and type selected.

$$Wt_{med} = \frac{2^{Med_{category}}}{2^{Med_{type}}} \qquad \text{[Equation 5]}$$

$$Med_{dose} = Wt_{med} \cdot Med_{dose} \qquad \text{[Equation 6]}$$

3.3.2 Optimal Input/Training Set Selection for Neural Network Using a Genetic Algorithm

Utilization of the eCIDL resulted in the collection of 131 different medical records and potential inputs to the neural network model for prediction of glucose. A total of 15 categories of medical records were logged using the developed eCIDL. The categories and number of medical records logged within each category are included in Table 3-1. Although there are a large number of medical records logged using the developed eCIDL, many of these records would not have an impact or be an indicator of glucose concentration in the critical care patient population. Furthermore, throughout the course of the investigation it was determined that a significant number of the medical records were not routinely logged by clinical staff throughout the course of the clinical investigation. Genetic algorithms were implemented to determine which variables logged during utilization of the eCIDL should be included in the neural network model training and input dataset. Genetic algorithms were implemented using Eigenvector Research® Solo-MIA© with PLS Toolbox 4.0 software.

Table 3-1. Medical Record Categories Logged Using eCIDL

Medical Record Category	# of Medical Records
Vital Signs	8
Intake	14
Output	7
Lab Results	4
Pulmonary Artery Data	12
Medications	8
Ventilation Data	14
Skin Risk	8
Organ Systems Analysis	8
Diabetic Flowsheet	5
Sedation Analgesia	10
Clinical (Special) Events	4
Lines Insertion	3
Pain Assessment	2
Total Parenteral Nutrition	24

The theory behind utilization of a genetic algorithm is that given an x-block of predictor data and y-block of data to be predicted, the variables from the x-block which can be used for prediction of the y-block can be determined. This is accomplished through cross-validation and regression to determine the root mean squared error of cross validation (RMSECV) obtained when a subset of variables from the x-block are utilized for prediction. This process is iterated to determine which variables from the x-block produce the lowest RMSECV. For this investigation, the x-block included medical records from the developed eCIDL, CGM device sensor current, and CGM values categorized as glycemic states. The y-block was defined as CGM glucose concentration values measured every five minutes.

Two renditions of genetic algorithms were utilized. The first rendition of genetic algorithm implemented a multiple linear regression based genetic algorithm. In this

genetic algorithm, the actual variable values were utilized. The second rendition of genetic algorithm was a partial least squared regression based algorithm. In this algorithm latent variables (i.e. not direct variable values but values derived via mathematical modeling) were utilized. This rendition of genetic algorithm was configured with 10 latent variables.

Both genetic algorithms were configured with a window width (i.e. number of adjacent variables to be grouped together at a time) of 1. In these algorithms, a population size (i.e. random selection of variables from x-block) of 64 was implemented. The algorithms were configured to initially have 30% of the variables in the initial variable subsets. Each of the populations (i.e. subsets of variables) has an associated RMSECV. After allocation of variable subsets, the genetic algorithm determines the fitness (error) of each of the variable subsets for prediction of the y-block. After determination of fitness, each of the variables was "bred" using single crossover. During this crossover, the variables from 2 random variable subsets were split at into two random subsets and combined with the other random variable subset from which the variables were not initially included. Following crossover, the variables are given a chance for random mutation. Mutation allows for a finite chance of adding or removing variables which may be over or under represented in the x-block. A mutation rate of 0.05 was chosen such that mutation did not occur frequently. The genetic algorithms were configured to terminate after a maximum of 100 generations and a percent convergence of 50%.

3.3.3 Data Acquisition for Neural Network Model Development

Critical care (trauma or cardiothoracic surgical) patients admitted to the University of Toledo Medical Center: ≥18 years of age, and elevated glucose ≥150 mg/dl (upon admission to the intensive care unit or upon arrival at UTMC) were approached for consent by clinical staff. The only exclusion criterion was defined as pregnancy.

After patient consent was obtained, a CGM device (Medtronic Diabetes CGMS Ipro®, Northridge, CA) was placed on the patient. All clinical personnel involved in the investigation were trained on insertion, setup, removal, downloading, and maintenance of the subcutaneous glucose sensors, and CGM device. CGM sensors were changed every three days in accordance with FDA and device manufacturer recommendations for optimum accuracy. Routine care utilizing the established University of Toledo Medical Center insulin infusion protocol was maintained throughout the patient's length of stay in the intensive care unit. Furthermore, routine documentation of medical records was maintained. When the patient was discharged from the intensive care unit, the CGM device and sensor was removed from the patient and the patient was removed from the investigation. **NOTE:** CGM values and model predictions generated throughout the course of the investigation were not utilized by clinical staff and no modifications to conventional care established at the University of Toledo Medical Center occurred.

Various study personnel were trained and provided with an instructional manual on the successful operation and utilization of the eCIDL (developed in 3.3.1) for conversion of paper-based medical records into an electronic format. Additionally, study personnel were trained to combine CGM and electronic medical records into data files to be used for subsequent neural network model development and testing.

Before initiation of the clinical study, it was estimated that a total of 40-45 trauma patients at a rate of 2 patients every 2-3 weeks would be enrolled in the investigation. During the investigative timeframe, patient enrollment was drastically decreased from initial expectations. Due to decreased enrollment, the IRB protocol was amended to include cardiothoracic surgical patients to increase patient enrollment. Various factors have lead to a reduced patient enrollment in the clinical investigation. One such factor was that trauma incidences were drastically decreased over the last year. This is hypothesized to be due to the current ongoing economic crisis and increased fuel cost. A large proportion of trauma incidences at the University of Toledo Medical Center (UTMC) are automobile and motorcycle accidents which may be decreased due to the current state of the economy. Another factor due to the decreased patient enrollment is the limited surgical/critical care staff at UTMC. Decreased clinical staff made enrollment and consenting of patients for the investigation more difficult. Key members of the cardiothoracic surgical staff at the UTMC also departed from the institution, which can also be directly attributed to the decreased patient enrollment.

The data acquisition process outlined in the section was continued until March 2010, at which time final renditions of the neural network models were developed and tested using all available patient data collected in the clinical investigation.

3.3.4 Neural Network Model Development for Prediction of Glucose in Critical Care Patients

Following determination of the optimal variables/predictors for use in the neural network model design by the genetic algorithms implemented in 3.3.2, neural network models were developed for forecasting glucose concentration in the critical care patient population. Initially, a training set comprised of 14 critical care patients consisting of 19,989 data points (CGM data and medical records information obtained from utilization of the developed eCIDL) was utilized for model development and training. The neural network model architecture implemented for prediction of glucose in this patient base was a feed forward neural network model architecture similar to the neural network models developed in 3.2.6 for real-time prediction of glucose in patients with insulin dependent diabetes. The implementation of this neural network architecture enables the prediction of glucose in real-time within the time constraints of the sampling rate of the CGM device (CGMS Ipro®, Medtronic Diabetes©, Northridge,CA). The neural network model inputs and training set were determined from genetic algorithm application (outlined in 3.3.2) and inputs/predictors used in the model training set are included in table 3-2. Neural network model architecture and design is included in Figure 3-6.

Table 3-2. Final Inputs for Neural Network Model based on Genetic Algorithm for Variable Selection

Variable Number	Variable
1	Time
2	Temperature
3	Heart Rate
4	Respiratory Rate

5	Blood/Colloids (Intake)
6	Packed Red Blood Cells (Intake)
7	5% Albumin
8	D5W
9	D5NS
10	NS
11	D5LR
12	Time Period Collected
13	NG (Resid)
14	Lab Category
15	Lab Type
16	Lab Results
17	Num Labs
18	PCWP
19	SVO2
20	SPO2
21	Medication Category
22	Medication Class
23	Medication Type
24	Medication Dose
25	Number of Medications
26	PAO2
27	pH
28	PACO2
29	Conciousness
30	Activity
31	Nutrition
32	Gen. Phys Cond
33	POC Test Time
34	POC Blood Glucose
35	Insulin Dosage
36	Insulin Delivery Type
37	Pain Level
38	CGM Value
39	CGM Sensor Current
40	Glycemic State

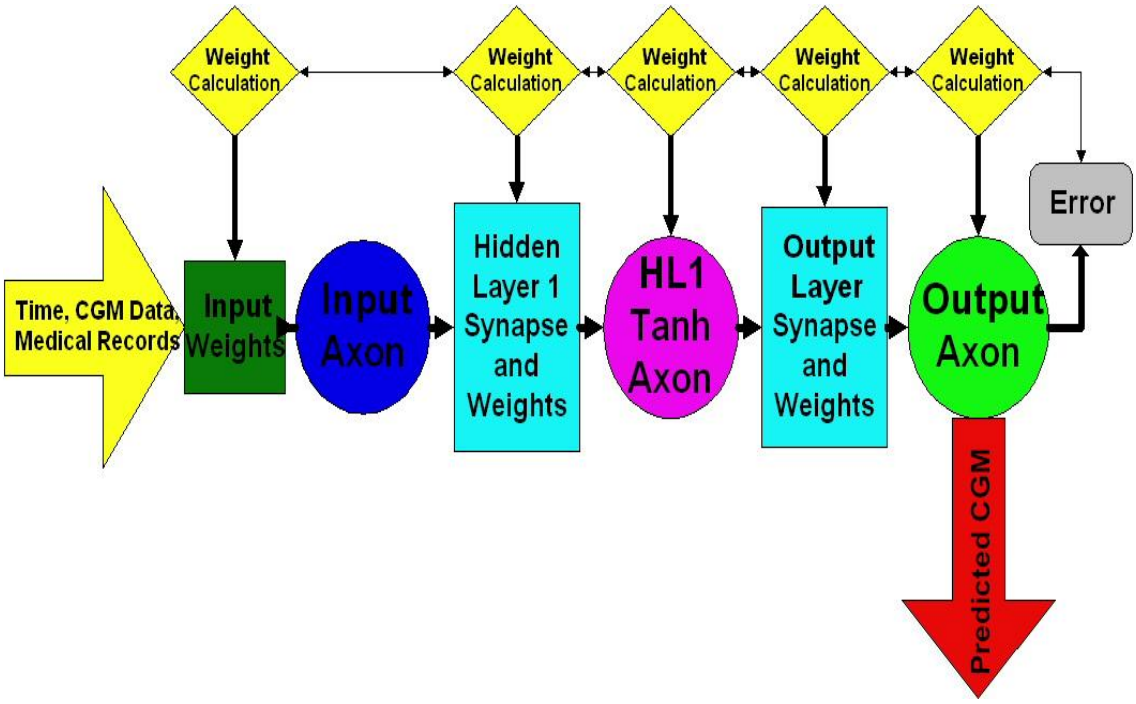

Figure 3-6. Feed Forward Neural Network Model Design and Architecture for Prediction of Glucose in Critical Care Patient Population

Neural network models were trained via the backpropagation training algorithm previously outlined in neural network model development for patients with diabetes (section 3.2.3). The neural networks were configured to terminate training if the mean squared error exceeded the threshold of 0.01 or after 1000 epochs (i.e. cycles through the dataset). Neural network models were configured as multifunctional neural network models to predict actual glucose concentration values and classified ranges of glycemic states (same ranges as outlined in section 3.2.8). Neural network models were initially configured to predict glucose using a prediction horizon of 75 minutes.

A prediction horizon of 75 minutes is the maximum prediction horizon chosen for implementation in this patient population. This maximum prediction horizon was determined via determining the amount of hyperglycemic and hypoglycemic excursions

detected by POC glucose monitoring implemented at UTMC. Determination of the percentage of hyperglycemic and hypoglycemic excursions detected via POC glucose monitoring was determined for the initial 19,989 data points used for initial model training and development. Table 3-3 demonstrates the percentage of hyperglycemic and hypoglycemic glucose extremes detected via conventional POC monitoring within a predefined time window. NOTE: A time window of 60 minutes is defined as 30 minutes before and 30 minutes after the detected event. Table 3-3 demonstrates that the prediction horizon of 75 minutes implemented in the models developed in this investigation is near ideal for this patient population and will provide insight where POC glucose values are not obtained. In addition to the 75 minute prediction horizon (which is the main prediction horizon implemented in this investigation), neural network models implementing prediction horizons of 30, and 60 minutes were also investigated. Models with reduced prediction horizons are hypothesized to have increased accuracy with respect to the models implementing larger prediction horizons, but will also be useful for intelligent therapeutic direction and clinical decision support

Table 3-3. Percentage of Hyperglycemia and Hypoglycemia detected Via POC Monitoring

	% Detected 40 Minutes	**% Detected 60 Minutes**	**%Detected 80 Minutes**
Hyperglycemia	44.2	64.1	83.9
Hypoglycemia	31.7	44.8	58.4

To assess the performance of neural network models implementing different prediction horizons, feed forward neural network models were developed and trained via the initial training set of 19,989 data points. These neural network models were developed via the aforementioned methodologies and configured for prediction of glucose using prediction horizons of 30, 60, and 75 minutes. Data from three patients not utilized for initial model development and training were utilized to test the performance of the models implementing 30, 60, and 75 minute prediction horizons. Performance analysis of the models was completed in MATLAB® and Clarke Error Grid Analysis (CEGA) was utilized to determine clinical acceptability of the predictions. In addition to CEGA, overall model error (MAD%) and the percentage of hypoglycemic, hyperglycemic, and normal glycemic extremes predicted was calculated.

3.3.5 Development of a Patient Specific Neural Network Model

Neural network models developed in this investigation have been general neural network models trained with data from multiple patients. In this investigation, a feed forward neural network model implementing the architecture/design outlined in 3.3.4 was trained using data from a single patient resulting in a patient specific neural network model.

A single trauma patient (38 year old, MVA (motor vehicle accident) victim, intubated, with multiple blunt force injuries) who met the aforementioned criteria, was admitted to the UTMC SICU. The patient was subjected to continuous glucose monitoring (CGM) (Medtronic Diabetes, CGMS Ipro®), and routine documentation of medical records throughout their length of stay in the ICU. The patient had an extended

length of stay in the ICU of 16 days. A patient specific feed forward neural network model was developed/trained using 243.6 hours (2,923 data points) of CGM and concurrent medical records data for prediction of glucose implementing a prediction horizon of 75 minutes. The neural network model was developed and trained using the same architecture included in Figure 3-6 and the model configuration as discussed in section 3.3.4. Model performance was compared with the performance of a general neural network model (trained with data from 5 critical care patients) on a segment of data from the patient utilized for patient specific model development not included in either model training set. The inputs to the patient specific and general neural network models were configured as time, CGM data, and data collected from the diabetic flow sheet maintained in the UTMC SICU. The diabetic flow sheet contained POC glucose values and test time, units of insulin delivered, and insulin delivery type (subcutaneous sliding scale or IV insulin infusion).

3.3.6 Development of a Multifunctional Complex (Time-Lagged Feed Forward) Neural Network Model

In addition to the reduced complexity feed forward neural network models generated in this investigation for prediction of glucose in critical care patients, a multifunctional complex time lagged feed forward (TLFF) neural network model was also generated. This model was designed using NeuroSolutions® software (Neurodimension©, Gainesville,FL) such that predictive performance could be compared with that of the feed forward neural network model generated in 3.3.4.

The complex TLFF neural network model was designed with the similar architecture implemented in the diabetes investigation in section 3.2.3 and included in

Figure 3-2. The major differences between complex TLFF and reduced complexity feed forward (FF) neural network architectures is that TLFF models have Laguarre Axons which contain memory structures to store historical values of neural network inputs. These memory structures give the system memory thus enabling the processing of information in time. Further differences in model architecture include the existence of two hidden processing layers equipped with memory components (Laguarre Axons) in the TLFF neural network model architecture. These hidden processing layers serve to limit the range of neural network input values within the hidden layer to a defined range which enables the neural network to process and interpret patterns in data more efficiently. A final difference existent between the TLFF neural network and FF neural network is the forward and backpropagation trajectories implemented in both approaches. The forward trajectory is the number of input and desired values of which the neural network model looks ahead and calculates gradient information for modification of model weights. The back propagation trajectory is the calculated error between neural network output and desired response which is backpropagated to other neural network layers for weight adaptation. In the FF neural network model, a forward and backpropagation trajectory of a single sample is implemented. Conversely, in the TLFF model architecture is configured to implement variable forward and back propagation trajectories and the number of exemplars (i.e. a single pass through forward and back propagation trajectory) experienced before the neural network model updates model weights. The existence of memory structures in the TLFF architecture make implementation of these variable trajectories more effective than the alternative FF model architecture.

The FF model architecture was the same architecture as implemented in section 3.3.4. The TLFF neural network model architecture was designed with an input layer containing a Laguarre Axon (memory component) containing two taps which function to store one historical and the current neural network input value. The TLFF model was also generated with two hidden layers each with an axon (with an associated Laguarre Axon) which were configured to implement a hyperbolic tangent transfer function, which served to limit input values within each layer to a range of -1 and 1. The first hidden layer was configured with a Laguarre Axon configured with five taps which stored memory of 4 historical and one current input values. A second hidden layer was configured with a Laguarre Axon configured with 2 taps which stored the memory of a single historical and current input value. Both neural network models were trained via the backpropagation of errors training algorithm as previously outlined in this document.

The TLFF and FF neural network models were developed/trained using the genetic algorithm optimized initial 14 patient comprehensive training set consisting of 19,989 input data vectors. The TLFF model was configured with variable forward and back propagation trajectories and tested on two patients not included in the original model training set. The FF neural network model was tested on the same 2 patient dataset. Variable trajectories implemented in the TLFF models included a forward trajectory of 5 and a back propagation trajectory of 2 and updating model weights after 10 exemplars (5-2-10), a forward trajectory of 5 and a back propagation trajectory of 2 and updating model weights after 100 exemplars (5-2-100), and a forward trajectory of 10 and a back propagation trajectory of 5 and updating weights after 100 exemplars (10-5-100). These trajectories were chosen based on initial design and testing of complex TLFF neural

network model architectures developed for prediction of glucose in insulin dependent diabetic patients as previously outlined in this document.

Performance of these multifunctional neural network model variations was measured via calculating overall model error (MAD%) between actual and predicted CGM data, percentage of hypoglycemic, hyperglycemic, and normal glucoses values predicted, percentage of general and specific glycemic states predicted, as well as clinical acceptability of model predictions determined via Clarke Error Grid Analysis (CEGA). Performance measures of the FF and TLFF model architectures are compared in this dissertation.

3.3.7 Real-Time Prediction of Glucose in the Critical Care Patient Population

Neural network models generated in this investigation were configured for real-time prediction of glucose and implemented in the C++ computer application included in Figure 3-4 of section 3.2.7. The neural network models were configured for real-time training and adaptation of model weights for generation of glycemic predictions. The neural network model functionality was integrated into a GUI-based C++ program via dynamic linked library (DLL) generation as previously discussed (3.2.7). A selected portion of the C++ source code implemented in the DLL for neural network implementation is included in Appendix B.1 of this dissertation. The C++ source code implemented in the previous diabetes application was enhanced in regards to how data was presented to the neural network for model training and subsequent prediction in real-time. In the previous rendition, unknown desired responses (future glycemic responses across model prediction horizon) were set to 0.

In the newly developed rendition of the real-time predictive application, the file

length (at each predictive iteration of the real-time predictive application) presented for training and prediction was kept constant and included 800 vectors of data points which consisted of the 40 optimal input/predictors determined from genetic algorithm implementation. Of these 800 vector values, 799 of these included an input and predicted (desired) response (i.e. glucose value ahead given prediction horizon). At the first iteration of the predictive application, the desired response of the final (800^{th}) vector of data points is set to the current real-time glucose value because no method of determining trend information in real-time glucose exists. After the first iteration of the real-time predictive application, the rate of change between the previous glucose value and the real-time glucose value is obtained, and the desired response (based on the prediction horizon implemented) is estimated based on the observe trends and rate of change in real-time glucose. The formula for estimation of the predicted (desired) response of glucose is included in Equation 7. In Equation 7, $Pr_{response}$ is the estimated predicted response, $Glucose_{RT}$ is the current real-time glucose value, $Glucose_{prev}$ is the previous glucose value, and $samp_{rate}$ is the sampling rate of the CGM device (5 minutes for the device implemented in this investigation). After this estimation is obtained, the predicted glucose is converted to the corresponding classified concentration range or glycemic state to facilitate the multifunctional neural network design and training process. After a total of N iterations of the predictive system (where N equals the samples in the prediction horizon) are completed, the current real-time glucose and glycemic state is appended to the desired file (containing desired response for real-time model training) at the index of the input/desired file length subtracted from the quantity (N-1). After each iteration of the predictive application, the first vector of data points in the input and desired files used for

real-time model training and prediction was removed and the next real-time vector of data points is appended at the end of each file.

$$\mathrm{Pr}_{response} = Glu\cos e_{RT} + \frac{Glu\cos e_{RT} - Glu\cos e_{prev}}{samp_{rate}} \qquad \text{[Equation 7]}$$

The neural network models were configured to update using a forward and backward trajectory of 1 sample. Furthermore, analysis of real-time predictions revealed that real-time training and updating model weights after a single exemplar (each forward and backward trajectory) led to increased predictive accuracy and the ability of the neural network model to predict trends in glucose. This is due to the fact that the real-time rate of change in glucose can be identified and incorporated into model predictions. Models were run for a total of 1000 epochs and configured to terminate training if a mean squared error (MSE) threshold of 0.01 was exceeded. Furthermore, if accuracy in neural network model did not improve after 100 epochs the neural network training and subsequent prediction process was terminated. This real-time application was configured to implement a prediction horizon of 75 minutes.

3.3.8 Performance Analysis of Neural Network Models for Critical Care Patients in Real-Time

The neural network models developed for prediction of glucose in the critical care patient population were tested in a real-time setting. Model performance analysis was completed via the same methodologies outlined for the insulin dependent diabetes patient population (3.2.9). Each patient enrolled in the investigation following the initial 14 patients (19,989 data points) used for comprehensive model training was utilized for model performance analysis. The utilization of this data provides a means of assessing

model accuracy in unseen patient data (data not used for model training), and provides a means of assessing performance of the models in a real-life hospital and patient setting. After performance analysis on an unseen patient record, the data from this patient is appended to the end of the comprehensive model training set, and the performance analysis process is completed on a new unseen patient record. This performance analysis was completed on data from 5 unseen critical care patients.

To test the performance of these real-time predictive models, Clarke Error Grid Analysis (CEGA) was implemented to determine the percentage of model predictions which can be deemed clinically acceptable. [114] A successful predictive model and system needs a majority of predicted CGM values to fall with regions A and B in the Clarke Error Grid. Furthermore, a higher percentage of values falling within region A of the Clarke Error Grid is most desireable.

Additional performance analysis was completed via calculating the overall error of the neural network model predictions with respect to actual CGM values. Overall error was determined via calculation of mean absolute difference percent (MAD%) via equations 3 and 4 in 3.2.4. Error of CGM devices with respect to gold standard handheld blood glucose meters has been reported to range between 14.0-21.0%. [115] A successful predictive model would therefore need predictive errors (MAD%) within this range. In addition to overall error, the percentage of hypoglycemic, hyperglycemic, and normal glucose extremes predicted was also calculated. For multifunctional neural network models, the percentage of general glycemic states (low (state 1), normal (states 2-4), and high (states 5-7)) was calculated in addition to the percentage of each specific glycemic state predicted.

In addition to the performance analysis of the real-time predictive application used for real-time model training and weight adaptation, utilization of the real-time predictive system for prediction of glucose implementing original model weights derived via comprehensive model training was completed. This performance analysis is also completed on the five patients not utilized for initial model training and development. The performance of the real-time models utilizing real-time training/weight adaptation (weight update method) and original model weights is compared.

3.3.9 Preliminary Weight Analysis: Neural Network Models for Critical Care Patient Population

MATLAB® source code was generated for preliminary weight analysis of the model weights which were updated in the real-time application as outlined in section 3.3.7. The real-time predictive application (outlined in 3.3.7) was configured to acquire neural network model weights in each layer of the neural network model design. Source code was generated such that the weights were acquired and logged into spreadsheets for subsequent analysis. Neural network model weights were acquired after every 800 exemplars during each iteration of the real-time predictive application. After model weights were acquired, the weight values were imported into MATLAB® for subsequent weight analysis.

Analysis of the weights in the output bias axon of the output layer was the focus of this preliminary weight analysis. The output bias axon weights consist of two weight values which serve as offsets which are added to the neural network data after the output layer synapse weights are applied to neural network data output from the hidden layer of

the neural network. The output bias axon weights derive the two outputs of the neural network which consist of predicted CGM value and predicted classified glycemic state. The analysis outlined in this section will provide a means of correlating real-time input/training data in the neural network with model predictive performance and accuracy. The focus of this preliminary weight analysis will be on the first output bias axon weight value.

The MATLAB® source code was configured to simulate the prediction (implementing a prediction horizon of 75 minutes) of the neural network model utilizing the weights which were acquired via the implementation of the real-time application in 3.3.7. After every 800 exemplars (single pass/epoch) through the test dataset, neural network predictions were generated via the MATLAB source code and the overall model error (MAD%), short term error (MAD% between first five predicted values and first five glucose values in the actual glycemic response), midterm error (MAD% between second five predicted values and second five glucose values in the actual glycemic response), and long term error (MAD% between last five predicted values and last five glucose values in the actual glycemic response) were calculated. These calculated errors and associated output bias axon weight values were categorized based on historical and real-time input data presented to the neural network model. Categorization was based on real-time CGM values (final 800^{th} value) in the test dataset. These CGM values were sorted based on glycemic threshold as well as whether insulin was delivered within 15 historical input values (model prediction horizon) preceding the current real-time CGM value. Glycemic thresholds were defined according to Table 3-4 below. Further categorization based on the occurrence of tachycardia (defined as heart rate $\geq$90 beats per minute) in

real-time or within 15 historical input values (model prediction horizon) preceding the current real-time CGM value was also completed.

Weight analysis was completed using the data and weights acquired from the real-time prediction of glucose in the 5 critical care patients outlined in section 3.3.7. Results of this weight analysis were combined based on the categorization defined previously and correlation analysis was completed. Pearson correlation coefficient values were acquired between model weights and error for each category (CGM glycemic threshold with historical insulin, CGM glycemic threshold without historical insulin, and tachycardia). This correlation analysis will indicate how real-time data and output axon weight values for each of the categories are correlated with model performance. This correlation analysis was performed on an individual patient basis as well as on all model weights obtain across the complete five critical care patient dataset.

Table 3-4. Glycemic Thresholds Implemented in Preliminary Weight Analysis

CGM Glycemic Threshold	Minimum CGM Value	Maximum CGM Value
1	40	70
2	71	149
3	150	190
4	190	240
5	241	400

3.3.10 Development of Preliminary Post-Processing Algorithms to Enhance Model Accuracy

This section will outline the procedures utilized for development of a post-processing algorithm for enhancing the performance of the real-time neural network models developed and tested in sections 3.3.7 and 3.3.8. The post-processing algorithm generated in this investigation takes into account two factors to be utilized for modifying neural network model predicted output to enhance model accuracy. The first factor taken into account in the post-processing algorithm design is the rate of change of the neural network predicted output as well as the offset existent between current real-time glucose and first predicted value in the output predicted vector of the neural network. Model predictions generated by the neural network model track the rate of change in glucose concentration accurately, however, at times this offset value is large and it is hypothesized that model predictions can be significantly improved if this calculated offset is applied to the initial predicted value in the neural network output predicted vector while maintaining the overall rate of change in the predicted output. The rate of change in predicted output is also adjusted via weighting the rate of change based on the glycemic threshold of the real-time glucose values. Given the threshold of this real-time glucose value the physiologic rate of change in glucose varies with time. For example, if real-time glucose is hyperglycemic, the value can decrease or increase at high rates across the model prediction horizon. On the contrary, if a hypoglycemic or near hypoglycemic glucose concentration is experienced, overall rate of change in glucose values will tend to be less then when potential for glycemic changes is greater at hyperglycemic extremes. To accommodate for this observed phenomena, the post-processing algorithm was

configured to weight rate of change values in the neural network predicted value based on the threshold of the current real-time glucose value. Ranges of glucose were defined and a percentage of the rate of change of the predicted output is utilized in the post-processing algorithm. Equation 8 includes the equation utilized to implement this post-processing algorithm to determine the post-processed predicted CGM value $PP_{CGM}(j)$ at the jth index of the neural network model predicted output. At initiation of the post-processing algorithm the first value in the post-processed predicted output applies the offset or difference between the current real-time CGM value and first predicted value in neural network output. $ROC_{\Pr}(j)$ is the rate of change at the jth index of the predicted neural network output. $Samp_{rate}$ is the sampling rate of the CGM device (for this investigation $Samp_{rate}$ is 5 minutes). W_i is the weight value of the rate of change given current real-time glycemic threshold. Table 3-5 includes the defined glycemic threshold ranges and the weight values (W_i) utilized to adjust rate of change in the post-processing algorithm.

$$PP_{CGM}(j) = CGM_{off}(j-1) + Samp_{rate} * W_i * ROC_{\Pr}(j) \qquad \text{[Equation 8]}$$

Table 3-5. Rate of Change/Offset Based Post-Processing Algorithm Weights and Associated Glycemic Thresholds

Glycemic Threshold	Min CGM Value in Threshold (mg/dl)	Max CGM Value in Threshold (mg/dl)	W_i
1	40	70	0.2
2	71	100	0.3
3	101	140	0.5
4	141	180	0.7
5	181	400	0.9

A second factor utilized in the developed post-processing algorithm will be the real-time data input to the neural network model. The effect of various factors recorded in the medical records and included in the neural network input structure can be correlated to subsequent glycemic responses. To determine an overall "trend" in future glycemic excursions based on the occurrence of these factors, the comprehensive model training set was analyzed and glycemic responses following the occurrence of these events/factors/states was determined. In the developed preliminary post-processing algorithm, factors to be correlated to future glycemic trends include: body temperature, respiratory rate, heart rate, and insulin dosages. These factors were chosen as they were recorded intensively (every hour) during the course of each patient's stay in the intensive care unit. Furthermore, classification of various states of these factors such as tachycardia (elevated heart rate) for example, can be made and interpreted for its effect on future glucose concentration. Analysis of the comprehensive model training set based on

different extremes of these factors were determined via grouping glycemic responses based on categorized values of these input factors/events (e.g. tachycardia, hypothermia, etc). Glycemic responses after each categorized input event/factor were grouped for the 75 minute prediction horizon (15 CGM samples) following the categorized input event/factor such that deduction of trends in glycemic excursions could be identified, modeled, and integrated into the post-processing algorithm. Given occurrence of these factors in real-time, when neural network model predictions differ from expected trends, the model predicted output will be modified to enhance model accuracy.

Analysis of respiratory rates, and temperature in the initial model training did not identify patterns in glycemic responses. Many of the patients in the investigation were on ventilators during their stay in SICU and MICU therefore respiratory rates documented in the medical records were artificially controlled and maintained within a physiologic range. For this reason it would be difficult to correlate changes in respiratory rate with subsequent glycemic responses. Body temperature can be correlated as an indicator/predictor of glucose, however, temperature changes do not occur rapidly, and subsequent changes in glucose concentration as a result of temperature changes do not occur or are not quantifiable within the defined 75 minute prediction horizon.

Analysis of heart rate specifically the occurrence of tachycardia resulted in patterns which when grouped with historical insulin delivery (insulin delivery occurring 75 minutes before the occurrence of tachycardia) could be successfully modeled. Glycemic responses after tachycardia were grouped based on whether glucose increased and decreased and whether any historical insulin was delivered. These responses were further classified based on the defining various ranges/degrees of tachycardia and the

glycemic threshold/extreme of the real-time glucose value at the instance of tachycardia. Tachycardia extremes are defined in Table 3-6. Conversely, glycemic thresholds are defined in Table 3-7.

Table 3-6. Tachycardic Extremes Utilized in Post Processing Algorithm Development

Tachycardic Extreme	Minimum Heart Rate (bpm)	Maximum Heart Rate (bpm)
Near Tachycardia	90	99
Onset Tachycardia	100	110
Moderate Tachycardia	110	119
Severe Tachycardia	120	All heart rates >120

Table 3-7. Glycemic Extremes Utilized in Post Processing Algorithm Development

Glycemic Extreme	Minimum Glucose Value (mg/dl)	Maximum Glucose Value (mg/dl)
Hypoglycemic	40	70
Normal	71	149
Hyperglycemic Extreme 1	150	190
Hyperglycemic Extreme 2	191	240
Hyperglycemic Extreme 3	241	300

After grouping glycemic responses 75 minutes after instances of tachycardia based on glycemic thresholds of real-time glucose and historical insulin delivery as outlined previously and in Tables 3-6 and 3-7, MATLAB® was used for fitting these

grouped glycemic responses to a third order polynomial functions in the form of $y = a_1x^3 + a_2x^2 + a_3x + a_4$. The MATLAB® function polyfit was used to obtain the best fit of a third order polynomial function while using the x data as time (up to 75 minutes following tachycardia) and the y data as interstitial glucose concentration (over this 75 minute time period) obtained via CGM. The model fits of the glycemic responses after tachycardia were utilized for final post-processing model generation if the correlation coefficient of the model fit was $\geq$ 0.85. For each of the grouped glycemic responses, average coefficients of the best model fits were obtained and implemented in the final post-processing algorithm.

Source code was generated in MATLAB® for this event-based post-processing algorithm implementation. This MATLAB source code is also included in Appendix B.2 of this dissertation. The source code was configured to analyze real-time medical records and CGM data and implement the two renditions of post-processing outlined in this section. If tachycardia is detected in real-time the event-based post-processing algorithm will be initiated. If no tachycardia is detected the rate of change and offset based post-processing algorithm is initiated. The post-processing algorithm was utilized to modify neural network model predictions in the five patients not included in original neural network model development/training subjected to performance analysis in section 3.3.8. Additionally, MATLAB® was utilized to compare performance of original neural network model predictions with predictions modified by the post-processing algorithm. Performance measures utilized for comparison included CEGA, overall model predictive accuracy (MAD%), and percentage of hypoglycemic, normal, and hyperglycemic extremes predicted.

CHAPTER 4

RESULTS

This section demonstrates the results obtained in the various clinical investigations outlined in this document for prediction of glucose using a neural network modeling approach. Prediction of glucose is demonstrated in both insulin dependent diabetic and critical care patient populations however, the emphasis of this dissertation is the prediction of glucose in the critical care patient population.

4.1 Neural Network Model Based Prediction of Glucose in Insulin Dependent Diabetic Patients

This section includes the results obtained via development of neural network models for prediction of glucose in patients with insulin dependent diabetes. In this section, predictive accuracy of the developed models is evaluated.

4.1.1 Initial Neural Network Model Development and Performance Analysis

Figure 4-1 is a plot containing neural network predictions using a 100 minute prediction horizon on a single patient whose data was not included in the training data during initial model development. This plot illustrates the effect of varying the number of patients (11, 14, and 17) utilized for training each neural network model. Figure 4-1 demonstrates that as the number of patients used in training is increased, the sensitivity of the neural network predictions at hyperglycemic extremes generally increased. Training sets of fewer patients (i.e., less data) appear to underestimate hyperglycemia to a greater

extent, which leads to some hyperglycemic reactions not being predicted. Table 4-1 includes the performance analysis results while varying the number of patients included in the initial training set in neural network development from 11–17 patients. There were a total of 128 hyperglycemic reactions and 94 hypoglycemic reactions in the unseen patient data that was used to validate model performance. The overall MAD% appears to be relatively consistent throughout, regardless of training set size ranging from 18.7 to 25.8% with an average of 22.7%. Neural network theory substantiates that as the quantity of training data is increased, neural network performance increases; however, this was not observed. A possible reason for the slight variability in overall MAD% is that the patients added to training set had different electronic diary data documenting similar lifestyle and emotional factors, which did not lead to the same glycemic trends as the patient chosen for analysis. Furthermore, the patient data used to validate these neural network models had a significant number of hypoglycemic reactions (as demonstrated in Figure 4-1). The neural networks generated with lower quantities of training data underestimate hyperglycemic extremes and are more accurate at the estimation of lower glucose extremes, thus leading to a smaller MAD% overall. This is realized as the MAD% at hypoglycemic extremes is greater when the neural network model overall MAD% does not follow the expected trend. As the amount of training data is increased, the percentage of hyperglycemic reactions predicted successfully by the neural network model increases from 49.2 to 69.5% for 11 and 17 patients, respectively. In addition, there is a corresponding decrease in MAD% at hyperglycemic extremes from 17.4 to 11.7% for 11 and 17 patients, respectively. Models routinely overestimate hypoglycemic

extremes due to the limited number of hypoglycemic CGM values in the training set used for neural network model development.

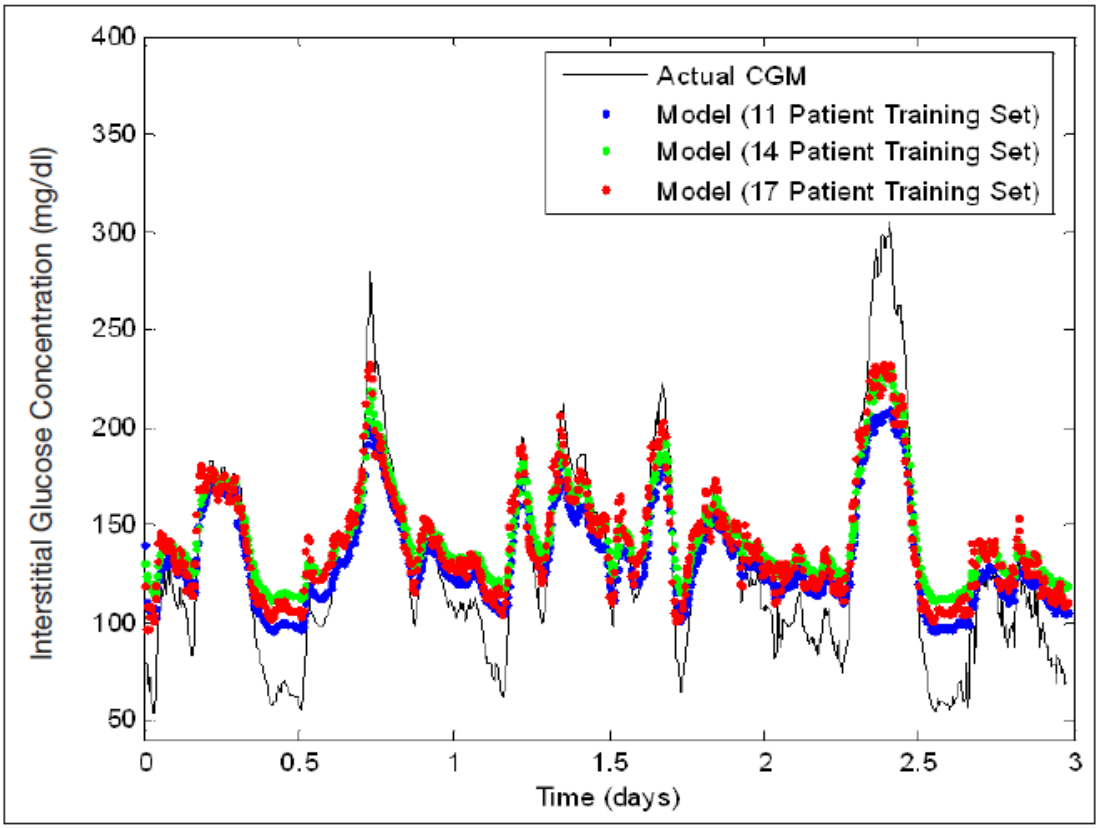

Figure 4-1. Neural Network Model Accuracy Generated Using Variable Length Training Sets

Table 4-1. Performance Analysis on Unseen Data: Variation of Training Set Length (100 min Prediction Horizon)

Number of Patients	Overall MAD%	MAD% Hyper	MAD% Hypo	Hyper Predicted (%)	Hypo predicted (%)
11	18.7	17.4	44.0	49.2	0
12	21.5	14.0	55.4	56.3	0
13	23.1	13.7	57.4	58.6	0
14	25.8	12.5	61.6	67.2	0
15	25.1	11.5	58.7	68.0	0
16	22.1	11.2	54.1	70.3	1.1
17	22.5	11.7	51.9	69.5	0

Figures 4-2 and 4-3 show neural network model predictions (implementing a prediction horizon of 100 minutes) made on two different patient datasets, while the number of patients, 15 and 16, respectively, were used for training the developed neural network model. Both neural network models accurately follow trends in data as well as predicting a significant percentage of hyperglycemic reactions. In Figure 4-3, the patient utilized for validation experiences extended hyperglycemic and hypoglycemic reactions, which occur at the maximum recorded value for the glucose sensor at 400 and 40 mg/dl, respectively. In each respective case, the neural network predictions underestimated and overestimated the glycemic extremes, which leads to a significant impact on overall MAD% as well as the MAD% at hyperglycemic and hypoglycemic extremes (i.e., 39.9,

24.1, and 30.0%, respectively, compared with 22.6%, 19.0%, and 3.0% for the 15-patient model—see Table 4-2). Calculation of overall model error is therefore very subjective to trends in the dataset used for validation. Table 4-2 summarizes the performance analysis and an assessment of neural network performance in predicting glucose values in multiple unseen patients while varying the length of the training data utilized during the initial model development. Because each patient is different, the number of hyperglycemic and hypoglycemic reactions in each dataset varies. In each case, the quantity of training data is increased, and the model is validated on a single patient dataset that was not used in the initial model formulation. As the quantity of training data is increased, there is an observed increase in model performance, and overall MAD% decreases with the exception of the final neural network model developed using the 16-patient training set for the reasons previously described. In addition to these reasons, it is also important to note that this patient exhibited the second highest number of hypoglycemic reactions of the unseen patient data that was tested. The respective models predict a significant percentage of hyperglycemic reactions ranging from 52.8–92.6%; however, they commonly overestimate hypoglycemic values. This correlates to the poor performance in the successful prediction of hypoglycemic extremes, and likely correlates to the decreased model accuracy in the model with the 16-patient training set.

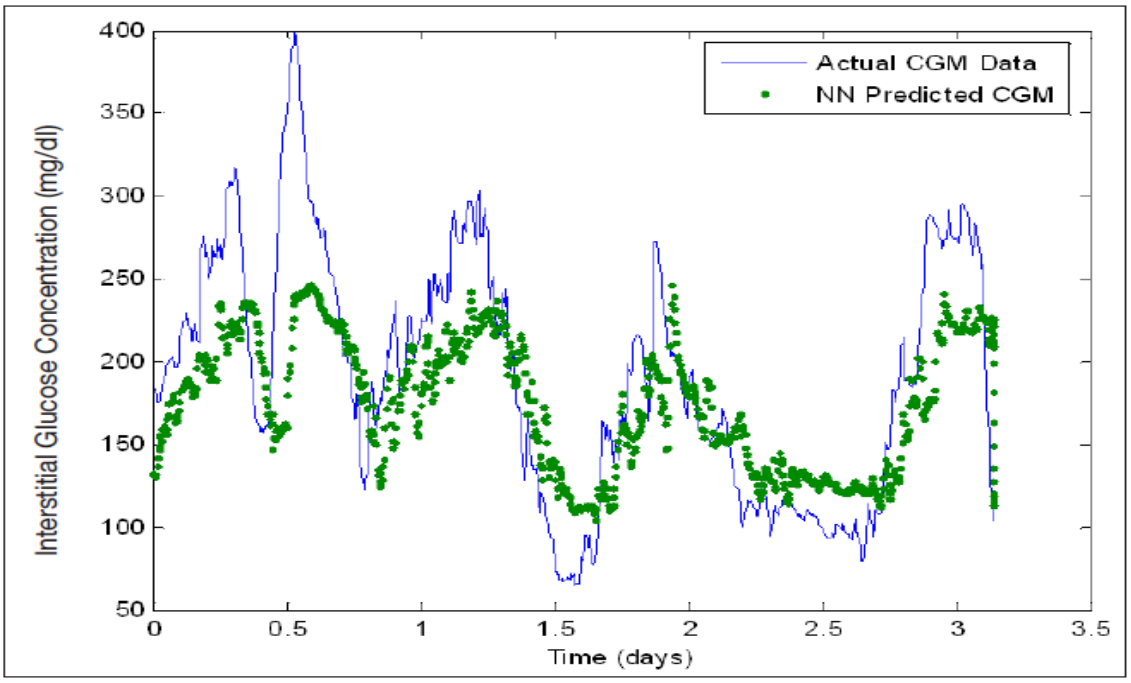

Figure 4-2. Neural network predictive abilities (generated using a 15-patient training set) (unseen data)

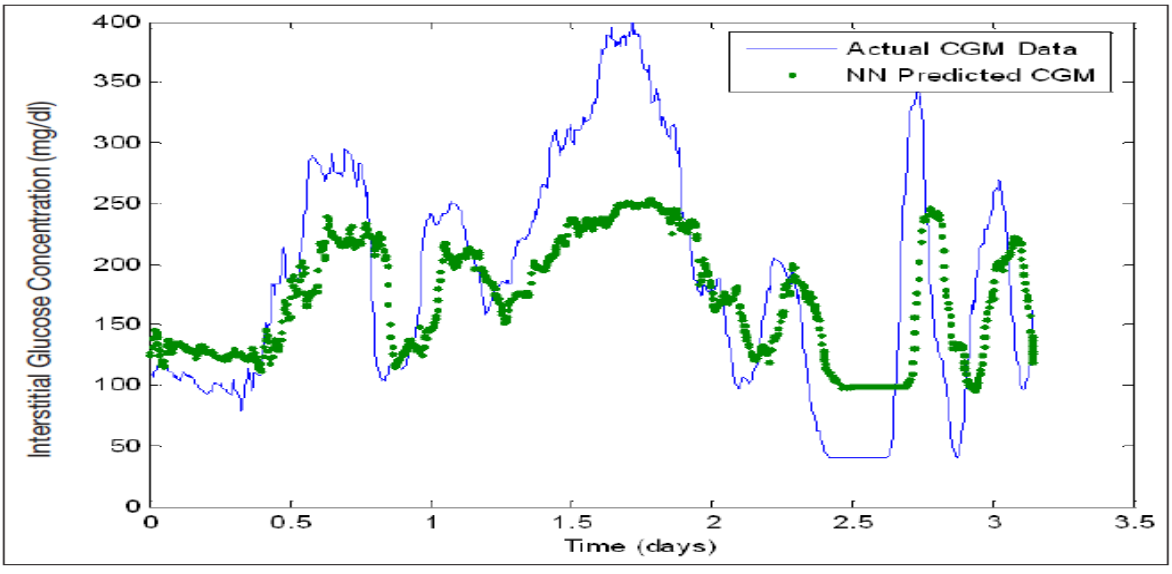

Figure 4-3. Neural network predictive abilities (generated using a 16-patient training set) (unseen data)

Table 4-2. Performance Analysis: Multiple Unseen Patients with Increasing Training Set Length (100 Minute Prediction Horizon)

Patients in Training Set	Overall MAD%	MAD% Hyper	MAD% Hypo	# Hyper Reactions	# Hypo Reactions	Hyper Predicted (%)
11	43.0	30.6	15.8	431	55	57.1
12	46.3	29.4	46.2	303	157	52.8
13	28.4	22.3	6.7	784	61	92.6
14	20.0	19.6	N/A	750	0	86.5
15	22.6	19.0	3.0	504	20	72.4
16	39.9	24.1	30.0	475	94	67.8

Figure 4-4 shows neural network models developed using a 17-patient training set and the predictions on a single unseen patient data record with variable prediction horizons of 50, 100, and 180 min. As the prediction horizon is increased, the accuracy in each model decreases, respectively. It is hypothesized that the underestimation of hyperglycemic extremes is due to the extension of the prediction horizon and the associated inability of the neural network to determine oscillations and trends in glycemia as well as the occurrence of other relevant input events such as lifestyle, emotional states, insulin dosages, and meals that may occur within the prediction horizon and may impact or change neural network weights.

Table 4-3 includes the performance analysis for the models generated with the 17-patient training set and variable prediction horizons. This dataset included 429 hyperglycemic reactions and 8 hypoglycemic reactions. A consistent increase in overall MAD% (6.7–18.9%) is observed with an increase in the prediction horizon. Similarly, the MAD% at hyperglycemic and hypoglycemic extremes increases from 6.6–22.1% and 0.6–1.7%, respectively. A majority of the hyperglycemic reactions in this dataset are predicted with 71.6–97.2% of hyperglycemic reactions being predicted by the models. Conversely, for reasons previously mentioned, hypoglycemic reactions are routinely overestimated, resulting in no hypoglycemic extremes being predicted successfully.

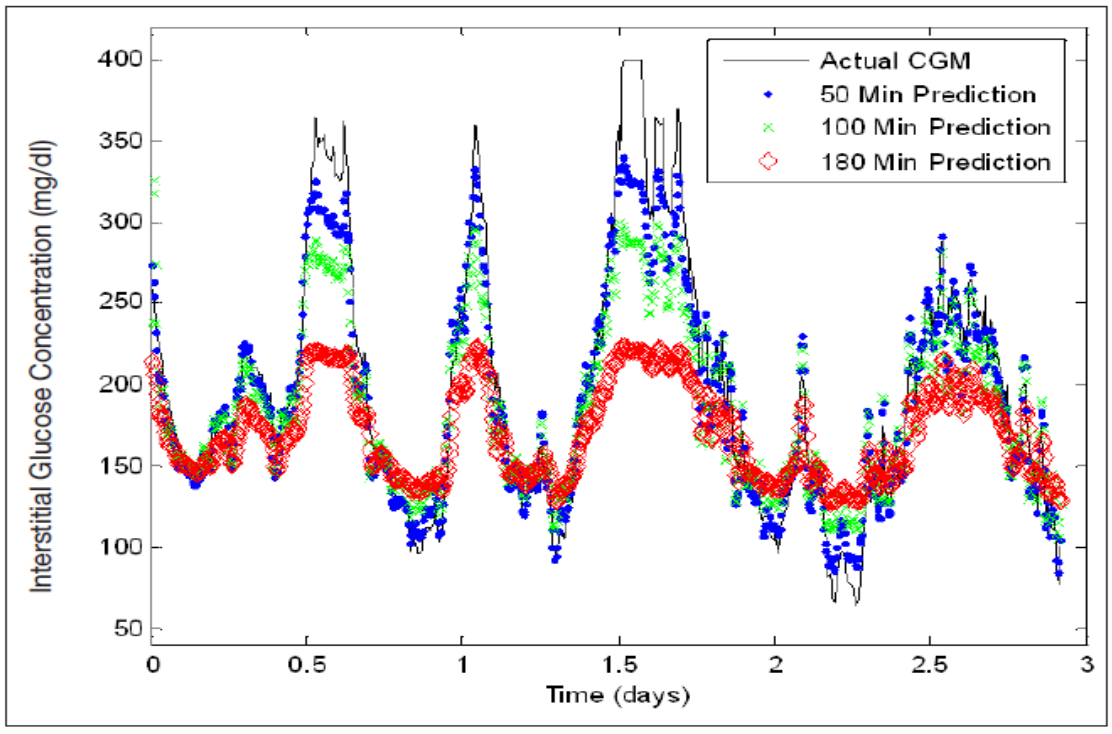

Figure 4-4. Neural Network Model Performance Analysis: Effect of Variation of Prediction horizon on Same Segment of Unseen Patient Data

Table 4-3. Performance Analysis: Prediction horizon Variation on Same Unseen Data Segment

Prediction horizon (min)	Overall MAD%	MAD% Hyper	MAD% Hypo	Hyper Predicted (%)	Hypo Predicted (%)
50	6.7	6.6	0.6	95.3	0.0
75	8.9	8.0	0.9	94.9	0.0
100	11.7	11.0	1.3	90.4	0.0
120	14.5	12.0	1.5	97.2	0.0
150	16.6	19.6	1.5	79.0	0.0
180	18.9	22.1	1.7	71.6	0.0

4.1.2 Performance Analysis of Predictive Models for Glucose in Real-time in Patients with Diabetes (Reduced complexity Model Architecture)

Figures 4-5 and 4-6 include the real-time predictions of glucose in a segment of CGM data derived from 10 patients not utilized for model training. Figures 4-5 and 4-6 include model predictive accuracy at hypoglycemic, normal, and hyperglycemic extremes. Due to the large number of predictions generated by the neural network model (15 predicted CGM values for each real-time CGM value acquired), the data was resampled to plot every 20^{th} predicted value such that trends in predictions can be more accurately displayed. Real-time predictions were generated via the real-time predictive computer program outlined in 3.2.5. A feed forward neural network model architecture was implemented and the model was trained using the same training set utilized in section

3.2.3 for model development. Real-time prediction of glucose was completed using two methodologies. Figure 4-5 includes model predictions generated using original model weights (no weight updating) determined via initial model training during each iteration of the real-time predictive program. Figure 4-6 includes model predictions generated using the real-time predictive program for real-time training to update model weights at each predictive iteration (weight update method).

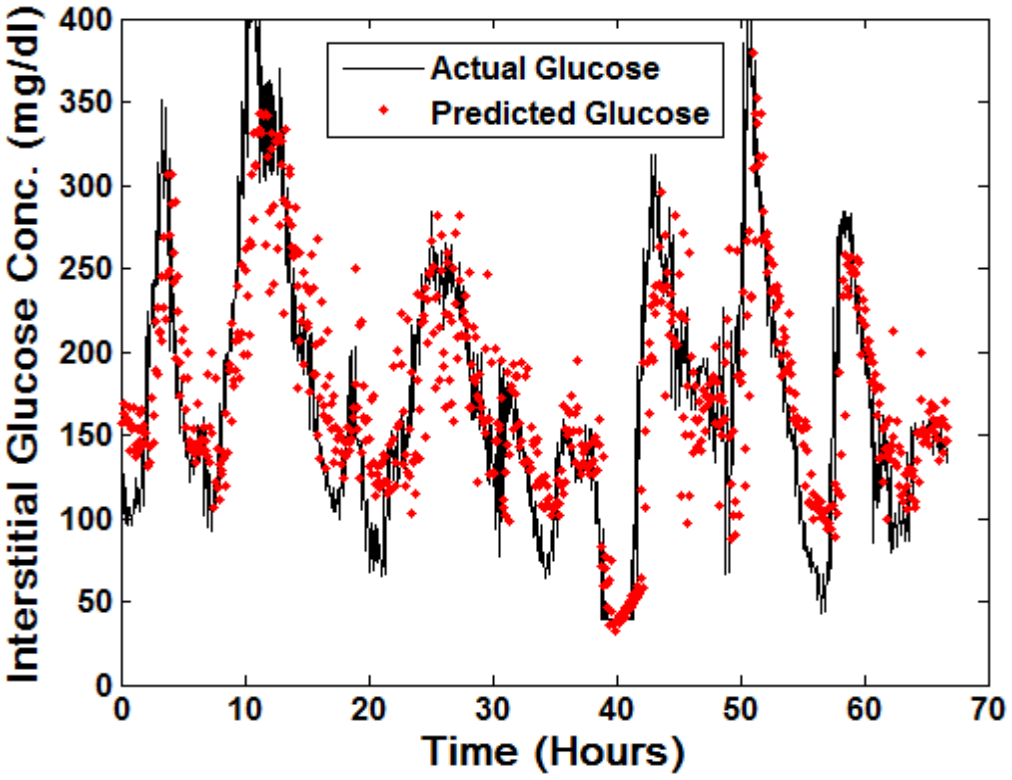

Figure 4-5. Real-Time Predictions in Insulin Dependent Diabetic Patients (No Weight Update)

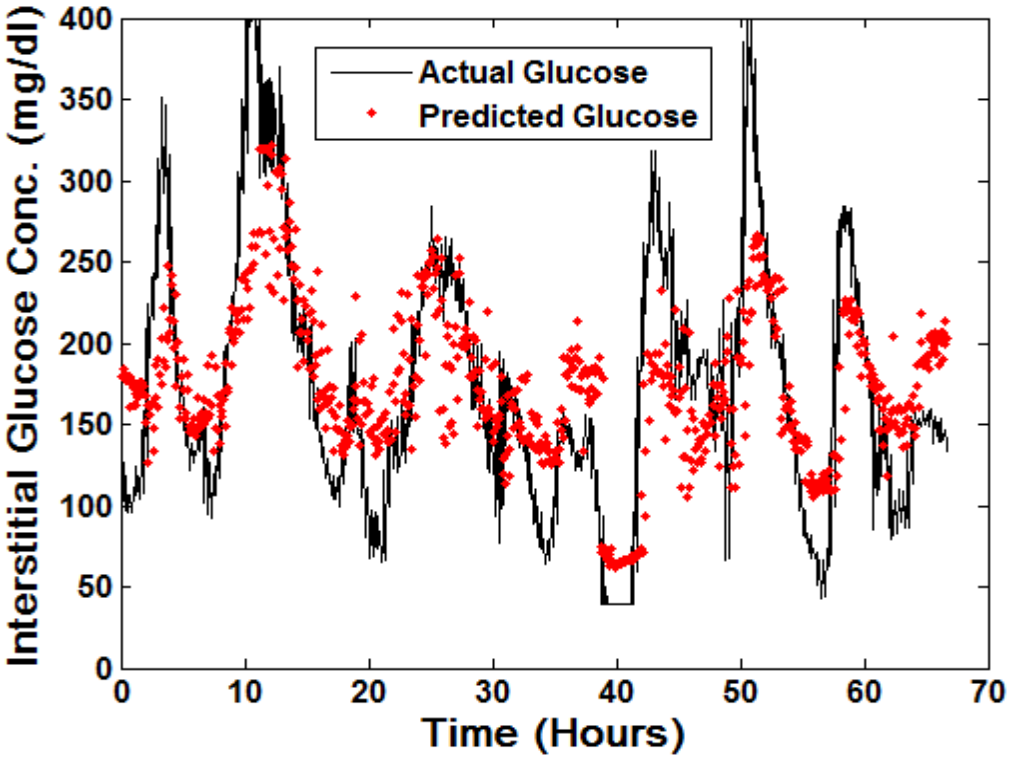

Figure 4-6. Real-Time Predictions in Insulin Dependent Diabetic Patients (Weight Update)

Figures 4-7 and 4-8 include Clarke Error Grids to demonstrate the predictive accuracy and clinical acceptability of the real-time model predictions. Figure 4-7 includes the Clarke Error Grid for the model implementing no weight update (model weights determined via initial comprehensive model training). Figure 4-8 includes the Clarke Error Grid for the model in which weights were updated using the real-time predictive model. Tables 4-4 and 4-5 include the summary of Clarke Error Grid Analysis (CEGA), model predictive error (MAD%), and the percentage of hypoglycemic (CGM $\leq$70 mg/dl), normal (CGM >70 and <180 mg/dl), and hyperglycemic (CGM $\geq$ 180 mg/dl) glucose values predicted successfully. Table 4-4 includes the summary of CEGA, and predictive results for the model implementing no weight update (model weights determined via

initial comprehensive model training). Table 4-5 includes the summary of CEGA, and predictive results for the model in which weights were updated using the real-time computer program.

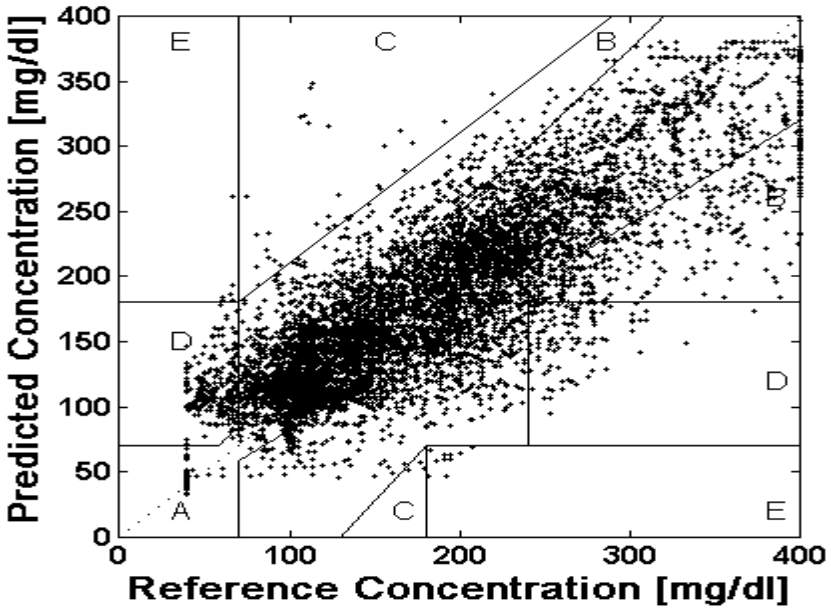

Figure 4-7. Clarke Error Grid of Real-time Predictions (No Weight Update)

Table 4-4. CEGA and Summary of Model Predictive Accuracy (No Weight Update)

Zone	A	B	C	D	E
Total in Zone	66112	34763	477	5291	202
Percentage Of Data in Zone	61.9	32.5	0.4	5.0	0.2
Total in Dataset	106845				
Overall MAD%	22.3				
MAD% (No Hypo)	19.2				
% data Hypo	4.4				
% Hypo Predicted	16.8				
% data Norm	37.3				
% Norm Predicted	73.0				
% data Hyper	58.3				
% Hyper Predicted	87.2				

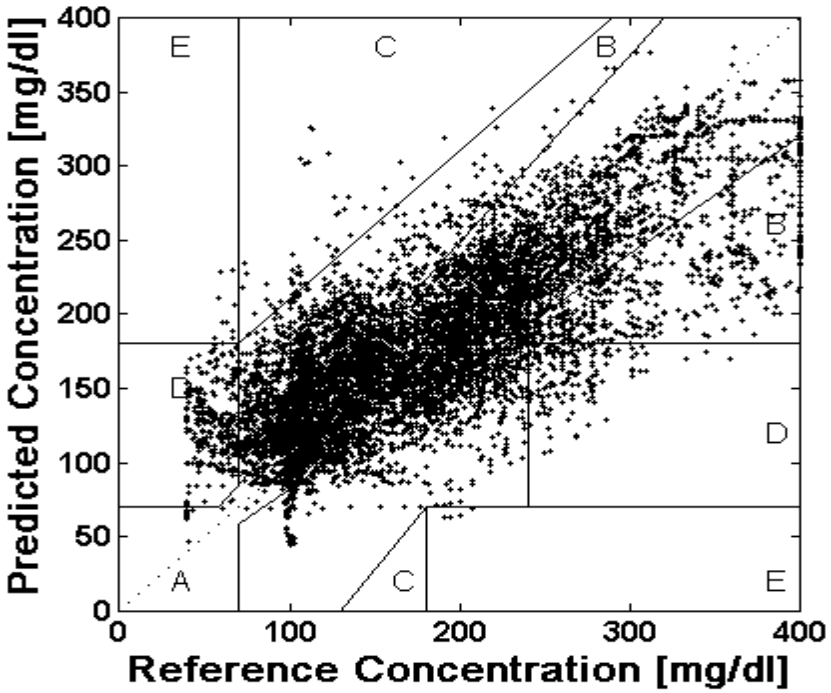

Figure 4-8. Clarke Error Grid of Real-time Predictions (Weight Update)

Table 4-5. CEGA and Summary of Model Predictive Accuracy (Weight Update)

Zone	A	B	C	D	E
Total in Zone	59201	41026	689	5775	154
Percentage Of Data in Zone	55.4	38.4	0.6	5.4	0.1
Total in Dataset	106845				
Overall MAD%	27.0				
MAD% (No Hypo)	22.4				
% data Hypo	4.4				
% Hypo Predicted	15.2				
% data Norm	37.3				
% Norm Predicted	61.8				
% data Hyper	58.3				
% Hyper Predicted	88.6				

Clarke Error Grid Analysis (CEGA) of real-time predictions revealed that a majority of predictions were clinically acceptable and would not lead to adverse

therapeutic direction or outcome. In utilizing the real-time program with no weight update/adaptation during each predictive iteration of the model (i.e. model weights determined via training as outlined in section 3.2.3), 61.9% and 32.5% (94.4%) of predicted values fell within regions A and B respectively of the error grid and could be classified as clinically acceptable. A total of 0.4%, 5.0%, and .2% of predicted values fell within regions C, D, and E of the error grid respectively, and could lead to inaccurate/adverse therapeutic direction. Utilization of the real-time predictive system for weight update/adaption (i.e. neural network model was retrained at each predictive iteration) resulted in slightly less predictions within regions A and B of the error grid with 55.4% and 38.4% (93.8%) respectively. A total of 0.6%, 5.4%, and .1% of predicted values fell within regions C, D, and E of the error grid respectively, and could lead to inaccurate/adverse therapeutic direction.

In utilizing original model weights (no weight update), the overall error (MAD%) of the model predictions was calculated as 22.3% for the entire dataset and 19.2% for the dataset at non-hypoglycemic extremes (CGM values $\leq$ 70 mg/dl). Utilizing this approach resulted in the prediction of 16.8% of hypoglycemia (CGM $\leq$70 mg/dl), 73.0% of normal glycemia (CGM >70 and <180 mg/dl), and 87.2% of hyperglycemia (CGM $\geq$180 mg/dl). Conversely, utilizing the real-time predictive system for weight adaptation resulted in less accurate predictions with an overall error (MAD%) of 27.0%, and 22.4% at non-hypoglycemic extremes. Utilizing this approach resulted in the prediction of less hypoglycemia (15.2%) and normal glycemia (61.8%) and an insignificant increase in percentage hyperglycemia predicted (88.6%) than utilizing original model weights.

4.1.3 Effect of Design Variation of Neural Networks Utilized for Real-time Prediction of Glucose in Insulin Dependent Diabetic Patients

This section outlines the effect of neural network model design differences on real-time glucose prediction. The neural network models developed in this investigation were designed with a prediction horizon of 75 minutes (i.e. prediction of 15 CGM values). The neural network models were configured as multifunctional neural network (MFNN) models and to predict glucose concentration, as well as glycemic states (i.e. ranges of glucose concentration classified numerically from 1-7). It is hypothesized that prediction of glycemic states may be more accurate than prediction of specific glucose concentration values. Furthermore, the prediction of two factors can be used for comparison. If both predictions coincide then the prediction is likely accurate. Differences in overall neural network model complexity are analyzed. Differences in trajectory and number of samples backpropagated to calculate gradient information for weight optimization are also investigated. The results of this analysis will provide insight towards the best and optimal architecture to be implemented in subsequent investigations.

In prediction of glucose concentration, there is often considerable predictive error. Due to the inherent nature of neural network models, it is hypothesized that prediction of ranges of glucose concentration (i.e. glycemic states) may have less associated errors in prediction. In this investigation, glycemic states were classified numerically from 1-7 as demonstrated in Table 4-6. Glycemic state 1 represents hypoglycemic glucose values. Glycemic state 2 represents lower-normal glucose values. Glycemic state 3 represents middle-normal glucose values. Glycemic state 4 represents upper-normal (i.e. near hyperglycemic) glucose values. Glycemic state 5 represents lower-hyperglycemic

glucose values. Glycemic state 6 represents middle-hyperglycemic values. Glycemic state 7 represents extremely elevated hyperglycemic glucose values. The prediction of these glycemic states may lead to enhanced predictive accuracy, and also allow for caregivers to adjust therapy (similar to sliding scale protocol) based on predicted glycemic states.

Table 4-6. Classification of Glycemic States for Multifunction Neural Network Models

Glycemic State	Glucose Concentration Range (mg/dl)
1	$\leq$70
2	>70 & $\leq$100
3	>100 & $\leq$140
4	>140 & <180
5	$\geq$180 & $\leq$220
6	>220 & $\leq$300
7	>300

4.1.4 Reduced complexity Feed Forward MFNN: Prediction of Glycemic States

Table 4-7 demonstrates the predictive accuracy of reduced complexity MFNN in prediction of general glycemic states. Comparison of performance of real-time models implementing weight adaptation and implementation of original model weights was analyzed. Utilizing the neural network model for real-time training (weight update) predicts a significantly smaller percentage of hypoglycemia (0.02 % versus 15.9%) with respect to implementation of original model weights. The model implementing original model weights (no weight updates) predict a slightly higher percentage of normal glycemic states (86.6% versus 85.2%). Furthermore, implementation of original model weights resulted in prediction of a significantly higher percentage of hyperglycemic states (79.3% versus 71.9%).

Table 4-7. Prediction of General Glycemic States in Reduced Complexity MFNN Models

Glycemic State	Low (State 1)	Normal (States 2-4)	High (States 5-7)
Percent Predicted (Weight Update)	0.02	85.20	71.90
Percent Predicted (Original Model Weights)	15.90	86.60	79.30

The performance of the MFNN models in prediction of specific glycemic states is presented in Table 4-8. Prediction of hypoglycemia is again higher in the model implementing original model weights (15.9% versus 0.02%). The percentage of glycemic states 2 and 3 predicted were significantly higher in the model implementing original model weights and no weight updating. Original model weights resulted in the prediction of 22.7% of glycemic state 2 and 54.8% of glycemic state 3. In comparison, the neural network model implementing real-time training resulted in the prediction of 12.3% and 46.9% of glycemic states 2 and 3 respectively. Models implementing original model weights therefore result in an improvement of 15.7%, 10.4%, and 7.9% in prediction of specific glycemic states 1, 2, and 3. Utilizing neural network models with real-time training resulted in increased accuracy in prediction of glycemic states 4, and 7. In these models 53.7% and 46.6% of glycemic states 4 and 7 were predicted successfully. In comparison, models implementing original weights predicted 43.7% and 28.4% of glycemic states 4 and 7 respectively. Models implementing weight adaptation therefore had an increase in performance in prediction of glycemic states 4 and 7 with increases in 10.0% and 18.2% respectively. Both modeling approaches predicted the same percentage

of glycemic state 6 (30.1%). In prediction of glycemic state 5, utilization of original model weights resulted in a higher performance in predicting 48.2% of glycemic state 5 versus 44.2% using the model implementing real-time training.

Table 4-8. Glycemic States Predictive Results (Specific Glycemic States)

Glycemic State	1 (Hypo)	2(>70&<=100)	3(>100&<=140)	4(>140<=179)	5(>=180&<=220)	6(>220&<=300)	7(>300)
Percent Predicted (Weight Update)	0.2	12.3	46.9	53.7	44.2	30.1	46.6
Percent Predicted (No Weight Update)	15.9	22.7	54.8	43.7	48.2	30.1	28.4

4.1.5 Enhanced Complexity Multifunctional Neural Network Models**:** Effect of Modifying Exemplars per Update

Multifunctional neural networks for real-time prediction of glucose and glycemic states in patients with diabetes are presented in this section. Neural networks were designed with enhanced complexity in design including an input layer with memory consisting of 3 taps and a tap delay line of 1 (1 sample delay between successive taps). The neural network thus had memory of the current input plus 2 historical inputs in the input layer. Additionally, the neural network was designed with two hidden layers both with hyperbolic tangent axons for processing neural network inputs to between a range of -1 and 1. The first hidden layer contained a memory structure with 8 taps and a tap delay line of 1 which maintained a memory of the current input and 7 historical inputs. The second hidden layer contained a memory structure with 4 taps and a tap delay line of 1

which maintained a memory of the current input and 3 historical inputs. The neural networks were designed with a forward trajectory of 50 samples and backpropagation of 40 samples (i.e. single exemplar) to acquire gradient information and modify weights accordingly. In the analysis below three real-time implementations of the neural network were investigated where the neural networks were configured to update weights after every 10, and 100 exemplars.

A neural network model was configured to update model weights after every 10 exemplars (i.e. forward trajectory of 50 samples and back-propagation of 40 samples). Figure 4-9 demonstrates the Clarke Error Grid for neural network model predictions. Clarke Error Grid Analysis (CEGA) indicated that 93.7% of the predictions were clinically acceptable with 59.9% and 33.8% of predictions falling within regions A and B of the error grid. This analysis also revealed that 0.7%, 76.4%, and 88.3% of hypoglycemic, normal, and hyperglycemic glycemic extremes were predicted successfully. CEGA results are displayed in Table 4-9. Only a small percentage of hypoglycemic extremes were predicted successfully. The overall error (MAD%) between actual and predicted CGM was 22.5%. If MAD% is recalculated at non-hypoglycemic extremes, error is improved to 19.2%, correlating to an improvement of 3.3%.

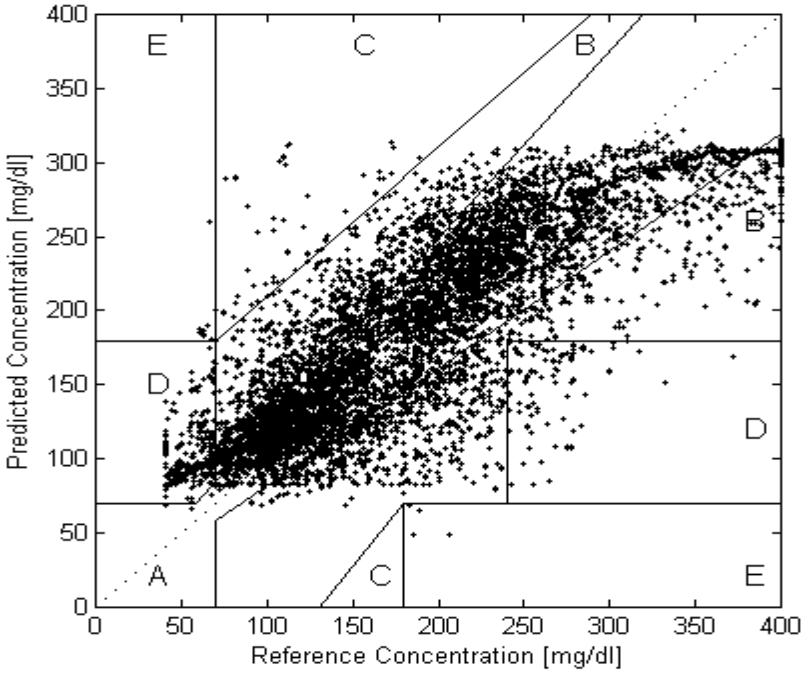

Figure 4-9. Clarke Error Grid of MFNN (10 Exemplar Per Update)

Table 4-9. Results: Clarke Error Grid Analysis (10 Exemplars Per Update)

Zone	A	B	C	D	E
Total in Zone	63138	35622	690	5700	195
Percentage Of Data in Zone	59.9	33.8	0.7	5.4	0.2
Total in Dataset	105345				
Overall MAD%	22.5				
MAD% (No Hypo)	19.2				
% data Hypo	4.4				
% Hypo Predicted	0.7				
% data Norm	36.9				
% Norm Predicted	76.4				
% data Hyper	58.7				
% Hyper Predicted	88.3				

The neural network model previously described was configured to update model weights after 100 exemplars. Figure 4-10 demonstrates the Clarke Error Grid for neural network model predictions. Clarke Error Grid Analysis (CEGA) indicated that 93.7% of the predictions were clinically acceptable with 62.7% and 31.0% of predictions falling within regions A and B of the error grid. This analysis also revealed that 1.6%, 85.7%,

and 82.6% of hypoglycemic, normal, and hyperglycemic glycemic extremes were predicted successfully. CEGA results are presented in Table 4-10. Only a small percentage of hypoglycemic extremes were predicted successfully. The model overestimates hypoglycemic extremes. This phenomenon is again attributed to the lack of hypoglycemic training data in the initial model training set which will be discussed later in this document. The overall error (MAD%) between actual and predicted CGM was 20.6%. If MAD% is recalculated at non-hypoglycemic extremes, error is improved to 17.8%, correlating to an improvement of 2.8%.

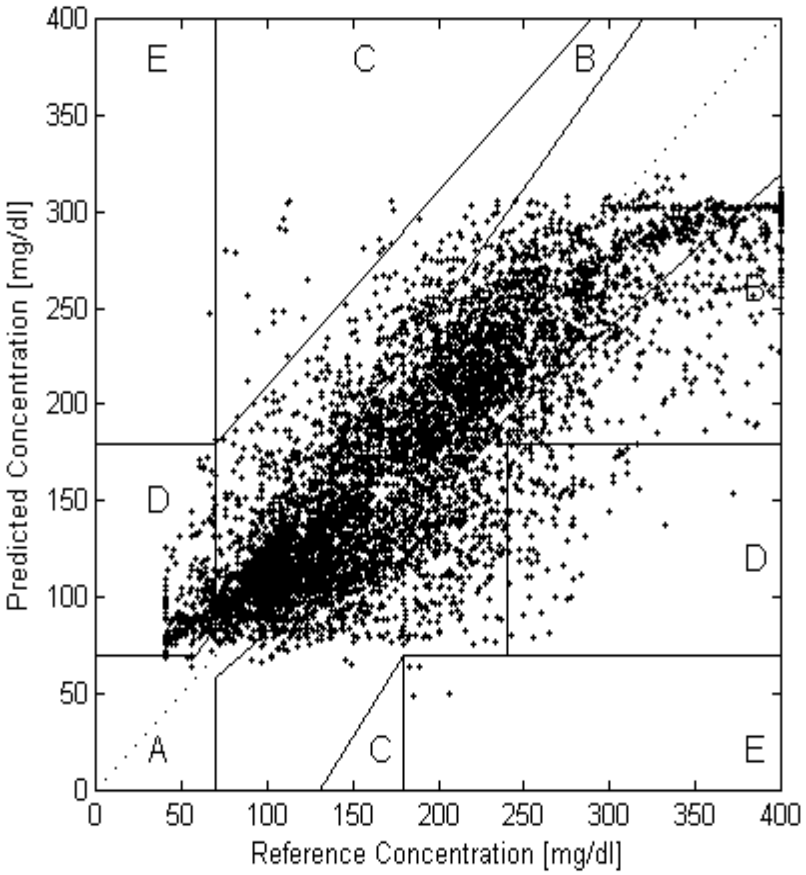

Figure 4-10. Clarke Error Grid (100 Exemplars Per Update)

Table 4-10. Results: Clarke Error Grid Analysis (100 Exemplars Per Update)

Zone	A	B	C	D	E
Total in Zone	66038	32692	360	6165	90
Percentage Of Data in Zone	62.7	31.0	0.3	5.9	0.1
Total in Dataset	105345				
Overall MAD%	20.6				
MAD% (No Hypo)	17.8				
% data Hypo	4.4				
% Hypo Predicted	1.6				
% data Norm	36.9				
% Norm Predicted	85.7				
% data Hyper	58.7				
% Hyper Predicted	82.6				

In addition to overall accuracy in prediction of glucose concentration, MFNN models were assessed for their abilities to predict glycemic states. Table 4-11 demonstrates model accuracy at prediction of general low, normal, and high glucose states. Prediction of normal glucose states is highest in the model which updates weights after 100 exemplars. More hyperglycemic (high) glucose states were predicted when weights were updated after 10 exemplars. Table 4-12 demonstrates the percentage of specific glycemic states predicted successfully by the real-time neural network model application. In prediction of specific glycemic states, models updating weights after 10 exemplars are more accurate at elevated glycemic extremes. Models updating weights after 100 exemplars are more accurate at normal glycemic extremes.

Table 4-11. Prediction of General Glycemic States in MFNN Models (Exemplars per Update)

Glycemic State	Low	Normal	High
10 Exemplars Per Update	0	88.6	79.6
100 Exemplars Per Update	0	93.5	70.6

Table 4-12. Prediction of Specific Glycemic States in MFNN Models (Exemplars per Update)

Glycemic State	1 (Hypo)	2 (>70&<=100)	3 (>100&<=140)	4 (>140<=179)	5 (>=180&<=220)	6 (>220&<=300)	7 (>300)
1 Exemplar Per Update	0	12.3	66.2	40.0	45.7	46.9	61.2
10 Exemplars Per Update	0	10.5	66.5	40.7	45.5	46.5	58.9
100 Exemplars Per Update	0	26.3	73.0	37.7	36.2	34.1	49.6

4.1.6 Enhanced Complexity Multifunctional Neural Network Models**:** Effect of Modifying Forward and Back-Propagation Trajectories

The multifunctional neural network models outlined in section 4.1.6 were investigated to gauge the effect of modifying the forward and backpropagation trajectories. The neural networks were designed with variable forward trajectories of 10 and 5 samples and backpropagation trajectories of 5, and 2 samples (i.e. single exemplar) to acquire gradient information and modify weights accordingly. All neural network models were configured to update weights after 100 exemplars. Additionally a neural network using a forward trajectory of 5 samples and backpropagation of 2 samples is utilized and configured to update after 10 exemplars. Trajectories are abbreviated in this section as 10-5 for 10 samples in forward trajectory and 5 samples back propagated.

Figure 4-11 demonstrates the Clarke Error Grid containing neural network model predictions generated by the MFNN model implementing a forward trajectory of 10 and a backpropagation trajectory of 5, and configured to update weights after 100 exemplars. Clarke Error Grid Analysis (CEGA) indicated that 93.7% of the predictions were

clinically acceptable with 62.7% and 31.0% of predictions falling within regions A and B of the error grid. This analysis also revealed that 1.6%, 85.7%, and 82.6% of hypoglycemic, normal, and hyperglycemic glycemic extremes were predicted successfully. CEGA results are presented in Table 4-13. The overall error (MAD%) between actual and predicted CGM was 20.6%. If MAD% is recalculated at non-hypoglycemic extremes, error is improved to 17.8%, correlating to an improvement of 2.8%.

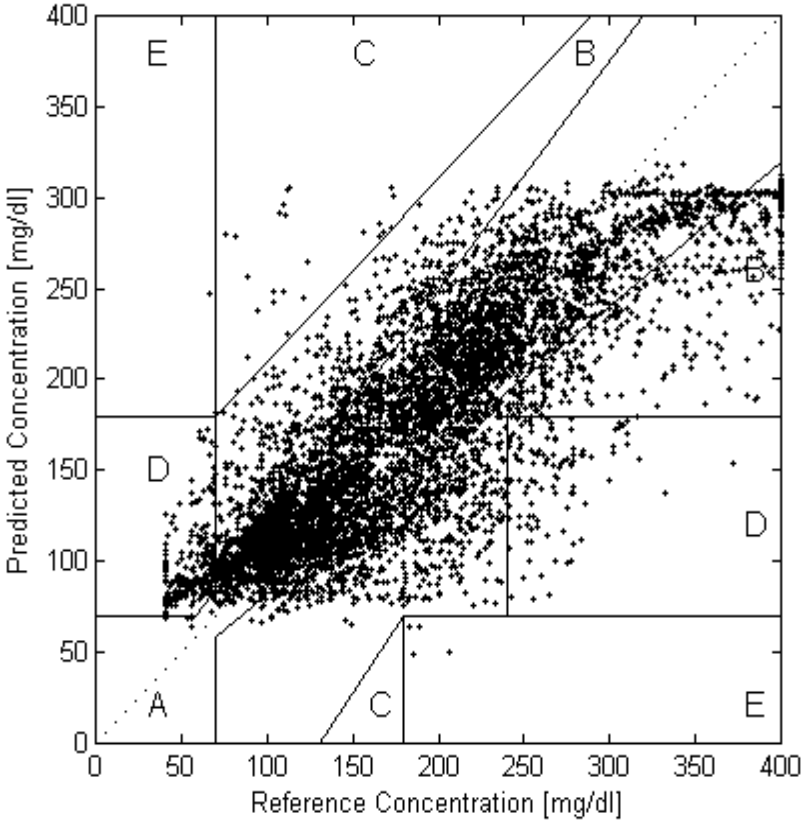

Figure 4-11. Clarke Error Grid (10-5 Trajectory/100 Exemplars Per Update)

Table 4-13. Results: Clarke Error Grid Analysis (10-5 100 Exemplars per Update)

Zone	A	B	C	D	E
Total in Zone	66038	32692	360	6165	90
Percentage Of Data in Zone	62.7	31.0	0.3	5.9	0.1
Total in Dataset	105345				
Overall MAD%	20.6				
MAD% (No Hypo)	17.8				
% data Hypo	4.4				
% Hypo Predicted	1.6				
% data Norm	36.9				
% Norm Predicted	85.7				
% data Hyper	58.7				
% Hyper Predicted	82.6				

A MFNN model was developed implementing a forward trajectory of 5 samples and the back propagation of 2 samples and configured to update weights after 100 exemplars. Figure 4-12 demonstrates the Clarke Error Grid containing predictions for the MFNN model implementing a forward trajectory of 5 samples and the backpropagation trajectory of 2 samples and configured to update weights after 100 exemplars. Clarke Error Grid Analysis (CEGA) indicated that 93.8% of the predictions were clinically acceptable with 59.9% and 33.9% of predictions falling within regions A and B of the error grid. This analysis also revealed that 0.7%, 76.4%, and 88.3% of hypoglycemic, normal, and hyperglycemic glycemic extremes were predicted successfully. CEGA results are presented in Table 4-14. Only a small percentage of hypoglycemic extremes were predicted successfully. The model overestimates hypoglycemic extremes. This is again due to the lack of hypoglycemic training data in the initial model training set. The overall error (MAD%) between actual and predicted CGM was 22.6%. If MAD% is recalculated at non-hypoglycemic extremes, error is improved to 19.2%, correlating to an improvement of 3.4%.

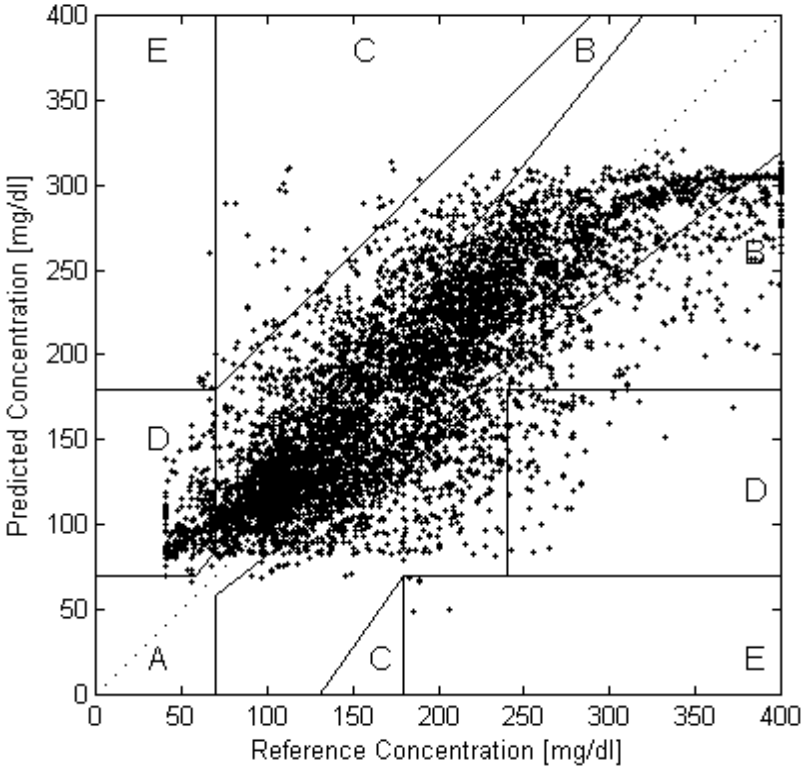

Figure 4-12. Clarke Error Grid (5-2 Trajectory/100 Exemplars Per Update)

Table 4-14. Results: Clarke Error Grid Analysis (5-2 100 Exemplars per Update)

Zone	A	B	C	D	E
Total in Zone	63118	35675	630	5727	195
Percentage Of Data in Zone	59.9	33.9	0.6	5.4	0.2
Total in Dataset	105345				
Overall MAD%	22.6				
MAD% (No Hypo)	19.2				
% data Hypo	4.4				
% Hypo Predicted	0.7				
% data Norm	36.9				
% Norm Predicted	76.4				
% data Hyper	58.7				
% Hyper Predicted	88.3				

A MFNN model was developed implementing a forward trajectory of 5 samples and the back propagation of 2 samples and configured to update weights after 10 exemplars. Figure 4-13 includes the Clarke Error Grid containing predictions generated by the MFNN implementing a forward trajectory of 5 and a backpropagation trajectory of 2 and configured to updated model weights after 10 exemplars. Clarke Error Grid Analysis (CEGA) indicated that 93.8% of the predictions were clinically acceptable with 59.7% and 34.1% of predictions falling within regions A and B of the error grid. This analysis also revealed that 0.7%, 75.9%, and 88.6% of hypoglycemic, normal, and hyperglycemic glycemic extremes were predicted successfully. CEGA results are presented in Table 4-15. The overall error (MAD%) between actual and predicted CGM was 22.7%. If MAD% is recalculated at non-hypoglycemic extremes, error is improved to 19.3%, correlating to an improvement of 3.4%.

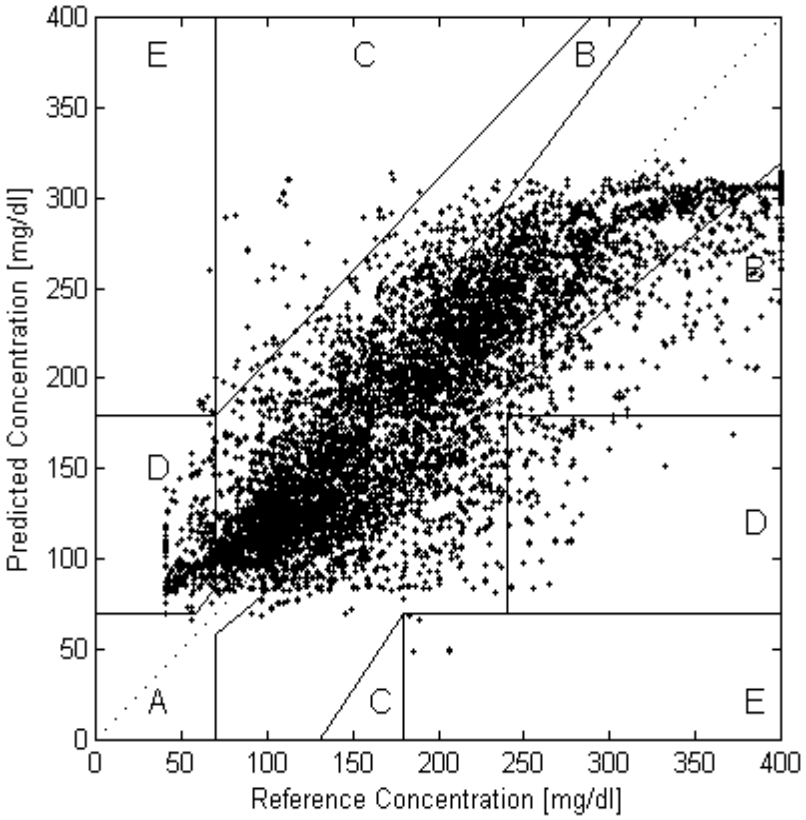

Figure 4-13. Clarke Error Grid (5-2 10 Exemplars Per Update)

Table 4-15. Results: Clarke Error Grid Analysis (5-2 10 Exemplars per Update)

Zone	A	B	C	D	E
Total in Zone	62846	35929	675	5700	195
Percentage Of Data in Zone	59.7	34.1	0.6	5.4	0.2
Total in Dataset	105345				
Overall MAD%	22.7				
MAD% (No Hypo)	19.3				
% data Hypo	4.4				
% Hypo Predicted	0.7				
% data Norm	36.9				
% Norm Predicted	75.9				
% data Hyper	58.7				
% Hyper Predicted	88.6				

In addition to overall accuracy in prediction of glucose concentration, MFNN models were assessed for their abilities to predict glycemic states. Table 4-16 demonstrates model accuracy at prediction of low, normal, and high (general) glucose states. Prediction of normal glucose states is highest in the model which updates weights after 100 exemplars with a trajectory of 10-5. Prediction of hyperglycemic (high) glucose states was increased with a trajectory of 5-2 while updating weights after 100 and 10 exemplars. Table 4-17 demonstrates the percentage of specific glycemic states predicted successfully by the real-time neural network model application. In prediction of specific glycemic states, the model implementing a trajectory of 10-5 is higher in accuracy at prediction of normal glycemic states 2 and 3. Models updating weights implementing trajectories of 5-2 and updating weights after 100 and 10 exemplars are more accurate at hyperglycemic states and extremes.

Table 4-16. Prediction of General Glycemic States in MFNN Models (Forward and Backpropagation Trajectory Variation)

Glycemic State	Low	Normal	High
10-5 (100 Exemplars/Update)	0	93.5	70.6
5-2 (100 Exemplars/Update)	0	88.7	79.5
5-2 (10 Exemplars/Update)	0	88.1	80.5

Table 4-17. Prediction of Specific Glycemic States in MFNN Models (Forward and Backpropagation Trajectory Variation)

Glycemic State	1 (Hypo)	2 (>70&<=100)	3 (>100&<=140)	4 (>140<=179)	5 (>=180&<=220)	6 (>220&<=300)	7 (>300)
10-5 (100 Exemplars/Update)	0	26.3	73.0	37.7	36.2	34.1	49.6
5-2 (100 Exemplars/Update)	0	10.3	66.6	40.6	45.6	46.7	56.6
5-2 (10 Exemplars/Update)	0	10.2	66.0	40.3	46.0	47.2	59.8

4.2 Prediction of Glucose in the Critical Care Patient Population

4.2.1 Justification for Predictability of Glucose in Critical Care Patients: Glycemic Patterns in Response to Insulin Delivery

Figure 4-14 demonstrates 12 patterns in glucose in patients when subjected to the UTMC insulin infusion protocol who experience an elevated glucose value of approximately 180 mg/dl. The data in Figure 4-14 is CGM data (sampled every five minutes) in response to the insulin infusion protocol at UTMC six hours after an elevated glucose value of ~180 mg/dl is experienced. Glycemic responses to the UTMC insulin infusion protocol are similar and there are indeed patterns which can be visualized. Previous research has substantiated the existence of ultradian glycemic patterns (in discrete metered glucose measurements) in the critical are patient population in response to insulin infusion. [57] These results support and are an extension of these findings in that patterns are demonstrated using CGM with glucose measurements obtained continuously every 5 minutes. Ideally, the insulin infusion protocol should lower glucose to within a target range of 90-140 mg/dl. This is demonstrated in this patient population. There are incidences however, where the insulin infusion protocol appears over aggressive and leads to hypoglycemia. Furthermore, there are incidences where insulin infusion is not adequate and glucose remains elevated $\geq$ 150 mg/dl which has been demonstrated in current literature to be correlated to decreased patient outcome. Table 4-18 includes insulin infusion in each patient over the 6 hour time period, as well as the time of the initial elevated glucose value (on a 24 hour scale).

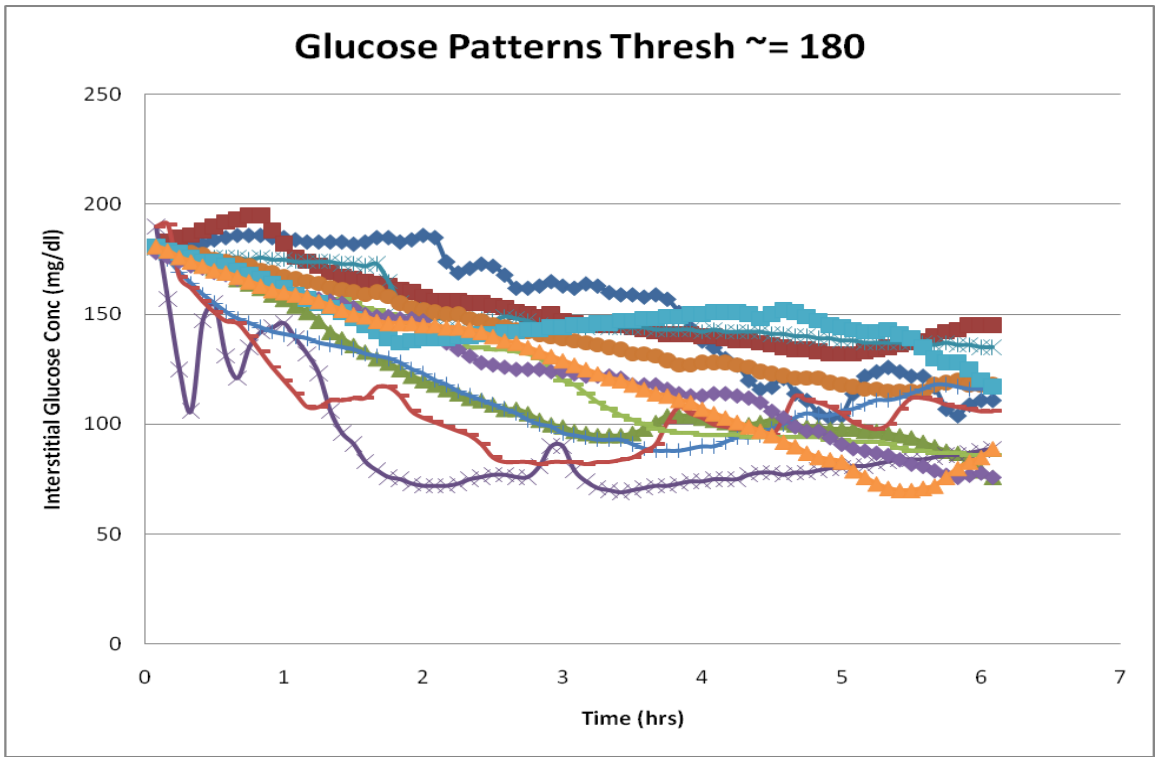

Figure 4-14. Patterns in Glucose: Critical Care Patients with Elevated Glucose (~180 mg/dl)

Table 4-18. Data Demographics of 12 Critical Care Patients in Figure 4-14

Pattern	Patient Type	Time Start (Hours)	Insulin Infused Over Time (units)
1	Cardiac	17.08	5.0
2	Trauma	11.16	11.0
3	Cardiac	3.67	18.0
4	Cardiac	0.08	0.0
5	Trauma	17.66	42.0
6	Cardiac	22.66	42.0
7	Cardiac	12.16	34.5
8	Trauma	12.00	0.0
9	Cardiac	17.91	42.5
10	Trauma	6.41	23.5
11	Trauma	10.00	61.0
12	Trauma	6.33	98.0

4.2.2 Determination of Optimal Neural Network Model Input/Predictor Variables Utilizing a Genetic Algorithm

A genetic algorithm implementing multiple linear regression (MLR) was generated for variable selection. In this genetic algorithm, 73 variables obtained through data-logging using the developed eCIDL were used as the x-block and the y-block was defined as CGM data. The genetic algorithm was utilized to effectively determine which variables are predictors of glucose concentration (i.e. CGM data). Figure 4-15 demonstrates the frequency of variable utilization at the 36th generation of this genetic algorithm. Variables used in each of the models/generations likely impact or are indicators of future glucose concentration. The variables utilized most frequently for prediction of glucose concentration as determined from genetic algorithm implementation are included in Table 4-19.

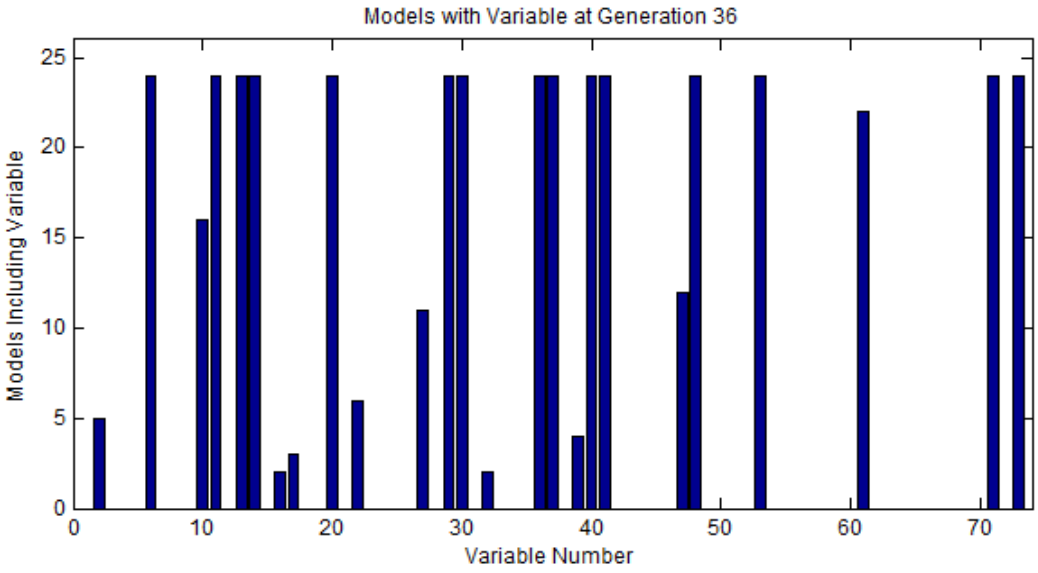

Figure 4-15. Number of MLR Based Genetic Algorithm Models Utilizing Each Variable

Table 4-19. Variables Determined as Predictors of Glucose (MLR based) Genetic Algorithm

Variable	Number of Models Utilizing Variable
Temperature	5
Heart Rate	24
Blood/Colloids	15
Packed Red Blood Cells	24
D5W	24
D5NS	24
NS	3
D5LR	4
NG (Resid)	6
Lab Category	11
Lab Results	24
Num Labs	24
PCWP	3
SVO2	24
SPO2	24
Med Class	4
Med Type	24
Med Dose	24
PAO2	12
PACO2	24
Gen. Phys Cond	24
POC Blood Glucose	24
CGM Sensor Current	24
Glycemic State	24

A second genetic algorithm implementing partial least squares (PLS) regression was generated for variable selection. In this genetic algorithm, the comprehensive 73 variable set was used as the x-block and the y-block was defined as CGM data. Figure 4-16 demonstrates the frequency of variable utilization at the 29th generation of this genetic algorithm. Variables used in each of the models/generations likely impact or are indicators of glucose concentration. The variables utilized most frequently for prediction

of glucose concentration as determined from genetic algorithm implementation are included in Table 4-20.

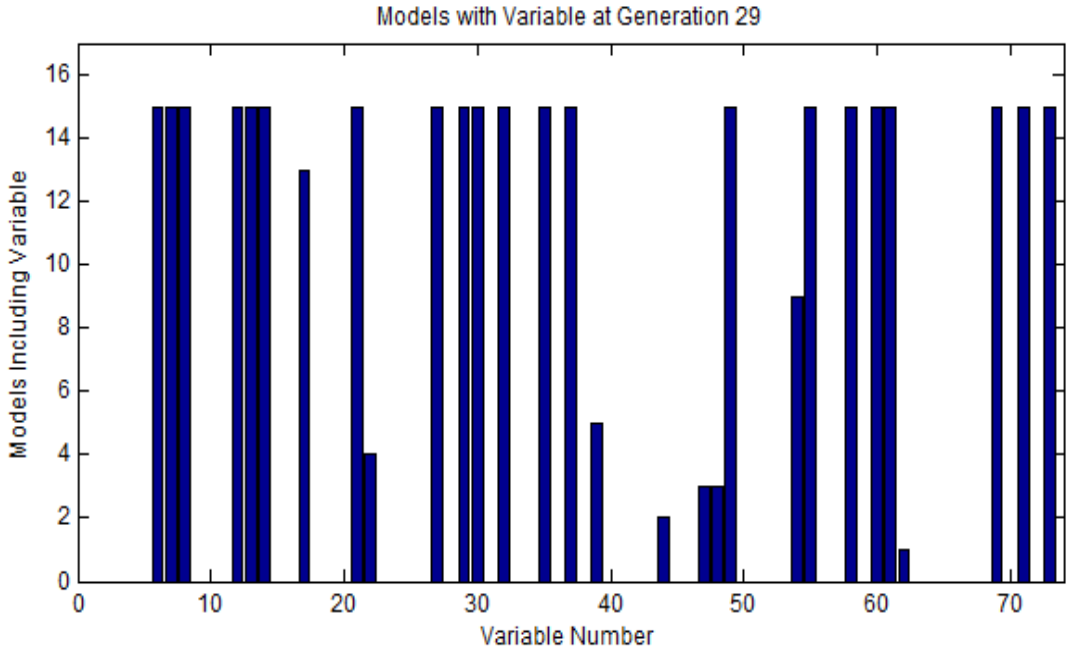

Figure 4-16. Number of PLS Based Genetic Algorithm Models Utilizing Each Variable

Table 4-20. Variables Determined As Predictors of Glucose (PLS based) Genetic Algorithm

Variable	Number of Models Utilizing Variable
HR	14
RR	14
SPO2	14
5% Alb	15
D5W	15
D5NS	15
D5LR	13
Time Period Collected	15
NG (Resid)	4
Lab Category	15
Lab Results	15
Num Labs	15
PCWP	15
SVR	15

SPO2	15
Med Class	4
Rate	2
PAO2	3
PACO2	3
pH	15
Conciousness	9
Activity	15
Nutrition	15
BG Test Time	15
POC BG(mg/dl)	15
Insulin	15
Pain Level	15
CGM Sensor Current	15
GS	15

4.2.3 Real-time Prediction of Glucose in Critical Care Patients Using Initial Model Weights

A neural network model implementing a reduced complexity feed forward neural network architecture was developed/trained with 6,188 (515.7 hours) data points from 5 critical care patients. Inputs/predictors to the neural network model included, CGM results, classified glycemic states, CGM device sensor current, POC glucose test times and results, insulin delivery type (infusion or subcutaneous), and units of insulin delivered. The neural network model's performance was tested on 5,444 data points (453.7 hours) from 4 patients not included in the original model training set. Model weights generated during initial model training/development were utilized during each iteration of the real-time predictive application.

Figure 4-17 contains the Clarke Error Grid containing the real-time predictions in 4 critical care patients. In this dataset, 81,660 predicted values were generated (15 predicted values for every CGM value). CEGA indicated that 97.5% of predicted values

were clinically acceptable with 67.9% and 29.6% falling within regions A and B of the error grid respectively. CEGA also indicated that .3%, 1.8%, and .3% of predicted values were in regions C, D, and E respectively, which would have resulted in predictions that would lead to inaccurate/adverse therapy.

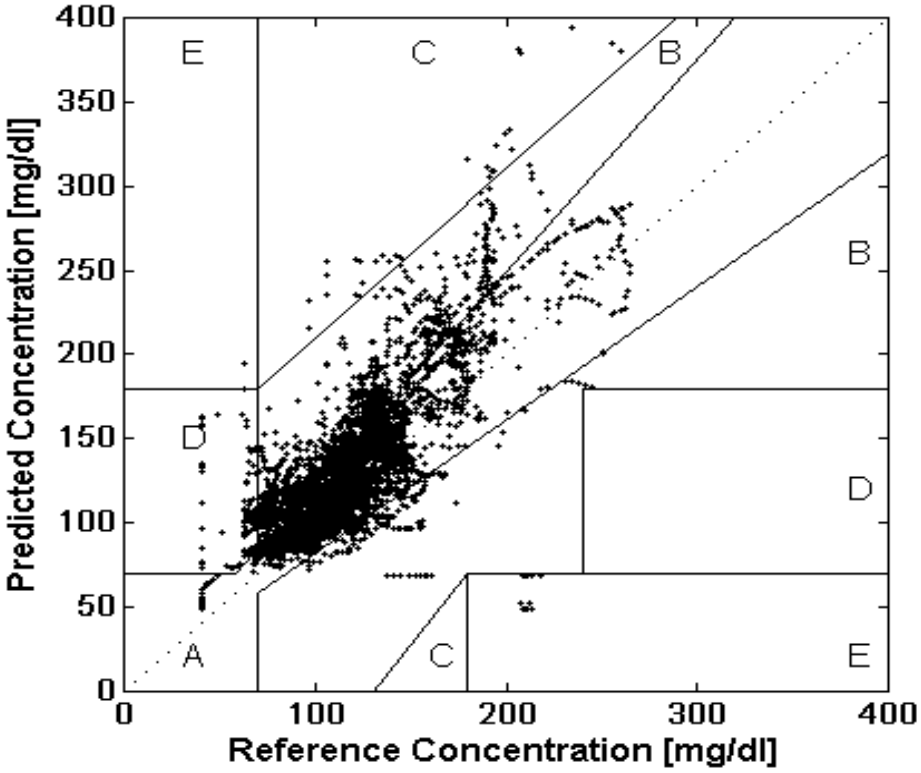

Figure 4-17. Clarke Error Grid of Predictions in 4 Critical Care Patients

Figure 4-18 contains the actual CGM and predicted CGM values generated by the real-time application for various glycemic extremes. Figure 4-18A demonstrates predictive accuracy at normal and near hypoglycemic extremes. Figure 4-18B includes predictions at hypoglycemic (≤70 mg/dl), normal, and elevated (≥150 mg/dl) glycemic extremes. Due to the large dataset of 81,660 predicted glucose values (i.e. 15 CGM values predicted for every CGM value in the test dataset) the data was re-sampled to demonstrate predictive accuracy in Figure 4-18. Re-sampling was completed via plotting

every 20th predicted CGM value and corresponding actual glucose value in the predictive dataset. The glycemic predictions track trends of the actual CGM values accurately. In calculating the overall error between actual and predicted CGM values, the MAD% was calculated as 17.3%. In this dataset, 86.7% of the hyperglycemic (elevated glucose ≥ 150 mg/dl) were predicted. In addition to this, 83.4% of normal glucose values (>70 and <150 mg/dl) were successfully predicted. A relatively small proportion of the test dataset was hypoglycemic (2.6%) and real-time prediction resulted in 14.7% of hypoglycemic glucose values (≤70 mg/dl) predicted.

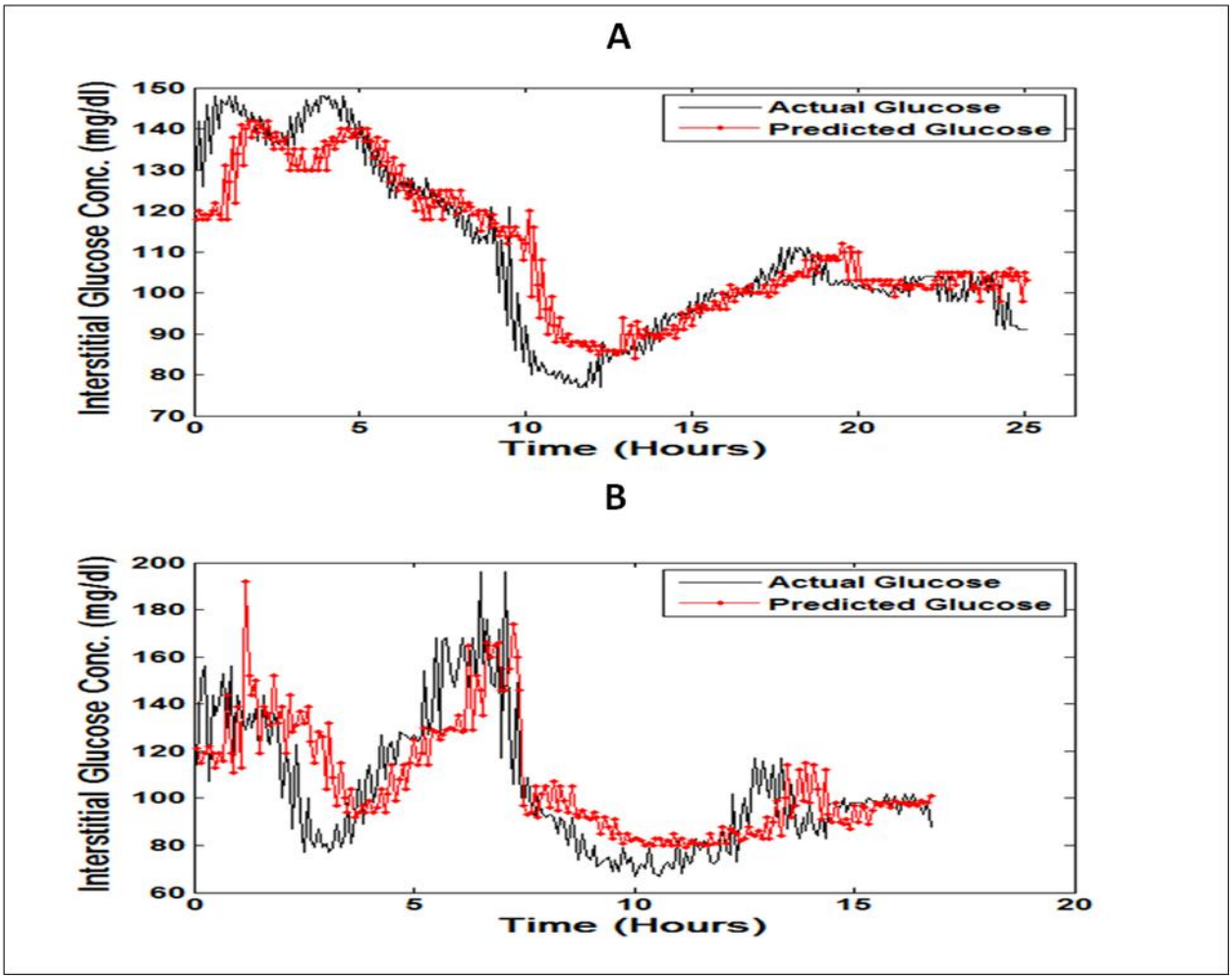

Figure 4-18. Real-time Prediction of Glucose at Various Glycemic Extremes in Critical Care Patient Data not Utilized for Model Training

4.2.4 Performance Analysis of a Patient Specific Neural Network Model

Figure 4-19 includes the real-time predictions on the test dataset using a patient specific neural network model. Due to the large dataset of 7,260 predicted glucose values (i.e. 15 CGM values predicted for every CGM value in the test dataset) the data was re-sampled to demonstrate predictive accuracy demonstrated in Figure 4-19. Re-sampling was completed by plotting every 20th predicted CGM value and corresponding actual glucose value in the predictive dataset. The overall error (MAD%) of the predictions generated using the patient specific model was calculated as 7.9%.

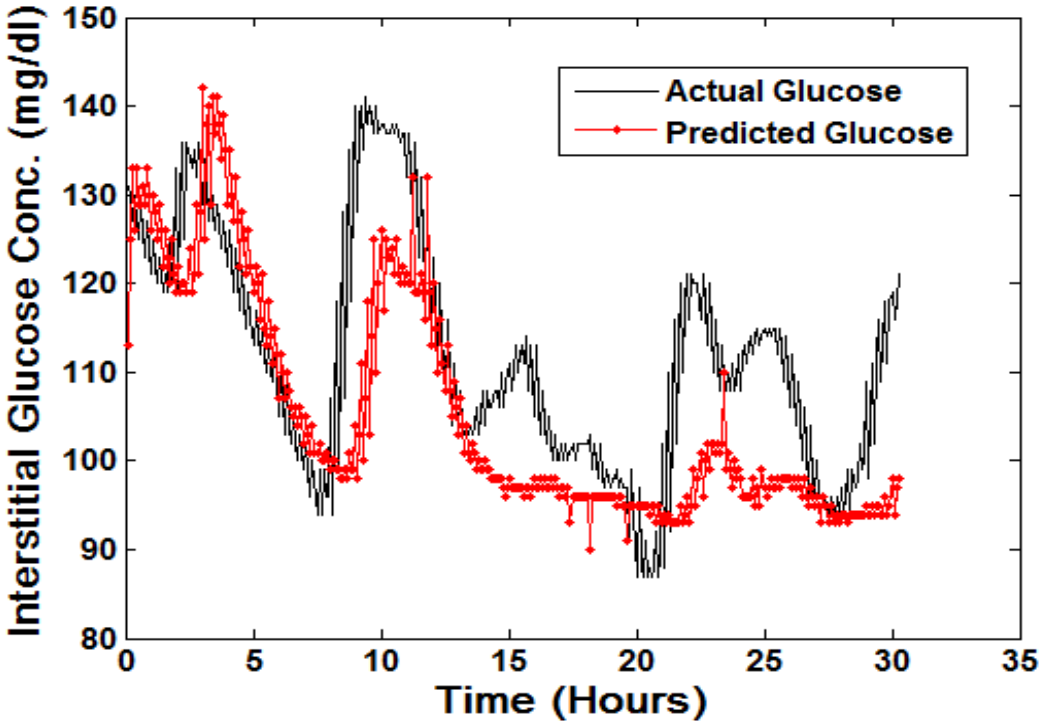

Figure 4-19. Prediction of Glucose Using Patient Specific Neural Network Model

Figure 4-20 includes the real-time predictions generated using the general neural network model analyzed in section 4.2.2. The overall error (MAD%) of the predictions generated using this general neural network model was calculated as 15.9%. The patient

specific model therefore generates more accurate predictions with a decrease in overall error of 8.0%.

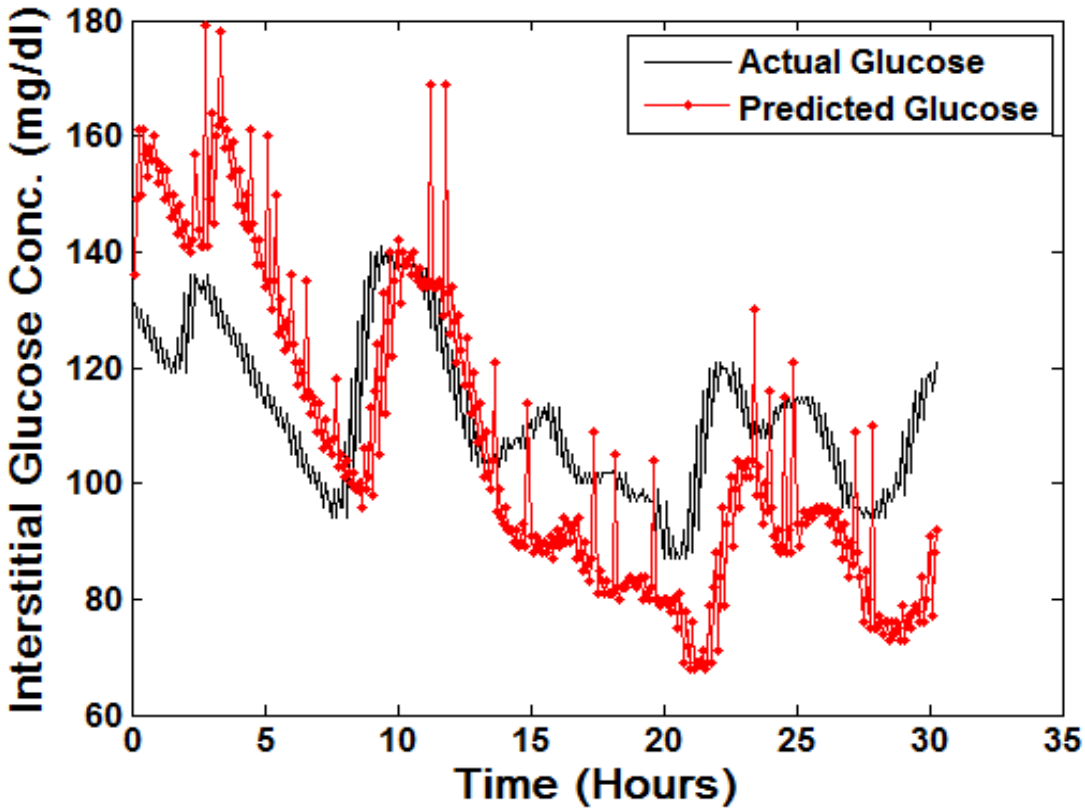

Figure 4-20. Prediction of Glucose Using General Neural Network Model

Figure 4-21 contains the Clarke Error Grid containing the real-time predictions generated via the patient specific neural network model. CEGA revealed that 95.1% of the predictions fell within region A of the error grid and 4.9% fell within region B of the error grid. Figure 4-22 contains the Clarke Error Grid containing the real-time predictions generated via the general neural network model. CEGA revealed that 69.8% of the predictions fell within region A of the error grid and 30.2% fell within region B of the error grid. In both instances 100% of the predicted CGM values could be considered clinically acceptable with no predicted values falling within regions C,D, or E of the error

grid. CEGA also revealed that the patient specific model generated predictions with a high degree of accuracy, as 95.1% of the values fell within region A of the error grid and had values within 20% of the reference glucose concentration.

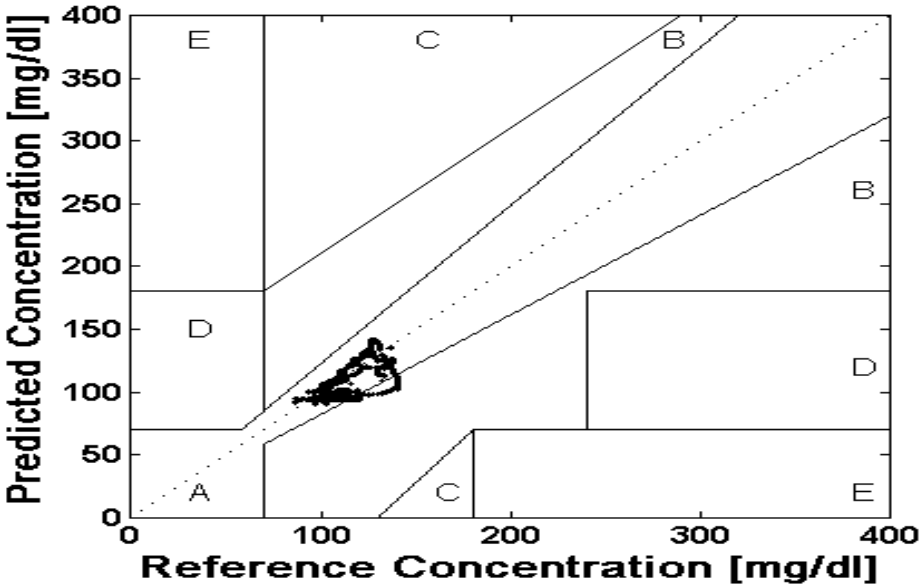

Figure 4-21. Clarke Error Grid of Predictions Generated by Patient Specific Model

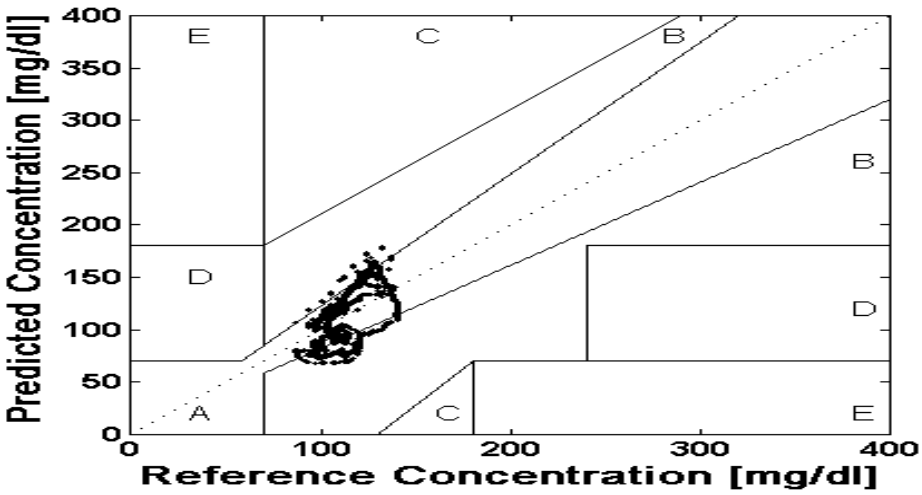

Figure 4-22. Clarke Error Grid of Predictions Generated by General Neural Network Model

4.2.5 Comparison of Predictive Performance in Models With Variable Prediction Horizons

Three feed forward neural network models were developed using the initial comprehensive model training set which included 19,989 data points. These models were developed with the optimized training set determined via genetic algorithm implementation presented in section 4.2.3. These neural network models were developed and configured to implement 30, 60, and 75 minute prediction horizons. Figure 4-23 demonstrates model predictive accuracy across the variable prediction horizons of 30, 60, and 75 minutes in three patients (A, B, and C) which were not utilized for model training. The models accurately predict trends in glucose concentration across various glycemic extremes. Figure 4-24 includes the Clarke Error Grid Analysis (CEGA) to assess clinical acceptability of each of the 30 (Figure 4-24-1), 60(Figure 4-24-2), and 75 (Figure 4-24-3) minute predictive models.

Table 4-21. Summary of Model Performance Given Variable Prediction Horizons

Prediction horizon (min)	**Overall Model Error (MAD%)**	**% of Normal Glucose Predicted**	**% of Hyperglycemia Predicted**
30	4.7	97.0	85.2
60	7.5	94.0	79.8
75	8.0	96.1	66.3

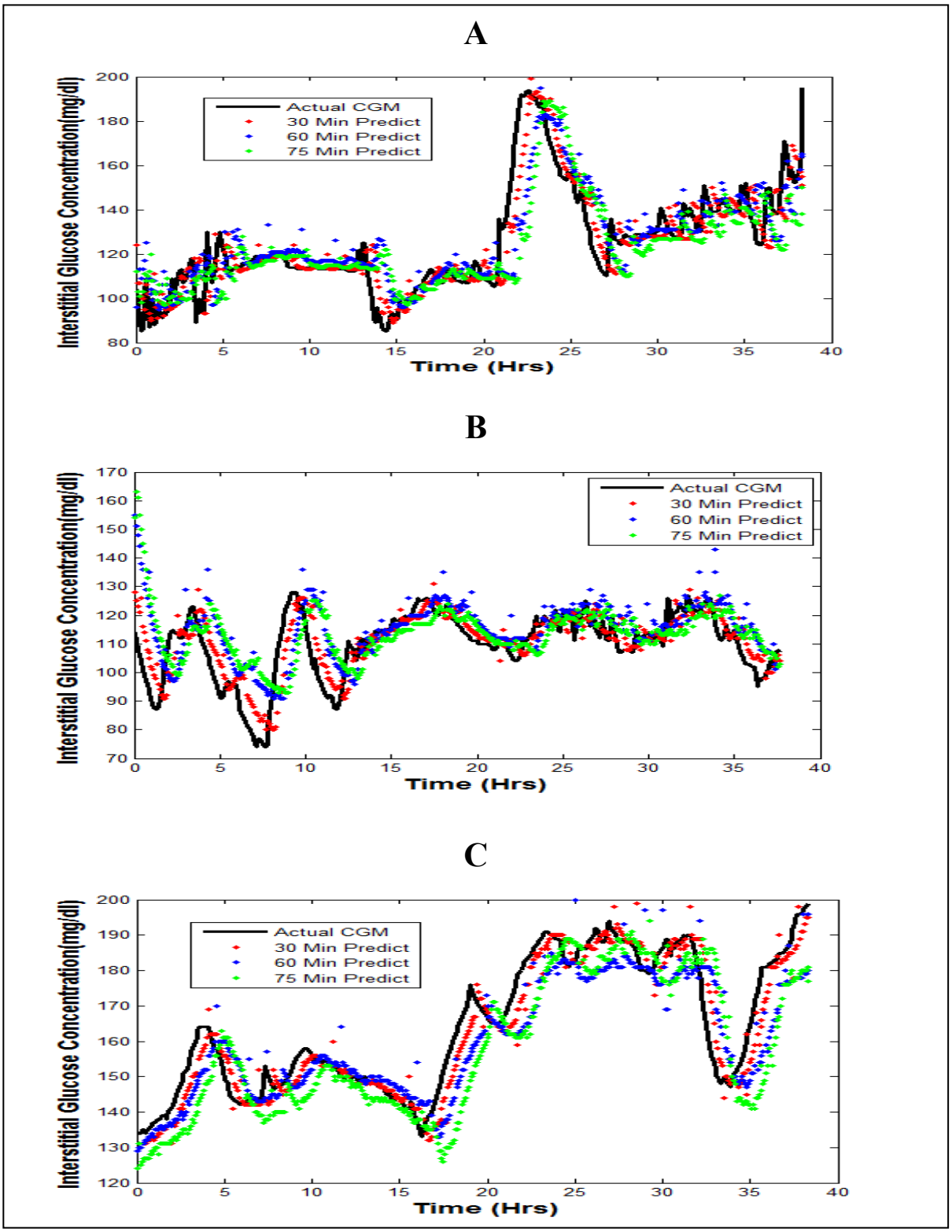

Figure 4-23. Models Implementing Variable Prediction horizons in 3 Critical Care Patients

Table 4-21 includes a summary of model performance given variable prediction horizons. As hypothesized, overall model error increases with an increase in prediction horizon. Furthermore, the percentage of hyperglycemic extremes decreases with an increase in prediction horizon. Percentage of normal glycemic extremes decreases between models implementing 30 and 60 minute prediction horizons, however, the model implementing a prediction horizon of 75 minutes predicts a higher percentage of normal glycemic extremes than the 60 minute predictive model. CEGA of the model predictions is summarized in Table 4-22. A majority of predictions generated by the predictive models fell within regions A and B and were considered clinically acceptable. The percentage of predictions in region A of the error grid decreased with an increase in prediction horizon. This correlates to an overall decrease in model accuracy with an increase in prediction horizon as hypothesized.

Table 4-22. Summary of Clarke Error Grid Analysis: Variable Prediction horizons

Prediction horizon (min)	**% Predictions in Region A**	**% Predictions in Region B**	**% Predictions in Region C**	**% Predictions in Region D**	**% Predictions in Region E**
30	98.6	1.40	0.00	0.00	0.00
60	91.5	8.20	0.20	0.00	0.10
75	91.0	9.00	0.00	0.00	0.00

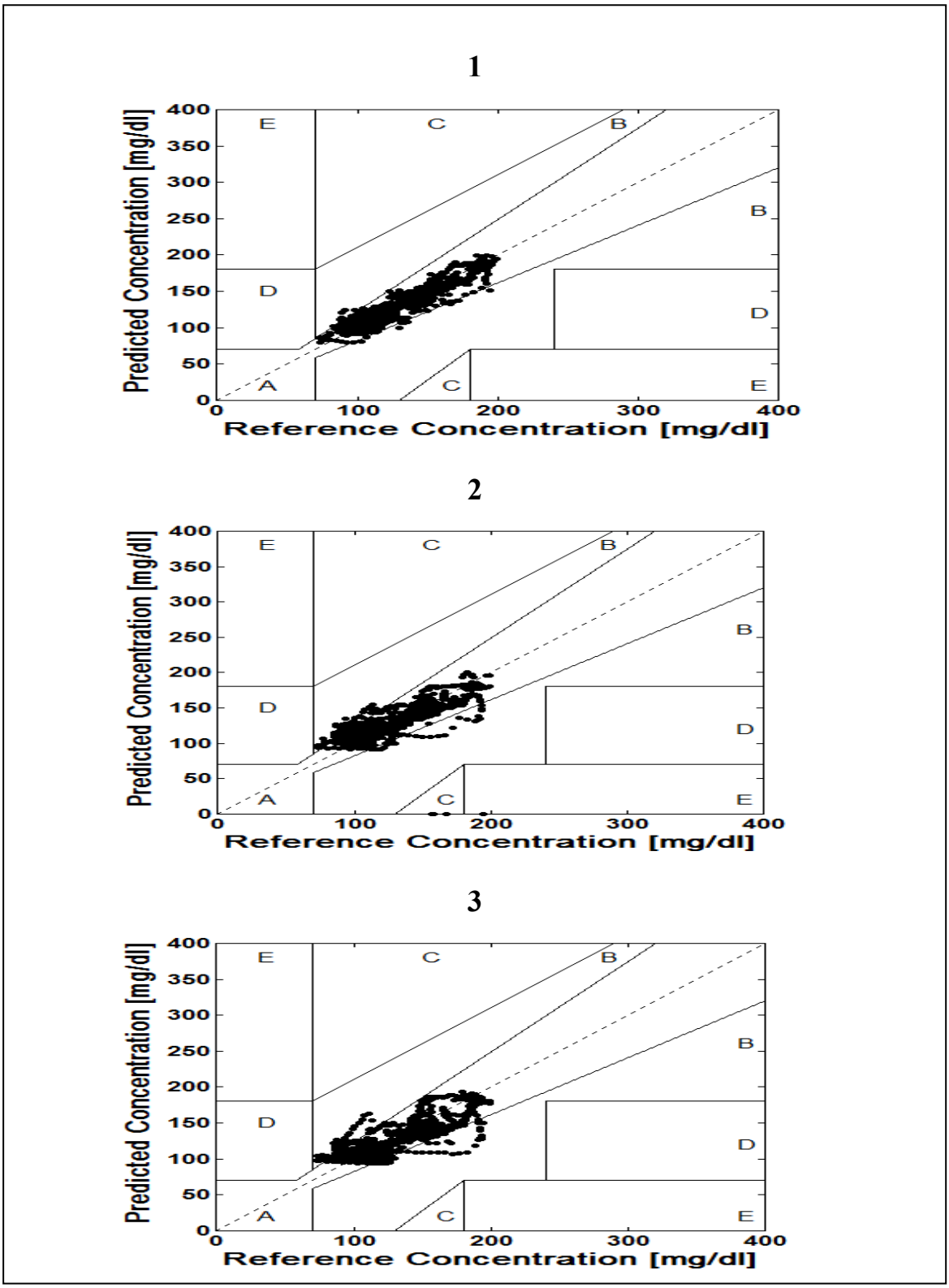

Figure 4-24. Clarke Error Grids of Models Implementing Variable Prediction Horizons

4.2.6 Comparison of Predictive Accuracy of Complex and Feed Forward Neural Network Model Architectures in Critical Care Patients

Figure 4-25 includes the comparison of predictive accuracy between multifunctional neural network (MFNN) models (with prediction horizons of 75 minutes) implementing time-lagged feed forward (TLFF) neural network (complex) architectures, and a reduced complexity feed forward neural network architecture. Performance analysis is completed on data from two patients (A and B) not included in the initial model training set. TLFF model architectures varied in terms of the forward and backpropagation trajectories, as well as the number of exemplars experienced before neural network model weights were updated. One TLFF neural network model was configured with a forward trajectory of 5, a backpropagation trajectory of 2 and configured to update model weights after 10 exemplars (5-2-10). A second TLFF neural network model was configured with a forward trajectory of 5, a backpropagation trajectory of 2 and configured to update model weights after 100 exemplars (5-2-100). A third TLFF neural network model was configured with a forward trajectory of 10, a backpropagation trajectory of 5 and configured to update model weights after 100 exemplars (10-5-100). A feed forward (FF) neural network model was developed and was configured with a forward trajectory of 1, a backpropagation trajectory of 1 and configured to update model weights after 100 exemplars (1-1-100). Overall, model predictions generated by TLFF (complex) neural networks architectures did not differ between the various configurations of forward and backpropagation trajectories, and exemplars per update as demonstrated in Figure 4-25A and 4-25B. Table 4-23 summarizes predictive accuracy of TLFF and reduced complexity feed forward (FF)

neural network architectures. Performance measures which were calculated include overall model error (MAD%), and percentage of hypoglycemic, hyperglycemic, and normal glycemic extremes predicted by each model implementation.

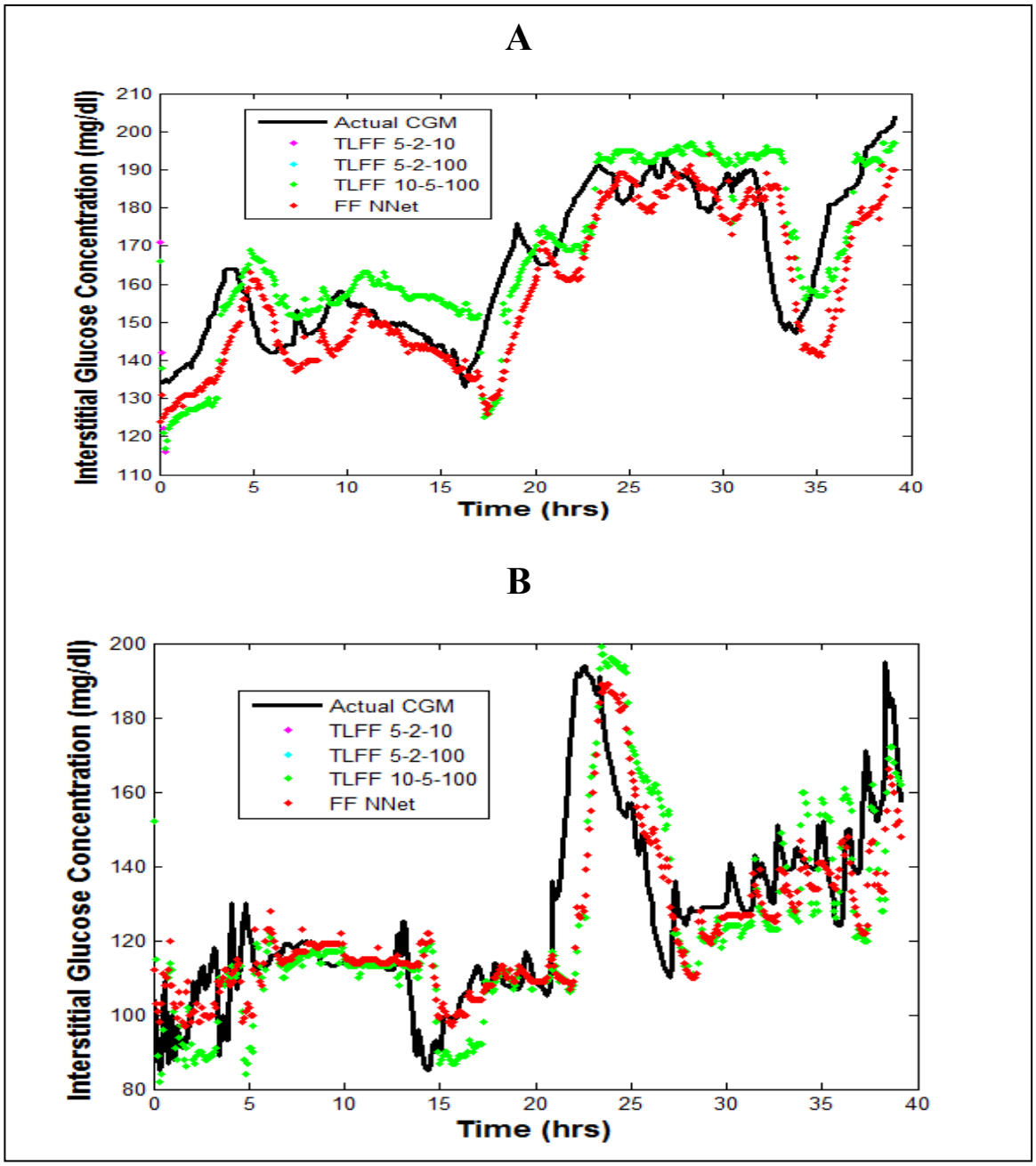

Figure 4-25. Predictive Accuracy: Complex and Reduced Complexity Model Architectures

Table 4-23. Summary of Predictive Accuracy Between TLFF and FF Model Architectures

Model Architecture	Overall Model Error (MAD%)	% Normal Glucose Predicted	% Hyperglycemia Predicted
TLFF	8.7	72.8	88.1
FF	7.4	93.8	67.6

Table 4-24 demonstrates the MFNN model predictive abilities of the TLFF and FF model architectures in prediction of general glycemic states in the two patients used for model performance analysis. Table 4-25 demonstrates model MFNN model predictive abilities of the TLFF and FF model architectures in prediction of specific glycemic states (1-7) in the two patients included for model performance analysis. Overall, a significant percentage of normal (>99.0%) and high general glycemic (88.6%) states were predicted via both modeling approaches. The performance of both model architectures in prediction of specific glycemic states demonstrated that performance varies between model architectures. The TLFF neural network model architecture performs more accurately overall at prediction of specific glycemic states than the FF modeling approach.

Table 4-24. Prediction of General Glycemic States in TLFF and FF Model Architectures

Glycemic State	Low	Normal	High
TLFF Model Architecture	N/A	99.6	88.6
FF Model Architecture	N/A	100	88.6

Table 4-25. Prediction of Specific Glycemic States in TLFF and FF Model Architectures

Glycemic State	1 (≤70)	2 (>70&<=100)	3 (>100&<=140)	4 (>140<=179)	5 (>=180&<=220)	6 (>220&<=300)	7 (>300)
TLFF Model Architecture	N/A	49.1	77.3	72.7	70.6	N/A	N/A
FF Model Architecture	N/A	47.4	80.8	74.6	42.2	N/A	N/A

Figure 4-26A and 4-26B includes the Clarke Error Grids containing predicted values obtained for TLFF (4-26A) and FF (4-26B) neural network model implementations applied in the two test patients. Table 4-26 summarizes Clarke Error Grid Analysis (CEGA) (in the two test patients) for both complex TLFF and FF neural network models. In both implementations 100% of predictions were clinically acceptable as indicated via CEGA. The FF neural network architecture had a higher percentage (94.2%) of its predictions which were more accurate and fell within region A of the error grid. Conversely, 90.7% of the predictions generated via TLFF neural network architecture fell within region A of the error grid.

Table 4-26. Summary of CEGA for TLFF and FF Model Implementations

Model Architecture	% Predictions in Region A	% Predictions in Region B	% Predictions in Region C	% Predictions in Region D	% Predictions in Region E
TLFF	90.7	9.30	0.00	0.00	0.00
FF	94.2	5.8	0.00	0.00	0.00

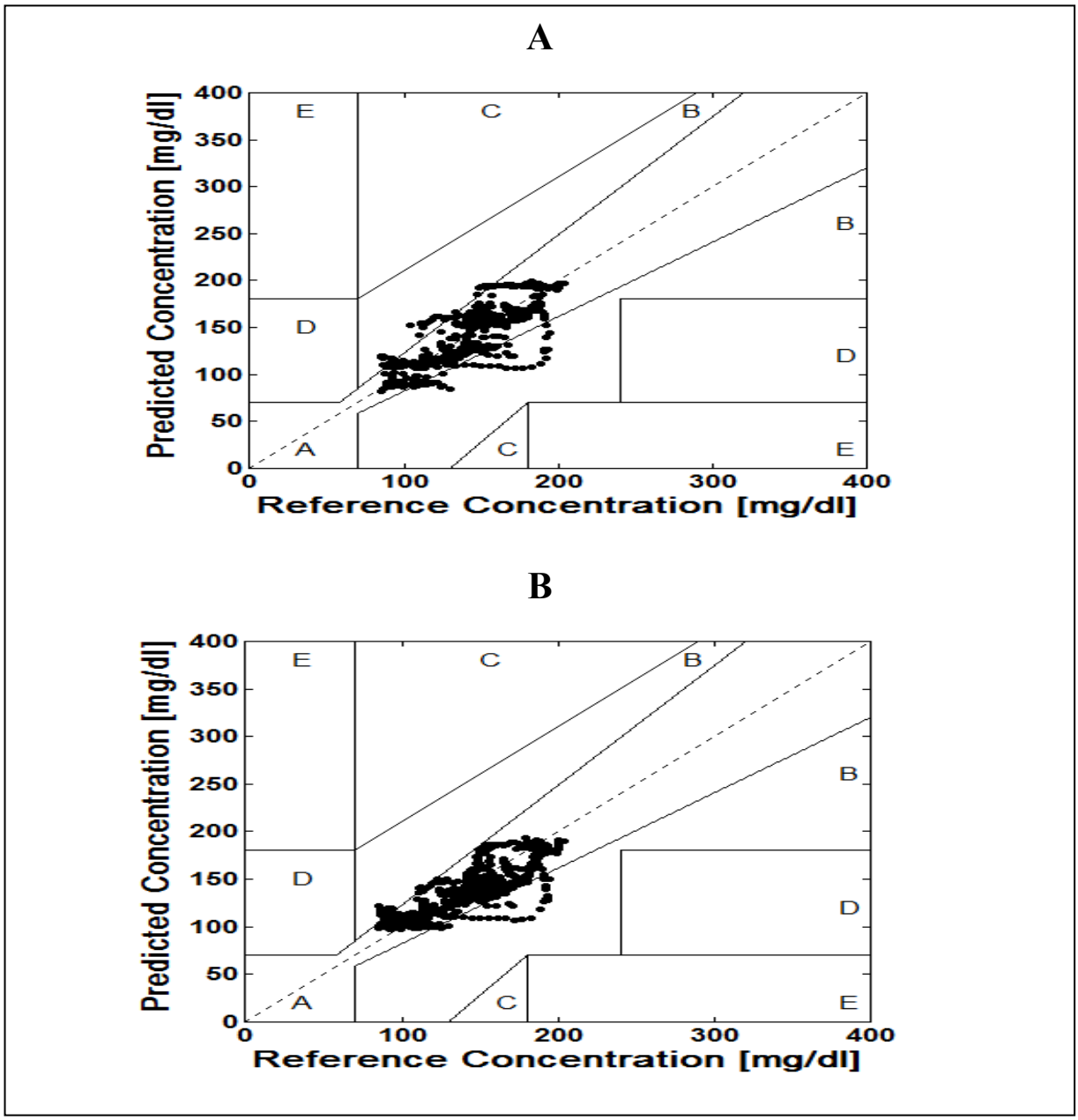

Figure 4-26. CEGA of Glycemic Predictions: TLFF(A) and FF(B) Neural Network Architecture

4.2.7 Preliminary Weight Analysis: Occurrence of Real-Time Events and Correlation to Neural Network Model Performance

This section contains the results obtained from the preliminary analysis of neural network model weights which were adapted using the neural network model implementing real-time training as outlined in section 3.3.7. In this analysis, weights from the output bias axon (main processing component in the output layer) are analyzed with respect to the reception of new neural network input data (CGM and medical records used for prediction) in real-time. Real-time input data was categorized according to the current real-time glucose threshold, historical insulin delivery, and occurrence of tachycardia. Output bias axon weights are grouped based on the occurrence of these real-time input data categories and performance of the neural network model in prediction of glucose (implementing a prediction horizon of 75 minutes) is correlated with these weight values. Model performance is divided into four categories: short term error (MAD% between first five actual and predicted glucose values), midterm error (MAD% between second five actual and predicted glucose values), long term error (MAD% between last five actual and predicted glucose values), and overall MAD% (MAD% across entire prediction horizon). Tables 4-27 through 4-33 contain the results of correlation analysis to calculate Pearson correlation coefficient values between the first output bias axon weight (offset value to calculate predicted glucose value) and each model performance category. The correlation analysis is focused on this only weight value as it is directly associated with the determination of the final predicted glucose concentration value of the neural network model.

The correlation analysis included in Table 4-27 reveals that there appears to be an increase in correlation with output axon weight values and model performance across the model prediction horizon (short term to long term MAD%) which is observed with the occurrence of tachycardia. This is indicative that adaptation of model weights in the output layer which occur with tachycardia will have more of an effect on predicting glucose in the long term than in the short term. This indicates that tachycardia may be an event which has effects on glucose which are seen in the time period 55-75 minutes after the detection of tachycardia in real-time.

Table 4-27. Tachycardia: Correlation of Output Axon Weights to Model Performance

Patient	Short Term MAD%	Midterm MAD%	Long Term MAD%	Overall MAD%
1	-0.14	-0.20	-0.23	-0.19
2	0.10	0.12	0.13	0.12
3	0.36	0.34	0.36	0.35
4	0.03	0.05	0.08	0.06
5	N/A	N/A	N/A	N/A
All	0.56	0.56	0.58	0.57

The correlation analysis included in Table 4-28 reveals that there appears to be a decrease in correlation with output axon weight values and model performance across the model prediction horizon (short term to long term MAD%) which is observed with the occurrence of a real-time glucose value (>70 and <150 mg/dl) and no historical insulin

delivery. This occurs in 3 of 5 test patients and is the trend in the 5 patients overall. This is indicative that adaptation of model weights in the output layer which occur with this glycemic threshold and no historical insulin delivery will have more of an effect on predicting glucose in the short term than in the long term. The occurrence of this glycemic threshold and no historical insulin delivery may be an event which has effects on glucose which are seen in the time period 5-25 minutes after its occurrence in real-time.

Table 4-28. Glycemic Threshold 2 (No Historical Insulin): Correlation of Output Axon Weights to Model Performance

Patient	Short Term MAD%	Midterm MAD%	Long Term MAD%	Overall MAD%
1	-0.26	-0.13	-0.09	-0.16
2	0.02	-0.00	0.13	0.03
3	0.08	0.53	0.62/	0.58
4	-0.12	-0.08	-0.02	-0.08
5	-0.21	-0.12	-0.15	-0.16
All	0.61	0.53	0.52	0.57

The correlation analysis included in Table 4-29 reveals that there appears to be an increase in correlation with output axon weight values and model performance across the model prediction horizon (short term to long term MAD%) which is observed with the occurrence of a real-time glucose value (>70 and <150 mg/dl) and historical insulin delivery. This occurrence is dominant in 1 of 2 test patients and is the overall trend

observed in both patients. This is indicative that adaptation of model weights in the output layer which occur with this glycemic threshold and historical insulin delivery will have more of an effect on predicting glucose in the long term than in the short term. The occurrence of this glycemic threshold and historical insulin delivery may be an event which has effects on glucose which are seen in the time period 55-75 minutes after its occurrence in real-time. This is likely attributed to the activity of the historical insulin dose.

Table 4-29. Glycemic Threshold 2 (Historical Insulin): Correlation of Output Axon Weights to Model Performance

Patient	Short Term MAD%	Midterm MAD%	Long Term MAD%	Overall MAD%
1	N/A	N/A	N/A	N/A
2	N/A	N/A	N/A	N/A
3	N/A	N/A	N/A	N/A
4	-0.21	-0.21	-0.40	-0.34
5	-0.02	-0.01	-0.01	-0.01
All	-0.09	-0.01	0.10	-0.01

The correlation analysis included in Table 4-30 reveals that there is a decrease in correlation with output axon weight values and model performance across the model prediction horizon (short term to long term MAD%) which is observed with the occurrence of a real-time glucose value ($\geq$150 and $\leq$190 mg/dl) and no historical insulin delivery. This correlation is observed in 2 of 3 test patients but is not established as the

overall trend in all patients. This is indicative that adaptation of output axon model weights in the output layer which occurs with this glycemic threshold and lack of historical insulin delivery may have more of an effect on predicting glucose in the short term than in the long term. The occurrence of this glycemic threshold and lack of historical insulin delivery may be an event which has effects on glucose which are seen in the time period 5-25 minutes after its occurrence in real-time.

Table 4-30. Glycemic Threshold 3 (No Historical Insulin): Correlation of Output Axon Weights to Model Performance

Patient	Short Term MAD%	Midterm MAD%	Long Term MAD%	Overall MAD%
1	-0.05	-0.07	-0.00	-0.04
2	N/A	N/A	N/A	N/A
3	0.23	0.24	0.25	0.24
4	N/A	N/A	N/A	N/A
5	0.03	0.02	0.01	0.02
All	0.10	0.11	0.10	0.10

The correlation analysis included in Table 4-31 reveals that there appears to be an increase in correlation with the output axon weight values and model performance across the model prediction horizon (short term to long term MAD%) which is observed with the occurrence of a real-time glucose value ($\geq$150 and $\leq$190 mg/dl) and historical insulin delivery. This occurrence is dominant in 1 of 2 test patients and is the trend across the 2

patients overall. This is indicative that adaptation of output axon model weights in the output layer which occurs with this glycemic threshold and historical insulin delivery will have more of an effect on predicting glucose in the long term than in the short term. The occurrence of this glycemic threshold and historical insulin delivery may be an event which has effects on glucose which are seen in the time period 55-75 minutes after its occurrence in real-time. This is likely attributed to the activity of the historical insulin dose.

Table 4-31. Glycemic Threshold 3 (Historical Insulin): Correlation of Output Axon Weights to Model Performance

Patient	Short Term MAD%	Midterm MAD%	Long Term MAD%	Overall MAD%
1	-0.10	-0.14	-0.22	-0.15
2	N/A	N/A	N/A	N/A
3	0.13	0.06	0.05	0.09
4	N/A	N/A	N/A	N/A
5	N/A	N/A	N/A	N/A
All	-0.10	-0.14	-0.21	-0.15

The correlation analysis included in Table 4-32 reveals that there appears to be an increase in correlation with the output axon weight values and model performance from short term to midterm MAD% which is observed with the occurrence of a real-time glucose value ($\geq$190 and $\leq$240 mg/dl) and no historical insulin delivery. After this

increase in correlation, the correlation coefficient returns to a similar value in long term MAD% as seen with short term MAD%. This increase in correlation is dominant in the only test patient which experienced this glycemic threshold and lack of insulin delivery. This is indicative that adaptation of output axon model weights in the output layer which occurs with this glycemic threshold and no historical insulin delivery will have more of an effect on predicting glucose in the midterm than in the short and long term. The occurrence of this glycemic threshold and historical insulin delivery may be an event which has effects on glucose which are seen in the time period 30-50 minutes after its occurrence in real-time.

Table 4-32. Glycemic Threshold 4 (No Historical Insulin): Correlation of Output Axon Weights to Model Performance

Patient	Short Term MAD%	Midterm MAD%	Long Term MAD%	Overall MAD%
1	N/A	N/A	N/A	N/A
2	N/A	N/A	N/A	N/A
3	0.22	0.40	0.28	0.29
4	N/A	N/A	N/A	N/A
5	N/A	N/A	N/A	N/A
All	0.22	0.40	0.28	0.29

The correlation analysis included in Table 4-33 reveals that there appears to be a decrease in correlation with the output axon weight values and model performance from

short term to long MAD% which is observed with the occurrence of a real-time glucose value ($\geq$190 and $\leq$240 mg/dl) and historical insulin delivery. This decrease in correlation is dominant in 1 of 2 test patients which experienced this glycemic threshold and historical insulin delivery. This trend is highly correlated when output weights are correlated to model performance in both patients. This is indicative that adaptation of output axon model weights in the output layer which occurs with this glycemic threshold and historical insulin delivery will have more of an effect on predicting glucose in the short term than in the long term. The occurrence of this glycemic threshold and historical insulin delivery may be an event which has effects on glucose which are seen in the time period 5-25 minutes after its occurrence in real-time. This may be attributed to glycemic responses following aggressive insulin delivery which occurs at this extremely elevated glycemic threshold.

Table 4-33. Glycemic Threshold 4 (Historical Insulin): Correlation of Output Axon Weights to Model Performance

Patient	Short Term MAD%	Midterm MAD%	Long Term MAD%	Overall MAD%
1	-0.67	-0.60	-0.55	-0.62
2	N/A	N/A	N/A	N/A
3	-0.64	-0.67	-0.67	-0.66
4	N/A	N/A	N/A	N/A
5	N/A	N/A	N/A	N/A
All	-0.93	-0.90	-0.85	-0.91

4.2.8 Real-time Prediction of Glucose in Five Critical Care Patients

This section includes the results of real-time prediction of glucose in five critical care patients not included in the comprehensive model training set. The neural network models were trained via methodology outlined in section 3.3.7 of this document. In this investigation, the real-time predictive application was configured for real-time training (updating and optimization of model weights) and prediction of glucose implementing a prediction horizon of 75 minutes. In addition to utilization of the real-time predictive system for weight adapation (hereafter referred to as the weight update method) the performance of neural network model (also implementing a prediction horizon of 75 minutes) which implements weights obtained via comprehensive model training (hereafter referred to as original weights) is compared with the weight update method. The real-time prediction of glucose (in the five critical care patients) for the weight update and original weights methodologies is included in Figure 4-27 [Figure 4-27A (weight update method) and Figure 4-27B (original weights method)]. Figure 4-27 demonstrates that the model implementing the original model weights is more accurate at prediction of glucose. The weight update method routinely overestimates glucose concentration values as well as overcompensates during rapid rates of change in glucose concentration. NOTE: The data was resampled to plot every 40^{th} actual and predicted value to better demonstrate predictive accuracy of the model with respect to changing glucose values. Clarke Error Grid Analysis (CEGA) and other methods of performance analysis was completed on all model predicted values.

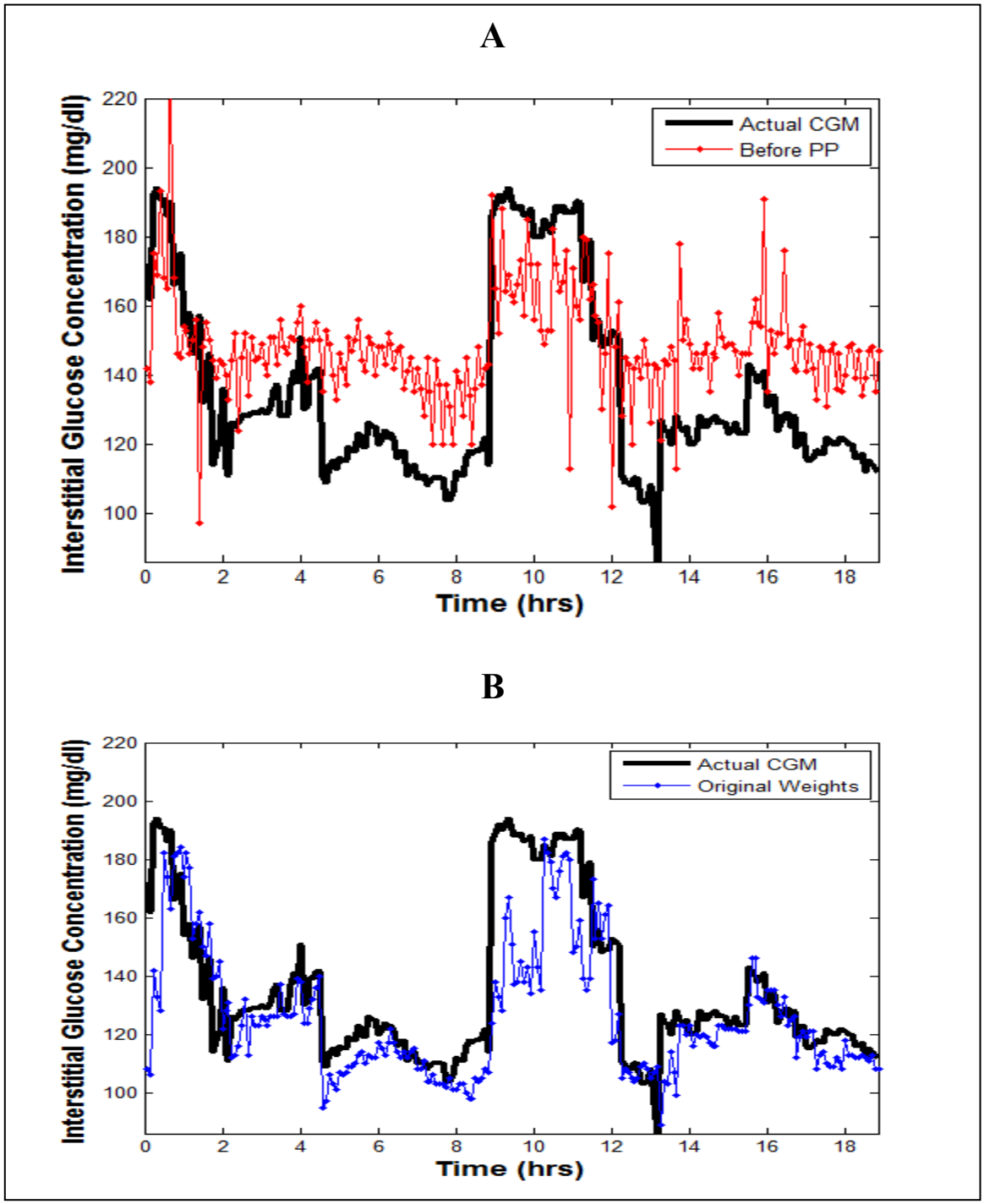

Figure 4-27. Real-time Prediction of Glucose in Five Critical Care Patients

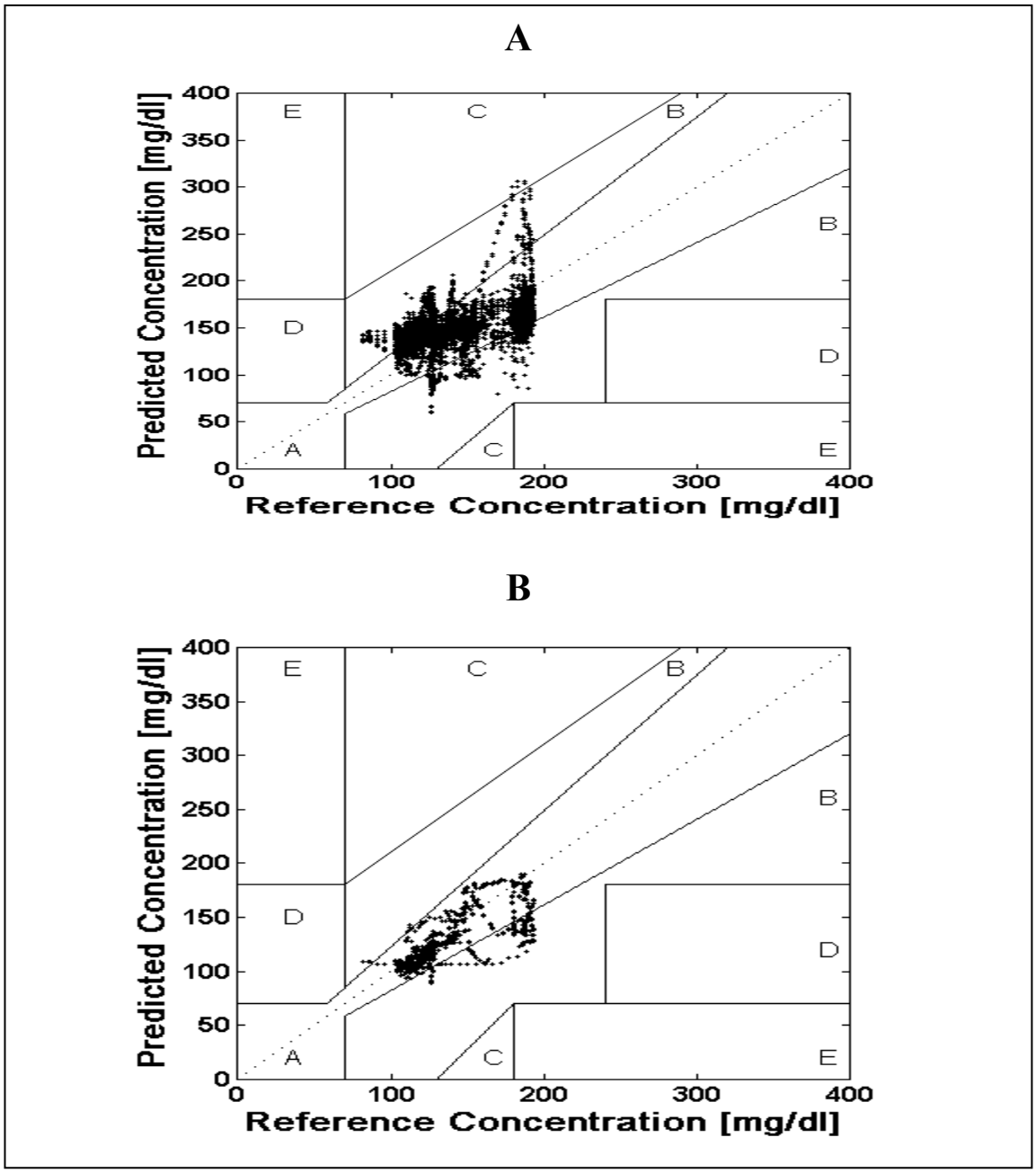

Figure 4-28. Clarke Error Grids: Real-Time Prediction of Glucose in Five Critical Care Patients

Clarke Error Grids containing real-time predictions are included in Figure 4-28. Figure 4-28A contains the Clarke Error Grid for the weight update model, and Figure 4-28B contains the Clarke Error Grid for the original weight method. Tables 4-34 and 4-35 summarize the CEGA and predictive accuracy of the weight update and original weight based models respectively. The model implementing original model weights was significantly more accurate than the weight update model (9.0 versus 18.0 MAD%). Furthermore, CEGA revealed that implementation of original model weights resulted in a significantly higher percentage of predictions falling within region A of the error grid (87.3% versus 62.1%). A higher percentage of normal glycemic extremes were predicted using the original model weights (96.7% versus 77.7%). The weight update model however, resulted in a significantly higher percentage of elevated/hyperglycemic glucose extremes (≥150 mg/dl) predicted successfully (80.0% versus 53.6%). This is due to the fact that the weight update model will update model weights when rapid rates of change in glucose are experienced which leads to detection of subsequent elevated glycemic excursions.

Table 4-34. Summary of CEGA and Predictive Accuracy (Weight Update Model)

Zone	A	B	C	D	E
Total in Zone	5617	3420	8	0	0
Percentage Of Data in Zone	62.1	37.8	0.1	0.0	0.0
Total in Dataset	9045				
Overall MAD%	18.0				
% data Hypo	0				
% Hypo Predicted	N/A				
% data Norm	76.6				
% Norm Predicted	77.7				
% data Hyper	23.4				
% Hyper Predicted	80.0				

Table 4-35. Summary of CEGA and Predictive Accuracy (Original Model Weights)

Zone	A	B	C	D	E
Total in Zone	7900	1145	0	0	0
Percentage Of Data in Zone	87.3	12.7	0.0	0.0	0.0
Total in Dataset	9045				
Overall MAD%	9.0				
% data Hypo	0				
% Hypo Predicted	N/A				
% data Norm	76.6				
% Norm Predicted	96.7				
% data Hyper	23.4				
% Hyper Predicted	53.6				

4.2.9 Development and Utilization of a Preliminary Post-Processing Algorithm to Increase Model Accuracy

Analysis of the data collected during the clinical investigation indicated the presence of patterns in future glycemic excursions in response to certain events. One such event was tachycardia, or an abnormal increased heart rate. Figure 4-29 demonstrates patterns in 15 critical care patients after a documented occurrence of tachycardia ($\geq$90 bpm). In these patients, no insulin was delivered 75 minutes before the occurrence of tachycardia and resulted in each patient having an overall increase in glucose concentration in the time domain 75 minutes after the detected occurrence of tachycardia. Patterns such as those included in Figure 4-29 provided the hypothetical construct for the development of an event-based post-processing algorithm for increasing overall model predictive accuracy.

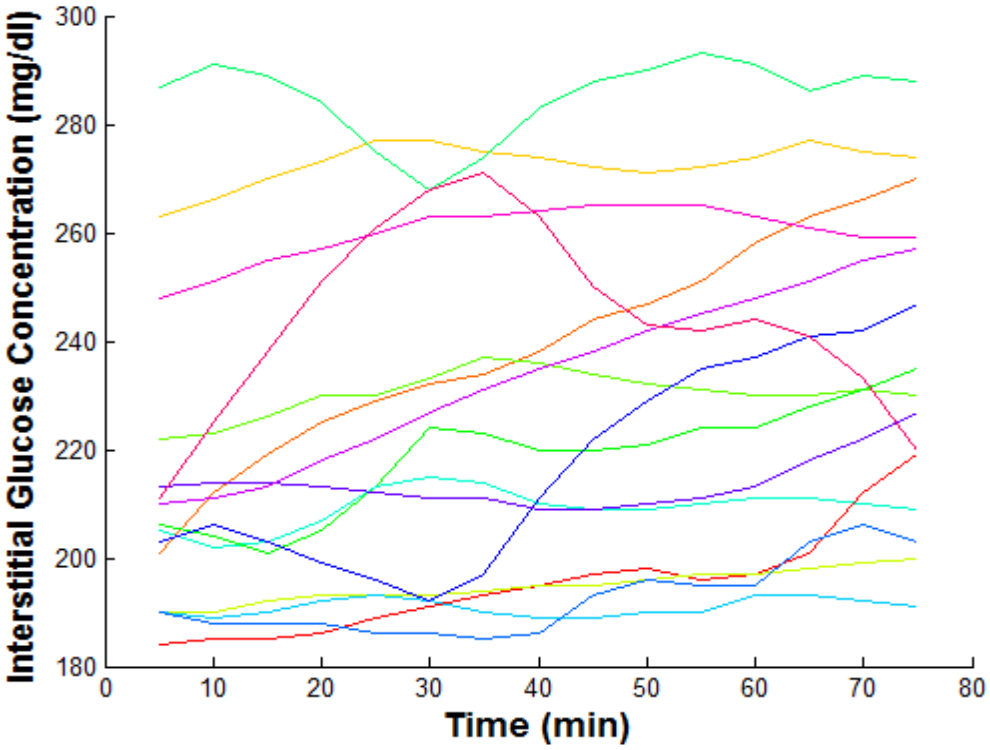

Figure 4-29. Patterns in Glucose in 15 Critical Care Patients Following Tachycardia

The post-processing algorithm generated in this investigation is outlined in section 3.3.10 of this document. This post-processing algorithm consisted of two post-processing implementations. The first method of post-processing consisted of an event-based post-processing algorithm, which modified neural network model output given occurrence of tachycardia, the current real-time glucose value (glycemic threshold), and whether or not historical insulin was delivered (within the time period 75 minutes before detected occurrence of tachycardia). There were a total of 10 detected occurrences of tachycardia in the 5 critical care patients utilized for real-time prediction of glucose concentration (presented in section 4.2.8). The post-processing algorithm was applied following these detected occurrences of tachycardia and model performance of the

unprocessed predictions was compared with the post-processed predictions. Figure 4-30 contains neural network model predictions (implementing a prediction horizon of 75 minutes) before and after post-processing.

Post-processed model predictions are more accurate but do not model the extent of glycemic variability (peaks and valleys) in the data. This is due to the limited nature of utilizing a third order polynomial model fit. The post-processed predictions estimate the final glucose value (glucose value 75 minutes after tachycardia) relatively accurately. Tables 4-36 and 4-37 summarize CEGA and predictive performance of the neural network predictions before and after post-processing in response to tachycardia. These results demonstrate that model accuracy is significantly higher after implementation of the post-processing algorithm with an MAD% of 12.1 whereas a MAD% of 26.7 was obtained without post processing. Prediction of glycemic extremes also improved after post-processing as 100.0% of normal (>70 and <150 mg/dl) and elevated ($\geq$150 mg/dl) glycemic extremes were predicted. Conversely, 63.7% and 53.3% of normal and elevated extremes were predicted before post-processing. Predictions with and without post-processing were all clinically acceptable as indicated by CEGA. CEGA revealed however, that post-processing implementation resulted in predictions with higher accuracy with 86.7% of predictions falling within region A of the error grid. In comparison only 27.3% of predictions fell within region A before post-processing.

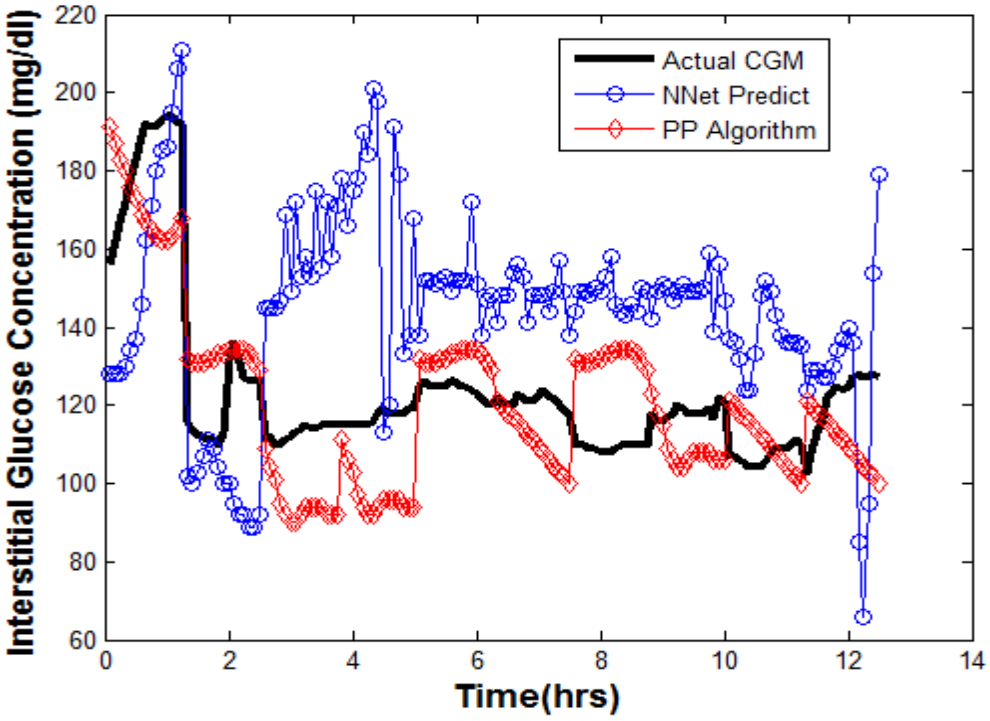

Figure 4-30. Application of Event-Based (Tachycardia) Post-Processing Algorithm

Table 4-36. CEGA and Predictive Accuracy: After Tachycardia (Before Post-Processing)

Zone	A	B	C	D	E
Total in Zone	41	109	0	0	0
Percentage Of Data in Zone	27.3	72.7	0.0	0.0	0.0
Total in Dataset	150				
Overall MAD%	26.7				
% data Hypo	0				
% Hypo Predicted	N/A				
% data Norm	90.0				
% Norm Predicted	63.7				
% data Hyper	10.0				
% Hyper Predicted	53.3				

Table 4-37. CEGA and Predictive Accuracy: After Tachycardia (After Post-Processing)

Zone	A	B	C	D	E
Total in Zone	130	20	0	0	0
Percentage Of Data in Zone	86.7	13.3	0.0	0.0	0.0
Total in Dataset	150				
Overall MAD%	12.1				
% data Hypo	0				
% Hypo Predicted	N/A				
% data Norm	90.0				
% Norm Predicted	100.0				
% data Hyper	10.0				
% Hyper Predicted	100.0				

The second method of post-processing included utilization of the offset existent between the current real-time glucose value and the first value in the neural network predicted output vector which was outlined in section 3.3.10. This post-processing algorithm was implemented when instances of tachycardia were not detected during the real-time prediction of glucose (implementing a prediction horizon of 75 minutes) in the five critical care patients presented in section 4.2.8. Figure 4-31 includes the real-time prediction of glucose before and after post-processing after post-processing (including tachycardia event-based post-processing) in the five critical care patients. NOTE: Data was resampled to plot every 40^{th} actual and predicted value to better demonstrate model predictive accuracy. Post-processing results in predictions which are significantly more accurate than model predictions generated before post-processing.

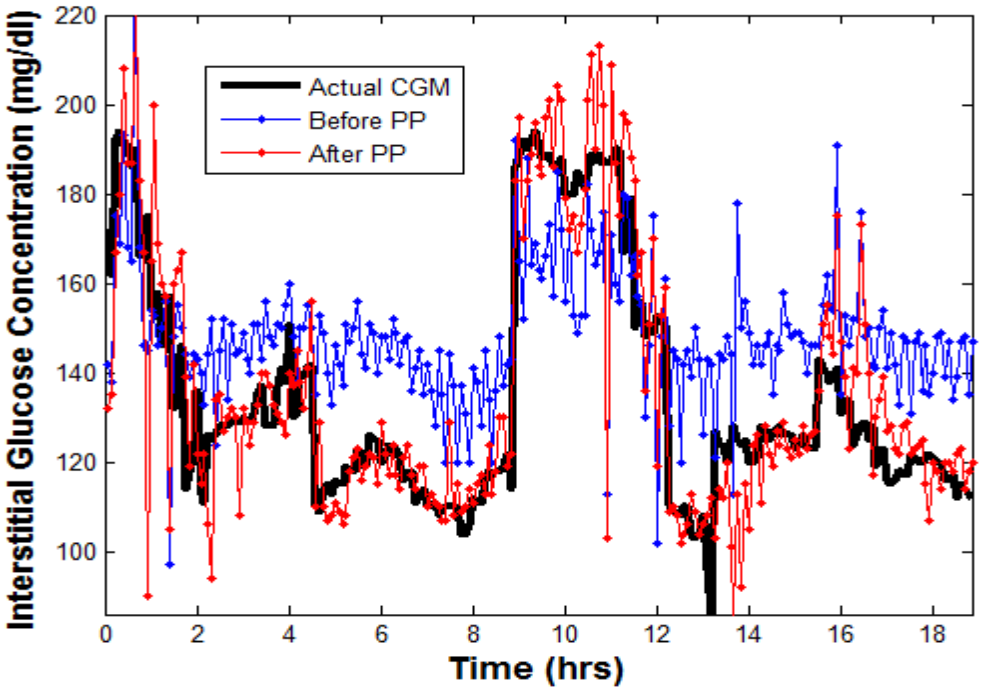

Figure 4-31. Real-time Prediction of Glucose: Before and After Post-Processing

Figure 4-32 contains the Clarke Error Grids generated for model predictions generated before (Figure 4-32A) and after post-processing (Figure 4-32B). Table 4-38 summarize CEGA and predictive accuracy of the model performance after post-processing in the complete five patient test dataset. Model performance before post-processing was previously included in Table 4-36. As is demonstrated in Figure 4-32, model predictions after post-processing are significantly more accurate with an overall MAD% of 7.1 in contrast to the MAD% of 18.0 obtained before post-processing. Furthermore, CEGA supported the observed increase in model accuracy after post-processing as 93.2% and 6.7% of predictions fell within regions A and B of the error grid. Before post-processing, only 62.1% and 37.8% of predictions fell within regions A and B of the error grid. Post-processing implementation is also correlated to an increase

in percentage of glycemic extremes predicted. After post-processing 94.5% and 86.8% of normal and elevated extremes were predicted, whereas only 77.7% and 80.0% of these extremes were predicted before post-processing. No hypoglycemia occurred in the five critical care patients used for model performance analysis.

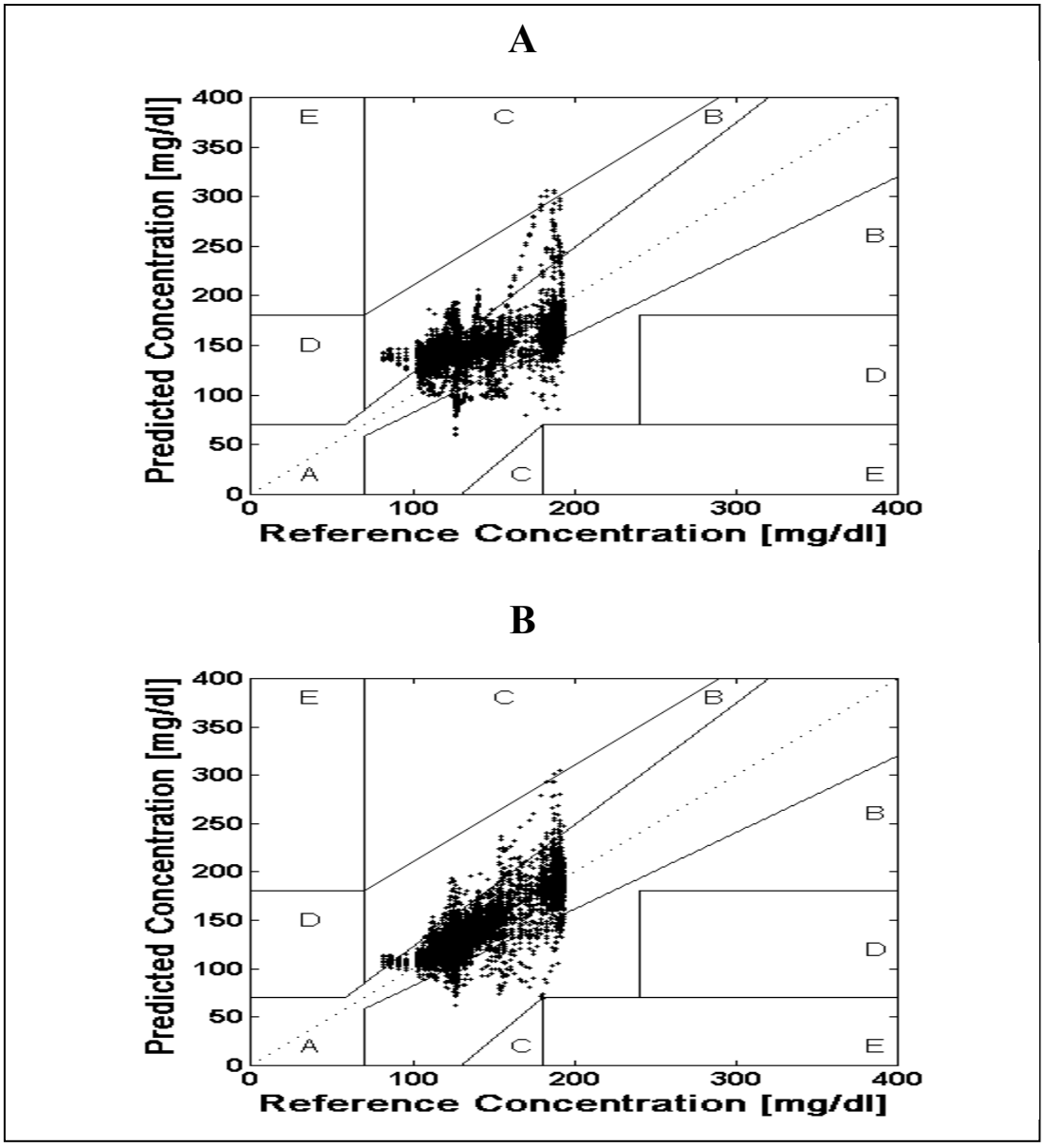

Figure 4-32. Clarke Error Grids: Glucose Prediction Before (A) and After Post-Processing (B)

Table 4-38. CEGA and Predictive Accuracy: After Post-Processing Implementation

Zone	A	B	C	D	E
Total in Zone	8430	609	3	0	3
Percentage Of Data in Zone	93.2	6.7	0.03	0.00	0.03
Total in Dataset	9045				
Overall MAD%	7.1				
% data Hypo	0				
% Hypo Predicted	N/A				
% data Norm	76.6				
% Norm Predicted	94.5				
% data Hyper	23.4				
% Hyper Predicted	86.8				

CHAPTER 5

DISCUSSION

5.1 Goals

The goal of this research was the development and performance evaluation of predictive models for glucose in insulin dependent diabetic and critical care patient populations. Literature review has established that tight glycemic control in both populations correlates to enhancement of patient outcomes. The decreased occurrence of complications such as but not limited to: retinopathy, neuropathy, and nephropathy in diabetic patients is an observed benefit of tight glycemic control. In the critical care patient population, observed decreases in morbidities, mortality, infections, and length of stay in the intensive care unit have been correlated to tight glycemic control. Neural network models for prediction of glucose and the performance of these models was the goal of this research investigation. To be defined as a clinically acceptable predictive model, an overall error (MAD%) of 14.0-21.0% (error of CGM device with respect to serum glucose values obtained via reference handheld glucose meter) is desired as well. Furthermore, Clarke Error Grid Analysis (CEGA) of the predictions should yield a majority of predictions with regions A and B of the error grid. A majority of predictions within region A is most desirable as it would indicate that predictions are clinically acceptable and have error less than 20% with respect to reference CGM device glucose measurements.

To date, glycemic predictive models in patients with diabetes have had limited prediction horizons of 30-60 minutes. These predictive models have variable complexity and range from simple rate of change based models to more complex models incorporating the effect of various variables on future glucose concentration. Historically, a majority of these predictive models predict discrete handheld metered glucose values which limit the accuracy and efficacy of predictions. Furthermore, most models which incorporate the effect of other variables on future glucose concentration have utilized insulin, exercise, and nutritional intake as input variables. In this investigation, the utilization of continuous glucose monitoring (CGM) enables the prediction of a complete vector of glucose values up to the length of the prediction horizon. Additionally, the utilization of CGM and more frequently sampled glucose values enables the prediction of glucose using significant prediction horizons. Furthermore, the effect of other variables known to effect glucose concentration such as emotional factors (e.g. stress, depression, etc), and lifestyle factors (e.g. sleep-wake cycles, work schedules, etc) were utilized as inputs into the neural network model. In this investigation, initial neural network model development implementing a time-lagged feed forward neural network architecture for prediction of glucose using prediction horizons/horizons of 50-180 minutes are demonstrated. Real-time prediction of glucose using a multifunctional feed forward neural network architecture implementing a prediction horizon of 75 minutes is also demonstrated.

The goal of this research was to substantiate that prediction of a complete vector of glucose values using a significant prediction horizon is possible. A further goal of this investigation was the evaluation of the clinical acceptability and accuracy of these models

in real-time is within the error of CGM devices and within regions of acceptability based on Clarke Error Grid Analysis (CEGA).

To date there has been little glycemic predictive model development for the critical care population. Furthermore, there has been relatively limited utilization of CGM in the critical care setting. Models have been developed for prediction of insulin delivery requirements for maintaining tight glycemic control and applied in a critical care setting. [68,70,71] While these models have experienced some success, most of these models base insulin delivery requirements on discrete point of care (POC) glucose values. A PID control algorithm for use in critical care patients was one of the few insulin delivery estimation algorithms which has been integrated with a CGM device. [70,85] Utilization of a PID control algorithm is reactive as insulin dosage estimates are based off of current (proportional), area under glucose curve (integral), and rate of change in glucose (derivative). These algorithms and the previous insulin estimation algorithms previously discussed do not take into account other factors such as but not limited to medications, vital signs, ventilation data, special clinical events and nutritional intake which may impact or be indicators of future glycemic excursions. A futher goal of this investigation is the development of neural network models for prediction of glucose in the critical care patient population. Neural network models have the ability to quantify the effect of a variety of input variables on future glycemic excursions. A secondary goal of this investigation is the performance analysis and determination of the clinical acceptability/applicability of the developed neural network models based on the criteria previously outlined in this section. Furthermore, analysis of neural network model weight adaptation based on changing input variables (temperature, heart rate, respiratory

rate, real-time CGM data, and insulin delivery) and the subsequent effect on glycemic predictions is evaluated. The utilization of these results for preliminary development of post-processing algorithms to enhance model accuracy is also investigated.

5.2 Limitations of the Developed Neural Network Models for Diabetic Patients

Neural network models developed and applied in patients with insulin dependent diabetes had various limitations. One such limitation was overestimation of hypoglycemic extremes observed in model predictions. This was due to the percentage of hypoglycemic data present in the initial model training set. The CGM dataset used for the training of the neural network models had a relatively low incidence of hypoglycemia (1460 CGM values $\leq$70 mg/dl), which corresponded to approximately 7.9% of the dataset. On the contrary, hyperglycemia comprised approximately 35.7% of the dataset (6560 CGM values $\geq$180 mg/dl), and euglycemic (normal) values allotted for 56.4% of the dataset (10,380 CGM values >70 and <180 mg/dl). This inadequacy in hypoglycemic training data can be correlated directly to the observed decrease in neural network performance for predictions at hypoglycemic extremes. Further data acquisition with an increased quantity of hypoglycemic data is a necessary step in future investigation and will likely correlate to improvement in the neural network model's ability to predict hypoglycemia.

Another limitation of the developed neural network models for diabetic patients was the possible inaccuracy of input variables documented using the handheld data-logger included in Figure 3-1. It is also important to note that data logged via the use of the electronic data-logger may have been entered incorrectly by patients involved in the study; however, it was difficult to identify such instances if they occurred. To mitigate

errors of this type, patients were instructed and trained on the methods to record data prior to their involvement in the study. If an input in the final patient dataset appeared to be inaccurate (e.g. an uncharacteristically large insulin dosage) the data was removed from the dataset and set to zero (i.e. no input). Given that patients with diabetes would need to utilize the glycemic predictive model in an outpatient setting, it is difficult to provide a –eontrolled" setting in which parameters logged using the data-logger can be deemed accurate. In this investigation patients were not instructed to use the data-logger at a specific frequency therefore the utilization of the data-logger varied amongst the patients enrolled in the investigation. Future investigation is warranted in which the patients are instructed to use the data-logger at a frequency of every 1-3 hours. The more intensive documentation of input variables utilizing the data-logger would likely provide a means for enhancement of model accuracy.

5.3 Limitation of Developed Neural Network Models for the Critical Care Patient Population

Neural network models developed in this investigation for prediction of glucose in the critical care patient population predict trends in future glycemic excursions accurately. Throughout the course of the clinical investigation however, various occurrences led to modification of methodologies involving patient recruitment/enrollment, conversion of paper based medical records to electronic medical records via the developed clinical intensive data-logger, and neural network model optimization/development.

Patient enrollment in the clinical investigation did not reach original expectations which were outlined in the initial project proposal. Various factors contributed to

decreased patient enrollment. One such factor was the departure from the University of Toledo Medical Center (UTMC) of our initial principal investigator for the clinical side of the investigation. This departure occurred during initial IRB approval phase, which resulted in a significant delay in achieving IRB approval for the clinical investigation. This delay in clinical investigation therefore contributed directly to a decrease in patient enrollment. Another factor which contributed to decreased patient enrollment in the investigation included the decreased incidences of trauma at UTMC. The decreased incidences of trauma are hypothesized to be due to the ongoing economic crisis in the United States. The majority of trauma patients admitted to UTMC are motor vehicle accident (MVA) victims. Due to the ongoing economic crisis and increasing prices of gasoline it is hypothesized that the incidences of MVAs were decreased and limited.

Due to the decreased enrollment of trauma patients in the clinical investigation, the IRB document was amended to include cardiothoracic surgical patients with elevated glucose ($\geq$150 mg/dl). The inclusion of this patient population resulted in increased patient enrollment, however, postoperative cardiothoracic patients have a decreased length of stay in the intensive care unit of 2-3 days relative to trauma patients which have an average length of stay of approximately 1-2 weeks. Although there was increased patient enrollment following inclusion of cardiothoracic surgical patients, the data derived from this patient population was not near original expectations. During the course of the clinical investigation the main cardiothoracic surgeon at UTMC departed the institution which also resulted in decreased patient enrollment.

Although patient enrollment did not reach expectations, neural network models developed in the investigation predict and follow trends in glucose accurately. It is

important to note however, that although neural network models developed in this investigation accurately predicted glycemic excursions, accuracy could have been dramatically improved with a larger and more extensive dataset on which to train neural network models. As encountered in the diabetes clinical investigation, neural network models were developed with a training set which contained a limited quantity of hypoglycemic data. The lack of a sufficient quantity of hypoglycemic data resulted in the neural network models routinely overestimating hypoglycemic extremes. Neural network models optimize predictive success via recognition of patterns, and trends in model training set, and a more extensive training set (including more CGM data at various hypoglycemic, normal, and hyperglycemic extremes) would provide a means for the model to determine more patterns/trends in data. This would directly result in an increase in overall model accuracy.

Data collected for the investigation was collected in a controlled setting in which the paper based medical records documented by clinical staff in the intensive care unit were presumed accurate. Various medical students, and graduate students at the University of Toledo Health Science Campus were recruited to utilize the developed electronic clinical intensive data-logger (eCIDL) to convert the paper medical records into an electronic format. All investigative personnel were initially trained in operation of the eCIDL, as well as merging data into a cumulative electronic spreadsheet for use in neural network model development. Investigative personnel were instructed to monitor that the data logged using the developed eCIDL was the same as documented in the paper based medical records. Although investigative personnel were heavily trained in this process, there still exists a significant possibility that data may have been logged

inaccurately. A factor leading to significant inaccurate data-logging included lack of uniformity by clinical staff in terms of how paper based medical records are documented. For example, some nursing staff members circle and date medications which are delivered, while others place a line through and date the medication to signify delivery. Another example of this includes nursing staff documentation of insulin delivery in the critical care patient population. Insulin infusion is recorded in a diabetic flowsheet where some nursing staff signify an increase/decrease in insulin infusion rate with an upwards/downwards arrow and the new insulin infusion rate next to the arrow. On the contrary, other nursing staff members log insulin infusion with an arrow and the number of units per hour increased/decreased from the previously implemented insulin infusion rate next to this arrow. These are only a few examples of the diversity existent in medical records documentation by clinical and nursing staff at UTMC, which may have lead to inaccurate recording of electronic medical records via the developed eCIDL. Another factor possibly leading to inconsistencies in electronic medical records obtained via utilization of the eCIDL included the legibility of the handwriting in the paper based medical records. Furthermore, delays in the data logging process due to missing medical records, and medical student/graduate student availability also resulted in delays in neural network model development/design.

A large number of clinical staff were involved in the investigation at the University of Toledo Medical Center. The clinical staff including nurses, residents, and attending physicians was constantly changing. Efforts were made to alert clinical staff about the research investigation such that patients who met eligibility requirements were approached for study consent. To facilitate this process, two large posters were generated

which included patient eligibility characteristics, investigation design, and contact information for obtaining consent. These posters were placed within the surgical intensive care unit, and the trauma bay at UTMC such that a majority of patients meeting eligibility requirements could be approached for consent. Although this process was completed, some patients meeting eligibility were not appropriately and timely identified for subsequent consent and enrollment in the clinical investigation. As previously discussed, if more of the eligible patients were recruited for the investigation this would result in a more extensive dataset and increased model accuracy.

5.4 Performance of Neural Network Models: Prediction of Glucose in Patients with Diabetes

Neural network modeling for the prediction of glucose in patients with insulin dependent diabetes as presented in this document represents a novel and unique methodology. Neural network modeling is well suited for modeling such a complex system in which multiple variables such as but not limited to physiologic, lifestyle, and emotional factors impact future glycemic excursions. Literature review and discussion with endocrinologists lead to the determination of inputs to be utilized by the neural network model for prediction of glucose in the diabetic patient population. This section will focus on the performance analysis of the neural network models developed for prediction of glucose in prediction of patients with diabetes. Furthermore, comparison of the models generated in this investigation with previously developed predictive models and models used for determination of insulin requirements to maintain a normal glucose concentration is discussed.

Prediction of glucose using various approaches has been the subject of many

historical research attempts. These predictive models have ranged in complexity from autoregressive models to model predictive control based algorithms. [35-37] In these modeling approaches prediction of glucose using prediction horizons of 30-120 minutes were obtained. Even though CGM was utilized in the development of autoregressive models, the prediction horizons of 30-60 minutes obtained via these modeling techniques limit their clinical and patient applications. In patients with diabetes, prediction of glucose 120 minutes ahead of time is extremely advantageous. Following a meal and insulin bolus to cover nutritional intake, a diabetic patient commonly experiences elevated glucose within the two hour time frame following this event if insulin dosages are not adequate. Two hour post prandial glycemic control is thus an extremely important measure in determining overall glycemic control a diabetic patient can achieve. The autoregressive model generated by Reifman et al was also designed to implement a prediction horizon of 120 minutes. This resulted in considerably less accuracy in overall model error and prediction of hyperglycemic and hypoglycemic extremes than the 30-60 minute predictive models. [37] A further limitation of the modeling techniques using CGM and prediction horizons of 30-60 minutes is the lag which exists between interstitial fluid and serum glucose concentration. [99-102] The time lag between interstitial glucose and serum glucose has been determined to range between 5 and 15 minutes. Therefore, given the prediction horizons of 30-60 minutes, the actual prediction of glucose can range from 15-45 minutes given a maximum time lag of 15 minutes. It is also important to note that in the modeling techniques discussed previously, meal intake, activity, lifestyle factors (e.g. sleep-wake cycles), emotional factors (e.g. stress, depression), time of day, etc were not fully incorporated into the predictive models.

Performance analysis of the initial time-lagged feed forward neural network models demonstrate that models accurately predict trends and patterns in glucose values across prediction horizons of 50-180 minutes. Accuracy of the models in prediction of glucose decreases with an increase in prediction horizon. An overall error (MAD%) of 6.9-18.9% across the prediction horizons of 50-180 minutes was achieved. The ability of the neural network model to predict the extent (overall magnitude) of hyperglycemia decreases as the prediction horizon is increased. This is an expected outcome, as large rates of change which lead to hyperglycemic extremes $\geq$250 mg/dl are not readily predictable given such large prediction horizons. In most cases however, although the overall magnitude of hyperglycemia is not predicted, the prediction of hyperglycemic extremes ($\geq$180 mg/dl) is accomplished. This is of direct benefit to clinician and patient in terms of therapeutic direction and support.

Neural network models generated in this investigation were demonstrated to predict glucose using prediction horizons of 50-180 minutes. In comparing the performance of the neural network models across the various prediction horizons, there is an observed increase in overall model error (MAD%) associated with an increase in model prediction horizon from 6.7% to 14.5%. It is important to note however, that the neural networks ability to predict hyperglycemic extremes ($\geq$180 mg/dl) remains relatively consistent across prediction horizons of 50-120 minutes. Using a prediction horizon of 120 minutes resulted in the prediction of 97.2% of hyperglycemic extremes. This is an important result which demonstrates that prediction of hyperglycemia remains consistent and performance does not decrease given an increase in prediction horizon.

Previous autoregressive model development by Reifman and colleagues did not

provide in depth predictive results obtained using a 120 minute prediction horizon and instead focused on 30-60 minute predictions. [37] There is no basis to compare model predictive ability between the neural network models generated in this investigation with previously developed modeling techniques as reported performance measures differ between each approach. It is important to note however, that utilizing the neural network model approach developed in this investigation results in consistent performance in prediction of hyperglycemia up to a prediction horizon 120 minutes. Using large prediction horizons of 120, 150, and 180 minutes resulted in the prediction of 97.2, 79.0, and 71.6% of hyperglycemic extremes, therefore, a majority of hyperglycemic extremes are successfully predicted implementing these significant prediction horizons.

Using a neural network model for prediction of glucose enables the assessment of multiple variables on future glycemic excursions and trends. This approach is advantageous due to the effect of many factors on glycemic excursions such as but not limited to: lifestyle, emotional, nutritional intake, and medication/insulin dosages. These factors being incorporated into a predictive model enabled the prediction of glucose using extended prediction horizons as demonstrated in this investigation. Prediction of glucose using such expanded prediction horizons may enable patients with diabetes to more accurately optimize therapy in anticipation of hypoglycemic or hyperglycemic excursions. Furthermore, the prediction of a complete vector of glucose values up to the prediction horizon will enable the assessment of trends in glucose in response to the various factors and therapy of the patient which has not yet been completed in research endeavors to date.

A majority of today's diabetes research is aimed at the development of a closed

loop artificial pancreas for maintaining tight glycemic control. A well known approach in development of a closed loop artificial pancreas for maintaining normal glucose concentration includes implementation of a classic control algorithm: the proportional integral derivative (PID) controller. [32-34] The classic PID control algorithm is used to control a system based on proportional, integral, and derivative values. In terms of glycemic control, the proportional value determines the reaction to the current glucose value, the integral value determines the reaction based on the sum of recent glucose values, and the derivative value determines the reaction based on the rate of change of glucose. The weighted sum of these three actions is used to adjust the process via a control element. The PID controller was chosen to be implemented in closed loop control due to the fact that it mimics physiologic β cell insulin secretion.[116] The β cell is responsible for secreting insulin in response to increases in glucose concentration to obtain normal glucose concentration.

While the PID control algorithm has been subject of many research attempts to develop a closed loop artificial pancreas, such a control algorithm is limited in functionality. The PID control algorithm cannot appropriately integrate the occurrence of the multiple factors which may impact or are indicators of future glycemic trends. Patients who have diabetes often have a degree of autonomic insufficiency in which the counter-regulatory hormonal response is delayed or in some circumstances inexistent. [117,118] Given utilization of a PID control algorithm there is no input or ability to quantify the occurrence of lifestyle and emotional factors such as exercise or stress which have a known effect on increasing adrenal response and a corresponding elevation of glucose. Utilization of a PID control algorithm would respond to this ―perceived"

elevation of glucose via delivery of insulin. This would be an inappropriate response, which may lead to the occurrence of hypoglycemia. Given the degree of autonomic insufficiency that patients with diabetes commonly experience, this would be a very dangerous occurrence. Patients with diabetes often experience hypoglycemic unawareness a condition in which the patient does not realize they are in a hypoglycemic state, which combined with autonomic insufficiency would lead to prolonged occurrences of hypoglycemia.[119-121]

A further limitation of implementing a PID algorithm for closed loop glycemic control is the inability to account for nutritional intake. A PID control algorithm would not be able to distinguish meal content and insulin dosage needed to maintain a normal glycemic state. While an observed increase in glucose concentration following a meal would be accounted for, the overall insulin to cover total nutritional intake could not be determined via utilization of the PID controller. A system which takes into account approximation of carbohydrate/caloric intake would be more capable of maintaining tight glycemic control in response to a meal. A closed loop PID controller would therefore need to have at least a ―meal button" to initiate to account for nutritional intake. Even in the presence of such a ―meal button", the meal content at specific meals and times of day would need to be consistent for optimizing glycemic control given the utilization of such a control algorithm.

To address the potential limitations of the PID controller algorithm and other previously employed modeling techniques, the neural network modeling approach outlined in this document was designed and investigated as an alternative modeling approach. A neural network model based predictive system is well suited to model the

effect of various factors on future glycemic excursions and trends. An implementation of a semi-closed loop system with automated therapy based on patient input of factors affecting glucose would be able to identify factors which correlate to a temporary elevation in glucose such as exercise and stress and not result in overly aggressive treatment in response to the perceived elevation in glucose. Research into the development of such a semi-closed loop system has been subject of research endeavors of Skevofilakas and colleagues. [122] In this investigation, Skevofilakas developed a system which integrates various factors on prediction of glucose and subsequent insulin needed for maintaining a normal glycemic control. Prediction of glucose and optimal insulin dosage was completed via utilization of a neural network model for short term glucose prediction as well as a compartmental model to model glucose absorption in the gut in response to nutritional intake. While such an implementation involves a more comprehensive model for glucose, the short term prediction of glucose, as well as lack of incorporating factors such as lifestyle and emotional state which impact glucose may limit this approach. A neural network approach such as the models developed in this investigation with prediction horizons of 50-180 minutes would provide more insight on which therapeutic guidance and automation may be optimized.

The accuracy of the neural network models developed in this investigation ranged from 6.7-27.0 MAD%. Real-time implementation of the neural network based predictive model with a prediction horizon of 75 minutes had MAD% values ranging from 19.0-27.0%. Lack of hypoglycemic data of which to train and develop the neural network models result in the overestimation of hypoglycemic extremes. If error was recalculated at non-hypoglycemic extremes, overall model error (MAD%) is considerably reduced.

Error of CGM devices with respect to serum glucose values has been reported to be between 14.0-21.0% (MAD%). [123] Therefore, the model accuracy and overall MAD% of the models generated in this investigation fall within this reported error range which makes them acceptable models for prediction and forecasting glucose concentration in the diabetic patient population. Furthermore, utilization of Clarke Error Grid Analysis (CEGA) revealed that real-time application of the neural network based models resulted in $\geq$90.0% of predicted values falling within regions A and B of the error grid. This result is indicative of the clinical acceptability of the predicted glucose values. Given that the error of the predictions falls within the reported error range of the CGM device and $\geq$90.0% of predictions could be regarded as clinically acceptable based on CEGA, such a predictive system has a significant degree of clinical applicability in its current state.

Although the predictive models in their current state provide significant accuracy, future research will be directed at optimization. A unique feature of the developed models is the multifunctional neural network approach in which the prediction of two outputs related to glucose concentration is achieved. The prediction of numerical glucose concentration values is often associated with considerable error. The models are configured to predict classified ranges of glucose concentration or glycemic states in addition to numerical concentration. This multifunctional approach can accomplish two tasks. First, the prediction of glycemic states may provide just as useful information to the patient/caregiver as prediction of numerical concentration values. Secondly, prediction of two variables will provide a means to gauge accuracy of predictions. If the two predicted values coincide with each other, the predictions are likely accurate. Preliminary multifunctional neural network model application in the diabetes patient population

resulted in successful prediction of a majority of general glycemic states predicting 88.0-94.0% of normal glycemic states, and 70.6-80.5% of hyperglycemic glucose states. Due to limited quantity of hypoglycemic training data models routinely overestimated hypoglycemic states. Prediction of specific glycemic states resulted in accuracy ranging from 10.2-73.0%. The reduced prediction of lower normal glycemic states was also attributed to the quantity of lower normal glycemic states (>70 and $\leq$100 mg/dl) present in the initial model training set. Further research aimed at enhancing the accuracy of model predictions such as development of post-processing algorithms will be subject of future research and will discussed in a later section of this document.

The neural network models developed in this investigation also predict a high percentage of normal (>70 and <180 mg/dl) and hyperglycemic ($\geq$180 mg/dl) extremes. Model performance in terms of the real-time prediction of normal glucose extremes is $\geq$ 75.0%, and $\geq$80.0% in prediction of hyperglycemic extremes. Utilization of such predictive models for therapeutic direction/assistance would therefore directly benefit patients with diabetes in gauging if insulin doses are adequate for maintaining normal glycemic control. The prediction of glucose using the extensive prediction horizons >60 minutes as demonstrated in this investigation may provide a construct for semi-closed loop and perhaps eventually closed loop automated and optimized therapy leading to tight glycemic control in patients with diabetes.

5.5 Prediction of Glucose in the Critical Care Patient Population

Point of care (POC) glucose monitoring of critical care patients and implementation of an insulin infusion protocol is the current standard of care to obtain tight glycemic control. This approach is limited in that POC glucose monitoring only provides discrete glucose values every 1-4 hours throughout a patient's length of stay in the ICU. Research has been completed to develop models to predict glucose and/or insulin requirements to maintain normal glucose concentration in critical care patients. [68,71] While these models have experienced success, it is hypothesized that modeling of glucose and insulin requirements for maintaining normal glucose concentration in the critical care patient population can be enhanced via the neural network model approach outlined in this dissertation. Neural network models have the ability to incorporate the effect of a variety of factors routinely documented in a critical care patient's medical record which may be predictors or indicators of future glycemic excursions. Furthermore, CGM technologies are only recently being investigated for their potential as a diagnostic/assistive tool in the ICU. [89] Based on the review of the current literature, the neural network model approach outlined in this investigation is one of the first predictive models utilizing CGM for prediction of glucose in this critical care patient population. Furthermore, utilization of this modeling approach (as will be outlined in this section) enables the ability to predict a complete vector of glucose values with large prediction horizons which have not be obtained in previous research investigations.

The neural network models developed in this investigation for glycemic forecasting in critical care patients accurately predict trends in glycemic excursions. Performance analysis revealed that a majority of predictions generated via this neural

network modeling approach were clinically acceptable as determined via Clarke Error Grid Analysis. Prediction of glucose via the developed approach can be utilized for intelligent therapy direction and ultimately automation given future development and increased model accuracy. Given the degree of accuracy of models generated in this investigation, models may be used in their current state by clinical staff to support their clinical judgments and assist in therapeutic direction for maintaining tight glycemic control in the critical care setting.

5.5.1 Patterns in Glucose in the Critical Care Population: A Foundation for Model Development

Previous research has eluded to patterns in glucose in critical care patients. [57-59] These patterns were identified via utilization of discrete POC glucose measurements which are routinely collected during a patient's length of stay in the ICU. In this investigation, similar patterns in response to insulin infusion were identified using CGM. CGM makes it possible to further identify trends in glucose in response to insulin infusion and other factors, which makes modeling glycemic excursions using the neural network model approach outlined in this document well suited for prediction of glucose.

Figure 4-14 demonstrates patterns in glucose in response to insulin infusion when glucose values of critical care patient reach a threshold of approximately 180 mg/dl. Most of the glycemic responses in these patients follow the expected trend of a decrease in glucose as the glycemic threshold is reached. Furthermore, most of the glycemic responses follow a similar rate of change in glucose over the 6 hour time period after the glycemic threshold was reached. This observed pattern in subsequent glucose may be correlated to a variety of factors such as but not limited to patient insulin sensitivity and

insulin requirements for maintenance of a normal glycemic state. For this reason, the hypothetical construct for development of the neural network models in this investigation is supported. The acquisition of a variety of factors and medical records which may be indicative of subsequent glycemic trends combined with CGM provides a significant source of data from which development of models for prediction of glucose was completed. Such an intensive dataset has previously not been collected and utilized for predictive model development.

5.5.2 Utilization of a Genetic Algorithm to Optimize Neural Network Model Training Set

A total of 131 possible medical records and variables acquired from CGM were acquired throughout the course of clinical investigation. Given this large quantity of variables, it is important to distinguish which variables are predictors/indicators of glucose concentration. Utilization of a genetic algorithm for determination of the medical records to be utilized for prediction of glucose was chosen as the best method of optimizing neural network model inputs. The utilization of the genetic algorithm approach was chosen based on literature review and genetic algorithm theory. [112,113]

Two renditions of the genetic algorithm implementation were used as subtle differences between multiple linear regression and partial least squares linear regression based genetic algorithms may lead to different results. The major difference between these approaches is the utilization of actual variable values and latent variable values would lead to different results. Due to these differences, results of both genetic algorithm implementations were combined and the optimal model input variables were finalized. These 131 variables were minimized to 40 variables which are included in Table 3-2.

To justify results obtained via genetic algorithm implementation, literature review

and discussion with clinical staff was completed. For example, increased heart rate or tachycardia has been correlated in the literature with increased glucose concentration. [124] Furthermore, research has substantiated that body temperature is an indicator of glucose concentration specifically the occurrence of hypoglycemia. [125] Other factors/inputs such as dextrose solutions (D5, D5W, etc) which are infused in critical care patients contain dextrose (glucose) which would correlate to an increase in glucose concentration. Therefore the optimized input set determined via implementation of the genetic algorithm coincides with literature review and discussion with clinical investigators.

5.5.3 Real-time Prediction of Glucose Using Initial Model Weights

A feed forward neural network model was developed using CGM results and data recorded in the diabetic flow sheet of the ICU. The model was trained using data from five critical care patients, and subsequently integrated into a real-time predictive application. Using data from four patients not included in the model training set, model performance was tested using original weights determined via comprehensive model training.

Overall, the model performed accurately at predicting trends in glucose in the test dataset. A majority of the predictions generated by the real-time application were clinically acceptable (97.5%) as indicated by Clarke Error Grid Analysis (CEGA). CEGA demonstrated that 67.9% and 29.6% of model predictions fell within regions A and B of the error grid respectively. CEGA also indicated that .3%, 1.8%, and .3% of predicted values fell within regions C, D, and E respectively, which would have resulted in predictions that would lead to inaccurate/adverse therapeutic direction.

A majority of normal and hyperglycemic extremes were predicted by the neural network model. In this test dataset, 86.7% of the hyperglycemic extremes (elevated glucose $\geq$ 150 mg/dl) were predicted and 83.4% of normal glucose values (>70 and <150 mg/dl) were successfully predicted. Overall model error (MAD%) was calculated as 17.3%. Model predictive accuracy is thus within the reported error range of the CGM device and a majority of predictions are within regions A and B of the Clarke Error Grid indicating overall model clinical acceptability. [114,123,126] Given the degree of accuracy, model predictions could therefore be utilized by clinical staff for intelligent therapeutic direction, and given future model development automation of insulin delivery for maintenance of tight glycemic control.

A limitation of the neural network model included the ability to predict hypoglycemic extremes. The model only predicted 14.7% of the hypoglycemic glucose values ($\leq$70 mg/dl). The predictions generated by the real-time application routinely overestimated hypoglycemic glucose values. This can be attributed to the lack of hypoglycemic training data. In the dataset used for training the neural network model, 93.6% of training data was normal and 6.4% of the training set was hyperglycemic. There was no hypoglycemic data present in the training set which can be directly attributed to the routine overestimation of hypoglycemic extremes in the test dataset.

The reduced complexity feed forward neural network model design enables the prediction of glucose within the sampling rate of the CGM device (five minutes). Furthermore, the results of this investigation indicate that prediction of glucose using original model weights generated via comprehensive model training for prediction result in accurate and clinically acceptable glycemic predictions. Utilization of such a neural

network based approach for glycemic forecasting is a promising concept and well suited to model glucose in this patient population.

Utilization of CGM in the critical care setting is only recently becoming part of research endeavors for establishing glycemic control. [85,89] The goal of this investigation was the development and optimization of a predictive system which integrates electronic medical records and CGM for prediction of glucose in real-time in the intensive care unit. The results of this investigation substantiate that utilization of CGM and a predictive model as developed in this investigation could be integrated into a routine bedside monitoring system. Such a bedside monitoring system could become as commonplace as an electrocardiograph system which is routinely implemented bedside in critical care patients.

5.5.4 Performance Analysis of a Patient Specific Neural Network Model

Models outlined in this document were primarily focused on the development of general neural network models, i.e. models developed/trained with data from multiple patients. While many of these general models have predictive accuracy within the error of CGM monitoring devices, and CEGA reveals that a large majority (>90%) of predicted values are clinically acceptable, it is hypothesized that a patient specific model may result in more accurate predictions. Neural network theory substantiates that performance increases given larger training sets covering a wide range of values to be predicted. The availability of a significant training set provides a basis for detecting more trends and patterns in data. Throughout the duration of the clinical investigation there was only a single patient who had an extended length of stay in intensive care suitable enough to

generate and test the performance of a patient specific neural network model.

In this investigation, a patient specific neural network model was developed/trained with data from a single patient who was in the intensive care unit for 16 days. This patient was a 38 year old trauma patient who was a motor vehicle accident victim, was intubated, and suffered multiple blunt force injuries. Performance of the patient specific model was compared against the performance of the general neural network (discussed in section 5.5.3) model on a segment of data from the 38 year old trauma patient which was not included in either model training set.

Performance analysis and comparison of the two modeling approaches demonstrated that the patient specific model was significantly more accurate at prediction of glucose than the general model approach. Overall model error (MAD%) of the patient specific model approach was calculated as 7.9% versus 15.9% using the general model. Furthermore, CEGA revealed that 100% of predictions generated by both modeling approaches were located within regions A and B of the error grid and could be classified as clinically acceptable. The patient specific modeling approach however, resulted in a larger majority of its predictions (95.1%) falling within region A of the error grid. On the contrary, the general model resulted in only 69.8% of prediction values falling within region A of the error grid. The patient specific model had 4.9% of predicted values falling within region B of the error grid. Conversely, the general model resulted in 30.2% of predictions falling within region B of the error grid. The patient specific modeling approach is the more desireable approach as 95.1% of the values fell within region A (the region of highest accuracy in CEGA) of the error grid which contains predicted values within 20% of the reference glucose concentration.

The patient specific modeling approach is more accurate due to the fact that it is tailored to model specific responses in a single patient. This makes the modeling approach more adapted to accommodating for a particular patient's insulin sensitivity, any insulin resistance a patient may have, as well as patient responses to particular events. The general modeling approach has a larger overall error due to the overestimation of glycemic responses when large rates of change in glucose are experienced as demonstrated in Figure 4-20. This does not occur in the patient specific model as demonstrated in Figure 4-19. This patient was subjected to IV insulin infusion throughout their stay in intensive care, and the difference in performance between the general and patient specific modeling approaches is likely correlated to fact that the general model is trained with glycemic responses to the insulin infusion protocol from a variety of critically ill patients, whereas the patient specific model is trained with glycemic responses to insulin infusion protocol in a single patient (test patient).

It is further hypothesized that increased model performance of the patient specific model would be achieved given the utilization of the optimized training set determined via the genetic algorithm. The patient specific model only utilized inputs which included point of care glucose test times and results, insulin delivered, insulin delivery type, and CGM data. Utilization of the optimal training set would enable the neural network to determine and quantify the effect of various other inputs within the patient medical records on future glucose concentration. These results indicate that a patient specific model may be a more desireable approach in patients who have an extended length of stay in the intensive care unit. The increased accuracy of a patient specific model would be of direct benefit when utilized for intelligent therapeutic direction/automation.

5.5.5 Comparison of Neural Network Performance Given Variable Prediction Horizons

Most neural network models developed in this investigation for prediction of glucose in the critical care patient population implemented a prediction horizon of 75 minutes. This prediction horizon was chosen due to the percentage of hypoglycemic and hyperglycemic reactions detected via conventional POC testing at the University of Toledo Medical Center. Table 3-3 summarizes this analysis and demonstrates that 83.9% of hyperglycemia and 58.4% of hypoglycemia is detected within an 80 minute window (40 minutes before and 40 minutes after detected hypoglycemic or hyperglycemic occurrence) via POC testing. Therefore, implementation of a prediction horizon of 75 minutes will be near optimal in providing insight on glycemic excursions during regions where POC glucose measurements are not acquired. The implementation of a prediction horizon of 75 minutes will provide a means for prediction of a majority of elevated/hyperglycemic glycemic extremes ($\geq$150 mg/dl) in this critical care patient population.

Although this clinical investigation primarily focused on development and optimization of neural network models implementing a prediction horizon of 75 minutes, neural network models were also developed with prediction horizons of 30 and 60 minutes. Performance of these neural network models in prediction of glucose in data from three critical care patients not utilized for model training was compared. Given results acquired previously in the diabetes investigation, it was hypothesized that an increase in prediction horizon would correlate to a increase in overall model error (MAD%).[127]

As hypothesized, an increase in the model prediction horizon is correlated with an increase in overall model error. Error was calculated as 4.8% , 7.5%, and 8.0% for models implementing 30, 60, and 75 minute prediction horizons respectively. The percentage of hyperglycemic glucose values ($\geq$150 mg/dl) predicted by the models also decreases with an increase in prediction horizon. Percentage of hyperglycemic extremes predicted by the models was calculated as 85.2%, 79.8%, and 66.3% for 30, 60, and 75 minute predictive models respectively. Percentage of normal glucose values (>70 and <150 mg/dl) predicted decreased when comparing 30 minute predictive models with 60 and 75 minute predictive models. There was not a decrease in percentage of normal values predicted between 60 and 75 minute predictive models. The percentage of normal glucose values predicted by the 30, 60, and 75 minute models was calculated as 97.0%, 94.0%, and 96.1% respectively. It is hypothesized that the model implementing the 75 minute prediction horizon predicted a higher number of normal glycemic extremes due to the increase in prediction horizon with respect to the 60 minute model. Given large rates of change which lead to hyperglycemia, the 75 minute prediction horizon does not always predict subsequent hyperglycemic states and predicts a normal glycemic state. Once glucose returns to a normal glycemic state the 75 minute predictive model successfully predicts the normal glucose values. Conversely, the 60 minute predictive model predicts more hyperglycemia then the 75 minute predictive model however predicts hyperglycemia when glucose returns to a normal glucose value resulting in the discrepancy in percentage of normal glucose values predicted by the 60 and 75 minute predictive models. Figures 4-23A, 4-23B, and 4-23C demonstrate this observed phenomena and model performance given the variable prediction horizons in three critical

care patients (A, B, and C).

CEGA of the predictions generated by each of the models implementing variable prediction horizons is included in Table 4-21. Overall, a large majority of the model predictions were clinically acceptable and fell within regions A and B of the error grid. Each model generated ≥ 91.0% of predicted values within region A of the error grid and had predicted values within 20% error of the reference CGM device measured interstitial glucose concentration. The 60 minute predictive model had 0.20% and 0.10% of predicted values within regions C and E of the error grid which would have lead to adverse therapeutic direction. This is a relatively small proportion of predictions and would likely not significantly limit the clinical acceptability of this model. Models implementing 30, and 75 minute prediction horizons had 100% of predicted values which could be considered clinically acceptable and were located within regions A and B of the error grid.

Although a 75 minute prediction horizon is the most well suited prediction horizon for critical care patients given the frequency of POC glucose monitoring maintained by clinical staff, models implementing smaller prediction horizons are more accurate overall. The implementation of models with reduced prediction horizons provide a foundation in which intelligent therapeutic direction and automation may be achieved. Given future development of a bedside monitoring and glycemic predictive system for critical care patients, multiple predictions implementing variable prediction horizons can be made available for caregivers. Caregivers can utilize the model predictions given implementation of variable prediction horizons for intelligent therapeutic direction, and give greater weight to predictions by the models implementing the smaller prediction

horizons as they area associated with higher accuracy.

5.5.6 Comparison of Performance in Complex and Reduced Complexity Neural Network Models

Various pros and cons exist based on choice of neural network model architecture/design. In this investigation, the performance of multifunctional neural network model implementing a complex time-lagged feed forward (TLFF) neural network architecture is compared with performance of a reduced complexity neural network model implementing a feed forward (FF) neural network architecture. The TLFF neural network model was configured with the variable forward and back propagation trajectories and the number of exemplars per weight update of the neural network model.

The model performance of the TLFF neural network model did not differ regardless of configuration of forward and back propagation trajectory. The prediction of glucose achieved via the complex TLFF architecture however, was different than the reduced complexity FF neural network model. Prediction of glucose in data from two critical care patients (A and B) not utilized for model training is included in Figure 4-25A and 4-25B. The TLFF neural network model architecture appears to overestimate normal glycemic extremes, which is most apparent in Figure 4-25A. On the contrary, the FF neural network model has the tendency to underestimate elevated glycemic extremes ($\geq$150 mg/dl). Due to these tendencies, the TLFF model predicted more elevated glycemic extremes (88.1%) than the FF neural network model (67.6%). Further performance analysis revealed that the FF neural network model predicted a higher percentage of the normal glycemic extremes (93.8%) than the TLFF model (72.8%).

Overall, the FF neural network model architecture generated more accurate predictions with an overall error (MAD%) of 7.4%. The TLFF neural network model had a higher overall error of 8.7%. CEGA revealed that 100% of predicted glucose values by each model approach were clinically acceptable with all predictions contained within regions A and B of the error grid. CEGA further substantiated that the FF model architecture generated more accurate predictions than the TLFF model. In comparing the two modeling approaches, the FF model had 94.2% of predicted values within region A of the error grid and 5.8% of predicted values within region B of the error grid. Conversely, the TLFF model had only 90.7% of predicted values within region A of the error grid and the remaining 9.3% of predictions within region B.

Comparison of the multifunctional model performance in predicting general and specific glucose states revealed that models perform similarly in prediction of general glycemic states with >99% of normal glycemic states being predicted by both modeling approaches. Furthermore, models predict the same percentage of general hyperglycemic (elevated glucose) states (88.6%). In comparing model predictive accuracy in prediction of specific glycemic states, prediction of the lower normal glycemic state 2 was slightly higher in the TLFF model (49.4%) versus the FF model (47.4%). Prediction of the normal glycemic state 3 was slightly higher in the FF model (80.8%) versus the TLFF model (77.3%). Prediction of the upper normal and elevated glycemic state 4 was slightly higher in the FF model (74.6%) versus the TLFF model (72.7%). The prediction of elevated glycemic state 5 was significantly higher in the TLFF model (70.6%) versus the FF model (42.2%).

A plausible explanation for the overestimation of normal glycemic extremes by

the TLFF and underestimation of the hyperglycemic extremes by the FF neural network model are the differences existent between model architectures. The TLFF architecture contains memory structures to store historical neural network input values which give the model the ability to process information in time. The glucose data from the two critical care patients utilized to test model performance contained regions where there were sustained incidences of elevated glycemic extremes. The TLFF modeling approach performs more accurately at prediction of such sustained elevated glucose extremes in that memory structures and variable forward and back propagation trajectories help identify that glucose concentrations have been sustained over time. On the contrary, the FF neural network model does not contain such memory structures or variable trajectories and therefore are more ~~"re~~active" to only recent changes in glucose. Overall, both model approaches have reduced accuracy when large rates of change in glucose are experienced. This is due to the implementation of a significant prediction horizon of 75 minutes. Larger prediction horizons are associated with reduced model predictive accuracy as demonstrated in section 4.2.5 and Figures 4-24A, 4-24B, and 4-24C.

Implementation of a complex TLFF model architecture is associated with an increased ability to predict elevated (hyperglycemic) glucose extremes. The implementation of a reduced complexity FF neural network model architecture resulted in an increased ability to predict normal glycemic extremes and had more accurate predictions overall. There are other pros and cons in regards to the implementation of TLFF or FF neural network models.

The existence of memory structures in the TLFF model design can have positive and negative implications. The utilization of memory structures to track changes in past

neural network inputs, is of significant benefit when changes in past neural network inputs are indicative of real-time changes in glucose. These memory structures can be detrimental to model predictive accuracy if past glucose values are stable and sustained and there is a sudden rapid increase or decrease in glucose. The memory provided to the model for predictions would not include this rapid change in glucose in subsequent predictions until the trend in glucose is integrated into model memory. Implementation of complex TLFF neural network models require more computation time in terms of training, and real-time prediction of glucose in the developed real-time application. The increased computation time is due to the more complex architecture containing more weights, hidden layers, and the existence of memory structures which require further processing time for weight adaptation and optimization. Implementation of such a TLFF model due to increased computational time does not easily generate predictions within the sampling rate (5 minutes) of the CGM device. Given further advances in computational technology the advent of portable computer technologies with higher processing power would likely be able to accommodate the implementation of complex TLFF models in real-time.

Implementation of reduced complexity FF models are associated with a higher degree of accuracy, and resulted in the prediction of a higher percentage of normal glucose values. These models are however limited in that lack of memory structures in the design do not enable the processing of data in time and pattern recognition in historical neural network input data. These neural network models are perhaps the most suitable model architecture in real-time applications (due to the reduced complexity of the model architecture) as the computation time required for training and real-time prediction

is much less than the complex TLFF model. These models are capable of generating predictions well within the sampling rate of a CGM device and allow additional time for post-processing of model output such that increased model accuracy can be achieved. FF models generated in this investigation also implement a forward and back propagation trajectory of a single sample which enables the adaptation of model weights based on the most recent changes in glucose, which allows the model to track rapid changes in glucose more accurately. There are limitations to this FF model architecture as well. When past glucose values remain stable and there is a sudden increase or decrease in glucose, the FF model predictions will react to this recent change. If this recent change does not persist and glucose returns to values near its previously sustained state, the generated model predictions may overcompensate for the sudden change in glucose and model accuracy will decrease.

In both model implementations overall model accuracy is well within the reported error range of the CGM device of 14.0-21.0%. [123] Furthermore, CEGA of the predictions generated by the modeling approaches indicated that 100% of predictions were clinically acceptable and fell with regions A and B of the error grid. [114,126] In both model implementations, a majority of the predictions (>90%) fell within region A of the error grid and had error within 20.0% of the reference CGM device glucose measurement. Further investigation into optimization of both TLFF and FF model implementations for glucose prediction is warranted. These preliminary results indicate that utilization of such a predictive system for intelligent therapeutic direction and automation for maintaining tight glycemic control in the critical care patient population may be possible within the near future.

5.5.7 Preliminary Weight Analysis: Correlation to Neural Network Model Performance

The preliminary weight analysis completed in this investigation and summarized in section 4.2.7 of this document provides insight which can be used for future model optimization, as well as insight into how real-time CGM values and medical records may impact future glycemic excursions and neural network model performance. This preliminary weight analysis focuses only on the first of two output bias axon weights. This output axon weight value acts as an offset value to determine the final predicted glucose concentration value via adding the weight value to the neural network value output from the hidden layer and after output synapse weights are applied. Weight values were updated during real-time model training and prediction of glucose was obtained using the developed real-time predictive application.

Weight analysis revealed that the detected occurrence of tachycardia in real-time has an increased correlation with model performance across the model prediction horizon (from short term to long term MAD%). This result indicates that adaptation of model weights in the output layer which occur with detection of tachycardia in real-time will have more of an effect on predicting glucose in the long term than in the short term. This finding is important to gauge the overall effect of tachycardia on future glucose concentration. Results acquired via weight analysis demonstrate that tachycardia has effects on glucose which are seen in the time period 55-75 minutes after the detection of tachycardia in real-time. As identified in Figure 4-29, there are patterns in glucose which occur after tachycardia and no insulin delivery in critical care patients. An overall increase in glucose is observed in the time period 75 minutes after this detected occurrence of tachycardia. Preliminary weight analysis determined that output axon

weight values will have more of an impact on predictions in the 55-75 minute range of the model prediction horizon. This time frame is therefore warranted of future investigation to determine the overall effect of tachycardia on glucose such that model accuracy can be optimized.

Correlation analysis of output axon weights with respect to the occurrence of various real-time glucose concentrations with and without delivery of insulin also alluded to various time domains with which model performance and weight values were associated. Insulin delivery and occurrence of various glycemic thresholds was correlated with model performance in the long term (55-75 minutes into the prediction horizon). It is hypothesized that this is due to the delivery of insulin which will is usually correlated to a reduction in glucose concentration. This reduction in glucose will likely occur across the model prediction horizon, and results of weight analysis indicate that modification of output axon weight values will affect performance in the latter duration of the model prediction horizon. Future research needs to be completed to identify glycemic responses after insulin delivery given the occurrence of real-time CGM at the various glycemic thresholds defined in this investigation.

Real-time occurrence of extremely elevated glucose concentrations ($\geq$190 and $\leq$240 mg/dl) and insulin delivery is highly correlated with model performance and output axon weight values in the short term time domain (5-25 minutes) of the model prediction horizon. This is hypothesized to be due to the aggressive delivery of insulin which is routinely administered via the University of Toledo Medical Center insulin infusion protocol. The delivery of this insulin will likely cause glucose concentration to rapidly decrease during the initial 5-25 minutes after the elevated glucose and corresponding

insulin delivery. This is hypothesized as the reason why model performance has a higher correlation during the short term duration of the model prediction horizon as insulin delivery dominates in this time domain. This preliminary weight analysis effectively identifies the time domain in which identification of glycemic responses following extremely elevated glucose concentration and insulin delivery needs to be completed such that model weights and overall predictive accuracy can be optimized.

Overall, the various time domains identified via weight analysis will need to be subjected to further investigation to determine patterns or trends in glucose which occur. After determining these patterns, weight values and consequently model performance during these time domains can be optimized. The determination of optimal model weights depending on the real-time occurrence of CGM values, and events such as insulin dosages, or tachycardia as utilized in this preliminary analysis will lead to development of algorithms which can be used to assist real-time training/prediction in the neural network models developed in this investigation. Further expansion of this weight analysis to analyze weight values in other neural network model layers and their correlation to real-time input data and model performance will be the subject of future research endeavors.

5.5.8 Real-time Prediction of Glucose: Testing Model Performance in Five Critical Care Patients

In this investigation, the model performance of the neural network models implementing a prediction horizon of 75 minutes were tested in real-time using data from five critical care patients not utilized for model training. The real-time predictive application was configured for two different implementations. The first implementation

included utilization of the real-time predictive application for real-time training (updating of model weights via backpropagation training with gradient descent with momentum training algorithm) and prediction of glucose. The second implementation was the prediction of glucose using original model weights determined via model training and no real-time training.

The prediction of glucose using the original model weights resulted in higher predictive accuracy than the implementation of the real-time training (weight update) method. Utilization of original model weights resulted in predictions with an overall error (MAD%) of 9.0%. Conversely, implementation of the weight update method resulted in predictions with an overall error (MAD%) of 18.0%. The error achieved via the weight update method therefore had double the predictive error of the model implementing original weights. Figure 4-27 demonstrates the prediction of each implementation. Figure 4-27A includes the prediction of glucose utilizing the real-time training (weight update) method. Glycemic predictions generated by the weight update method track trends and rate of change in glucose concentration accurately, however, there are numerous instances where overestimation of glucose values occur. Overestimation of glucose values generally occurs at normal glucose values ($\geq$90 & $\leq$ 120 mg/dl). This observed overestimation can be attributed to the fact that real-time training and prediction was completed using a training set of only 800 values. Models trained using such a limited training set would result in decreased model performance which may explain the overestimation and error experienced in predicting glucose at these glycemic extremes. It is important to note that this training set length was selected as it was the maximum length in which model predictions could be generated within the sampling rate of the

CGM device given implementation of real-time model training. Implementation of this training set length would therefore be ideal for a real-time predictive application in its current state.

Predictions derived from real-time model training sometimes overcompensate for real-time rates of change in glucose. This phenomena is demonstrated in Figure 4-27A. This is due to the fact that model weights are updated after each CGM value (exemplar) in the training set. Weights updated after the 800^{th} (current real-time) CGM value will incorporate the current real-time rate of change into model predictions. The overcompensation for real-time rates of change in glucose does not occur frequently, and the ability of the neural network model to accommodate for real-time rates of change in glucose may be more beneficial to overall model performance.

Although overestimation of glucose values within the normal glycemic range ($\geq$90 &$\leq$ 120 mg/dl) was experienced, real-time training/prediction resulted in the prediction of a large majority of both normal (>70 and <150 mg/dl) and elevated ($\geq$150 mg/dl) glycemic extremes (77.7% and 80.0% respectively). Implementation of original model weights predicted a significantly higher percentage of normal extremes, but predicted less hyperglycemia than the weight update method. The original model weight method predicted 96.7% of normal glycemic extremes but only 53.6% of elevated glycemic extremes. The reduced ability of the original weight method to predict elevated glycemic extremes is likely due to the fact that weight values are maintained during prediction. Conversely, in the weight update method, weights are updated due to real-time rates of change in glucose and would result in the model to have an increased ability to predict elevated glycemic extremes. This is an excellent example where real-time model training

for prediction of glucose is beneficial to model performance.

CEGA of predictions generated via both model implementations indicated that greater than 99.8% of predicted glucose values were clinically acceptable and fell within regions A and B of the error grid. The original weight method had 100% of predictions which could be considered as clinically acceptable determined via CEGA, with 87.3% and 12.7% of predictions falling within regions A and B respectively. The real-time training method resulted in 99.9% of model predictions which could be considered as clinically acceptable determined via CEGA, with 62.1%, 37.8% predictions falling within regions A and B of the error grid respectively. There were a small number 8 predicted values (0.1%) which fell within region C of the error grid which could lead to inaccurate and adverse therapeutic direction.

The data from the five patients utilized for model performance analysis did not contain any hypoglycemic extremes (CGM $\leq$70 mg/dl). The models generated in this investigation were not developed with training sets which contained a significant quantity of hypoglycemia. The training sets utilized for model development contained only 901 hypoglycemic glucose values which corresponded to only 4.5% of the comprehensive model training sets. There were however, a significantly larger number of elevated and normal glycemic extremes in the model training sets. The model training sets consisted of 83.8% of normal and 11.7% of elevated glycemic extremes. It is hypothesized that the developed neural network models would overestimate hypoglycemic extremes due to this training set composition. This reduced ability to predict hypoglycemic extremes was observed in preliminary neural network model development for prediction of critical care patients included in section 4.2.3 and in insulin dependent diabetic patients. [127]

Overall, implementation of both modeling implementations exhibited considerable predictive accuracy with errors falling within the reported range of CGM devices of 14.0-21.0%.[123] CEGA of the predictions generated via each implementation indicated that ≥99.8% of model predictions could be considered clinically acceptable and not lead to inaccurate therapeutic direction. Neural network modeling is well suited for prediction of glucose in a real-time critical care setting given the model's ability to adapt to trends/patterns observed in medical records and CGM data. Given changes to patient state which correlate to future changes in glucose, a neural network model such as the model implementing real-time training developed in this investigation may be ideal for prediction of glucose and intelligent therapeutic direction and automation. Future research will be completed to optimize such model implementations. Techniques to enhance model predictive accuracy include the development of post-processing algorithms which will modify neural network model output given the occurrence of certain events, real-time medical records, and given changes in real-time CGM data. Preliminary post-processing algorithm implementation will be discussed in the next section of this chapter (5.5.9).

5.5.9 Preliminary Post-Processing Algorithm Implementation to Enhance Predictive Accuracy

The models developed in this investigation successfully predict trends/patterns in glycemic excursions within various critical care patients. The models were configured with a significant prediction horizon of 75 minutes, which leads to a reduction of model accuracy at times. Improvement of modeling accuracy can be achieved via generation of a post-processing algorithm which modifies neural network predictive output given the

detection of events and CGM values in real-time. In this investigation, the development and testing of a preliminary post-processing algorithm which modifies neural network output given the occurrence of various levels of tachycardia (near, onset, moderate, and severe) at a variety of CGM values (glycemic thresholds) was completed. In addition to post-processing based on the occurrence of tachycardia, a post-processing algorithm which accommodates for differences in real-time and predicted CGM values is assessed.

Research completed by Palatini et al demonstrated that high blood pressure and corresponding tachycardia can be linked to increased glucose concentration. [128] The current literature does not fully correlate the occurrence of tachycardia with future glycemic responses. The utilization of CGM provides a significant source of data in which trends in glucose following tachycardia can be identified. Figure 4-29 includes patterns in CGM results in 15 critical patients with elevated glucose and tachycardia who did not receive any insulin and resulted in an overall increase in glucose concentration in the time period 75 minutes after the detected occurrence of tachycardia ($\geq$90 bpm). Patterns such as these provide the hypothetical construct for development of an event based post-processing algorithm to adjust model predicted output due to real-time occurrence of tachycardia.

The event based post-processing algorithm implemented various third order polynomial functions to model future glycemic responses at various CGM glycemic thresholds and degrees of tachycardia. A third order polynomial function was chosen to model these responses as such a function would be able to model some of the variability in glycemic responses which occur in this patient base more effectively than first or second order models. Further investigation into generating higher order models or

alternative modeling techniques to estimate these glycemic responses will be subject of future investigation.

There were a total of 10 detected occurrences of tachycardia in the 5 critical care patients utilized for model performance analysis. The post-processing algorithm was applied following these detected occurrences of tachycardia and model performance of the unprocessed predictions was compared with the post-processed predictions. Figure 4-30 contains neural network model predictions (implementing a prediction horizon of 75 minutes) before and after event-based post-processing. It is demonstrated that post-processing results in increased accuracy. The post-processed model output does not model the overall extent of glycemic variability (peaks and valleys). This performance is due to the limited nature of utilizing a third order polynomial model fit as previously discussed. The post-processed predictions provide an accurate estimation of the final glucose value in model prediction horizon (glucose value 75 minutes after tachycardia). Tables 4-36 and 4-37 summarize CEGA and predictive performance of the neural network predictions before and after post-processing. These results demonstrate that model accuracy is significantly higher after implementation of the post-processing algorithm as a MAD% of 12.1% is obtained in comparison to the MAD% of 26.7 obtained without application of the post processing algorithm.

Prediction of glycemic extremes also improved after post-processing as 100.0% of normal (>70 and <150 mg/dl) and elevated (≥150 mg/dl) glycemic extremes were predicted. Conversely, 63.7% and 53.3% of normal and elevated extremes were predicted without post-processing implementation. Predictions with and without post-processing were all clinically acceptable as indicated by CEGA. CEGA revealed however, post-

processing implementation resulted in predictions with significantly higher accuracy as 86.7% of predictions falling within region A of the error grid. In contrast, only 27.3% of predictions fell within region A without post-processing.

The data set utilized for neural network model training and prediction contains a variety of factors/events in patient medical records which are indicators or impact future glycemic trends. Development of further event based post-processing such as the tachycardia based post-processing algorithm outlined in this dissertation will lead to enhancement in model performance. For example, post-processing algorithms can be generated which account for the effect of certain medications on future glucose concentrations. As demonstrated in this investigation, the utilization of such event-based post-processing algorithms may lead to enhancement and increased applicability of the neural network based models for glycemic forecasting in the critical care setting.

Predictions generated by the neural network model implementing real-time training and weight adaptation track the overall trends in glycemic excursions across the model prediction horizon accurately. A major source of error in model predictions is the existence of an offset between actual and predicted glucose values which occurs when overestimation of glucose occurs. CGM provides a tremendous advantage in that it provides glucose measurements every five minutes. Using the frequent sampling of glucose concentration by the CGM device can provide a secondary method of post-processing. During time periods where model predictions overestimate or underestimate glucose concentration, the offset existent between the current real-time CGM measurement and the first predicted CGM in the neural network model output can be calculated. The addition of this offset to the initial predicted glucose value may be

utilized to enhance model predictive accuracy. If this calculated offset is not large and the model predictions are accurate, model accuracy will not be affected. Due to the fact that model predictions accurately follow rates of change in glucose across the model prediction horizon, the rate of change in the predicted glucose concentration is maintained. Given the threshold of the current real-time glucose concentration, the rate of change in predicted concentration is weighted as outlined in section 3.3.10 of this document. This weighting is completed as glucose values will have more potential to change at elevated glucose extremes than at hypoglycemic or lower normal glucose concentrations. The implementation of this glycemic offset based post-processing algorithm was applied to the predictions generated using the five critical care patient data set for model performance analysis.

Implementation of both event-based (tachycardia) and glycemic offset based post-processing algorithms significantly increased model predictive accuracy. Figure 4-31 demonstrates the increased accuracy obtained via implementation of the post-processing algorithm implementations. Regions where overestimation or underestimation of glucose values occur are compensated for via post-processing algorithm implementation. In terms of overall model performance, post-processing resulted in reduction of overall model error (MAD%) from 18.0% to 7.1% (an improvement of 10.9%). Furthermore, CEGA of post-processed model predictions supported the observed increase in model accuracy as 93.2% and 6.7% of predictions fell within regions A and B of the error grid. Before post-processing implementation 62.1% and 37.8% of predictions fell within regions A and B of the error grid. Post-processing did result in 0.06% of predicted values falling within regions C and E of the error grid which would have led to

adverse therapeutic direction. These undesirable predictions are infrequent and occur when model predictions overcompensate for a positive (increasing) rate of change in glucose. The addition of the offset incurred via post-processing therefore results in overestimation of glucose concentration and prediction of a false elevated glucose concentration. Post-processing implementation was also correlated with an increase in percentage of glycemic extremes predicted. After post-processing 94.5% and 86.8% of normal (>70 and <150 mg/dl) and elevated extremes (≥150 mg/dl) were predicted, whereas only 77.7% and 80.0% of these extremes were predicted before post-processing.

Preliminary implementation of event-based and glycemic offset based post-processing algorithms resulted in a significant increase in model performance. Overall model error and the percentage of predictions which could be regarded as clinically acceptable were well within desired ranges. [114,123,126] The application of neural network models coupled with post-processing for prediction of glucose in real-time for intelligent therapeutic direction/guidance and ultimately automation in the critical care setting is therefore, an extremely promising concept. These results warrant future investigation and optimization of post-processing implementations such that further enhancement in model performance may be achieved.

5.6 Summary of Neural Network Models for Prediction of Glucose

While previous modeling techniques for prediction and control of glucose in critical care patients, and patients with diabetes have had considerable success, it is hypothesized that a modeling technique which can account for the effect of a variety of factors on future glycemic excursions may be a useful alternative modeling approach.

Neural network models are modeling techniques capable of determining the effect of various input/predictor variables on a variable to be predicted. The application of neural network modeling toward prediction of glucose in these patient populations is therefore well suited.

Neural network models generated in this investigation and utilized for real-time prediction of glucose in critical care patients, and patients with insulin dependent diabetes provide a promising technique for providing therapeutic direction/guidance. Future research leading to increased predictive accuracy will result in a predictive system which can be used for therapeutic automation via semi-closed loop and closed loop insulin infusion. Models generated in this investigation in their current state can be potentially utilized (using clinical judgement) for intelligent therapeutic guidance. Models have accuracy which fall within the reported error ranges of CGM devices with respect to serum glucose concentration, and CEGA established that $\geq$90.0% of model predictions can be regarded as clinically acceptable and not lead to adverse therapeutic direction.

Results of this investigation substantiate that utilization of a patient specific model (i.e. neural network model trained for prediction in single patient) results in more accurate predictions than a general model (trained using data from multiple patients). Such a patient specific model would be beneficial for both patient populations, however, may be of more significant benefit in patients with diabetes. These outpatients have considerable variability in daily glycemic excursions which can be attributed to day to day differences in factors such as but not limited to: lifestyle/activities (sleep-wake cycles, exercise, etc), nutritional/dietary intake, and emotional states (i.e. stress, depression, etc). Patients with diabetes only monitor glucose 3-6 times daily therefore, utilization of CGM and

predictive models for glucose would be of direct benefit. Conversely, critical care patients are monitored in a hospital setting where such factors are controlled. For example, POC glucose values are obtained more frequently every 1-4 hours. Due to this increased monitoring and utilization of aggressive insulin infusion protocols, glycemic variability in critical care patients is much less than the variability present in insulin dependent diabetic. While a patient specific model in critical care has been shown to have increased accuracy, a general model would have more applicability than in insulin dependent diabetic patients.

Neural network models developed in this investigation were configured as multifunctional neural network models i.e. the models predict two outputs: glucose concentration and classified ranges of glycemic states. A majority of general glycemic states (normal, and high/hyperglycemic) were predicted in both patient populations. In the diabetic patient population >88.0% of general normal and >70.0% of general hyperglycemic states were predicted. In the critical care population, >99.0% and >88.0% of general normal and hyperglycemic extremes were predicted successfully. The predictions of specific glycemic states 1-7, were not as accurate as prediction of general glycemic states, but more accurate in the critical care patient population. A multifunctional neural network model as implemented in this investigation will provide a means of assessing accuracy of model predictions. If both predicted glucose concentration and glycemic state values coincide with each other, the generated model predictions are likely accurate. Further development and optimization of these multifunctional neural network models will result in increased model performance.

While various modeling techniques such as but not limited to: autoregressive

models, control algorithms, and neural network modeling have been implemented for prediction and optimization of glycemic control, the neural network models designed in this investigation differ from previous modeling techniques. These neural network models incorporate the effect of various factors to predict future glycemic trends, and provide a unique alternative modeling approach with the ability to predict glucose using significant prediction horizons >60 minutes. Modeling is completed using CGM technology which provides glucose measurements every 1-5 minutes depending on technology. The utilization of neural network modeling utilizing CGM technology is a promising technique and an innovate concept, and has only recently been addressed in the literature.[127] Sparacino and colleagues who previously developed an autoregressive model for prediction of glucose have recently shifted focus of their research efforts towards development of a neural network approach for real-time prediction of glucose (implementing prediction horizons of 15,30, and 45 minutes) using CGM technology. [36,129] Neural network model development and application in the critical care patient population has not been addressed in the literature to date, and the investigation outlined in this document is an innovative concept. Research regarding development and optimization of such predictive models is warranted and will be subject of future investigation for optimization of therapy and outcome in the diabetic and critical care patient populations.

There is no controversy that optimized and tight glycemic control in patients with diabetes is needed to avoid adverse outcomes and complications such as but not limited to nephropathy, neuropathy, and retinopathy. [1-4] A current study (NICE-SUGAR) is being completed to determine if tight glycemic control in hosptial/critical care patients is

beneficial or not, and has led to controversy in the field. [130] Preliminary results of this study indicate that tight glycemic control is linked to adverse outcomes in critical care patients. This may be associated with an increased occurrence of a significant number of incidences of hypoglycemia in the patient populations studied due to aggressive insulin therapy. Hypoglycemia has been linked to adverse outcomes in critically ill patients as well. [110] Although the advent of the NICE-SUGAR study has raised questions in terms of whether tight glycemic control is beneficial, more research exists which affirms there is improvement in patient outcomes (i.e. reduction of morbidities and mortality) associated with tight glycemic control.[49-52,54,56,65,131]

Models for prediction of glucose and optimization of tight glycemic control has been a common focus of research efforts in patients with diabetes, but has not received considerable attention in the critical care patient population. The utilization of the neural network models developed in this investigation for real-time prediction of glucose is a promising technique. Models generated in this investigation predict glucose concentration using significant prediction horizons (>60 minutes) which have not been obtained in many modeling techniques to date. Given the accuracy of the developed models, the utilization of these models for intelligent therapeutic direction/guidance for patients and clinicians may be within the near future. Optimization of model accuracy will enable model predictions to be used for automation of therapy to obtain tight glycemic control and avoid unwanted hypoglycemic and hyperglycemic excursions.

5.7 Future Research

This dissertation has focused on the development and optimization of neural network models for prediction of glucose in diabetic and critical care patients. While the models generated in this investigation are accurate in predicting glycemic excursions in both patient populations, future research will be focused on further optimization of these models and applications to implement these models for intelligent therapeutic guidance, recommendation, and automation.

The development of patient specific neural network models for prediction of glucose will be a major focus of future research. In this investigation, comparison of a patient specific model was compared with a general model. The patient specific model was significantly more accurate than the general model in predicting glucose concentration. Patient specific models will only be possible and beneficial in the critical care setting when patients have an extended length of stay in the intensive care unit. A significant quantity of CGM and medical records data from a single patient is needed to train an accurate neural network model. Therefore, patients with lengths of stay $\geq$10 days would be candidates for development of patient specific modeling.

Patient specific modeling would be extremely beneficial in diabetic patients who experience significant glycemic variability on a daily basis. Patients with insulin dependent diabetes are required to routinely measure glucose concentration and deliver insulin to maintain a normal glucose concentration. Various factors impact and are indicators of a patient's daily glycemic variability. These factors include but are not limited to lifestyle/activities (e.g. sleep-wake cycles, exercise), emotional states (e.g. stress, depression), and nutritional intake. A patient specific neural network model would

be able to determine patterns and trends in response to such factors which correlate to future trends in glucose. Due to the routine monitoring of glucose in patients with diabetes, large datasets containing CGM data and factors which impact future glycemic excursions will be easily acquired. Given availability of such large datasets, training and development of patient specific models is an attainable goal for patients with diabetes and warranted of future investigation.

Neural network models generated in the clinical investigations were multifunctional neural network models. These neural network models were configured to predict two outputs: actual numerical glucose concentration values and classified ranges of glucose values (glycemic states). Preliminary analysis of the predictive accuracy of the models in prediction of glycemic states demonstrated that models predict general glycemic states (hypoglycemic, normal, and hyperglycemic) accurately. Prediction of specific glycemic states (glucose concentration ranges classified from 1-7) was not as accurate as prediction of general glycemic states. The reduced accuracy in prediction of specific glycemic states is likely due to the limited number of each of the glycemic states present in the model training sets. Future research will be aimed at data collection in both patient populations, and the acquisition of more CGM data with significant quantities of each specific glycemic state. Models generated via larger training sets should result in enhancement of model performance in prediction of specific glycemic states.

Another focus of future research will be the optimization of predictive accuracy of the neural network models in predicting actual numerical glucose concentration values. Models generated in this investigation were developed with training sets which did not contain a significant number of hypoglycemic reactions. As a result of these limited

training sets, model predictions have the tendency to overestimate hypoglycemic extremes. Further research will be dedicated to CGM data acquisition in both patient populations such that training sets with adequate hypoglycemic data may be achieved. The acquisition of further data in both patient populations will provide considerably more training data containing hypoglycemic, normal, and hyperglycemic extremes. These training sets will result in development of models which should be able to predict each glycemic extreme more effectively.

The development and implementation of the preliminary post-processing algorithm which modified neural network output in response to tachycardia and occurrence of real-time CGM data resulted in a significant increase in model performance. These results warrant future investigation aimed at development and optimization of similar post-processing algorithms. There are many factors in both populations which are predictors of future glycemic trends. The analysis of glycemic responses in the time periods after occurrence of these various factors will be subject of future investigative efforts. The development of post-processing algorithms which predict glycemic responses due to the detection of various real-time data presented to the neural network model will lead to increased model performance. Furthermore, the analysis of trends in real-time CGM data such as rate of change, glycemic thresholds, and offset values existent between actual and predicted glycemic responses will enable further post-processing for enhancement of model accuracy.

The key feature of neural network models is the ability to update and optimize model weights based on trends and patterns in data presented to the model. The real-time predictive application generated in this investigation for prediction of glucose requires

further optimization such that real-time training can be optimized. Future research will be dedicated to optimization of real-time model training, and analysis of model weights and how they are updated in response to various neural network model inputs. Preliminary weight analysis completed in this investigation identified time periods within the model prediction horizon with which model weight values and predictive accuracy of the model are correlated. Analysis of trends in glucose during these identified time domains in response to various neural network model inputs will provide a means for optimization of real-time model training.

A major limitation of the clinical investigations was the data acquisition using the developed data-logging software applications. Certain data logged by the patients (diabetes investigation) and co-investigators (critical care investigation) may have been erroneous due to a variety of factors discussed in sections 5.2 and 5.3 of this dissertation. The limitations of these investigations will be addressed in future studies. Future collaboration with various institutions is planned to optimize results. Future investigation at institutions where electronic medical records are present will enable the optimization of the data collection process as well as integrity of the data collected.

The models generated in this investigation have predictive error within the reported error range of the CGM device. Furthermore, Clarke Error Grid Analysis revealed that a majority of predictions generated by the models were clinically acceptable and would not lead to adverse therapeutic direction. Given this accuracy, the real-time predictive system can be implemented for intelligent therapy assistance, recommendation, and ultimately automation. The utilization of the real-time predictive system for such therapeutic interventions will be subject of future research endeavors. Glycemic control

obtained via the real-time prediction of glucose will be subjected to future analysis to determine the benefit in patient outcome of utilizing the developing modeling approach.

The goal of all future research will be the generation of real-time predictive systems for diabetic and critical care patients for intelligent therapeutic assistance, recommendation, and automation. In patients with diabetes, such a real-time predictive system would be incorporated into CGM devices and/or insulin infusion pumps such that prediction of glucose will be utilized by patient for therapeutic direction. Given increased model accuracy, model predictions can be utilized for semi-closed loop and closed loop insulin delivery. In the critical care patient population, a real-time predictive system will be a routinely implemented in bedside monitoring (such as an ECG monitor). This system will be integrated with electronic medical records and utilization of CGM. Prediction of glucose will be available to clinical staff, and ultimately used for closed loop insulin delivery for automated tight glycemic control. Implementation of these predictive modeling approaches will result in better glycemic control in both patient populations and enhancement of patient safety and care.

REFERENCES

1. The Diabetes Control and Complications Trial Research Group. *The effect of intensive treatment of diabetes on the development and progression of long-term complications in insulin-dependent diabetes mellitus*. N Engl J Med 1993;329:977-986

2. The Diabetes Control and Complications Trial Research Group. *Retinopathy and nephropathy in patients with type 1 diabetes four years after a trial of intensive therapy*. N Engl J Med 2000;342:381-389

3. The Diabetes Control and Complications Trial Research Group. *Sustained effect on intensive treatment of type 1 diabetes Mellitus on development and progression of diabetic nephropathy*. JAMA 2003;2003:2159-2167

4. The Diabetes Control and Complications Trial Research Group. *Intensive diabetes treatment and cardiovascular disease in patients with type 1 diabetes*. N Engl J Med 2005;354:2643-2653

5. Reed C, Stewart R, Sherman M, Myers J, Corneille M, Larson N, Gerhardt S, Beadle R, Gamboa C, Dent D, Cohn S, Pruitt B. *Intensive Insulin Protocol Improves Glucose Control and is Associated with a Reduction in Intensive Care Unit Mortality*. Journal of the American College of Surgeons 2007;204:1048-1054

6. Chipkin SR, Klugh SA, Chasan-Tabere L. *Exercise and diabetes*. Cardiol Clin 2000;19:489-505

7. Cox DJ, Gonder-Fredrick L, Kovatchev BP, Clarke WL. *The metabolic demands of driving for drivers with type 1 diabetes mellitus*. Diab Metab Res Rev 2002;18:381-385

8. Dutour A, Boiteau V, Dadoun F, Feissel A, Atlan C, Oliver C. *Hormonal response to stress in brittle diabetes*. Psychoneuroendocrinology 1996;21:525-543

9. Ficker JH, Dertinger SH, Siegfried W, et al. *Obstructive sleep apnoea and diabetes mellitus: the role of cardiovascular autonomic neuropathy*. Eur Resp Journal 1998;11:14-19

10. Hargreaves M, et al. *Effect of heat stress on glucose kinetics during exercise*. Journ App Physiol 1996;81:1594-1597

11. Jones TW, Porter P, Sherwin RS, et al. *Decreased epinephrine responses to hypoglycemia during sleep*. N Engl J Med 1998;338:1657-1662

12. Nomura M, Fujimoto K, Higashino A, et al. *Stress and coping behavior in patients with diabetes mellitus*. Acta Diabetologia 2000;37:61-64

13. Resnick HE, Redline S, Shahar E, et al. *Diabetes and sleep disturbances: findings from the sleep heart health study*. Diabetes Care 2003;26:702-709

14. Trief PM, et al. *Impact of the work environment on glycemic control and adaptation to diabetes*. Diabetes Care 1999;22:569-574

15. Van Cauter E, Polonsky KS, Scheen A. *Roles of circadian rhythmicity and sleep in human glucose regulation*. Endocrine Reviews 1997;18:716-738

16. Winokur A, Maislin G, Phillips J, Amsterdam J. Insulin resistance after oral glucose tolerance testing in patients with major depression. Am J Psychiatry 1988;145:325-330

17. Jarrett R. *Rhythms in insulin and glucose*. Endocrine Rhythms 1979:247-258

18. Simon C , Brandenberger G , Saini J , Ehrhart J , Follenius M. *Ultradian oscillations of plasma glucose, insulin, and C-peptide in man during continuous enteral nutrition*. J Clin Endocrinol Metab 1987;64:669-674

19. Simon C, Brandenberger G , Saini J , Ehrhart J , Follenius M *Slow oscillations of plasma glucose and insulin secretion rate are amplified during sleep in humans under continuous enteral nutrition*. Sleep 1994;17:333-338

20. Tato F, Tato S, Beyer J, Schrezenmeir, J., . *Circadian variation of basal and postprandial insulin sensitivity in healthy individuals and patients with type 1 diabetes*. Diabetes Res Clin Prac 1991;17:13-24

21. Trumper B, Reschke K, Molling J, . *Circadian variation of insulin requirement in insulin dependent diabetes mellitus: the relationship between circadian change in insulin demand and diurnal patterns of growth hormone, cortisol, and glucagon during euglycemia*. Horm Metab Res 1995;27:141-147

22. Van Cauter E, Shapiro E, Tillil H, Polonsky K,. *Circadian modulation of glucose and insulin responses to meals: relationship to cortisol rhythm*. Amer Journ Phys 1992;262:E467-475

23. Campbell PJ, Gerich JE. *Occurrence of dawn phenomenon without change in insulin clearance in patients with insulin-dependent diabetes mellitus*. Diabetes 1986;35:749-752

24. De Feo P, Perriello G, Ventura MM. *Studies on overnight insulin requirements and metabolic clearance rate of insulin in normal and diabetic man : Relevance to the pathogenesis of the dawn phenomenon*. Diabetologia 1986;29:475-480

25. Dodt C, Breckling U, Derad I. *Plasma epinephrine and norepinephrine concentrations of healthy humans associated with nighttime sleep and morning arousal*. Hypertension 1997;30:71-76

26. Dux S, White NH, Skor DA. *Insulin clearance contributes to the variability of nocturnal insulin requirement in insulin-dependent diabetes mellitus*. Diabetes 1985;34:1260-1265

27. Shapiro ET, Polonsky KS, Copinschi G. *Nocturnal elevation of glucose levels during fasting in noninsulin-dependent diabetes*. J Clin Endocrinol Metab 1991;72:444-454

28. Skor DA, White NH, Thomas L. *Relative roles of insulin clearance and insulin sensitivity in the prebreakfast increase in insulin requirements in insulin-dependent diabetic patients*. Diabetes 1984;33:60-63

29. Van Cauter E, Desir D, Decoster C. *Nocturnal decrease in glucose tolerance during constant glucose infusion*. J Clin Endocrinol Metab 1989;69:604-611

30. Van Cauter E, Leproult R, Kupfer DJ. *Effects of gender and age on the levels and circadian rhythmicity of plasma cortisol*. J Clin Endocrinol Metab 1996;81:2468-2473

31. Wu MS, Ho LT, Jap TS *Diurnal variation of insulin clearance and sensitivity in normal man*. Proc Natl Sci Counc Repub China B 1986;10:64-69

32. Steil G, Rebrin K,Mastrototaro J *Metabolic modelling and the closed-loop insulin delivery problem*. Diabetes Res Clin Prac 2006;74:S183-S186

33. Steil GM, Clark B, Kanderian S, Rebrin K *Modeling insulin action for development of a closed-loop artificial pancreas*. Diabetes Tech Ther 2005;7:94-108

34. Steil GM, Panteleon AE, Rebrin K. *Closed-loop insulin delivery-the path to physiological glucose control*. Adv Drug Deliv 2004;56:125-144

35. Schaller HC, Schaupp L, Bodenlenz M, et al. On-line adaptive algorithm with glucose prediction capacity for subcutaneous closed loop control of glucose: evaluation under fasting conditions in patients with Type 1 diabetes. Diabetic Medicine 2006;23:90-93

36. Sparacino G, Zanderigo F, Corazza S, Maran A, Facchinetti A, Cobelli C *Glucose Concentration can be Predicted Ahead in Time From Continuous Glucose Monitoring Sensor Time-Series*. IEEE Transactions on Biomedical Engineering 2007;54:931-937

37. Reifman J, Rajaraman S, Gribok A,Ward WK. *Predictive Modeling for Improved Management of Glucose Levels*. Journal of Diabetes Science and Technology 2007;1:479-486

38. Robinson LE, van Soeren MH. *Insulin resistance and hyperglycemia in critical illness: role of insulin in glycemic control*. AACN Clin Issues 2004;15:45-62

39. Sung J, Bochicchio G, Joshi M. *Admission hyperglycemia is predictive of outcome in critically ill trauma patients*. J Trauma 2005;59:80-83

40. Bochicchio G, Sung J, Joshi M. *Persistent hyperglycemia is predictive of outcome in critically ill trauma patients*. J Trauma 2005;58:921-924

41. Collier B, Diaz Jr J, and Forbes R. *The impact of a normoglycemic management protocol on clinical outcomes in the trauma intensive care unit*. J Parenter Enteral Nutr 2005;29:353-358

42. Gore DC, Chinkes D, Heggers J. *Association of hyperglycemia with increased mortality after severe burn injury*. J Trauma 2001;51:540-544

43. Laird AM, Miller PR, Preston R, Kilgo PD, Meredith, JW, Chang MC. . *Relationship of early hyperglycemia to mortality in trauma patients*. J Trauma 2004;56:1058-1062

44. Doenst T, Wijeysundera D, Karkouti K, Zechner C, Maganti M, Rao V, Borger MA, . *Hyperglycemia during cardiopulmonary bypass is an independent risk factor for mortality in patients undergoing cardiovascular surgery*. Journal of Thoracic and Cardiovascular Surgery 2005;130:1144-1152

45. Furnary A, Cheek D, Holmes S, Lyall Howell, Kelly S,. *Achieving Tight Glycemic Control in the Operating Room: Lessons Learned from 12 Years in the Trenches of a Paradigm Shift in Anesthetic Care*. Seminars in Thoracic and Cardiovascular Surgery 2006;18:339-345

46. Jessen M. *Glucose Control During Cardiac Surgery: How Sweet it is*. Journal of Thoracic and Cardiovascular Surgery 2003;125:985-987

47. Jones KW, Cain AS, Mitchell JH, Millar RC, Rimmasch HL, French TK, Abbate SL, Roberts CA, Stevenson SR, Marshall D, Lappe DL. *Hyperglycemia predicts mortality after CABG: postoperative hyperglycemia predicts dramatic increases in mortality after coronary artery bypass graft surgery*. Journal of Diabetes and its Complications 2008;22:365-370

48. Rassias A. *Intraoperative Management of Hyperglycemia in the Cardiac Surgical Patient*. Seminars in Thoracic and Cardiovascular Surgery 2006;18:330-338

49. Furnary AP, Wu Y, Bookin S. *Effect of Hyperglycemia and Continuous Intravenous Insulin Infusions on Outcomes of Cardiac Surgical Procedures: the Portland Diabetic Project*. Endocrine Prac 2004;10:21-33

50. Furnary AP, Zerr KJ, Grunkemeier GL. *Continuous intravenous insulin infusion reduces the incidence of deep sternal wound infection in diabetic patients after cardiac surgical procedures*. Ann Thoracic Surg 1999;67:352-360

51. Furnary AP, Zerr KJ, Grunkemeier GL, Heller CA. *Hyperglycemia: a predictor of mortality following CABG in diabetics*. Circulation 1999;100:I591

52. Furnary AP, Chaugle H, Zerr K, Grunkemeier G. *Continuous insulin infusion reduces mortality in patients with diabetes undergoing coronary artery bypass grafting*. Journal of Thoracic and Cardiovascular Surgery 2003;125:1007-1021

53. Zerr KJ, Furnary AP, Grunkemeier GL, Bookin S, Kanhere V, Starr A. *Glucose control lowers the risk of wound infection in diabetics after open heart operations*. Ann Thoracic Surg 1997;63:356-361

54. Furnary AP, Chaugle H, Zerr K, Grunkemeier G. *Postoperative hyperglycemia prolongs length of stay in diabetic CABG patients*. Circulation 2000;102:II556

55. Van Den Berghe G, Wouters P, Weekers F. *Intensive insulin therapy in critically ill patients*. N Engl J Med 2001;345:1359-1367

56. Van den Berghe G, Wouters PJ, Bouillon R. *Outcome benefit of intensive insulin therapy in the critically ill: insulin dose versus glycemic control*. Crit Care Med 2003;31:359-366

57. Smith S, Ovenson K, Strauss W, et al. *Ultradian Variation of Blood Glucose in Intensive Care Unit Patients Receiving Insulin Infusions* Diabetes Care 2007;30:2503-2505

58. Smith SM, Oveson KE, Strauss W, Ahmann AJ, Hagg DS. *Diurnal and other variations in blood glucose in ICU patients receiving insulin infusions*. Crit Care 2007;11:133

59. Smith S, Hagg D. *Glucose Variance in ICU Patients Receiving Insulin Infusions* Chest 2008;133:1288

60. De Feo P, Perriello G, Torlone E, et al. Contribution of cortisol to glucose counterregulation in humans. Am J Physiol Endocrinol Metab 1989;257:E35-42

61. Vanhorebeek I, Peeters RP, Vander Perre S, et al. Cortisol Response to Critical Illness: Effect of Intensive Insulin Therapy. J Clin Endocrinol Metab 2006;91:3803-3813

62. Hamrahian AH, Oseni TS, Arafah BM. Measurements of Serum Free Cortisol in Critically Ill Patients. N Engl J Med 2004;350:1629-1638

63. Finney SJ, Zekveld C, Elia A, Evans TW. Glucose Control and Mortality in Critically Ill Patients. JAMA 2003;290:2041-2047

64. Ingels C, Debaveye Y, Milants I, et al. Strict blood glucose control with insulin during intensive care after cardiac surgery: impact on 4-years survival, dependency on medical care, and quality-of-life. Eur Heart J 2006;27:2716-2724

65. Van den Berghe G. How does blood glucose control with insulin save lives in intensive care? The Journal of Clinical Investigation 2004;114:1187-1195

66. Grey N, Perdrizet G. *Reduction of Nosocomial Infections in the Surgical Intensive Care Unit By Strict Glycemic Control* Endocrine Prac 2004;10:46-52

67. Kanji S, Buffie J, Hutton B, et al. Reliability of point-of-care testing for glucose measurement in critically ill adults *. Critical Care Medicine 2005;33:2778-2785

68. Plank J, Blaha J, Cordingley J, et al. *Multicentric, Randomized, Controlled Trial to Evaluate Blood Glucose Control by the Model Predictive Control Algorithm Versus Routine Glucose Management Protocols in Intensive Care Unit Patients* Diabetes Care 2006;29:271-276

69. Wintergerst KA, Deiss D, Buckingham B, et al. Glucose Control in Pediatric Intensive Care Unit Patients Using an Insulin-Glucose Algorithm. Diabetes Technology & Therapeutics 2007;9:211-222

70. Chee F, Fernando T, Savkin A, van Heerden V. Expert PID control system for blood glucose control in critically ill patients. IEEE Trans Inf Technol Biomed 2003;7:419 - 425

71. Vogelzang M, Zijlstra F, Nijsten M. Design and implementation of GRIP: a computerized glucose control system at a surgical intensive care unit. BMC Medical Informatics and Decision Making 2005;5:38

72. Klonoff DC. A Review of Continuous Glucose Monitoring Technology. Diabetes Technology & Therapeutics 2005;7:770-775

73. Mastrototaro JJ. The MiniMed Continuous Glucose Monitoring System. Diabetes Technology & Therapeutics 2000;2:13-18

74. Wilson D, Beck R, Tamborlane W,. *The Accuracy of the FreeStyle Navigator Continuous Glucose Monitoring System in Children With Type 1 Diabetes* Diabetes Care 2007;30:59-64

75. Boland E, Monsod T, Brandt C, et al. *Limitations of Conventional Methods of Self-Monitoring of Blood Glucose Lessons learned from 3 days of continuous glucose sensing in pediatric patients with type 1 diabetes*. Diabetes Care 2001;24:1858-1862

76. Bailey TS, Zisser HC, Garg SK. Reduction in Hemoglobin A1c with Real-Time Continuous Glucose Monitoring: Results from a 12-Week Observational Study. Diabetes Technology & Therapeutics 2007;9:203-210

77. Chico A, Vidal-Rios P, Subira M. *The Continuous Glucose Monitoring System Is Useful for Detecting Unrecognized Hypoglycemias in Patients With Type 1 and Type 2 Diabetes but Is Not Better Than Frequent Capillary Glucose Measurements for Improving Metabolic Control*. Diabetes Care 2003;26:1153-1157

78. Deiss Dorothee, Bolinder J, Riveline J, Battelino T, et al. *Improved Glycemic Control in Poorly Controlled Patients with Type 1 Diabetes Using Real-Time Continuous Glucose Monitoring* Diabetes Care 2006;29:2730-2732

79. Francine Ratner K, Juliana A, Aaron N, et al. Nocturnal hypoglycemia detected with the continuous glucose monitoring system in pediatric patients with type 1 diabetes. The Journal of pediatrics 2002;141:625-630

80. Garg S, Zisser H, Schwartz S, Bailey T, et al. *Improvement in Glycemic Excursions With a Transcutaneous, Real-Time Continuous Glucose Sensor: A randomized controlled trial* Diabetes Care 2006;29:44-50

81. Gross TM, Bode BW, Einhorn D, et al. Performance Evaluation of the MiniMed® Continuous Glucose Monitoring System During Patient Home Use. Diabetes Technology & Therapeutics 2000;2:49-56

82. Hay LC, Wilmshurst EG, Fulcher G. Unrecognized Hypo- and Hyperglycemia in Well-Controlled Patients with Type 2 Diabetes Mellitus: The Results of Continuous Glucose Monitoring. Diabetes Technology & Therapeutics 2003;5:19-26

83. Skyler JS. The Economic Burden of Diabetes and the Benefits of Improved Glycemic Control: The Potential Role of a Continuous Glucose Monitoring System. Diabetes Technology & Therapeutics 2000;2:7-12

84. Goldberg PA, Siegel MD, Russell RR, et al. Experience with the Continuous Glucose Monitoring System in a Medical Intensive Care Unit. Diabetes Technology & Therapeutics 2004;6:339-347

85. Chee F, Fernando T, van Heerden P. *Closed-loop glucose control in critically ill patients using continuous glucose monitoring system (CGMS) in real time*. IEEE Trans Inf Technol Biomed 2003;7:43-53

86. Price GC, Stevenson K, Walsh TS. Evaluation of a continuous glucose monitor in an unselected general intensive care population. Crit Care Resusc 2008;10:209-216

87. De Block C, Manuel-y-Keenoy B, Rogiers P, Jorens P, Van Gaal L. Glucose control and use of continuous glucose monitoring in the intensive care unit: a critical review. Curr Diabetes Rev 2008;4:234-244

88. Allen HF, Rake A, Roy M, Brenner D, McKiernan CA. Prospective detection of hyperglycemia in critically ill children using continuous glucose monitoring. Pediatr Crit Care Med 2008;9:153-158

89. Goldberg PA, Siegel MD, Russell RR, et al. Experience with the continuous glucose monitoring system in a medical intensive care unit. Diabetes Technol Ther 2004;6:339-347

90. Holzinger U, Warszawska J, Kitzberger R, et al. Real-Time Continuous Glucose Monitoring in Critically Ill Patients. Diabetes Care;33:467-472

91. Buckingham B, Caswell K, Wilson DM. Real-time continuous glucose monitoring. Current Opinion in Endocrinology, Diabetes and Obesity 2007;14:288-295

92. Buckingham B, Block J, Burdick J, et al. Response to Nocturnal Alarms Using a Real-Time Glucose Sensor. Diabetes Technology & Therapeutics 2005;7:440-447

93. Tubiana-Rufi N, Riveline JP,Dardari D. *Real-time continuous glucose monitoring using Guardian®RT: from research to clinical practice* Diabetes and Metabolism 2007;33:415-420

94. Weinstein R, Schwartz S, Brazg R, Bugler J, et al. *Accuracy of the 5-Day FreeStyle Navigator Continuous Glucose Monitoring System: Comparison with frequent laboratory reference measurements* Diabetes Care 2007;30:1125-1130

95. Bode B, Gross K, Rikalo N, et al. Alarms Based on Real-Time Sensor Glucose Values Alert Patients to Hypo- and Hyperglycemia: The Guardian Continuous Monitoring System. Diabetes Technology & Therapeutics 2004;6:105-113

96. Fanelli C, Pampanelli S, Epifano L, et al. Long-term recovery from unawareness, deficient counterregulation and lack of cognitive dysfunction during hypoglycaemia, following institution of rational, intensive insulin therapy in IDDM. Diabetologia 1994;37:1265-1276

97. Cryer PE, Davis SN, Shamoon H. *Hypoglycemia in Diabetes* Diabetes Care 2003;26:1902-1912

98. Cryer PE. Diverse Causes of Hypoglycemia-Associated Autonomic Failure in Diabetes. N Engl J Med 2004;350:2272-2279

99. Rebrin K, Steil GM. Can Interstitial Glucose Assessment Replace Blood Glucose Measurements? Diabetes Technology & Therapeutics 2000;2:461-472

100. Cengiz E, Tamborlane W. *A Tale of Two Compartments: Interstitial Versus Blood Glucose Monitoring*. Diabetes Tech Ther 2009;11:s11-s16

101. Kovatchev BP, Shields D, Breton M. *Graphical and Numerical Evaluation of Continuous Glucose Sensing Time Lag*. Diabetes Tech Ther 2009;11:139-143

102. Wentholt IME, Hart AAM, Hoekstra JBL, Devries JH. Relationship Between Interstitial And Blood Glucose in Type 1 Diabetes Patients: Delay And The Push-Pull Phenomenon Revisited. Diabetes Technology & Therapeutics 2007;9:169-175

103. Sjöbom N, Adamson U, Lins P. The prevalence of impaired glucose counter-regulation during an insulin-infusion test in insulin-treated diabetic patients prone to severe hypoglycaemia. Diabetologia 1989;32:818-825

104. Kinsley B, Simonson D. Evidence for a hypothalamic-pituitary versus adrenal cortical effect of glycemic control on counterregulatory hormone responses to hypoglycemia in insulin-dependent diabetes mellitus. J Clin Endocrinol Metab 1996;81:684-691

105. Cryer PE, Childs BP. Negotiating the Barrier of Hypoglycemia in Diabetes. Diabetes Spectrum 2002;15:20-27

106. Tresp V, Briegel T,Moody J. Neural Network Models for Blood Glucose Metabolism of a Diabetic. IEEE Trans on Neural Networks 1999;10:1204-1212

107. Prank K, Jurgens C, von zur Muhlen A, Brabant G. Predictive Neural Networks for Learning the Time Course of Blood Glucose Levels from the Complex Interaction of Counterregulatory Hormones. Neural Computation 1998;10:941-953

108. Davide D, Francesco T, Alessandra G, et al. The control of blood glucose in the critical diabetic patient: a neuro-fuzzy method. Journal of Diabetes and its Complications 2001;15:80-87

109. El-Jabali A. Neural network modeling and control of type 1 diabetes mellitus. Bioprocess and Biosystems Engineering 2005;27:75-79

110. Krinsley JS, Grover A. Severe hypoglycemia in critically ill patients: Risk factors and outcomes. Critical Care Medicine 2007;35:2262-2267

111. Renner G, Ainko E. *Genetic Algorithms in Computer Aided Design*. Computer Aided Design 2003;35:709-726

112. McShane MJ, Cameron BD, Cote GL, Spiegelman CH. *Improving complex near-IR calibrations using a new wavelength selection algorithm*. Applied Spectroscopy 1999;53:1575-1581

113. McShane MJ CB, Cote GL, Motamadi M, Spiegelman CH. *A novel peak-hopping stepwise feature selection method with application to Raman spectroscopy*. Analytical Chemica Acta 1999;388:251-264

114. Clarke WL, Cox D, Gonder-Frederick LA, Carter W, Pohl SL. Evaluating clinical accuracy of systems for self-monitoring of blood glucose. Diabetes Care 1987;10:622-628

115. Klonoff DC. Continuous Glucose Monitoring. Diabetes Care 2005;28:1231-1239

116. Steil GM, Rebrin K, Janowski R, Darwin C, Saad MF. Modeling Î²-Cell Insulin Secretion - Implications for Closed-Loop Glucose Homeostasis. Diabetes Technology & Therapeutics 2003;5:953-964

117. Segel SA, Paramore DS, Cryer PE. Hypoglycemia-Associated Autonomic Failure in Advanced Type 2 Diabetes. Diabetes 2002;51:724-733

118. Dagogo-Jack SE, Craft S, Cryer PE. *Hypoglycemia-associated autonomic failure in insulin dependent diabetes mellitus*. Journ Clin Invest 1993;91:819-828

119. Mokan M, Mitrakou A, Veneman T, et al. Hypoglycemia unawareness in IDDM. Diabetes Care 1994;17:1397-1403

120. Gerich JE, Mokan M, Veneman T, Korytkowski M, Mitrakou A. Hypoglycemia Unawareness. Endocr Rev 1991;12:356-371

121. Hoeldtke RD, Boden G, Shuman CR, Owen OE. Reduced Epinephrine Secretion and Hypoglycemia Unawareness in Diabetic Autonomic Neuropathy. Annals of Internal Medicine 1982;96:459-462

122. Skevofilakas M, Mougiakakou SG, Zarkogianni K, Aslanoglou E, Pavlopoulos SA, Vazeou A, Bartsocas CS, Nikita KS *A Communication and Information Technology Infrastructure for Real Time Monitoring and Management of Type 1 Diabetes Patients*. Engineering in Medicine and Biology: 29th Annual Conference of IEEE 2007:3685-3688

123. Klonoff DC. *Continuous glucose monitoring: roadmap for 21st century diabetes therapy.* Diabetes Care 2005;28:1231-1239

124. Filipovsky J, Ducimetiere P, Eschwege E, et al. The relationship of blood pressure with glucose, insulin, heart rate, free fatty acids and plasma cortisol levels according to degree of obesity in middle-aged men. Journal of Hypertension 1996;14:229-235

125. Molnar GW, Read RC. Hypoglycemia and Body Temperature. JAMA 1974;227:916-921

126. Clarke WL. The Original Clarke Error Grid Analysis (EGA). Diabetes Technology & Therapeutics 2005;7:776-779

127. Pappada SM, Cameron BD, Rosman PM. *Development of a Neural Network for Prediction of Glucose Concentration in Type 1 Diabetes Patients*. Journal of Diabetes Science and Technology 2008;2:793-801

128. Palatini P, Casiglia E, Pauletto P, et al. Relationship of Tachycardia With High Blood Pressure and Metabolic Abnormalities : A Study With Mixture Analysis in Three Populations. Hypertension 1997;30:1267-1273

129. Perez-Gandia C, Facchinetti A, Sparacino G, et al. Artificial Neural Network Algorithm for Online Glucose Prediction from Continuous Glucose Monitoring. Diabetes Technology & Therapeutics 2010;12:81-88

130. Inzucchi SE, Siegel MD. Glucose Control in the ICU -- How Tight Is Too Tight? N Engl J Med 2009;360:1346-1349

131. Umpierrez G, Isaacs S, Bazargan N, et al. Hyperglycemia: an independent marker of in-hospital mortality in patients with undiagnosed diabetes. J Clin Endocrinol Metab 2002;87:978 - 982

APPENDIX

APPENDIX A

A.1 Biomedical Institutional Review Board Approval (#106204) for Critical Care Investigation at University of Toledo Medical Center

THE UNIVERSITY OF TOLEDO
1872

The University of Toledo
Department for Human Research Protections
Biomedical Institutional Review Board
Center for Creative Education Building – Room 0106
3025 Arlington Avenue, Toledo, Ohio 43614-2570
Phone: 419-383-6796 Fax: 419-383-3248
(FWA00010686)

TO: **Thomas Papadimos, M.D.**
UT Department of Anesthesiology

FROM: Roland Skeel, M.D., Chair
Deepak Malhotra, M.D. Vice Chair
Gregory Siegel, R.Ph., J.D., Chair Designee
UT Biomedical Institutional Review Board

SIGNED: _____ **DATE** 1-20-09

SUBJECT: **IRB # 106204**
TITLE: Effects of Using a Laser Cane as a Visual Cue to Improve Gait in Patients with Parkinson's Disease

---

The above project was reviewed and **approved** by the Chair and Chair Designee of the University of Toledo Institutional Review Board as an **expedited review** (categories #1b, #4 and #5). A signed and dated Informed Consent/Authorization form is required from each participant prior to that individual taking part in this research. This research is approved for a period of up to one year from the date of this review and approval. This action will be reported to the committee at its meeting on 02/19/2009.

Items Reviewed:

- IRB Application requesting Initial Review of Expedited Research
- Protocol Description/Grant Application (assigned version date 11/06/2008)
- Consent/Authorization form (version date 01/07/2009)
- Data Collection Tool (assigned version date 08/31/2007)

This research is **approved** until the expiration date listed below, unless the IRB notifies you otherwise.

APPROVAL DATE: 01/12/2009	**EXPIRATION DATE: 01/11/2010**

Please read the following attachment detailing Principal Investigator responsibilities.

THE UNIVERSITY OF TOLEDO
1872

Department of Surgery
University of Toledo Medical Center
Mailstop 1137, 3000 Arlington Ave
Toledo, Ohio 43614
Phone: (419) 383-6298

ADULT RESEARCH SUBJECT INFORMATION AND CONSENT FORM and AUTHORIZATION FOR USE AND DISCLOSURE OF PROTECTED HEALTH INFORMATION

Glycemic Prediction in Trauma Patients: for Improved Treatment Outcomes

Principal Investigators:	Thomas Papadimos, MD.
Other Staff (identified by role):	Brent Cameron, Ph.D., Co-Investigator Sonia Najjar, Ph.D., Co-Investigator Brian Lane, M.D., Co-Investigator Marilyn Borst, M.D., Co-Investigator Scott Pappada, Co-Investigator
Contact Phone number(s):	(419) 383-6298

What you should know about this research study:

- We give you this consent/authorization form so that you may read about the purpose, risks, and benefits of this research study. All information in this form will be communicated to you verbally by the research staff as well.
- Routine clinical care is based upon the best-known treatment and is provided with the main goal of helping the individual patient. The main goal of research studies is to gain knowledge that may help future patients.
- We cannot promise that this research will benefit you. Just like routine care, this research can have side effects that can be serious or minor.
- You have the right to refuse to take part in this research, or agree to take part now and change your mind later.
- If you decide to take part in this research or not, or if you decide to take part now but change your mind later, your decision will not affect your routine care.
- Please review this form carefully. Ask any questions before you make a decision about whether or not you want to take part in this research. If you decide to take part in this research, you may ask any additional questions at any time.
- Your participation in this research is voluntary.

RR050

NO TEXT THIS PAGE

PURPOSE (WHY THIS RESEARCH IS BEING DONE)

You are being asked to take part in a research study of glucose values in the Critical Care Unit. The purpose of the study is to determine if a sophisticated computer program can learn to predict glucose values far enough in the future to allow physicians time to intervene beforehand.
You were selected as someone who may want to take part in this study because you or your family member has an elevated glucose value due to the severity of injuries, and is expected to be in the Intensive Care Unit for several days. During this time as standard care nursing will be frequently checking the glucose values by fingersticks, and providing insulin if needed based upon the glucose value. There will be 25 patients involved in the study, and your involvement in this study will end once you or your family member is discharged from the Intensive Care Unit.

DESCRIPTION OF THE RESEARCH PROCEDURES AND DURATION OF YOUR INVOLVEMENT

If you decide to take part in this study, you will be asked to have a FDA approved continuous glucose sensor placed into your skin, and information related to your care while in the Intensive Care Unit collected. The sensor has a thin fiber that goes into the skin, usually on the abdominal wall. It has a transmitter that sends information to a monitor by the bedside. Patients with diabetes often use the device to monitor their glucose values while at home. They can leave the device in place for up to seven days. The device will not change what care you will receive, but it will alarm if the glucose value goes below normal to help call nursing attention to this. Information about nutrition intake, medication infusions, vital signs, and other events in your care will be put into a sophisticated computer program (neural network) and when all of the information is in, the program will be trained to predict glucose values in advance. In future research, the computer will help control glucose values, but not during this current study.

RISKS AND DISCOMFORTS YOU MAY EXPERIENCE IF YOU TAKE PART IN THIS RESEARCH

Please see the picture of the sensor provided with this consent form. The fiber inserted in the skin is smaller than the needles used to draw blood, and can stay in place for several days. Other than mild discomfort during insertion, it is not expected to be painful or place you at serious risk. If any problems related to the sensor fiber occur they will be treated by the Intensive Care Unit physicians. Nurses will still need to routinely check your glucose values the standard way with finger stick measurements, and they will continue to adjust your medication based upon the fingerstick values, not based upon the sensor values. Other than an additional alarm if your glucose values are low, this device and this study are not expected to alter your care in any way. Your condition may not get better or may become worse while you are in this research.

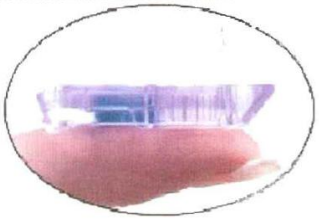

The main risk is not physical, but relates to use of your personal medical information as part of the research. In order to protect confidentiality of your information, we do not collect identifying information such as name, home address, or telephone number. The research does not require any personal identifying information and once medical information related to your Intensive Care Unit stay has been collected, the information which distinguishes you from other patients will be erased. The risk of physical injury or loss of your identifying information is minimal.

POSSIBLE BENEFIT TO YOU IF YOU DECIDE TO TAKE PART IN THIS RESEARCH

The research project is not expected to alter the type of care that you receive. Other than the potential for an additional alarm for low glucose values, it is not expected to offer any additional benefit. We cannot and do not guarantee or promise that you will receive any benefits from this research.

COST TO YOU FOR TAKING PART IN THIS STUDY

There is no cost to you for taking part in this study. There will be no additional cost to your insurance company because you are taking part in this study. The cost of the monitor is covered by a University of Toledo research grant.

PAYMENT OR OTHER COMPENSATION TO YOU FOR TAKING PART IN THIS RESEARCH

There is no compensation or monies paid for taking part in this study. If you decide to take part in this research you will not receive any additional care or products.

PAYMENT OR OTHER COMPENSATION TO THE RESEARCH SITE

The University of Toledo, the University of Toledo Medical Center, and the researchers are not receiving any monies from industry or outside groups for performing this study.

ALTERNATIVE(S) TO TAKING PART IN THIS RESEARCH

You may choose to take part in this project or you may choose to decline the offer. It will not alter the care that you will receive while you are in the Intensive Care Unit. You will still receive standard care while you are in the Intensive Care Unit.

CONFIDENTIALITY - (USE AND DISCLOSURE OF YOUR PROTECTED HEALTH INFORMATION)

By agreeing to take part in this research study, you give to the University of Toledo Medical Center, the Principal Investigator and all personnel associated with this research study your permission to use or disclose health information that can be identified with you that we obtain in connection with this study. We will use this information to help train the computer program to predict glucose values in advance.

The information that we will use or disclose includes information related to your care while in the Intensive Care Unit. This will include information on medications, height, weight, vital signs such as heart rate and blood pressure, nutrition, laboratory tests, and events while in the Critical Care Unit. It will not include items such as address or phone number. When you leave the Critical Care Unit, a study number will be used to replace your name when the information is stored, so if future researchers look at the information there will not be any way to identify you as the participant in the study. We may use this information ourselves, or we may disclose or provide access to the information to the Food and Drug Administration or other applicable governmental agencies if they request it. As the monitor is already FDA approved, it is not expected that they will want access to this information as part of the research study. Under some circumstances, the Institutional Review Board and Research and Sponsored Programs of the University of Toledo may review your information for compliance audits.

The University of Toledo is required by law to protect the privacy of your health information, and to use or disclose the information we obtain about you in connection with this research study only as authorized by you in this form. There is a possibility that the information we disclose may be re-disclosed by the persons we give it to, and no longer protected. However, we will encourage any person who receives your information from us to continue to protect and not re-disclose the information.

RR050

Your permission for us to use or disclose your personal health information as described in this section is voluntary. However, you will not be allowed to participate in the research study unless you give us your permission to use or disclose your personal health information by signing this document.

You have the right to revoke (cancel) the permission you have given to us to use or disclose your personal health information at any time by giving written notice to Dr. Thomas Papadimos, MD, University of Toledo Medical Center, Mail Stop 1095, Toledo, Ohio, 43614-5807. However, a cancellation will not apply if we have acted with your permission, for example, information that already has been used or disclosed prior to the cancellation. Also, a cancellation will not prevent us from continuing to use and disclose information that was obtained prior to the cancellation as necessary to maintain the integrity of the research study.

Except as noted in the above paragraph, your permission for us to use and disclose personal health information will be limited to information related to your stay in the Intensive Care Unit, and long term storage of this information will not include personal identifying information. Any publication of the results from this research will not include identifying information about you.

A more complete statement of University of Toledo's Privacy Practices is set forth in its Joint Notice of Privacy Practices. If you have not already received this Notice, a member of the research team will provide this to you. If you have any further questions concerning privacy, you may contact the University of Toledo's Privacy Officer at 419-383-3413.

IN THE EVENT OF A RESEARCH-RELATED INJURY

In the event of injury resulting from your taking part in this study, treatment can be obtained at a health care facility of your choice. You should understand that the costs of such treatment will be your responsibility. Financial compensation is not available through The University of Toledo or The University of Toledo Medical Center. By signing this form you are not giving up any of your legal rights as a research subject.

In the event of an injury, or if you have questions about the research or research subjects rights, you can talk with the Surgical Intensive Care Service attending providing care during the day, or have the hospital operator page either the Surgical Intensive Care Service attending or the Trauma Surgery Attending on call, at (419) 383-4000. If the concerns are not urgent you can contact the Dept. of Anesthesia at (419) 383-3556, or contact Dr. Brian Lane through the Dept. of Surgery at (419) 383-6298.

VOLUNTARY PARTICIPATION

Taking part in this study is voluntary. You may refuse to participate or discontinue participation at any time without penalty or a loss of benefits to which you are otherwise entitled. If you decide not to participate or to discontinue participation, your decision will not affect your future relations with the University of Toledo or The University of Toledo Medical Center.

NEW FINDINGS

You will be notified of new information that might change your decision to be in this study if any becomes available.

RR050

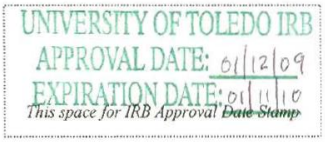

OFFER TO ANSWER QUESTIONS

Before you sign this form, please ask any questions on any aspect of this study that is unclear to you. You may take as much time as necessary to think it over. If you have questions regarding the research at any time before, during or after the study, you may contact Brian Lane, MD, Department of Surgery, University of Toledo Medical Center, Mail Stop 1095, Toledo, Ohio, 43614-5807.

If you have questions beyond those answered by the research team or your rights as a research subject or research-related injuries, please feel free to contact the Chairperson of the University of Toledo Biomedical Institutional Review Board at 419-383-6796.

SIGNATURE SECTION (Please read carefully)

YOU ARE MAKING A DECISION WHETHER OR NOT TO PARTICIPATE IN THIS RESEARCH STUDY. YOUR SIGNATURE INDICATES THAT YOU HAVE READ THE INFORMATION PROVIDED ABOVE, YOU HAVE HAD ALL YOUR QUESTIONS ANSWERED, AND YOU HAVE DECIDED TO TAKE PART IN THIS RESEARCH.

BY SIGNING THIS DOCUMENT YOU AUTHORIZE US TO USE OR DISCLOSE YOUR PROTECTED HEALTH INFORMATION AS DESCRIBED IN THIS FORM.

The date you sign this document to enroll in this study, that is, today's date, MUST fall between the dates indicated on the approval stamp affixed to the bottom of each page. These dates indicate that this form is valid when you enroll in the study but do not reflect how long you may participate in the study. Each page of this Consent/Authorization Form is stamped to indicate the form's validity as approved by the UT Biomedical Institutional Review Board (IRB).

Name of Subject (please print)	Signature of Subject or Their Representative	Date
Relationship to the Subject (Legal Guardian or other Healthcare Power of Attorney)		Time a.m. p.m.
Name of Person Obtaining Consent (please print)	Signature of Person Obtaining Consent	Date
Name of Witness to Consent Process (when required by ICH Guidelines) (please print)	Signature of Witness to Consent Process (when required by ICH Guidelines)	Date

YOU WILL BE GIVEN A SIGNED COPY OF THIS FORM TO KEEP.

Data Collection Tools

The electronic clinical data logging program, (eCIDL) is a computer program initially written by the researchers to allow patients at home to input information into the neural network program as part of an outpatient study on glucose predictions. Based upon the success of this project, the TRSA grant was submitted. Modification of the eCIDL has been performed to allow information from the care of the patient while in the Intensive Care Unit to be entered. Information that reflects the traumatic stress of the patient, medications or activities that may alter the stress of the patient will be abstracted. Figure 1. Shows the initial screen from the eCIDL demonstrating the breadth of information collected. The data reflects the Intensive Care Unit flow sheet.

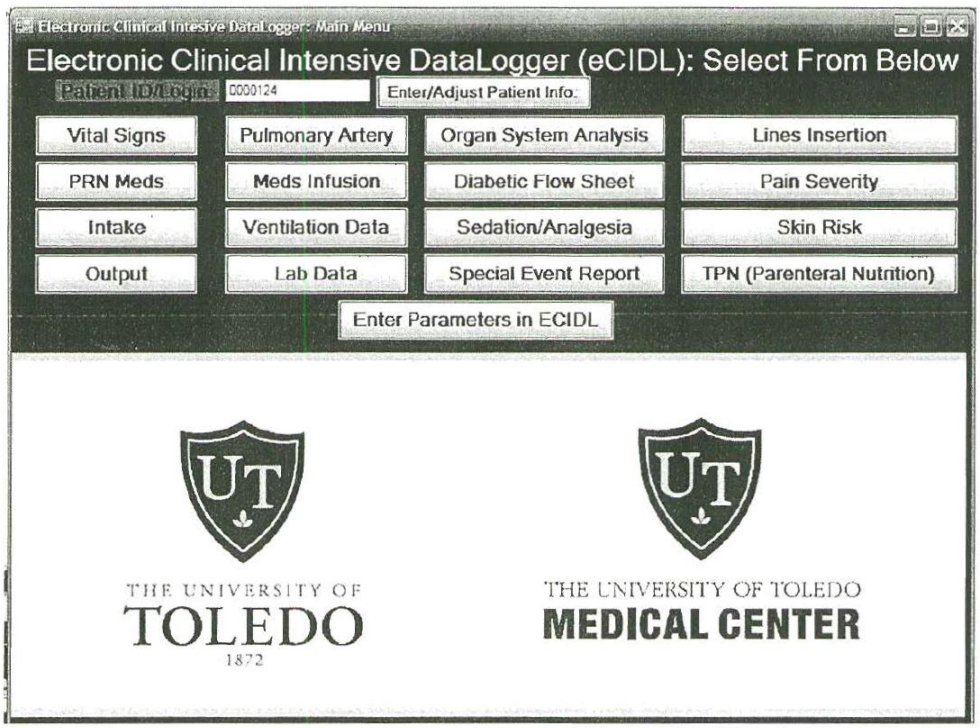

Figure 1. eCIDL Menu page demonstrating the breadth of data collected.

The continuous glucose monitoring device is made up of a sensor with transmitter (biomedical engineering approved), and a monitor which stores the readings. These are depicted in Figure 2. The monitor display will be turned off so as to not influence the routine care of the patient. However, the low glucose alarm will remain on to provide added safety to the routine care of the patient.

Figure 2. Transmitter and Glucose monitor.

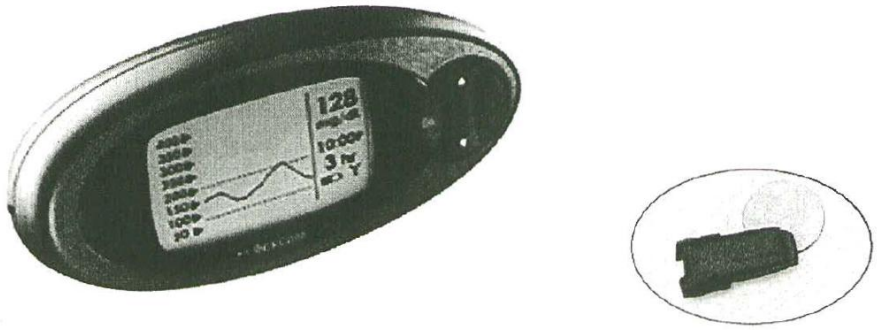

The implanted portion of the sensor is depicted by the thin fiber in Figure 3. This is small enough to represent minimal risk of complication within the subcutaneous tissue. This product was designed for comfortable outpatient use, and represents minimal risk within the critical care unit.

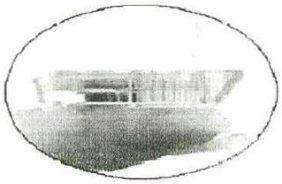

Figure 3. Sensor component of the Continuous Glucose Monitor. Note the size of the inserted fiber.

APPENDIX B

B.1 Neural Network Model Source Code for Real-time Training/Prediction (Dynamic Linked Library Implementation)

```
// Create Neural Network Model Components
LaguarreAxon inputAxon; //Input Axon
BackLaguarreAxon inputAxonBackprop; //Input Axon Backpropagation Element
//Backpropagation Element For Calculating Weights Via Gradient Descent With
Momentum (Input Axon)
Momentum inputAxonBackpropGradient;
DataFile inputFile; //Input File Containing Neural Network Input Data
FullSynapse hidden1Synapse; //Hidden 1 Layer Synapse
BackFullSynapse hidden1SynapseBackprop; // Backpropagation Element (Hidden Layer
1 Synapse)
Momentum hidden1SynapseBackpropGradient; //Backpropagation Element For
Calculating Weights Via Gradient Descent With Momentum (Hidden Layer 1 Synapse)
TanhAxon hidden1Axon; //Hidden Layer 1 Tanh Axon
BackTanhAxon hidden1AxonBackprop; //Backpropagation Element (Hidden Layer 1
Tanh Axon)
Momentum hidden1AxonBackpropGradient; //Backpropagation Element For Calculating
Weights Via Gradient Descent With Momentum (Hidden Layer 1 Tanh Axon)
FullSynapse outputSynapse; //Outpu Layer Synapse
BackFullSynapse outputSynapseBackprop; //BackPropagation Element (Output Synapse)
Momentum outputSynapseBackpropGradient; //Backpropagation Element For
Calculating Weights Via Gradient Descent With Momentum (Output Layer Synapse)
BiasAxon outputAxon; //Output Bias Axon
BackBiasAxon outputAxonBackprop; // Output Axon Backpropagation Element
Momentum outputAxonBackpropGradient; //Backpropagation Element For Calculating
Weights Via Gradient Descent With Momentum (Output Bias Axon)
DataFile outputDesiredDataGraph; //Output Desired File (Neural Network Predicted
Output and Desired Data)
DataFile CVOutputDesiredDataGraph; //Output Desired File (Neural Network Predicted
Output and Desired Data) for Cross Validation
L2Criterion criterion; //Error Element
BackCriteriaControl criterionBackprop; //Backpropagation of Model Error from Error
Element
DataFile desiredFile; //File Containing Desired Response for Network to Model
DataFile desiredViewer; //Desired Response Viewer
DataFile CVDesiredViewer;//Desired Response Viewer for Cross Validation
DataFile learningCurveDataGraph; // Learning Curve For Neural Network Model
DataFile MSEViewer; //Mean Squared Error of Model Output
DataFile CVMSEViewer;//Mean Squared Error of Model Output for Cross Validation
DynamicControl control;
BackDynamicControl controlBackprop;
```

```
DataFile bestFitnessGraph; //Best error for Neural Network Model

//Source Code to Initialize Neural Network Model Configuration
extern void __cdecl set_pstrauma_params(void)
{
	AFX_MANAGE_STATE(AfxGetStaticModuleState());
	srand((unsigned)time(NULL));
// Component Initialization Within Neural Network Model
	inputAxon.setTemporalDimension(2);
	inputAxon.setRows(40); //Set Number of Neural Network Inputs
	inputAxonBackprop.setTemporalDimension(2);
	inputAxonBackprop.setRows(40);
	inputAxonBackpropGradient.setDefaultMomentum(0.0000000000000000e+000);
	inputAxonBackpropGradient.setDefaultStepSize(0.0000000000000000e+000);
	inputAxonBackpropGradient.setStepDivisor(200); //Set Divisor for Step Size
	inputFile.setFilePath("inputFile.asc"); //Set Path for Input File
	inputFile.setMode(READ,ASCII);
	inputFile.setSpatialDimension(40,1);
	hidden1Synapse.setWeightVariance(2.0000000000000000e-002);
	hidden1SynapseBackpropGradient.setDefaultMomentum(2.413e- 003);
	hidden1SynapseBackpropGradient.setDefaultStepSize(9.9999998e-003);
	hidden1SynapseBackpropGradient.setStepDivisor(200);
	hidden1Axon.setRows(5); //Set Inputs to Hidden Layer 1
	hidden1AxonBackprop.setOffset(1.000000000e-003); //Offset  Hidden Layer 1
	hidden1AxonBackprop.setRows(5);
	hidden1AxonBackpropGradient.setDefaultMomentum(1.668e-001);
	hidden1AxonBackpropGradient.setDefaultStepSize(1.5714603662490845e-001);
	hidden1AxonBackpropGradient.setStepDivisor(200);
	outputSynapse.setWeightVariance(2.3999999999999999e+000);
	outputSynapseBackpropGradient.setDefaultMomentum(7.7313e-002);
	outputSynapseBackpropGradient.setDefaultStepSize(2.7087e-001);
	outputSynapseBackpropGradient.setStepDivisor(200);
	outputAxon.setRows(2); //Inputs to Output Axon
	outputAxonBackprop.setRows(2);
	outputAxonBackpropGradient.setDefaultMomentum(1.384e-002);
	outputAxonBackpropGradient.setDefaultStepSize(2.8379e-002);
	outputAxonBackpropGradient.setStepDivisor(200);
	outputDesiredDataGraph.setFilePath("outputDesiredDataGraph.asc");
	outputDesiredDataGraph.setMode(WRITE,ASCII);
	outputDesiredDataGraph.setSpatialDimension(2,1);
	CVOutputDesiredDataGraph.setAccessTesting(TRUE);
	CVOutputDesiredDataGraph.setFilePath("CVOutputDesiredDataGraph.asc");
	CVOutputDesiredDataGraph.setMode(WRITE,ASCII);
	CVOutputDesiredDataGraph.setSpatialDimension(2,1);
	criterion.setAutoSave(TRUE);
	criterion.setCheckCostEvery(1000); //Check Error After Every 1000 epochs
```

```
        criterion.setConfusionThreshold(0.0000000000000000e+000);
        criterion.setOnIncrease(TRUE);
        criterion.setBestCost(1.0224302723032389e-002); //Initial Best Error For Model
        criterion.setTotalNetworkWeights(257); //Total # of Model Weights
        criterion.setRows(2);
        criterionBackprop.setRows(2);
        desiredFile.setFilePath("desiredFile.asc");
        desiredFile.setMode(READ,ASCII);
        desiredFile.setSpatialDimension(2,1);
        desiredViewer.setFilePath("desiredViewer.asc");
        desiredViewer.setMode(WRITE,ASCII);
        desiredViewer.setSpatialDimension(2,1);
        CVDesiredViewer.setAccessTesting(TRUE);
        CVDesiredViewer.setFilePath("CVDesiredViewer.asc");
        CVDesiredViewer.setMode(WRITE,ASCII);
        CVDesiredViewer.setSpatialDimension(2,1);
        learningCurveDataGraph.setFilePath("learningCurveDataGraph.asc");
        learningCurveDataGraph.setMode(WRITE,ASCII);
        learningCurveDataGraph.setSpatialDimension(1,1);
        MSEViewer.setFilePath("MSEViewer.asc");
        MSEViewer.setMode(WRITE,ASCII);
        MSEViewer.setSpatialDimension(1,1);
        CVMSEViewer.setAccessTesting(TRUE);
        CVMSEViewer.setFilePath("CVMSEViewer.asc");
        CVMSEViewer.setMode(WRITE,ASCII);
        CVMSEViewer.setSpatialDimension(1,1);
        control.setTerminateWOImprovement(FALSE);
        control.setMaxEpochsWOImprovement(100);
        control.setPhases(1);
        control.setCostOfBestWeights(1.0000000000000000e+009);
        control.setEpochOfBestWeights(0); //First Epoch Cotains Best Model Weights
        control.setLearningType((NLearningType)0);
        control.allocateNewLearningGlobals();
        control.setWeightsRandomized(FALSE);
        control.setOptimizeInitialWeights(FALSE);
        control.setInitialLambda(1.0000000000000000e-002);
        controlBackprop.setGradientClassName("Momentum");
        bestFitnessGraph.setFilePath("bestFitnessGraph.asc");
        bestFitnessGraph.setMode(WRITE,ASCII);
        bestFitnessGraph.setSpatialDimension(1,1);

}

//Source Code to Connect Various Processing Elements Within Feed Forward Neural
Network Architecture
extern void __cdecl pstrauma_connect_components(void)
```

```
{
AFX_MANAGE_STATE(AfxGetStaticModuleState());
// Connect Various Elements Within Neural Network Architecture
inputAxon.setPreActivityAccess(&inputFile);
inputAxonBackprop.setDual(&inputAxon);
hidden1SynapseBackprop.setDual(&hidden1Synapse);
hidden1AxonBackprop.setDual(&hidden1Axon);
outputSynapseBackprop.setDual(&outputSynapse);
outputAxon.setActivityAccess(&outputDesiredDataGraph);
outputAxonBackprop.setDual(&outputAxon);
outputDesiredDataGraph.setStackedAccess(&CVOutputDesiredDataGraph);
outputDesiredDataGraph.setPerformNormalization(TRUE);
CVOutputDesiredDataGraph.setPerformNormalization(TRUE);
criterion.setCostAccess(&learningCurveDataGraph);
criterion.setDesiredAccess(&desiredFile);
criterionBackprop.setDual(&criterion);
desiredFile.setStackedAccess(&desiredViewer);
desiredViewer.setStackedAccess(&CVDesiredViewer);
desiredViewer.setPerformNormalization(TRUE);
CVDesiredViewer.setPerformNormalization(TRUE);
learningCurveDataGraph.setStackedAccess(&MSEViewer);
MSEViewer.setStackedAccess(&CVMSEViewer);
inputAxon.setNext(&hidden1Synapse);
inputAxonBackprop.setLast(&hidden1SynapseBackprop);
hidden1Synapse.setLast(&inputAxon);
hidden1Synapse.setNext(&hidden1Axon);
hidden1SynapseBackprop.setLast(&hidden1AxonBackprop);
hidden1SynapseBackprop.setNext(&inputAxonBackprop);
hidden1Axon.setLast(&hidden1Synapse);
hidden1Axon.setNext(&outputSynapse);
hidden1AxonBackprop.setLast(&outputSynapseBackprop);
hidden1AxonBackprop.setNext(&hidden1SynapseBackprop);
outputSynapse.setLast(&hidden1Axon);
outputSynapse.setNext(&outputAxon);
outputSynapseBackprop.setLast(&outputAxonBackprop);
outputSynapseBackprop.setNext(&hidden1AxonBackprop);
outputAxon.setLast(&outputSynapse);
outputAxon.setNext(&criterion);
outputAxonBackprop.setLast(&criterionBackprop);
outputAxonBackprop.setNext(&outputSynapseBackprop);
criterion.setLast(&outputAxon);
criterionBackprop.setNext(&outputAxonBackprop);
inputAxonBackpropGradient.setErrorSoma(&inputAxonBackprop);
inputAxonBackpropGradient.setForwardSoma(&inputAxon);
inputAxonBackpropGradient.setIndividualSteps(FALSE);
hidden1SynapseBackpropGradient.setErrorSoma(&hidden1SynapseBackprop);
```

```
        hidden1SynapseBackpropGradient.setForwardSoma(&hidden1Synapse);
        hidden1SynapseBackpropGradient.setIndividualSteps(FALSE);
        hidden1AxonBackpropGradient.setErrorSoma(&hidden1AxonBackprop);
        hidden1AxonBackpropGradient.setForwardSoma(&hidden1Axon);
        hidden1AxonBackpropGradient.setIndividualSteps(FALSE);
        outputSynapseBackpropGradient.setErrorSoma(&outputSynapseBackprop);
        outputSynapseBackpropGradient.setForwardSoma(&outputSynapse);
        outputSynapseBackpropGradient.setIndividualSteps(FALSE);
        outputAxonBackpropGradient.setErrorSoma(&outputAxonBackprop);
        outputAxonBackpropGradient.setForwardSoma(&outputAxon);
        outputAxonBackpropGradient.setIndividualSteps(FALSE);
        }



//Source Code for Setting Up Neural Network Model for Training/Prediction Via
Backpropagation
extern void __cdecl pstrauma_setup_run(void)
        {
   AFX_MANAGE_STATE(AfxGetStaticModuleState());
        // Get Ready to Run Network
        control.prepareToFire(&controlBackprop);
        inputAxon.setStaticControl(&control);
        inputAxon.preFireGetReady();
        inputAxonBackprop.setStaticControl(&control);
        inputAxonBackprop.preFireGetReady();
        inputAxonBackpropGradient.setStaticControl(&control);
        inputAxonBackpropGradient.preFireGetReady();
        inputFile.setStaticControl(&control);
        inputFile.preFireGetReady();
        hidden1Synapse.setStaticControl(&control);
        hidden1Synapse.preFireGetReady();
        hidden1SynapseBackprop.setStaticControl(&control);
        hidden1SynapseBackprop.preFireGetReady();
        hidden1SynapseBackpropGradient.setStaticControl(&control);
        hidden1SynapseBackpropGradient.preFireGetReady();
        hidden1Axon.setStaticControl(&control);
        hidden1Axon.preFireGetReady();
        hidden1AxonBackprop.setStaticControl(&control);
        hidden1AxonBackprop.preFireGetReady();
        hidden1AxonBackpropGradient.setStaticControl(&control);
        hidden1AxonBackpropGradient.preFireGetReady();
        outputSynapse.setStaticControl(&control);
        outputSynapse.preFireGetReady();
        outputSynapseBackprop.setStaticControl(&control);
```

```
outputSynapseBackprop.preFireGetReady();
outputSynapseBackpropGradient.setStaticControl(&control);
outputSynapseBackpropGradient.preFireGetReady();
outputAxon.setStaticControl(&control);
outputAxon.preFireGetReady();
outputAxonBackprop.setStaticControl(&control);
outputAxonBackprop.preFireGetReady();
outputAxonBackpropGradient.setStaticControl(&control);
outputAxonBackpropGradient.preFireGetReady();
outputDesiredDataGraph.setStaticControl(&control);
outputDesiredDataGraph.preFireGetReady();
CVOutputDesiredDataGraph.setStaticControl(&control);
CVOutputDesiredDataGraph.preFireGetReady();
criterion.setStaticControl(&control);
criterion.preFireGetReady();
criterionBackprop.setStaticControl(&control);
criterionBackprop.preFireGetReady();
desiredFile.setStaticControl(&control);
desiredFile.preFireGetReady();
desiredViewer.setStaticControl(&control);
desiredViewer.preFireGetReady();
CVDesiredViewer.setStaticControl(&control);
CVDesiredViewer.preFireGetReady();
learningCurveDataGraph.setStaticControl(&control);
learningCurveDataGraph.preFireGetReady();
MSEViewer.setStaticControl(&control);
MSEViewer.preFireGetReady();
CVMSEViewer.setStaticControl(&control);
CVMSEViewer.preFireGetReady();
controlBackprop.setStaticControl(&control);
controlBackprop.preFireGetReady();
bestFitnessGraph.setStaticControl(&control);
bestFitnessGraph.preFireGetReady();
control.preFireGetReady(TRUE);
control.setCrossValidationEnabled(FALSE);
control.clearEnginesToFire();
control.addToEnginesToFireList(&inputAxon, FALSE);
control.determineFiringSequence();
control.fireConfirmReady();
if (control.phases() > 1) {
if (control.backpropLearningOn()) {
        outputDesiredDataGraph.m_bAccessEnabled = FALSE;
        CVOutputDesiredDataGraph.m_bAccessEnabled = FALSE;
        desiredViewer.m_bAccessEnabled = FALSE;
        CVDesiredViewer.m_bAccessEnabled = FALSE;
        learningCurveDataGraph.m_bAccessEnabled = FALSE;
```

```
                MSEViewer.m_bAccessEnabled = FALSE;
                CVMSEViewer.m_bAccessEnabled = FALSE;
                bestFitnessGraph.m_bAccessEnabled = FALSE;
        }
        else {
                outputDesiredDataGraph.m_bAccessEnabled = TRUE;
                CVOutputDesiredDataGraph.m_bAccessEnabled = TRUE;
                desiredViewer.m_bAccessEnabled = TRUE;
                CVDesiredViewer.m_bAccessEnabled = TRUE;
                learningCurveDataGraph.m_bAccessEnabled = TRUE;
                MSEViewer.m_bAccessEnabled = TRUE;
                CVMSEViewer.m_bAccessEnabled = TRUE;
                bestFitnessGraph.m_bAccessEnabled = TRUE;
        }
        }
                inputAxonBackpropGradient.fireGetReady();
                hidden1SynapseBackpropGradient.fireGetReady();
                hidden1AxonBackpropGradient.fireGetReady();
                outputSynapseBackpropGradient.fireGetReady();
                outputAxonBackpropGradient.fireGetReady();
                criterion.fireGetReady();
        int updateCounter=0;
        FILE *loadStream = fopen("PSNNET75.nsw","r");
        if (!loadStream) {
                fprintf(stderr, "Could not open weight file PSNNET75.nsw");
                exit(1);
        }
        weightFileVersion = getWeightFileVersion(loadStream);

        }



//Load Neural Network Input File Normalization Coefficients
extern void __cdecl pstrauma_load_norm_coeff(void)
{
        AFX_MANAGE_STATE(AfxGetStaticModuleState());
        loadStream = fopen("PSNNet75.nsw","r");
        weightFileVersion = getWeightFileVersion(loadStream);
        //weightFileVersion=243;

        // Load Normalization Coefficients of Files
        inputFile.loadWeights(seekComponent(loadStream, "File",
"inputFile"),weightFileVersion);
        desiredFile.loadWeights(seekComponent(loadStream, "File",
"desiredFile"),weightFileVersion);
```

```
        outputDesiredDataGraph.loadWeights(seekComponent(loadStream, "DataGraph",
"outputDesiredDataGraph"),weightFileVersion);
        CVOutputDesiredDataGraph.loadWeights(seekComponent(loadStream,
"DataGraph", "CVOutputDesiredDataGraph"),weightFileVersion);
        desiredViewer.loadWeights(seekComponent(loadStream, "MatrixViewer",
"desiredViewer"),weightFileVersion);
        CVDesiredViewer.loadWeights(seekComponent(loadStream, "MatrixViewer",
"CVDesiredViewer"),weightFileVersion);

}



//Load Model Weights for Axons/Processing Elements Within Neural Network
Architecture
        extern void __cdecl pstrauma_load_axon_coeff(void)
        {
        AFX_MANAGE_STATE(AfxGetStaticModuleState());
        loadStream = fopen("PSNNet75.nsw","r");
        weightFileVersion = getWeightFileVersion(loadStream);
        //weightFileVersion=243;

        // Load Axon Weights
        inputAxon.loadWeights(seekComponent(loadStream, "LaguarreAxon",
"inputAxon"),weightFileVersion);
        hidden1Axon.loadWeights(seekComponent(loadStream, "TanhAxon",
"hidden1Axon"),weightFileVersion);
        outputAxon.loadWeights(seekComponent(loadStream, "BiasAxon",
"outputAxon"),weightFileVersion);
        criterion.loadWeights(seekComponent(loadStream, "L2Criterion",
"criterion"),weightFileVersion);

}

//Load Model Weights (Synapses of Neural Network Model)
        extern void __cdecl pstrauma_load_synapse_coeff(void)
        {
        AFX_MANAGE_STATE(AfxGetStaticModuleState());
        loadStream = fopen("PSNNet75.nsw","r");
        weightFileVersion = getWeightFileVersion(loadStream);
        //weightFileVersion=243;

        // Load Synapse Weights
        hidden1Synapse.loadWeights(seekComponent(loadStream, "FullSynapse",
"hidden1Synapse"),weightFileVersion);
```

```
	hidden1SynapseBackprop.loadWeights(seekComponent(loadStream,
"BackFullSynapse", "hidden1SynapseBackprop"),weightFileVersion);
	outputSynapse.loadWeights(seekComponent(loadStream, "FullSynapse",
"outputSynapse"),weightFileVersion);
	outputSynapseBackprop.loadWeights(seekComponent(loadStream,
"BackFullSynapse", "outputSynapseBackprop"),weightFileVersion);
	inputAxonBackpropGradient.loadWeights(seekComponent(loadStream,
inputAxonBackpropGradient.className(),
"inputAxonBackpropGradient"),weightFileVersion);
	hidden1SynapseBackpropGradient.loadWeights(seekComponent(loadStream,
hidden1SynapseBackpropGradient.className(),
"hidden1SynapseBackpropGradient"),weightFileVersion);
	hidden1AxonBackpropGradient.loadWeights(seekComponent(loadStream,
hidden1AxonBackpropGradient.className(),
"hidden1AxonBackpropGradient"),weightFileVersion);
	outputSynapseBackpropGradient.loadWeights(seekComponent(loadStream,
outputSynapseBackpropGradient.className(),
"outputSynapseBackpropGradient"),weightFileVersion);
	outputAxonBackpropGradient.loadWeights(seekComponent(loadStream,
outputAxonBackpropGradient.className(),
"outputAxonBackpropGradient"),weightFileVersion);
	control.loadWeights(seekComponent(loadStream, control.className(),
"control"),weightFileVersion);
	fclose(loadStream);
	}




//Source Code to Save Neural Network Model Weights After Updating Via Gradient
Descent Algorithm
extern void _cdecl saveAllWeights(char *weightsFilePath)
{
	AFX_MANAGE_STATE(AfxGetStaticModuleState());


	//Save Neural Network Model Weights at Each Layer to Path char
*WeightsFilePath

	FILE *saveStream = fopen(weightsFilePath,"w");
	if (!saveStream) {
		fprintf(stderr, "Could not open weight file %s\n", weightsFilePath);
		exit(1);
	}
	writeWeightFileVersion(saveStream);
```

```
        inputFile.saveWeights(putComponent(saveStream, "File", "inputFile"));
        desiredFile.saveWeights(putComponent(saveStream, "File", "desiredFile"));
        outputDesiredDataGraph.saveWeights(putComponent(saveStream, "DataGraph",
"outputDesiredDataGraph"));
        CVOutputDesiredDataGraph.saveWeights(putComponent(saveStream,
"DataGraph", "CVOutputDesiredDataGraph"));
        desiredViewer.saveWeights(putComponent(saveStream, "MatrixViewer",
"desiredViewer"));
        CVDesiredViewer.saveWeights(putComponent(saveStream, "MatrixViewer",
"CVDesiredViewer"));
        inputAxon.saveWeights(putComponent(saveStream, "LaguarreAxon",
"inputAxon"));
        hidden1Synapse.saveWeights(putComponent(saveStream, "FullSynapse",
"hidden1Synapse"));
        hidden1SynapseBackprop.saveWeights(putComponent(saveStream,
"BackFullSynapse", "hidden1SynapseBackprop"));
        hidden1Axon.saveWeights(putComponent(saveStream, "TanhAxon",
"hidden1Axon"));
        outputSynapse.saveWeights(putComponent(saveStream, "FullSynapse",
"outputSynapse"));
        outputSynapseBackprop.saveWeights(putComponent(saveStream,
"BackFullSynapse", "outputSynapseBackprop"));
        outputAxon.saveWeights(putComponent(saveStream, "BiasAxon",
"outputAxon"));
        criterion.saveWeights(putComponent(saveStream, "L2Criterion", "criterion"));
        inputAxonBackpropGradient.saveWeights(putComponent(saveStream,
inputAxonBackpropGradient.className(), "inputAxonBackpropGradient"));
        hidden1SynapseBackpropGradient.saveWeights(putComponent(saveStream,
hidden1SynapseBackpropGradient.className(), "hidden1SynapseBackpropGradient"));
        hidden1AxonBackpropGradient.saveWeights(putComponent(saveStream,
hidden1AxonBackpropGradient.className(), "hidden1AxonBackpropGradient"));
        outputSynapseBackpropGradient.saveWeights(putComponent(saveStream,
outputSynapseBackpropGradient.className(), "outputSynapseBackpropGradient"));
        outputAxonBackpropGradient.saveWeights(putComponent(saveStream,
outputAxonBackpropGradient.className(), "outputAxonBackpropGradient"));
        control.saveWeights(putComponent(saveStream, control.className(),
"control"));
        fclose(saveStream);

}
```

```
//Source Code for Real-Time Training and Prediction of Glucose
extern void _cdecl predictGlucose(int infile_length, int outfile_length, int epochs)
{
	//Log Initial Model Weights for Weight Analysis
   //acquire_weights();

	// Run Network
	int samples = 1; //Forward Trajectory
	int samplesBackprop = 1; //Backpropagation Trajectory
	//int epochs = 1000; //Number of Epochs
	int exemplars = infile_length; // Number of Exemplars
	int exemplarsPerUpdate = 1; //Number of Exemplars Before Weight Update
	//Counter to Determine Number of Exemplars Before Acquiring Weights for
	Weight Analysis
	int wtcount=0;

	//Set up Neural Network Model Training Configuration
	control.setBackpropLearningOn(TRUE);  //Enable Backpropagation Training
	control.setActiveNumberOfExemplars(infile_length); /
	control.postFireGetReady();
	control.setEpochs(epochs);
	control.setExemplars(exemplars);
	control.setEpochCounter(0);
	for (; control.epochCounter()<control.epochs();) {
		int phases = control.backpropLearningOn() ? control.phases() : 1;
		control.setPhaseCounter(0);
		while (control.phaseCounter()<phases) {
			control.setExemplarCounter(0);
for (; control.exemplarCounter()<control.exemplars();
control.incrementExemplarCounter())
{
				control.setSampleCounter(0);
	for (; control.sampleCounter()<samples; control.incrementSampleCounter())
	{
		control.fireEngines();
	}
	if (control.backpropLearningOn() || forceBackpropLearning)
	{
		inputAxonBackprop.backpropStarting();
		hidden1SynapseBackprop.backpropStarting();
		hidden1AxonBackprop.backpropStarting();
		outputSynapseBackprop.backpropStarting();
		outputAxonBackprop.backpropStarting();
		criterionBackprop.backpropStarting();
for (int backOffset=0; backOffset<samplesBackprop; backOffset++)
```

```
{
        criterionBackprop.fire();
}
        inputAxonBackprop.backpropComplete();
        hidden1SynapseBackprop.backpropComplete();
        hidden1AxonBackprop.backpropComplete();
        outputSynapseBackprop.backpropComplete();
        outputAxonBackprop.backpropComplete();
        criterionBackprop.backpropComplete();
        control.backpropComplete();
        wtcount=wtcount+1;
        if (++updateCounter >= exemplarsPerUpdate) {
                //Update Weights Via Gradient Descent With Momentum
                control.updateNetworkWeights();

                inputAxonBackpropGradient.updateWeights(&inputAxon);

                hidden1SynapseBackpropGradient.updateWeights(&hidden1Synapse);

                hidden1AxonBackpropGradient.updateWeights(&hidden1Axon);

                outputSynapseBackpropGradient.updateWeights(&outputSynapse);

                outputAxonBackpropGradient.updateWeights(&outputAxon);
                control.networkWeightsUpdated();
                updateCounter = 0;
                if(wtcount==800)
                {
                        //After 800 Exemplars Acquire Weights for Weight Analysis
                        saveAllWeights("PSNNet75.nsw"); // Save Model Weights
                        acquire_weights();
                        wtcount=0;
                 }
                }
                        forceBackpropLearning = FALSE;
                }
                        if (control.networkPaused())
                        {
                                criterion.reportCost();
                                goto ConcludeFiring;
                          }
                        }
                        control.incrementPhaseCounter();
                        if (control.phaseCounter() < phases) {
                        if (control.phases() > 1) {
                                control.phaseEnded(control.phaseCounter());
```

```
                outputDesiredDataGraph.m_bAccessEnabled = TRUE;
                CVOutputDesiredDataGraph.m_bAccessEnabled = TRUE;
                desiredViewer.m_bAccessEnabled = TRUE;
                CVDesiredViewer.m_bAccessEnabled = TRUE;
                learningCurveDataGraph.m_bAccessEnabled = TRUE;
                MSEViewer.m_bAccessEnabled = TRUE;
                CVMSEViewer.m_bAccessEnabled = TRUE;
                bestFitnessGraph.m_bAccessEnabled = TRUE;
        }
        }
}
control.incrementEpochCounter();
if(control.epochCounter()==control.epochs())
                {

                }
                else
                {
                        //Delete Predictions Until Last Epoch
                        desiredViewer.deleteData();
                        outputDesiredDataGraph.deleteData();

                }

NSFloat cost5 = criterion.reportCost();
        criterion.m_bIgnoreNextError = FALSE;
if (criterion.checkForSaveBest(cost5, FALSE))
{
        //If Cost Function (Model Error Improves)
        //Save Best Model Weights
        saveAllWeights("PSNNet75.bst");
        acquire_bstweights();
}
criterion.epochEnded();
control.epochEnded();
if ((control.phases() > 1) && control.backpropLearningOn()) {
        outputDesiredDataGraph.m_bAccessEnabled = FALSE;
        CVOutputDesiredDataGraph.m_bAccessEnabled = FALSE;
        desiredViewer.m_bAccessEnabled = FALSE;
        CVDesiredViewer.m_bAccessEnabled = FALSE;
        learningCurveDataGraph.m_bAccessEnabled = FALSE;
        MSEViewer.m_bAccessEnabled = FALSE;
        CVMSEViewer.m_bAccessEnabled = FALSE;
        bestFitnessGraph.m_bAccessEnabled = FALSE;
}
if (control.networkPaused())
```

```
                goto ConcludeFiring;
        }

        ConcludeFiring:
                control.fireConclude();
                if (criterion.checkForSaveBest(criterion.lastUncheckedCost(), TRUE))
                {
                        //If (Model Error Improves)
                        //Save Best Model Weights
                        saveAllWeights("PSNNet75.bst");
                        acquire_bstweights();
                }

                //After Training/Prediction Save Model Weights for

                saveAllWeights("PSNNet75.nsw");

                //Final Weights State Acquired for Weight Analysis
                //acquire_weights();

//Close Access to Neural Network Input and Desired Files
inputFile.closeFile();
desiredFile.closeFile();
}
```

B.2 MATLAB® Source Code for Post-Processing Algorithm Implementation

```
%%%%Post Processing Algorithm for Enhancement of NNet Model Accuracy
%%%%Critical Care Patients

clear all;
clc;


%Load Actual and Neural Network Model Predictions

predict_results = dlmread('PredictCGM1.xls','\t');

actual_cgm = predict_results(:,1);

predict_nnet = predict_results(:,2);


%Load Real-Time Data

rtdata = csvread('inputdatart.csv');



rt_hr = rtdata(:,3);

insulin_rt = rtdata(:,35);

rt_cgm = rtdata(:,38);


beg_file_length = 800;

%num_iter = length(rt_data)-beg_file_length;



%Predictive Horizon

pw = 15;

num_iter = length(predict_nnet)/pw;
```

```
%Define Tachycardic Extremes

near_tachy= 90;

onset_tachy = 100;

mod_tachy = 110;

severe_tachy = 120;


%Define Glycemic Extremes

hypo_thresh = 70;

norm_thresh = 149;

hyper_thresh1 =  190;

hyper_thresh2 = 240;

hyper_thresh3 = 300;




%Cycle Through Real-Time CGM Data and Apply Post Processing Algorithm
%Initial Start and End Indices
start_ind = 1;
end_ind = pw;

start_ind_rt = beg_file_length;

%Keep track of historical ROC of CGM
hist_roc_cgm=[];

%Cumulative PP results

pp_cum=[];


%Cumulative PP Values Due to TachyCardia
tachy_pp=[];
```

```
tachy_iter=[];

tachy_nnet =[];

for i=1:num_iter

   %Real-Time CGM Value
   rt_cgm_val = rt_cgm(start_ind_rt);

   %Real-Time Insulin Dosage
   rt_insulin_val = insulin_rt(start_ind_rt);

   predicted_cgm = predict_nnet(start_ind:end_ind);

   if(i>1)
      rt_roc_cgm = (rt_cgm(i)-rt_cgm(i-1))/5;
      hist_roc_cgm = [hist_roc_cgm;rt_roc_cgm];

      if(length(hist_roc_cgm)==pw-1)
         for j=1:length(hist_roc_cgm)
            if(j<length(hist_roc_cgm))
            hist_roc_cgm(j)=hist_roc_cgm(j+1);
            else
               hist_roc_cgm(j)=rt_roc_cgm;
            end
         end
      end

   end

   %Determine Tachycardic extreme

   near_tachy_ind=0;
   onset_tachy_ind=0;
   mod_tachy_ind=0;
   severe_tachy_ind=0;

   %Near Tachycardia
   if(rt_hr(start_ind_rt)>=near_tachy&rt_hr(start_ind_rt)<onset_tachy)
      near_tachy_ind=1;
   end

   %Onset Tachycardia
   if(rt_hr(start_ind_rt)>=onset_tachy&rt_hr(start_ind_rt)<mod_tachy)
      onset_tachy_ind=1;
   end
```

```
%Moderate Tachycardia
if(rt_hr(start_ind_rt)>=mod_tachy&rt_hr(start_ind_rt)<severe_tachy)
   mod_tachy_ind=1;
end

%Severe Tachycardia
if(rt_hr(start_ind_rt)>=near_tachy&rt_hr(start_ind_rt)<onset_tachy)
   severe_tachy_ind=1;
end


%Determine Which Post Processing Algorithm Implementation to Implement


%If Tachycardia Detected Implement Event Based PP Algorithm

if(near_tachy_ind==1|onset_tachy==1|mod_tachy==1|severe_tachy==1)

   if(near_tachy_ind==1)

      hist_insulin = sum(insulin_rt(start_ind_rt-15:start_ind_rt));


      %If Hypoglycemic Extreme
      if(rt_cgm_val<=hypo_thresh)

         %Model Fit Coefficients
         c1 =  5.53E-05;
         c2 = -5.35E-03;
         c3 = 2.11E-01;
         c4 = 6.55E+01;

         time = 5:5:pw*5;
         pp_predict_fix = c1.*time.^3+c2.*time.^2+c3.*time+c4;
      end



      %Normal Glycemic Extremes
      if(rt_cgm_val>hypo_thresh&rt_cgm_val<=norm_thresh)

         %Historical Insulin

         hist_insulin = sum(insulin_rt(start_ind_rt-15:start_ind_rt));
```

```
%No Insulin Delivery and Decrease in Glucose
if(hist_insulin==0&rt_roc_cgm<0)

   %Model Fit Coefficients
   c1 =  -2.67E-05;
   c2 = 3.01E-03;
   c3 = -2.00E-01;
   c4 = 1.18E+02;

   time = 5:5:pw*5;
   pp_predict_fix = c1.*time.^3+c2.*time.^2+c3.*time+c4;

end

%Insulin Delivery and Decrease in Glucose
if(hist_insulin>0&rt_roc_cgm<0)

   %Model Fit Coefficients
   c1 =  1.35E-05;
   c2 = -1.81E-03;
   c3 = -6.22E-02;
   c4 = 1.13E+02;

   time = 5:5:pw*5;
   pp_predict_fix = c1.*time.^3+c2.*time.^2+c3.*time+c4;

end

%No Insulin Delivery and Increase in Glucose
if(hist_insulin==0&rt_roc_cgm>0)

   %Model Fit Coefficients
   c1 =  -5.11E-05;
   c2 = 5.69E-03;
   c3 = 6.44E-02;
   c4 = 1.08E+02;

   time = 5:5:pw*5;
   pp_predict_fix = c1.*time.^3+c2.*time.^2+c3.*time+c4;

end

%Insulin Delivery and Increase in Glucose
if(hist_insulin>0&rt_roc_cgm>0)

   %Model Fit Coefficients
```

```
        c1 =  -1.96E-05;
        c2 = 2.97E-03;
        c3 = -8.92E-04;
        c4 = 1.11E+02;

        time = 5:5:pw*5;
        pp_predict_fix = c1.*time.^3+c2.*time.^2+c3.*time+c4;

    end


end %End Normal Extreme


%Hyperglycemic Extreme 1
if(rt_cgm_val>norm_thresh&rt_cgm_val<=hyper_thresh1)

    %Historical Insulin

    hist_insulin = sum(insulin_rt(start_ind_rt-15:start_ind_rt));

    %No Insulin Delivery and Decrease in Glucose
    if(hist_insulin==0&rt_roc_cgm<0)

        %Model Fit Coefficients
        c1 =  -1.55E-05;
        c2 = 2.97E-03;
        c3 = -3.38E-01;
        c4 = 1.72E+02;

        time = 5:5:pw*5;
        pp_predict_fix = c1.*time.^3+c2.*time.^2+c3.*time+c4;

    end

    %Insulin Delivery and Decrease in Glucose
    if(hist_insulin>0&rt_roc_cgm<0)

        %Model Fit Coefficients
        c1 =  5.63E-06;
        c2 = -5.62E-05;
        c3 = -2.3E-1;
        c4 = 1.68E+02;

        time = 5:5:pw*5;
        pp_predict_fix = c1.*time.^3+c2.*time.^2+c3.*time+c4;
```

```
    end

    %No Insulin Delivery and Increase in Glucose
    if(hist_insulin==0&rt_roc_cgm>0)

        %Model Fit Coefficients
        c1 =  -2.16E-05;
        c2 = 1.31E-04;
        c3 = 1.74E-01;
        c4 = 1.60E+02;

        time = 5:5:pw*5;
        pp_predict_fix = c1.*time.^3+c2.*time.^2+c3.*time+c4;

    end

    %Insulin Delivery and Increase in Glucose
    if(hist_insulin>0&rt_roc_cgm>0)

        %Model Fit Coefficients
        c1 =  1.63E-06;
        c2 = 3.07E-03;
        c3 = -1.13E-01;
        c4 = 1.654E+02;

        time = 5:5:pw*5;
        pp_predict_fix = c1.*time.^3+c2.*time.^2+c3.*time+c4;

    end

end %End Hyper1 Extreme




%Hyperglycemic Extreme 2
if(rt_cgm_val>hyper_thresh1&rt_cgm_val<=hyper_thresh2)

    %Historical Insulin

    hist_insulin = sum(insulin_rt(start_ind_rt-15:start_ind_rt));

    %No Insulin Delivery and Decrease in Glucose
    if(hist_insulin==0&rt_roc_cgm<0)
```

```
    %Model Fit Coefficients
    c1 =  -2.08E-05;
    c2 = 9.31E-03;
    c3 = -9.81E-01;
    c4 = 1.994E+02;

    time = 5:5:pw*5;
    pp_predict_fix = c1.*time.^3+c2.*time.^2+c3.*time+c4;

end

%Insulin Delivery and Decrease in Glucose
if(hist_insulin>0&rt_roc_cgm<0)

    %Model Fit Coefficients
    c1 =  1.24E-06;
    c2 = -7.2E-04;
    c3 = -2.16E-1;
    c4 = 2.14E+02;

    time = 5:5:pw*5;
    pp_predict_fix = c1.*time.^3+c2.*time.^2+c3.*time+c4;

end

%No Insulin Delivery and Increase in Glucose
if(hist_insulin==0&rt_roc_cgm>0)

    %Model Fit Coefficients
    c1 =  3.92E-04;
    c2 = -6.61E-02;
    c3 = 3.28;
    c4 = 1.90E+02;

    time = 5:5:pw*5;
    pp_predict_fix = c1.*time.^3+c2.*time.^2+c3.*time+c4;

end

%Insulin Delivery and Increase in Glucose
if(hist_insulin>0&rt_roc_cgm>0)

    %No Model Data Run ROC/Offset PP
```

```
    end

end %End Hyper2 Extreme



%Hyperglycemic Extreme 3
if(rt_cgm_val>hyper_thresh2&rt_cgm_val<=hyper_thresh3)

    %Historical Insulin

    hist_insulin = sum(insulin_rt(start_ind_rt-15:start_ind_rt));

    %No Insulin Delivery and Decrease in Glucose
    if(hist_insulin==0&rt_roc_cgm<0)

        %Model Fit Coefficients
        c1 =  3.15E-04;
        c2 = -4.22E-02;
        c3 = 1.25;
        c4 = 2.574E+02;

        time = 5:5:pw*5;
        pp_predict_fix = c1.*time.^3+c2.*time.^2+c3.*time+c4;

    end

    %Insulin Delivery and Decrease in Glucose
    if(hist_insulin>0&rt_roc_cgm<0)

        %Model Fit Coefficients
        c1 =  -3.17E-05;
        c2 = -3.88E-03;
        c3 = -4.98E-1;
        c4 = 2.62E+02;

        time = 5:5:pw*5;
        pp_predict_fix = c1.*time.^3+c2.*time.^2+c3.*time+c4;

    end

    %No Insulin Delivery and Increase in Glucose
    if(hist_insulin==0&rt_roc_cgm>0)
```

```
            %Model Fit Coefficients
            c1 =  -4.7E-04;
            c2 = 6.3E-02;
            c3 = -2.32;
            c4 = 3.04E+02;

            time = 5:5:pw*5;
            pp_predict_fix = c1.*time.^3+c2.*time.^2+c3.*time+c4;

        end

        %Insulin Delivery and Increase in Glucose
        if(hist_insulin>0&rt_roc_cgm>0)

            %No Model Data Run ROC/Offset PP



        end

    end %End Hyper3 Extreme

end %End Near Tachycardia



%%Onset Tachycardia
if(onset_tachy_ind==1)


    hist_insulin = sum(insulin_rt(start_ind_rt-15:start_ind_rt));

    %If Hypoglycemic Extreme
    if(rt_cgm_val<=hypo_thresh)


        if(hist_insulin>0&rt_roc_cgm<0)

            %Model Fit Coefficients
            c1 =  5.53E-06;
            c2 = -2.5E-04;
            c3 = -1.03E-01;
            c4 = 6.96E+01;

            time = 5:5:pw*5;
            pp_predict_fix = c1.*time.^3+c2.*time.^2+c3.*time+c4;
```

```
    end

end



%Normal Glycemic Extremes
if(rt_cgm_val>hypo_thresh&rt_cgm_val<=norm_thresh)

    %Historical Insulin

    hist_insulin = sum(insulin_rt(start_ind_rt-15:start_ind_rt));

    %No Insulin Delivery and Decrease in Glucose
    if(hist_insulin==0&rt_roc_cgm<0)

        %Model Fit Coefficients
        c1 =  6.01E-05;
        c2 = -6.32E-03;
        c3 = -3.85E-02;
        c4 = 1.19E+02;

        time = 5:5:pw*5;
        pp_predict_fix = c1.*time.^3+c2.*time.^2+c3.*time+c4;

    end

    %Insulin Delivery and Decrease in Glucose
    if(hist_insulin>0&rt_roc_cgm<0)

        %Model Fit Coefficients
        c1 =  3.86E-05;
        c2 = -4.44E-03;
        c3 = -8.72E-03;
        c4 = 1.16E+02;

        time = 5:5:pw*5;
        pp_predict_fix = c1.*time.^3+c2.*time.^2+c3.*time+c4;

    end

    %No Insulin Delivery and Increase in Glucose
    if(hist_insulin==0&rt_roc_cgm>0)

        %Model Fit Coefficients
```

```
        c1 =  1.19E-05;
        c2 = -7.46-04;
        c3 = 1.27E-01;
        c4 = 1.09E+02;

        time = 5:5:pw*5;
        pp_predict_fix = c1.*time.^3+c2.*time.^2+c3.*time+c4;

    end

    %Insulin Delivery and Increase in Glucose
    if(hist_insulin>0&rt_roc_cgm>0)

        %Model Fit Coefficients
        c1 =  -1.62E-05;
        c2 = 2.42E-03;
        c3 = 3.64E-02;
        c4 = 1.09E+02;

        time = 5:5:pw*5;
        pp_predict_fix = c1.*time.^3+c2.*time.^2+c3.*time+c4;

    end


end %End Normal Extreme


%Hyperglycemic Extreme 1
if(rt_cgm_val>norm_thresh&rt_cgm_val<=hyper_thresh1)

    %Historical Insulin

    hist_insulin = sum(insulin_rt(start_ind_rt-15:start_ind_rt));

    %No Insulin Delivery and Decrease in Glucose
    if(hist_insulin==0&rt_roc_cgm<0)

        %Model Fit Coefficients
        c1 =  7.47E-05;
        c2 = -5.37E-03;
        c3 = -3.96E-01;
        c4 = 1.62E+02;

        time = 5:5:pw*5;
        pp_predict_fix = c1.*time.^3+c2.*time.^2+c3.*time+c4;
```

```
    end

    %Insulin Delivery and Decrease in Glucose
    if(hist_insulin>0&rt_roc_cgm<0)

        %Model Fit Coefficients
        c1 =  -1.76E-05;
        c2 = 2.78E-03;
        c3 = -3.59E-1;
        c4 = 1.71E+02;

        time = 5:5:pw*5;
        pp_predict_fix = c1.*time.^3+c2.*time.^2+c3.*time+c4;

    end

    %No Insulin Delivery and Increase in Glucose
    if(hist_insulin==0&rt_roc_cgm>0)

        %Model Fit Coefficients
        c1 =  2.3E-05;
        c2 = -2.93E-03;
        c3 = 4.61E-01;
        c4 = 1.572E+02;

        time = 5:5:pw*5;
        pp_predict_fix = c1.*time.^3+c2.*time.^2+c3.*time+c4;

    end

    %Insulin Delivery and Increase in Glucose
    if(hist_insulin>0&rt_roc_cgm>0)

        %Model Fit Coefficients
        c1 =  -5.30E-05;
        c2 = 7.69E-03;
        c3 = -1.9E-01;
        c4 = 1.61E+02;

        time = 5:5:pw*5;
        pp_predict_fix = c1.*time.^3+c2.*time.^2+c3.*time+c4;

    end

end %End Hyper1 Extreme
```

```
%Hyperglycemic Extreme 2
if(rt_cgm_val>hyper_thresh1&rt_cgm_val<=hyper_thresh2)

   %Historical Insulin

   hist_insulin = sum(insulin_rt(start_ind_rt-15:start_ind_rt));

   %No Insulin Delivery and Decrease in Glucose
   if(hist_insulin==0&rt_roc_cgm<0)

      %Model Fit Coefficients
      c1 =  -1.1E-04;
      c2 = 1.78E-02;
      c3 = -8.82E-01;
      c4 = 1.994E+02;

      time = 5:5:pw*5;
      pp_predict_fix = c1.*time.^3+c2.*time.^2+c3.*time+c4;

   end

   %Insulin Delivery and Decrease in Glucose
   if(hist_insulin>0&rt_roc_cgm<0)

      %No Model Fit Implement ROC and Offset Based PP

   end

   %No Insulin Delivery and Increase in Glucose
   if(hist_insulin==0&rt_roc_cgm>0)

      %Model Fit Coefficients
      c1 =  2.35E-04;
      c2 = -1.93E-02;
      c3 = .332;
      c4 = 2.12E+02;

      time = 5:5:pw*5;
      pp_predict_fix = c1.*time.^3+c2.*time.^2+c3.*time+c4;

   end
```

```
    %Insulin Delivery and Increase in Glucose
    if(hist_insulin>0&rt_roc_cgm>0)

        %Model Fit Coefficients
        c1 =  -9.18E-05;
        c2 = 9.80E-03;
        c3 = .455;
        c4 = 2.061E+02;

        time = 5:5:pw*5;
        pp_predict_fix = c1.*time.^3+c2.*time.^2+c3.*time+c4;



    end

end %End Hyper2 Extreme




%Hyperglycemic Extreme 3
if(rt_cgm_val>hyper_thresh2&rt_cgm_val<=hyper_thresh3)

    %Historical Insulin

    hist_insulin = sum(insulin_rt(start_ind_rt-15:start_ind_rt));

    %No Insulin Delivery and Decrease in Glucose
    if(hist_insulin==0&rt_roc_cgm<0)

        %No Model Fit Implement ROC and Offset Based PP

    end

    %Insulin Delivery and Decrease in Glucose
    if(hist_insulin>0&rt_roc_cgm<0)

        %Model Fit Coefficients
        c1 =  -6.00E-04;
        c2 = 4.63E-02;
        c3 = -1.81;
        c4 = 2.532E+02;

        time = 5:5:pw*5;
```

```
        pp_predict_fix = c1.*time.^3+c2.*time.^2+c3.*time+c4;

    end

    %No Insulin Delivery and Increase in Glucose
    if(hist_insulin==0&rt_roc_cgm>0)

        %%No Model Fit Implement ROC/Offset PP

    end

    %Insulin Delivery and Increase in Glucose
    if(hist_insulin>0&rt_roc_cgm>0)

        %Model Fit Coefficients
        c1 =  1.51E-05;
        c2 = -1.13E-02;
        c3 = .959;
        c4 = 2.43E+02;

        time = 5:5:pw*5;
        pp_predict_fix = c1.*time.^3+c2.*time.^2+c3.*time+c4;



    end

  end %End Hyper3 Extreme



end %End Near Tachycardia




%%Moderate Tachycardia
if(mod_tachy_ind==1)


  hist_insulin = sum(insulin_rt(start_ind_rt-15:start_ind_rt));

  %If Hypoglycemic Extreme
  if(rt_cgm_val<=hypo_thresh)

    if(hist_insulin>0&rt_roc_cgm<0)
```

```
    %Model Fit Coefficients
    c1 =  1.74E-05;
    c2 = 9.01E-04;
    c3 = -4.22E-01;
    c4 = 5.9E+01;

    time = 5:5:pw*5;
    pp_predict_fix = c1.*time.^3+c2.*time.^2+c3.*time+c4;

  end


  if(hist_insulin==0&rt_roc_cgm>0)

    %Model Fit Coefficients
    c1 =  -9.2E-04;
    c2 = .109;
    c3 = -2.73;
    c4 = 78.8E+01;

    time = 5:5:pw*5;
    pp_predict_fix = c1.*time.^3+c2.*time.^2+c3.*time+c4;

  end


  if(hist_insulin>0&rt_roc_cgm>0)

    %Model Fit Coefficients
    c1 =  1.17E-04;
    c2 = -1.433E-04;
    c3 = .702;
    c4 = 6.3E+01;

    time = 5:5:pw*5;
    pp_predict_fix = c1.*time.^3+c2.*time.^2+c3.*time+c4;

  end



end
```

```
%Normal Glycemic Extremes
if(rt_cgm_val>hypo_thresh&rt_cgm_val<=norm_thresh)

   %Historical Insulin

   hist_insulin = sum(insulin_rt(start_ind_rt-15:start_ind_rt));

   %No Insulin Delivery and Decrease in Glucose
   if(hist_insulin==0&rt_roc_cgm<0)

      %Model Fit Coefficients
      c1 =  -4.67E-06;
      c2 = 4.60E-03;
      c3 = -.619;
      c4 = 1.29E+02;

      time = 5:5:pw*5;
      pp_predict_fix = c1.*time.^3+c2.*time.^2+c3.*time+c4;

   end

   %Insulin Delivery and Decrease in Glucose
   if(hist_insulin>0&rt_roc_cgm<0)

      %Model Fit Coefficients
      c1 =  1.77E-05;
      c2 = -2.15E-03;
      c3 = -1.1E-01;
      c4 = 1.19E+02;

      time = 5:5:pw*5;
      pp_predict_fix = c1.*time.^3+c2.*time.^2+c3.*time+c4;

   end

   %No Insulin Delivery and Increase in Glucose
   if(hist_insulin==0&rt_roc_cgm>0)

      %Model Fit Coefficients
      c1 = 2.91E-05;
      c2 = -3.22E-03;
      c3 = 2.87E-01;
      c4 = 1.20E+02;

      time = 5:5:pw*5;
```

```
        pp_predict_fix = c1.*time.^3+c2.*time.^2+c3.*time+c4;

    end

    %Insulin Delivery and Increase in Glucose
    if(hist_insulin>0&rt_roc_cgm>0)

        %Model Fit Coefficients
        c1 =  8.71E-06;
        c2 = -3.97E-04;
        c3 = 1.55E-01;
        c4 = 9.99E+01;

        time = 5:5:pw*5;
        pp_predict_fix = c1.*time.^3+c2.*time.^2+c3.*time+c4;

    end


end %End Normal Extreme


%Hyperglycemic Extreme 1
if(rt_cgm_val>norm_thresh&rt_cgm_val<=hyper_thresh1)

    %Historical Insulin

    hist_insulin = sum(insulin_rt(start_ind_rt-15:start_ind_rt));

    %No Insulin Delivery and Decrease in Glucose
    if(hist_insulin==0&rt_roc_cgm<0)

        %Model Fit Coefficients
        c1 =  5.71E-05;
        c2 = 3.87E-03;
        c3 = -8.64E-01;
        c4 = 1.59E+02;

        time = 5:5:pw*5;
        pp_predict_fix = c1.*time.^3+c2.*time.^2+c3.*time+c4;

    end

    %Insulin Delivery and Decrease in Glucose
    if(hist_insulin>0&rt_roc_cgm<0)
```

```
        %Model Fit Coefficients
        c1 =  3.66E-06;
        c2 = 1.29E-04;
        c3 = -3.13E-01;
        c4 = 1.76E+02;

        time = 5:5:pw*5;
        pp_predict_fix = c1.*time.^3+c2.*time.^2+c3.*time+c4;

    end

    %No Insulin Delivery and Increase in Glucose
    if(hist_insulin==0&rt_roc_cgm>0)

        %Model Fit Coefficients
        c1 =  1.48E-04;
        c2 = -1.77E-02;
        c3 = 7.6E-01;
        c4 = 1.73E+02;

        time = 5:5:pw*5;
        pp_predict_fix = c1.*time.^3+c2.*time.^2+c3.*time+c4;

    end

    %Insulin Delivery and Increase in Glucose
    if(hist_insulin>0&rt_roc_cgm>0)

        %Model Fit Coefficients
        c1 =  -5.13E-05;
        c2 = 1.01E-02;
        c3 = -3.26E-01;
        c4 = 1.80E+02;

        time = 5:5:pw*5;
        pp_predict_fix = c1.*time.^3+c2.*time.^2+c3.*time+c4;

    end

end %End Hyper1 Extreme



%Hyperglycemic Extreme 2
if(rt_cgm_val>hyper_thresh1&rt_cgm_val<=hyper_thresh2)
```

```
%Historical Insulin

hist_insulin = sum(insulin_rt(start_ind_rt-15:start_ind_rt));

%No Insulin Delivery and Decrease in Glucose
if(hist_insulin==0&rt_roc_cgm<0)


   %No Model Fit Implement ROC and Offset PP

end

%Insulin Delivery and Decrease in Glucose
if(hist_insulin>0&rt_roc_cgm<0)

   %Model Fit Coefficients
   c1 =  6.67E-05;
   c2 = -4.08E-03;
   c3 = -.323;
   c4 = 2.15E+02;

   time = 5:5:pw*5;
   pp_predict_fix = c1.*time.^3+c2.*time.^2+c3.*time+c4;


end

%No Insulin Delivery and Increase in Glucose
if(hist_insulin==0&rt_roc_cgm>0)

   %No Model Fit Implement ROC and Offset Based PP

end

%Insulin Delivery and Increase in Glucose
if(hist_insulin>0&rt_roc_cgm>0)

   %Model Fit Coefficients
   c1 =  -6.6E-04;
   c2 = 9.24E-02;
   c3 = -2.91;
   c4 = 2.218E+02;

   time = 5:5:pw*5;
   pp_predict_fix = c1.*time.^3+c2.*time.^2+c3.*time+c4;
```

```
    end

end %End Hyper2 Extreme



%Hyperglycemic Extreme 3
if(rt_cgm_val>hyper_thresh2&rt_cgm_val<=hyper_thresh3)

    %Historical Insulin

    hist_insulin = sum(insulin_rt(start_ind_rt-15:start_ind_rt));

    %No Insulin Delivery and Decrease in Glucose
    if(hist_insulin==0&rt_roc_cgm<0)

        %No Model Fit Implement ROC and Offset Based PP

    end

    %Insulin Delivery and Decrease in Glucose
    if(hist_insulin>0&rt_roc_cgm<0)

        %Model Fit Coefficients
        c1 =  7.23E-05;
        c2 = -6.73E-03;
        c3 = -.189;
        c4 = 2.69E+02;

        time = 5:5:pw*5;
        pp_predict_fix = c1.*time.^3+c2.*time.^2+c3.*time+c4;

    end

    %No Insulin Delivery and Increase in Glucose
    if(hist_insulin==0&rt_roc_cgm>0)

        %%No Model Fit Implement ROC/Offset PP

    end

    %Insulin Delivery and Increase in Glucose
    if(hist_insulin>0&rt_roc_cgm>0)

    end
```

```
    end %End Hyper3 Extreme

end %End Moderate Tachycardia


%%Severe Tachycardia
if(severe_tachy_ind==1)


    hist_insulin = sum(insulin_rt(start_ind_rt-15:start_ind_rt));

    %If Hypoglycemic Extreme
    if(rt_cgm_val<=hypo_thresh)

        if(hist_insulin>0&rt_roc_cgm<0)

            %No Model Fit Implement ROC/Offset Based PP

        end


        if(hist_insulin==0&rt_roc_cgm>0)

            %No Model Fit Implement ROC/Offset Based PP

        end


        if(hist_insulin>0&rt_roc_cgm>0)

            %No Model Fit Implement ROC/Offset Based PP

        end



    end



    %Normal Glycemic Extremes
    if(rt_cgm_val>hypo_thresh&rt_cgm_val<=norm_thresh)

        %Historical Insulin
```

```
hist_insulin = sum(insulin_rt(start_ind_rt-15:start_ind_rt));

%No Insulin Delivery and Decrease in Glucose
if(hist_insulin==0&rt_roc_cgm<0)

   %Model Fit Coefficients
   c1 =  -1.1E-04;
   c2 = 1.1E-02;
   c3 = -2.54E-01;
   c4 = 1.33E+02;

   time = 5:5:pw*5;
   pp_predict_fix = c1.*time.^3+c2.*time.^2+c3.*time+c4;

end

%Insulin Delivery and Decrease in Glucose
if(hist_insulin>0&rt_roc_cgm<0)

   %Model Fit Coefficients
   c1 =  2.56E-05;
   c2 = -3.16E-03;
   c3 = -1.96E-01;
   c4 = 1.22E+02;

   time = 5:5:pw*5;
   pp_predict_fix = c1.*time.^3+c2.*time.^2+c3.*time+c4;

end

%No Insulin Delivery and Increase in Glucose
if(hist_insulin==0&rt_roc_cgm>0)

   %Model Fit Coefficients
   c1 = -1.46E-05;
   c2 = 2.80E-03;
   c3 = -2.46E-02;
   c4 = 1.09E+02;

   time = 5:5:pw*5;
   pp_predict_fix = c1.*time.^3+c2.*time.^2+c3.*time+c4;

end

%Insulin Delivery and Increase in Glucose
```

```
    if(hist_insulin>0&rt_roc_cgm>0)

        %Model Fit Coefficients
        c1 =  5.37E-05;
        c2 = -7.03E-03;
        c3 = 3.89E-01;
        c4 = 1.16E+01;

        time = 5:5:pw*5;
        pp_predict_fix = c1.*time.^3+c2.*time.^2+c3.*time+c4;

    end


end %End Normal Extreme


%Hyperglycemic Extreme 1
if(rt_cgm_val>norm_thresh&rt_cgm_val<=hyper_thresh1)

    %Historical Insulin

    hist_insulin = sum(insulin_rt(start_ind_rt-15:start_ind_rt));

    %No Insulin Delivery and Decrease in Glucose
    if(hist_insulin==0&rt_roc_cgm<0)

        %Model Fit Coefficients
        c1 =  1.40E-04;
        c2 = -6.55E-03;
        c3 = -6.44E-01;
        c4 = 1.94E+02;

        time = 5:5:pw*5;
        pp_predict_fix = c1.*time.^3+c2.*time.^2+c3.*time+c4;

    end

    %Insulin Delivery and Decrease in Glucose
    if(hist_insulin>0&rt_roc_cgm<0)

        %Model Fit Coefficients
        c1 =  1.78E-05;
        c2 = -2.66E-04;
        c3 = -4.11E-01;
        c4 = 1.68E+02;
```

```
        time = 5:5:pw*5;
        pp_predict_fix = c1.*time.^3+c2.*time.^2+c3.*time+c4;

    end

    %No Insulin Delivery and Increase in Glucose
    if(hist_insulin==0&rt_roc_cgm>0)

        %Model Fit Coefficients
        c1 =  -2.09E-04;
        c2 = 1.64E-02;
        c3 = 1.07E-02;
        c4 = 1.64E+02;

        time = 5:5:pw*5;
        pp_predict_fix = c1.*time.^3+c2.*time.^2+c3.*time+c4;

    end

    %Insulin Delivery and Increase in Glucose
    if(hist_insulin>0&rt_roc_cgm>0)

        %Model Fit Coefficients
        c1 =  1.82E-04;
        c2 = -1.45E-02;
        c3 = 2.95E-01;
        c4 = 1.57E+02;

        time = 5:5:pw*5;
        pp_predict_fix = c1.*time.^3+c2.*time.^2+c3.*time+c4;

    end

end %End Hyper1 Extreme



%Hyperglycemic Extreme 2
if(rt_cgm_val>hyper_thresh1&rt_cgm_val<=hyper_thresh2)

    %Historical Insulin

    hist_insulin = sum(insulin_rt(start_ind_rt-15:start_ind_rt));

    %No Insulin Delivery and Decrease in Glucose
```

```
if(hist_insulin==0&rt_roc_cgm<0)


   %No Model Fit Implement ROC and Offset PP

end

%Insulin Delivery and Decrease in Glucose
if(hist_insulin>0&rt_roc_cgm<0)

   %Model Fit Coefficients
   c1 =  -3.69E-05;
   c2 = 3.22E-03;
   c3 = -2.80E-01;
   c4 = 2.09E+02;

   time = 5:5:pw*5;
   pp_predict_fix = c1.*time.^3+c2.*time.^2+c3.*time+c4;


end

%No Insulin Delivery and Increase in Glucose
if(hist_insulin==0&rt_roc_cgm>0)

   %Model Fit Coefficients
   c1 =  1.98E-04;
   c2 = -2.58E-02;
   c3 = 1.85;
   c4 = 1.95E+02;

   time = 5:5:pw*5;
   pp_predict_fix = c1.*time.^3+c2.*time.^2+c3.*time+c4;

end

%Insulin Delivery and Increase in Glucose
if(hist_insulin>0&rt_roc_cgm>0)

   %Model Fit Coefficients
   c1 =  1.28E-04;
   c2 = -2.27E-02;
   c3 = 1.18;
   c4 = 2.15E+02;

   time = 5:5:pw*5;
```

```
        pp_predict_fix = c1.*time.^3+c2.*time.^2+c3.*time+c4;

    end

end %End Hyper2 Extreme



%Hyperglycemic Extreme 3
if(rt_cgm_val>hyper_thresh2&rt_cgm_val<=hyper_thresh3)

    %Historical Insulin

    hist_insulin = sum(insulin_rt(start_ind_rt-15:start_ind_rt));

    %No Insulin Delivery and Decrease in Glucose
    if(hist_insulin==0&rt_roc_cgm<0)

        %No Model Fit Implement ROC and Offset Based PP

    end

    %Insulin Delivery and Decrease in Glucose
    if(hist_insulin>0&rt_roc_cgm<0)

        %Model Fit Coefficients
        c1 =  9.74E-05;
        c2 = -1.61E-02;
        c3 = -.600;
        c4 = 2.59E+02;

        time = 5:5:pw*5;
        pp_predict_fix = c1.*time.^3+c2.*time.^2+c3.*time+c4;

    end

    %No Insulin Delivery and Increase in Glucose
    if(hist_insulin==0&rt_roc_cgm>0)

        %Model Fit Coefficients
        c1 =  2.51E-04;
        c2 = -3.44E-02;
        c3 = 1.44;
        c4 = 2.56E+02;

        time = 5:5:pw*5;
```

```
            pp_predict_fix = c1.*time.^3+c2.*time.^2+c3.*time+c4;
        end

        %Insulin Delivery and Increase in Glucose
        if(hist_insulin>0&rt_roc_cgm>0)

            %No Model Fit Implement ROC/Offset Based PP

        end

    end %End Hyper3 Extreme

end %End Severe Tachycardia

for j=1:length(pp_predict_fix)

pp_cum=[pp_cum;pp_predict_fix(j)];
end

tachy_iter= [tachy_iter;actual_cgm((i*15-14):(i*15))];

tachy_nnet= [tachy_nnet;predict_nnet((i*15-14):(i*15))];

for j=1:length(pp_predict_fix)

tachy_pp=[tachy_pp;pp_predict_fix(j)];
end


else
  %Implement ROC/Offset Based PP Algorithm

  %Calculate Offset Between First Predicted Value and Current RT CGM
  offset = rt_cgm_val-predicted_cgm(1);

  roc_predict_cgm = diff(predicted_cgm)./5;


 %%%%Based on Glycemic Threshold set ROC Threshold Weight

 w_roc = 1.0;

 if(rt_cgm_val<=hypo_thresh)
    w_roc=.2;
 end
```

```
    if(rt_cgm_val>hypo_thresh&rt_cgm_val<=100)
       w_roc=.3;
    end

    if(rt_cgm_val>100&rt_cgm_val<=140)
       w_roc=.5;
    end

    if(rt_cgm_val>140&rt_cgm_val<=180)
       w_roc=.7;
    end

    if(rt_cgm_val>180)
       w_roc=.9;
    end




     for j = 1:length(predicted_cgm)
        if(j==1)
        pp_predict_fix(j)=predicted_cgm(j)+offset;
        else
           pp_predict_fix(j) = 5*w_roc*roc_predict_cgm(j-1)+pp_predict_fix(j-1);
        end
     end

     for j=1:length(pp_predict_fix)
     pp_cum=[pp_cum;pp_predict_fix(j)];
     end


  end



  start_ind_rt = start_ind_rt+1;

  start_ind = start_ind+pw;
  end_ind = end_ind+pw;

end

%%% Comparison of PP and Predicted Results
```

```
ad_predict = abs(actual_cgm-predict_nnet)./actual_cgm*100;
mad_predict = mean(ad_predict);

ad_pp = abs(actual_cgm-pp_cum)./actual_cgm*100;
mad_pp = mean(ad_pp);
```